Order Number 9405561

# Hydraulic relationships between shallow groundwater sub-systems discharging to surface water bodies and underlying regional systems

Modica, Edward, Ph.D.

City University of New York, 1993



U·M·I
300 N. Zeeb Rd.
Ann Arbor, MI 48106

14

# HYDRAULIC RELATIONSHIPS BETWEEN SHALLOW GROUNDWATER SUB-SYSTEMS DISCHARGING TO SURFACE WATER BODIES AND UNDERLYING REGIONAL SYSTEMS

by

**EDWARD MODICA**

A dissertation submitted to the Graduate Faculty in Earth and Environmental Sciences in partial fulfillment of the requirements for the degree of Doctor of Philosophy, The City University of New York

1993

This manuscript has been read and accepted for the Graduate Faculty in Earth and Environmental Sciences in satisfaction of the dissertation requirements for the degree of Doctor of Philosophy.

9/3/93
Date

H. L. Franke
Chair of Examining Committee

9/13/93
Date

Daniel Habib
Executive Officer

Thomas E. Reilly

David W. Pollock

David Thurber

**Supervisory Committee**

**THE CITY UNIVERSITY OF NEW YORK**

Abstract

**HYDRAULIC RELATIONSHIPS BETWEEN SHALLOW GROUNDWATER SUB-SYSTEMS DISCHARGING TO SURFACE WATER BODIES AND UNDERLYING REGIONAL SYSTEMS**

by

Edward Modica

Adviser: Professor O. L. Franke

Hypothetical flow models and a flow simulation of the Upper Rancocas watershed system in New Jersey were used to characterize the boundary zone separating stream sub-system flow and regional flow, and to determine the flow patterns within stream sub-systems. Estimates of flow in three-dimensional aquifer systems consisting of regional and stream sub-system flow regimes were made with numerical flow solutions and particle tracking analysis. Hydraulic parameters that affect stream system flow patterns were systematically modified in order to evaluate cause-and-effect relations and to determine the degree to which parameters can influence flow in the system. Stream sub-system geometry and its flow patterns are largely controlled by the quantity and distribution of stream discharge. The relative amount and location of discharge

along a stream channel is in turn affected by variations in anisotropy, aquifer thickness, recharge rates, streambed elevation, and drainage density. The "bounding surface" is an interaction zone between the stream sub-system and the adjacent flow system, the form of which is sensitive to system boundaries and hydraulic properties of the aquifer and stream sub-system. Regional flow is restricted in thin aquifer systems. Stream source areas in thin aquifers tend to be more extensive. Thin systems limit the development of flow to remote or major regional sinks that serve as common discharge outlets for the system. Thick aquifers allow for development of deeper flow systems under local stream sub-systems. Streams are line-sinks that induce complex flow patterns in a flow field whereby flow from near and far source areas are drawn into common discharge zones. The age range of groundwater that discharges along the stream varies as a function of distance downstream from the start-of-flow. The highest age ranges occur near the stream terminus.

# TABLE OF CONTENTS

# LIST OF TABLES

# LIST OF ILLUSTRATIONS

# INTRODUCTION

## Background

Hydrologists have long had a special interest in flow patterns and dynamics of aquifer systems. Recent concerns over groundwater contamination and water supply have sharpened this interest inasmuch as such knowledge is an indispensable tool for effective water supply management.

Flow nets have long been an effective way of conceptualizing the flow in an aquifer system in vertical section. Flow nets contain, in a form easy to visualize, much information about groundwater flow geometry, velocities, and residence times.

In the early sixties Toth developed what is now considered a classic series of flow-net-solutions for cross-sections of a small watershed in Alberta (1963). Toth formulated analytical solutions to a series of boundary-value flow problems for systems that are characterized by a hummocky terrain. Figure 1 shows one of these solutions; the model is bounded by no-flow boundaries along the lateral and bottom borders of the modeled section and by specified head values along the top. The head values vary according to a prescribed sine-wave function.

An important finding in Toth's analysis was that his model produced several flow regimes consisting of deep regional flow, intermediate flow, and a shallow system flow component. Flow patterns in the shallow system are nested on top of the deeper regional system and are characterized by an alternating pattern of

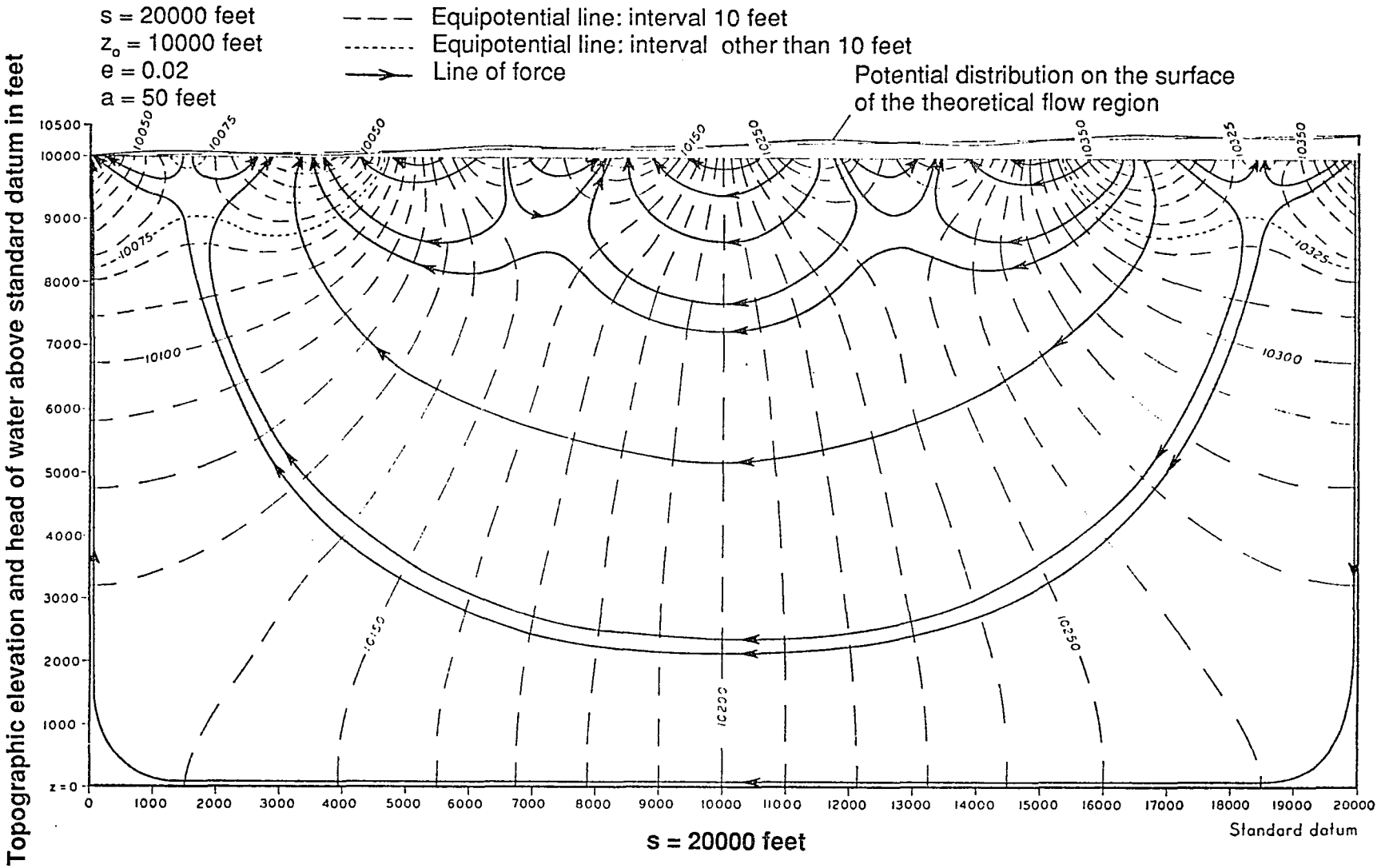


Figure 1--Flow patterns and potential distribution in cross-section of a valley flank in a small drainage basin. (after Toth, 1963)

recharge and discharge. Toth found that the depth to which this shallow system propagates into the aquifer is determined largely by the amplitude and frequency of the function describing the head values along the surface and by the aquifer thickness.

The interest in this classic work lies in the fact that the composite flow regime structure is typical of many aquifer systems where there is a deeper regional flow system underlying a shallow stream sub-system, the flow of which is controlled by surface features, such as topographic relief and stream drainage patterns, and by aquifer geometry and the location of other discharge outlets. The purpose of the present study is to analyze a specific type of composite flow system consisting of a stream sub-system and the underlying regional flow system.

In many aquifer systems where streams occur as part of distinct shallow sub-systems within larger regional systems the stream sub-systems are recharged at the water table and the shallow groundwater is discharged to a stream channel. The source of groundwater discharging to a stream is defined by a contributing area of recharge on the free surface, the shape of which is characterized by the flow dynamics of the system. The flow lines that travel into the system within the contributing area follow varying and winding paths in the stream sub-system to points of discharge on the stream channel. These paths are optimal responses to the flow gradients in a particular system. Collectively, these flow lines define a stream sub-system flow domain that is characterized by

a definite volume and limiting extent that marks the interface between regional- and stream-sub-system flow.

The stream network functions as a sink that dissipates groundwater; groundwater discharge to streams is commonly referred to as base flow. Changes in base flow are a reflection, in part, of the dynamic relation between the local and regional systems. Stresses applied to either system can change base flow as well as the configuration and position of flow lines. Such stresses occur naturally during the annual hydraulic cycle in which seasonal variations in recharge intensity and frequency of occurrence induce both immediate and lagged responses in both systems. Stresses can also be applied artificially to the aquifer system by extended periods of pumping or by artificial recharge.

Because of the complex hydrodynamic interactions between the shallow and deeper systems and their varied responses to stress, a detailed, three-dimensional characterization of the shallow sub-system boundaries and internal flow pattern has been difficult to obtain. Much of the present information on shallow stream system flow configuration is typically based on models that assume horizontal flow or flow within vertical sections. Although these models provide general information on quantities of flow in the shallow system, they cannot adequately represent the stream system boundaries and internal flow patterns.

Furthermore, a two-dimensional analysis of an aquifer system must also assume that flow is parallel to the modeled section. Stream sub-systems, however, are inherently three-dimensional and are not amenable to

two-dimensional analysis because their velocity-vector field changes in magnitude and direction in both the vertical and lateral directions. Therefore, flow analysis of such systems must necessarily include three spatial dimensions in order to adequately represent the system.

**Purpose & Scope**

This study focuses on the inter-relationships involving the free surface (water table), the stream sub-system flow pattern, and the deeper regional flow pattern. A hydraulic feature that is crucial to the understanding of these relationships is the nature of the interface between regional- and stream sub-system flow regimes.

A major objective of this study is to define the boundary that separates the stream sub-system from the regional flow system and determine factors that influence its form. A second objective is to determine the flow pattern within the stream sub-system and quantify its flow processes. A third objective is to determine what hydraulic parameters affect most significantly stream system flow geometry and dynamics and to indicate what these affects are.

An understanding of the geometry of the shallow sub-system and its flow processes is important in distinguishing contributing areas of flow to streams from other recharge areas. These studies will increase understanding of the wide variations in residence times that occur in groundwater flow systems. Flow direction and travel times are important characterizations for studies involving transport of solute or contaminant plume migration.

## Approach

The method of analysis used in this study involves the design of and experimentation with a suite of three-dimensional hypothetical, steady-state models of drainage-basin aquifer systems. These systems were developed using hydrogeologic parameters typical of the Atlantic Coastal Plain, particularly systems found in the Coastal Plain of New Jersey and Long Island, New York. Streams that comprise the drainage networks in these areas are typically gaining streams inasmuch as most stream discharge consists of base flow.

There are several advantages to using a hypothetical flow model rather than a real system as a means of obtaining a general understanding for the contribution of shallow groundwater to stream flow. Aquifer geometries and hydraulic parameters can be systematically and conveniently modified in order to study cause-and-effect relations on the system without regard to calibrating heads and flows against those of an actual system. Secondly, aquifer geometry can be designed without regard for complicated structural, stratigraphic, or even morphological features of real aquifer systems. Instead, features can be made simple and linear without appreciable loss of applicability. Although generic models do not require calibration, the hypothetical systems of this study were constrained by patterning them after hydrologic, geometric, and geologic properties similar to Atlantic Coastal Plain systems as noted above.

The computer flow model Modflow (McDonald and Harbaugh, 1988) was used to solve for hydraulic heads in all simulations. The model output also provides volumetric flow rates which were used to calculate vector fields and

specific discharges. Because a major component of the analysis involved understanding the orientation of flow paths in three dimensions, a particle tracking post-processing algorithm (Pollock, 1989) was used to simulate flow paths in the modeled aquifer systems.

A primary generic model was developed to serve as a hypothetical coastal plain system and to provide an index simulation for comparing 15 additional hypothetical flow systems (see table 1). The design of the other models was similar to that of the reference except that for each one a different parameter modification was made so as to evaluate how the parameter change affected the geometry, velocities, flow paths, and fluxes of the stream sub-system.

A final aspect of the study involved the comparison and analysis of flow patterns between the hypothetical systems and a real coastal plain aquifer system. A calibrated flow model of the Upper Rancocas Drainage Basin, New Jersey was developed for this purpose.

**Previous Studies**

A variety of studies exist in the literature that deal with the lagged response of the aquifer-stream system to a stress such as a rain storm. Most studies dealing with aquifer-stream interactions focus mainly on storm runoff and storm peaks that produce potentially damaging floods and soil erosion and are, therefore, of interest to engineers concerned about the design load of structures. These studies utilize mathematical flow models designed to predict the

hydrologic behavior of a local aquifer and related stream flow in response to a precipitation event (Hall, 1968; Eshett and Bittinger, 1965; Barnes, 1939). Many of these models are based on the relation:

$$(1) \quad \frac{d^2h^2}{dx^2} = \frac{S_s}{K}\frac{dh}{dt}$$

where h is the hydraulic head

x is the horizontal distance,

$S_s$ is the specific storage ,

K is the hydraulic conductivity and,

t is time.

Hornberger and others (1970) developed a numerical technique to obtain solutions to the Boussinesq equation that was used to determine groundwater flow and recession in response to changes in stream stage. Their model was amenable to problems involving time-varying boundary conditions at the stream and non-uniform initial conditions. Cooper and Rorabaugh (1963) derived analytical solutions for changes in groundwater heads, flows, and bank storage that would occur due to a sinosoidal flood event. Their analysis includes a family of asymmetric flood-wave stage hydrographs that show a wide variety of flood shapes in groundwater.

Singh (1968) developed solutions that would predict recession rates for shallow aquifers with fully penetrating streams and for deep aquifers with shallow entrenched streams. The results were presented as dimensionless-base-flow

curves that showed parameter values that caused a stream to become influent or to gain at a constant rate. Cases for loss due to evapotranspiration or gains from confined aquifers were also evaluated.

Flow and head variations in stationary linear stream-aquifer systems have been obtained by application of convolution equations (Hall and Moench, 1972; Venetis, 1970). Head fluctuations in the aquifer due to arbitrary varying flood pulse were obtained for a finite aquifer with and without a semi-impervious stream bank. Pinder and Sauer (1971) performed several numerical simulations to show that flood waves are affected by bank storage, especially in long segments of a long reach, and that the magnitude of effect is controlled by the hydraulic conductivity of the aquifer.

Morel-Seytoux (1975) developed what he refers to as discrete kernel generators for isolated alluvial aquifers and isolated streams that were combined to characterize interactions between both systems and to solve for flood problems. Relations involving simulated results, initial conditions, and controllable decision variables, or economic considerations, are also established through a set of 'influence coefficients' in order to render the model amenable to optimization-type management applications (Illangasekare and Morel-Seytoux, 1982).

Another category of studies deals with the complex relations among infiltration of precipitation, watershed morphology, and drainage characteristics (Strahler, 1967, Ritter, 1982). Horton (1945) laid down the basis of standard geomorphic analysis of drainage basins by attempting to express quantitatively

stream origins and basin hydrology. Horton hypothesized that when rainfall intensity exceeds infiltration capacity then runoff or overland flow would occur and erosion would ensue. Kirkby and Chorley (1967), however, argued that Horton's infiltration model had limited application but that 'throughflow' was the dominant process of erosion.

Freeze (1971, 1972, 1975) explored the mechanism of base-flow generation and watershed response by use of a model that coupled three-dimensional, transient, variably saturated groundwater flow to one-dimensional, unsteady, channel flow. His simulation of a hypothetical basin showed a wide range of response attributed to variations in rainfall and antecedent moisture conditions of the unsaturated zone. His simulation experiments also showed the limitations of classic Hortonian flow. Studies carried out by Dunne and Black in a New England watershed (1970a, 1970b) show that overland flow is generated by rainfall on varying source areas adjacent to stream channels and that overland flow occurs when the soil is saturated at the surface from below by the rising water table. Hewlett and Nutter (1970) concluded that source or contributing areas of flow to stream channels reach out to tap the subsurface flow system.

A number of studies have examined features of aquifer systems by determining streamlines or defining of source areas to streams. Simulations of stream flow or of shallow groundwater flow sub-systems on Long Island include studies by Harbaugh and Getzen (1977) and Prince et al (1988). Franke and Cohen (1972) considered rates of groundwater movement through different parts

of the aquifer system. They developed flow nets of both a generalized cross-section of the Island and a map view of East Meadow Brook. The study showed that residence times of 25 to 30 years are typical for water entering the shallow system compared with 800 years and 3000 years for water entering the Magothy and Lloyd aquifers, respectively. Buxton and others (1991) defined source areas of Long Island's aquifer system with a three-dimensional model and the particle tracking algorithm. They simulated minimum and maximum limiting case recharge areas in order to bracket actual recharge areas for different stress scenarios.

Winter (1976) analyzed flow nets of vertical sections derived from steady state numerical flow simulations that involved interactions between lakes and groundwater. The study demonstrated that movement of water from lakes to groundwater systems is prevented if the minimum head value along a continuous hydrologic divide encircling a lake is greater than lake-level head. Finally, Toth (1962) showed how a lens of highly permeable material embedded in an aquifer of less permeability causes flow in the aquifer to converge on the lens; the degree of flow convergence depends on the ellipticity of the lens and conductivity contrast between the lens and aquifer.

# GOVERNING EQUATIONS OF FLOW AND THEIR IMPLEMENTATION

## The LaPlacian System

A fundamental relation governing flow through porous media is based on the second-order partial differential Laplace equation used in potential theory:

$$(2) \qquad \frac{\partial^2 \Phi}{\partial x^2} + \frac{\partial^2 \Phi}{\partial y^2} + \frac{\partial^2 \Phi}{\partial z^2} = 0$$

In the above expression $\Phi$ is the fluid potential and is equal to g x h (gravity times hydraulic head). At the earths surface g is close to constant,$\Phi$ and h are correlated and, therefore, h can be used as a suitable potential. The solution of equation (2) is a function h(x,y,z) that describes the value of hydraulic head at every point in a three-dimensional flow domain that is homogeneous and isotropic. According to equation (2) the replenishment rate in a confined aquifer is equal to the outflow; there is no change in aquifer storage and piezometric heads do not change with time.

The description of flow in real aquifer systems is more complex due to the heterogeneity and anisotropy of the aquifer material, recharge and discharge along system boundaries, and aquifer storage characteristics that change with time. A linear partial differential equation that represents piezometric head in time and space for confined aquifers and that takes these complications into account is:

$$(3) \qquad \frac{\partial}{\partial x}\left(K_x \frac{\partial h}{\partial x}\right) + \frac{\partial}{\partial y}\left(K_y \frac{\partial h}{\partial y}\right) + \frac{\partial}{\partial z}\left(K_z \frac{\partial h}{\partial z}\right) = R + S_s \frac{\partial h}{\partial t}$$

where

$K_x$, $K_y$, $K_z$ are values of hydraulic conductivity along the x, y, and z coordinate axis;

h is potentiometric head;

R is the volumetric flux rate per unit volume and represents sources-sinks of water;

$S_s$ is specific storage of porous media; and

t is time.

The sink-source term can apply to points, lines, or be distributed over an area. In the generic system formulated in this study recharge is a distributed source of water. The streams of this system constitute line-sinks because they are gaining streams; groundwater discharges along stream channels as long as hydraulic heads exceed the altitude at a point on the stream.

The simulations of this study are assumed to be steady state for unconfined flow conditions. Hence, equation (3) is not strictly applicable because it characterizes confined flow conditions. ($S_s$ applies to water released from the aquifer under confinement). Also, under steady state there are no net changes in aquifer storage over time and therefore storage terms are not used.

**Relations Involving Unconfined Flow**

Because flow in the generic system is unconfined, the saturated thickness varies with the water table height. A difficulty exists inasmuch as the water table position is an outcome of the solution and yet its position is needed to define the

flow domain. In principle, the position of the water table in space can be computed by solving for equation (3) if the storage term is set to zero. In practice, however, the rigorous solution of this equation for unconfined flow leads to a complicated, non-linear expression. For example, Bear (1972) shows that unconfined and steady flow in three dimensions can be expressed by the following equation:

$$(4) \qquad K_x\left(\frac{\partial h}{\partial x}\right)^2+K_y\left(\frac{\partial h}{\partial y}\right)^2+K_z\left(\frac{\partial h}{\partial z}-\frac{K_z+R}{2K_z}\right)^2=K_z\left(\frac{K_z-R}{2K_z}\right)^2 ,$$

The terms used in the above equation have the same definitions as terms used in equation (3). The above expression is difficult to solve and is amenable only to a limited number of analytical solutions.

There have been less rigorous, more practical methods used to solve for flow under water-table conditions that involve solutions based on linearized boundary conditions or continuity equations describing unconfined flow; examples of approximate analytical solutions are the Dupuit-Forchheimer approximations or the Boussinesq Equation (see Bear, 1972, page. 361 for discussion). However, in order to apply these methods either specific flow conditions must be satisfied or particular boundary and initial conditions must be specified.

## Finite-Difference Formulation

In order to avoid these limitations a solution to the unconfined flow problem was sought using a computer flow model that solved by the method of finite-differences (see Modflow documentation for development of finite difference form of equation (3)). Because of the flexibility of the algorithm, the model can simulate many aquifer conditions and is especially effective in simulating water-table conditions through successive approximations. Also the sink and source boundary conditions required for unconfined flow problems are easily implemented and are easily modified.

## Stream Function

As mentioned earlier flow nets have been used effectively to represent flow patterns in vertical sections of aquifers. Flow nets are graphic representations of lines of equipotential and streamlines under steady-state conditions. In isotropic systems each family of lines is mutually perpendicular. Mathematically this relation is expressed by the Cauchy-Riemann equations for a two dimensional system:

$$(5) \quad \frac{\partial \Phi}{\partial x} = \frac{\partial \Psi}{\partial y}, \qquad \frac{\partial \Phi}{\partial y} = -\frac{\partial \Psi}{\partial x}$$

where,

$\Psi(x,y)$ is the stream function in x and y coordinate space and,

$\Phi(x,y)$ is the potential function in x and y.

The stream function describes flow patterns by a family of curves that are everywhere tangent to the velocity vector $\overleftarrow{q}$. The locus of points for which $\Psi(x,y)$

is constant is called a streamline. It follows that the stream function is also related to velocity components x and y by $q_x = -\frac{d\Psi}{dy}$ and $q_y = \frac{d\Psi}{dx}$.

According to Bear (1972, see p.224), the solution to equations that describe the geometry in three dimensions takes the form of two independent relationships: $\lambda = \lambda(x,y,z) = \text{const}$ and $\chi = \chi(x,y,z) = \text{const}$. These equations represent two families of surfaces whose intersections are streamlines. Along each streamline, both $\lambda$ and $\chi$ are constant. Streamlines are imbedded in these surfaces; these surfaces are referred to as stream surfaces. The functions $\chi$ and $\lambda$ are called stream functions of three-dimensional flow.

In principle the flow in a three-dimensional system can be characterized by stream surfaces. This is accomplished by interrelating the pair of constants $\chi$ and $\lambda$ to an arbitrary function such as a no-flow boundary surface. In practice, however, this is difficult to achieve in complicated flow systems involving multiple sinks and a distributed source. In such systems stream surfaces cannot be uniquely defined throughout the system.

## Particle Tracking Formulation

The geometric and quantitative flow characteristics of the three dimensional flow system are more conveniently represented by streamlines than by stream surfaces. In order to generate streamlines in three dimensional space, a particle tracking post-processor, Modpath (Pollack, 1989), was used for this study. The post-processor uses inter-cell velocities calculated from finite-difference model output. Modpath determines the path line that a particle of water follows from where it originates in the system to where it leaves. Modpath uses a semi-analytical method that assumes each directional velocity component to

vary linearly within a grid cell in its own coordinate direction (Pollack, 1988, 1989). Each simulated path line represents a discrete quantity of flow which, in turn, corresponds to a fraction of total model volumetric flow rate. Therefore, particle tracking simulations are found to be internally consistent with the way in which the finite-difference model calculates its flow solution.

**Simulation Artifact**

The finite-difference model and particle tracking processor can help establish flow patterns in complex, three-dimensional systems involving a variety of discharge outlets which would otherwise be difficult to do with an analytical solution. Yet, there are several limitations inherent to numerical approximation and specifically to flow solutions involving stream discharge.

Stream channel form and depositional characteristics that influence rates and distribution of groundwater seepage to channels are represented by a single 'lumped' parameter in flow simulations. This means that features such as channel geometry, bedding thickness, or other local features that affect discharge are not explicitly modeled.

For a finite-difference solution of a flow problem, recharge is distributed over the area of the top cells including the cells that are designated as sinks. Therefore, recharge and discharge to streams are combined for these cells to produce a net flow in or out of the top of the cell. When recharge is significantly greater than discharge the model calculates only a net downward flow from the water table over the entire cell surface. In a real system a component of flow

entering near the stream would flow directly to the stream whereas a component of flow just slightly farther away from the stream would travel deeper into the system. These local variations can not be differentiated in a numerical formulation within the cell.

There are also some limitations with respect to how the volumetric flow rate is estimated by the particle tracker. When flow paths are calculated from a model representation of a flow field in an aquifer system with the particle tracker, flow is estimated by a specified number of particles placed on top of the cells. An evenly-spaced array of particles is placed on the top surface where the algorithm uses the model's inter-cell velocities to determine the paths that the particles will take through the system to their final discharge points. Flow from a cell on the water table can be represented by any number of particles. The greater the number, the better the delineation of the flow issuing from a cell. Because particles are generally introduced into the system as evenly-spaced arrays, the relative spacing of the pathlines in the system serve to estimate flow rates, with closer spacing indicating higher volumetric flow and wider spacing indicating less flow. In many cases the absence of flow lines can represent slow or relatively stagnant zones of flow domains in the system. This situation would occur if there are a small number of particles positioned on the source area of a flow that passes through a low-velocity zone in the aquifer. Examples of such zones are near no-flow boundaries or in zones of diverging flow.

# HYPOTHETICAL COASTAL PLAIN AQUIFER SYSTEM

## Formulation of Primary Generic System

Figure 2 shows the basic features and labeling conventions used for the hypothetical aquifer system used in this study. The system is shaped like a simple, rectangular box and is deep enough to allow for the occurrence of both a regional and sub-stream flow systems. The box represents a homogeneous aquifer that is twelve-hundred feet deep and twelve miles in length. The system is designed to be wide enough to allow for the development of three separate stream sub-systems.

### *Grid design*

The aquifer system was divided into blocks 500 by 500 feet in plan view and was further divided into four layers 400 feet thick; the thickness of the uppermost layer depends on the final calculated position of the water table. This division of the aquifer system is somewhat arbitrary but the fine-scaled subdivision makes possible a detailed estimation of the flow patterns.

The orientation of the three coordinate directions x, y, and z are also shown in figure 2 and will be referred to in later discussions of velocity and vector components. The origin is located in the rear-left-top corner of the box. Model rows are parallel to the x-axis whereas model columns run parallel to the y-axis.

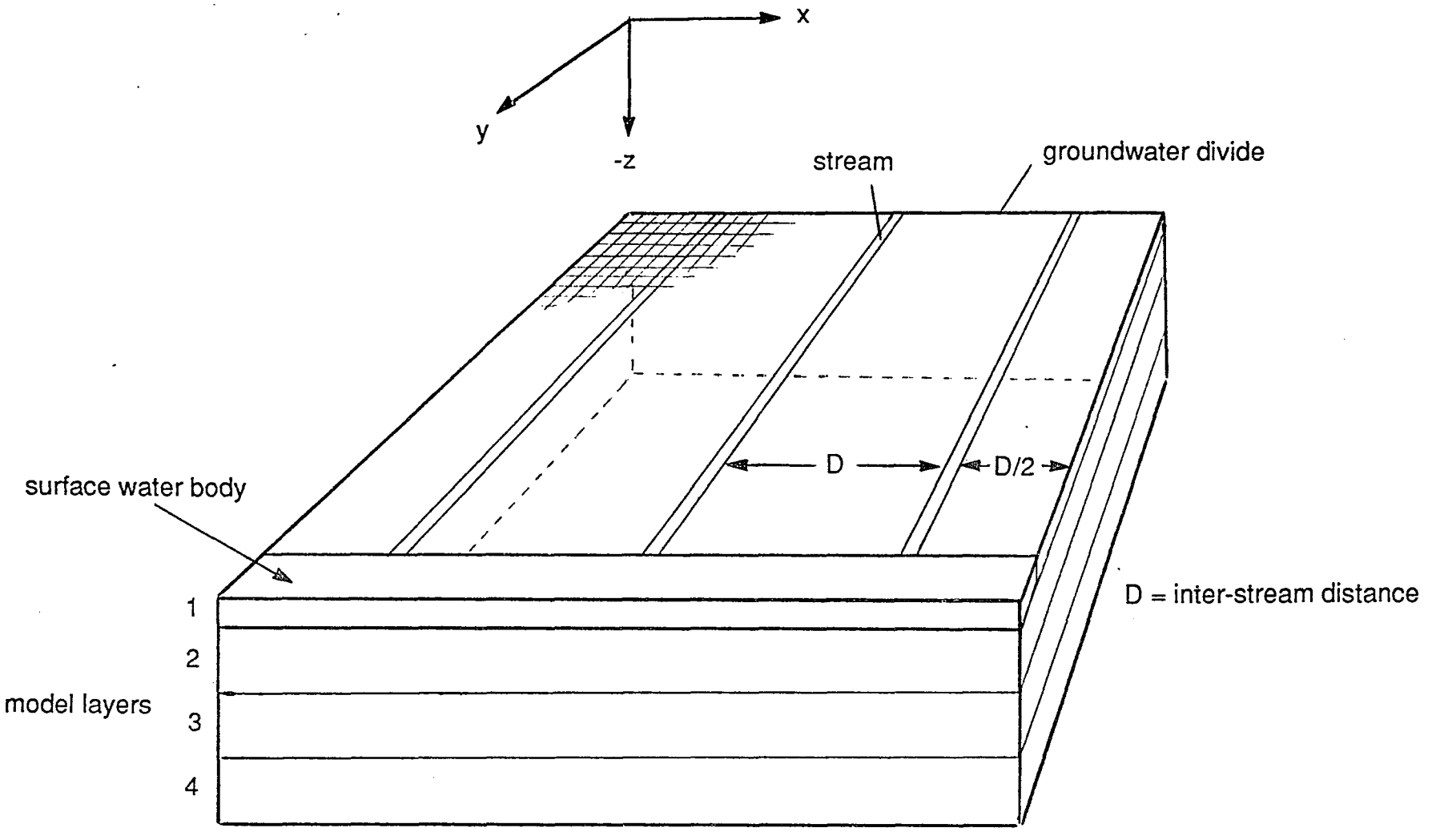


Figure 2--Geometric relations and Cartesian coordinate convention used for the hypothetical reference aquifer system.

*Boundary Conditions*

Except for the top surface, all surfaces of the modeled aquifer represent no-flow boundaries, that is, flow is tangential to these surfaces. The rear model face is assumed to coincide with the groundwater divide. The bottom face of the model represents the top of a relatively impermeable material such as bedrock or a massive confining unit. The lateral extents of the modeled aquifer represent hydraulic surfaces. It is assumed that there are other watersheds adjacent to this system and that each lateral surface is a common surface to identical watershed systems.

Figure 2 also shows an area spanning the width of the top layer at the front of the system. This area represents a surface water body such as a relatively large lake or sea outlet. The water body is simulated by setting the head values of nodes on the top layer within this area to zero. This surface water body functions as a general, regional sink that draws recharge not caught in the stream's sub-system flow and creates an additional discharge outlet that, in turn, generates a regional gradient. In a real world system a competing discharge outlet for groundwater flow could be the sea, a large lake, or even a remotely located stream sub-system.

*Stream system*

The streams of the hypothetical reference system are shown in figure 2 as three columns of nodes that trend from the divide to the edge of the surface water body. The hydraulic behavior between stream and aquifer is simulated as

a head-dependent flux condition; as long as heads in the aquifer are greater than the elevation of the streambed at any point on the stream, groundwater is discharged from the aquifer in proportion to the difference between the aquifer head and stream bed elevation at that point. Otherwise, discharge does not occur. This behavior is characteristic of a gaining stream.

The finite-difference model used for this study can simulate a number of different head-dependent leakage conditions. The drain package (see Modflow documentation, McDonald and Harbaugh, 1988) was used to simulate the stream system. This simulation is accomplished by designating nodes along three columns, arranged as illustrated in figure 2, as model drains. The elevations of a sequence of nodes in a column are set at elevations that increase by constant increments. For this reference system the stream channel is designed with a simple, constant slope, although in actuality, stream channels are characteristically concave (see section on stream channel slope). The slope that the stream channels make with the horizontal is typical of stream channel slopes occurring in coastal plain drainage basins.

For the hypothetical systems of this study streams are parallel and equi-distant. The distance between the outer two streams and the lateral boundary of the system is half the inter-stream distance, the distances measured between nodes. Because the simulated stream channel is allowed to extend up to the divide, the water-table position is generally below the streambed elevation near the divide area. At some point downstream from the divide the water table intersects the stream channel; at this point groundwater begins to seep into the

channel. This point will be referred to as the location of start-of-flow and, for this and other simulations, its location along the stream channel depends on the solution.

Groundwater discharging to streams converges along their channels. In real systems the discharge is resisted by streambed sediment and underlying aquifer material. The resistivity of stream bed sediment, its thickness, the stream channel profile, and vertical hydraulic properties of the aquifer influence seepage rates to the stream. However, in a finite-difference approximation, these features can only be represented simply as a lumped parameter called stream-bed conductance. Additionally, the scale of grid discretization will affect the conductance value used. The conductance parameter is a coefficient of proportionality that relates stream discharge to head difference according to the relation:

$$Q = C(h_{aquifer} - h_{stream})$$

where,

Q is the stream discharge;

C is the coefficient of proportionality;

h is the hydraulic head;

Because of this relation, the effects resulting from stream bed characteristics, the hydraulic properties of the aquifer, and model grid size cannot be individually established. For the reference simulation, a value of 5000 $ft^2$/day was chosen for all drains. This value was arbitrarily increased from a lower value that was

initially established from grid cell dimensions and aquifer vertical conductivity values.

*Stress*

Recharge is assumed to be constant and uniformly distributed over the modeled surface. A recharge rate of 0.00548 feet per day was used for the reference simulation. This rate is equivalent to about 24 inches per year of recharge, a value which is typical of the Northeastern Atlantic Coastal Plain where about half of the precipitation actually infiltrates down to the water table. The remainder of the precipitation is consumed by evapotranspiration, is intercepted by vegetation, or flows over the land surface directly into streams or open water bodies; the latter flow component can become significant during sustained, intense precipitation events where rainfall rates exceed soil infiltration capacity.

*Aquifer conductivity*

A horizontal conductivity value of 100 feet per day was used to represent the aquifer's water transmitting properties. Generally, this is a common value for medium to coarse unconsolidated sands. The aquifer is considered to be everywhere homogeneous in order to simplify the flow problem. An anisotropy of about 33:1 was used to represent a moderate degree of compaction of aquifer material. The effects of anisotropy on flow will be considered in a later section.

## Characteristics of the flow system

### *System symmetry*

Figure 3 shows the contributing areas of flow for each of the three streams in the reference flow system. The contributing areas and model output for flow in the stream system show that stream system flow is apportioned in a bilaterally symmetrical distribution with respect to a vertical plane along the center stream channel; this means that the center stream has the only truly symmetric flow configuration with respect to its stream channel whereas the left- and right-handed streams are slightly asymmetric with respect to their channels and are mirror images of each other.

The bilateral symmetry of the system is a model discretization effect. Because the model uses a block-centered finite-difference approach, the model boundary is at the edge of the grid even though the node is located 250 feet to the interior of the cell. In the case of the center stream, the interstream divide is located along a column of nodes that is common to the center and lateral streams; the model blocks that function as interstream divide contribute their recharge to both streams. However, along the edges of the grid, the entire recharge on the block flows to the left- and right-stream channels. Consequently, the left and right streams receive more flow than does the center stream causing a slight asymmetry in the contributing areas of the left and right streams.

Each of the model columns running through the left-handed stream system has a unique water-table profile. The profiles are repeated entirely in the

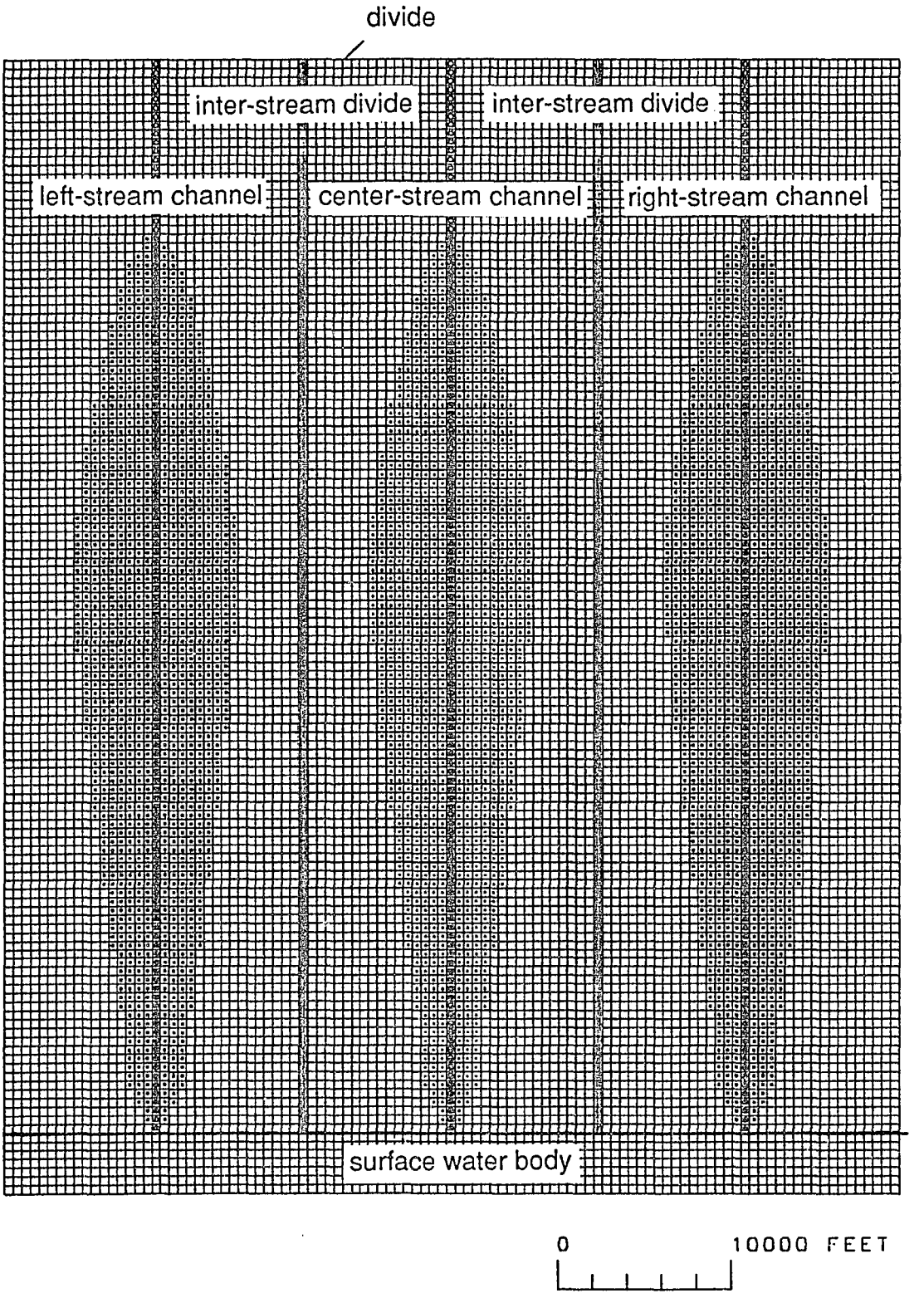


Figure 3--Map view of discretized hypothetical system showing bilateral symmetry of stream source areas.

right-handed stream system but in reverse order. Because of the symmetry of the center stream system, water-table profiles along its channel and either one of its inter-stream divides are end-members of a set of unique profiles which is repeated on either side of the stream. Because the solution to the flow problem is discrete, there are a finite number of water-table profiles that run parallel to the model's y-axis that are the same as the number of columns in the model. Flow patterns in the system are unique in half the aquifer.

As a matter of convenience the center stream will provide the basis for analysis in this study. It is used to represent basic stream sub-system flow characteristics for each flow simulation. Although there are small differences in water-table position, base-flow characteristics, and geometry between the middle and lateral streams, these differences are due to discretization effects and were not significant enough to justify separate analysis of these latter stream systems.

*Head and discharge profiles*

Figure 4a shows the simulated head profiles along the center stream channel and along an inter-stream divide. The streambed profile, from divide to its terminus, is also shown. (A map view of these profile traces is shown in figure 3.) An inspection of the head profiles shows that both are similar from divide to start-of-flow, but the inter-stream head profile is higher from the start-of-flow to the boundary of the water body. The differences in head between the two profiles suggest that there is a lateral component of flow (in the x-coordinate direction) between the inter-stream divide and stream channel which begins just

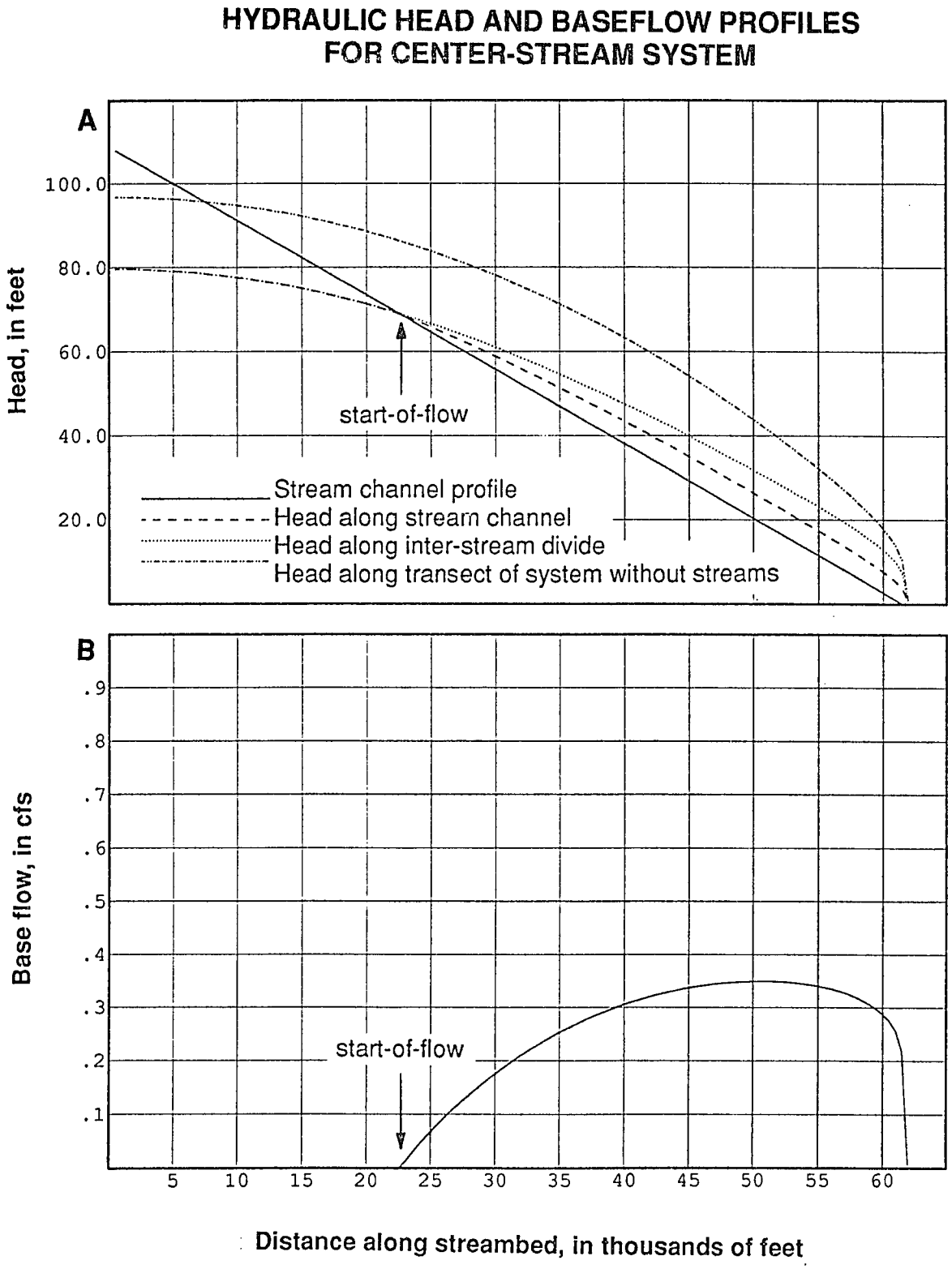


Figure 4a--Profiles of water table along stream channel and inter-stream divide for the reference simulation and typical profile for non-drainage simulation.

Figure 4b--Profile of groundwater discharge to center-stream channel (along model column 52) for reference simulation.

downstream of the start-of-flow and increases in proportion to head differences. However, because other components of flow are involved within this area, the relation is more complex.

Figure 4b shows discharge to each point on the center streambed (note that discharges to the stream as shown in figure 4b are not cumulative but represent discharge values for individual nodes along the streambed). The discharge profile is related to the head and streambed profiles of 4a. Start-of-flow occurs at the point where head and stream channel profiles intersect. Where heads are below the stream channel elevation, as they are upstream of the start-of-flow, discharge cannot take place. From the start-of-flow to the end of the channel the head profile is parabolic and everywhere above the streambed. The profiles of discharge rates along the stream channel are similarly parabolic. The maximum difference between streambed altitude and aquifer head corresponds to the maximum volumetric discharge rate into the stream channel. This indicates that stream discharge is proportional to head difference which is simply the application of Darcy's Law. The non-linear, parabolic shape of the water table is commuted to a non-linear, parabolic discharge pattern along the stream. (It should be noted that base flow to the left- and right-handed streams is slightly higher than that of the center stream owing to the discretization effects discussed previously. This follows from the higher head profiles that occur in these stream sub-systems.)

Because base flow varies parabolically in the simulated system, groundwater is drawn from the aquifer to the stream in a uniform but varying

quantity along the entire reach of stream. The aquifer response to this varying discharge should, therefore, be reflected in its flow patterns. Each simulated flow line of a finite-difference solution represents a discrete fraction of total recharge entering the system. When groundwater is discharged from the simulated system in a parabolic distribution along the stream channel, the number of flow lines representing this discharge must also vary parabolically; the peak base-flow value estimated for those cells that simulate streams should correspond to the greatest number of streamlines that terminate at these cells on the stream. In this way the flow patterns are a geometric expression of the parabolic form of the flow equation. The relation between the distribution of recharge within the stream source area and specific points of discharge on a stream will be evaluated in another section.

*Jacob's model of vertical accretion*

The concept of unconfined flow and vertical accretion, developed by Jacob (1943) for an infinite strip of aquifer that is recharged at a constant rate, is relevant to the flow system used in this study. In Jacob's steady-state model groundwater mounds along the axis of symmetry of an infinitely long island strip and develops an equilibrium configuration that is maintained by the dynamics of recharge to the aquifer and discharge to the adjacent water body. The system is considered to be sufficiently thick so that changes in water table position have negligible effects on the saturated thickness of the aquifer. Therefore, a transmissivity term is used in his analysis. In the adjacent water body on either

side of the strip constant heads are assumed to be zero. Because of the symmetry of an island-aquifer system, a section between the hydrologic divide, the highest position of the mound, and one border completely characterizes flow in the system. The water table is characterized by a parabolic profile that increases in slope from the divide to the shore. The distribution of head in the water-table profile is, to some measure, a function of the degree to which the system can resist groundwater discharge.

The generic system of this study can be thought of as a rectangular zone of an elongate island between its divide and shore but, unlike Jacob's model, has a system of parallel streams that act as line sinks for groundwater in the aquifer. The stream system dissipates much of the head in the aquifer and locally reduces the water-table gradient from what it would be had the stream sub-system not been in place.

Figure 4a shows the position of the water table that results from running the reference model without simulating the effects of streams (dash-dotted lines). The simulated system is comparable to Jacob's model except that in Jacob's model the shoreline constant-head boundary completely penetrates the aquifer system. Because there is no lateral component of flow for this simulation, a cross section of unit width would completely characterize its flow. By comparing head profiles of the system without streams to that of the original reference system (from hereon referred to as 'non-drainage' system and 'drainage' system respectively) it is evident that the 'non-drainage' system heads are much higher everywhere in the system than heads for the 'drainage' system

and that 'drainage' system heads are significantly lower even at the inter-stream and divide areas, which are farthest from the streams. It is apparent that the stream sub-system significantly modifies heads and the flow regime of the aquifer system and generates additional components of flow.

*Velocity-vector representation of the flow system*

An understanding of the flow dynamics of an aquifer system is enhanced by determining the distribution of relatively slow and fast zones of groundwater movement. One method of characterizing variation in water-movement rates throughout the 'non-drainage' and 'drainage' systems is by generating a vector representation of specific discharges or Darcy velocities. The Darcy velocity (from hereon referred to simply as *v*) is derived from dividing model cell volumetric flow rates along a given coordinate direction by the orthogonal inter-cell area. Figure 5a shows *v* vectors in a section of the 'non-drainage' system. The velocity field is predominantly horizontal (in the y-direction) for each of the four model layers with a small vertical or z-direction component (vertical exaggeration is 10X in figure 5). Because there is no lateral flow component (x-direction) for this system flow direction and magnitude are completely represented in section.

Figure 5a shows that the y-component of *v* increases with proximity to the surface water body. This increase corresponds to the increase in slope of the water table with proximity to the surface water body. The vertical flow

A

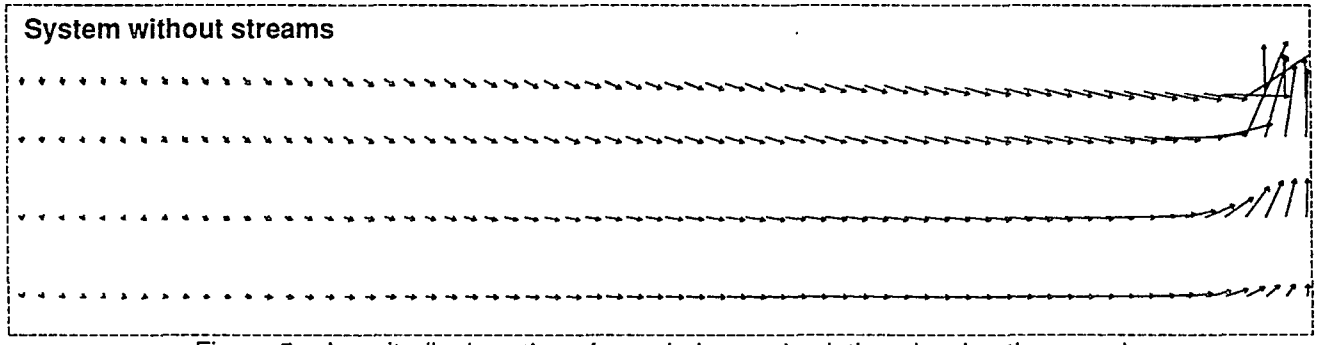


Figure 5a--Longitudinal section of non-drainage simulation showing the y- and z-coordinate components of velocity vectors.

B

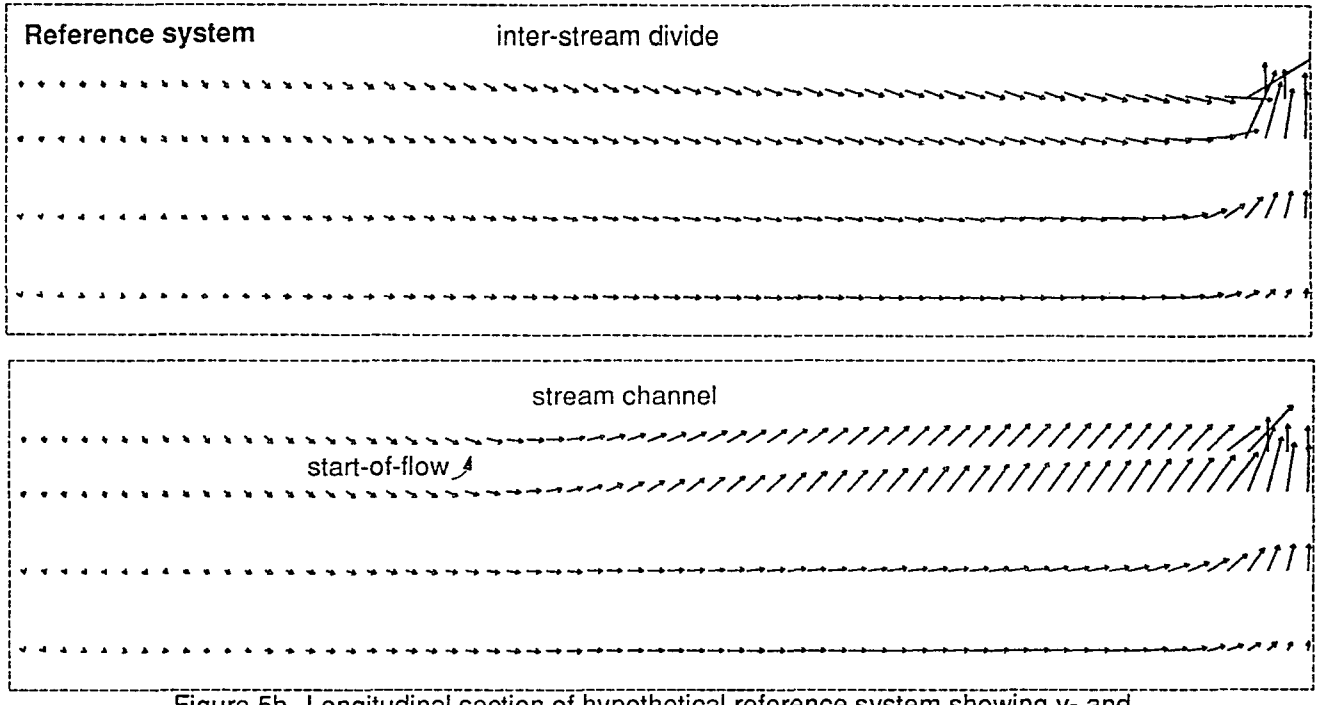


Figure 5b--Longitudinal section of hypothetical reference system showing y- and z-coordinate components of velocity vectors along the center stream channel and along the inter-stream divide.

V. E. is 10X

component diminishes in magnitude with depth. There is also a directional change from slightly down to up with proximity to the water body. The vertical component of flow near the divide area is the dominant flow component only because of diminished horizontal flow.

Flow in the 'drainage' system is three-dimensional and requires three mutually perpendicular views in order to completely characterize the velocity field. Figure 5b shows the y-z-vector components along the inter-stream and stream channel columns. The vector distribution in the inter-stream column is similar to that shown in 5a; there is, however, a smaller flow component in the y-direction and a slight increase in its vertical flow component.

Vectors along the stream channel boundary show the greatest vertical magnitudes downstream from the start-of-flow. The vertical *v* component is in the down direction (-z ) between the divide and the start-of-flow but in the up direction (+z) between the start-of-flow and the stream terminus where flow magnitude increases significantly. There is a similar pattern in the deeper part of the system but at lesser magnitudes with increasing depth as shown by shorter vector lengths. Sections represented in figure 5b correspond to sections in which head profiles are shown in figure 4.

Figure 6a shows a plan view of the vector field (x-y-components) for the top layer of part of the center stream system; the area is bounded at the sides by the inter-stream divides. The vector orientations are distributed symmetrically with respect to the stream channel and show a converging pattern about the stream. In general, vectors show an increasingly stronger lateral component of

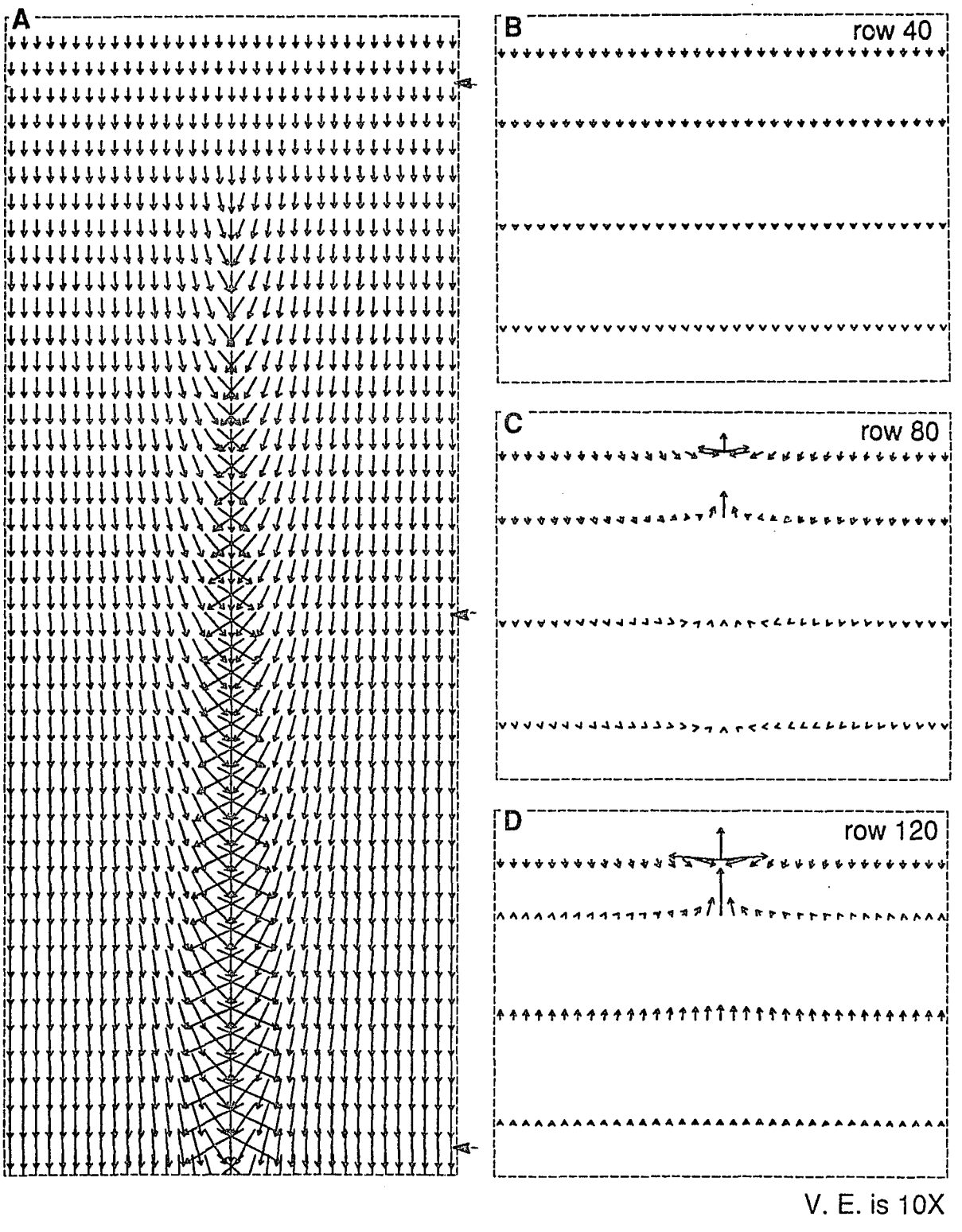


Figure 6--Map view showing x- and y-coordinate components of velocity vectors in model layer 1 for the central portion of the reference system (A) and three transects showing x- and z-coordinate components of velocity vector (B, C, and D).

velocity with proximity to the stream and in the downstream direction. Also, the magnitude of y-component of *v* increases near the surface water body.

Figures 6b through 6d illustrate the x-z-components of *v* for the center stream system at three sections oriented perpendicular to the stream channel. Figure 6b is a section located upstream from the start-of-flow. For all layers, the direction of flow is downward although the magnitude becomes negligible with depth. Section 6c is located 13,000 feet down from the start-of-flow. Vectors indicate that stronger lateral *v* occurs near the stream channel. The vectors reverse from the down direction near the inter-stream divide the to up direction in the stream channel. The vector pattern for lower model layers reflects stream influence as vectors point upward just under the stream channel. However, the magnitudes become progressively diminished with increased depth. Figure 6d is located about 7000 feet from the surface water body and shows a vector pattern similar to that shown in 6c. The lower layers reflect a stronger influence from the stream system.

*Energy distribution in the system*

The position of the water-table can be thought of as an indication of the level of potential energy in the system. Inasmuch as the water-table position is a measure of elevation head, it is a measure of potential. The potential is also used in the Bernoulli Equation for problems in fluid mechanics to express energy loss during fluid flow and is defined by the following equation:

(6) $\Phi = gz + \frac{v^2}{2} + \int_{p_0}^{p} \frac{dp}{\rho}$ where,

z is the elevation
g is the force to gravity
v is the velocity of the fluid;
ρ is the fluid density
p is the fluid pressure
$p_0$ is atmospheric pressure

The above expression (6) for potential reduces to $\Phi = g \bullet z$ at the water table because the velocity component of $\Phi$ is negligible in porous-media flow and the pressure is a constant at atmospheric so that fluid density does not depend on pressure; hence the last two terms go to zero.

As discussed earlier, the water table in the 'drainage' system is everywhere lower than that of the 'non-drainage' system. The lowering results from loss of groundwater through the drainage network. The stream system provides additional outlets through which groundwater can discharge. In effect, the energy of the drainage system is greatly dissipated along, and adjacent to, the sinks in the system.

Both the 'non-drainage' and 'drainage' systems were simulated using an identical rate of recharge applied over the modeled area. Because inflow in both systems is the same, their outflow must also be equivalent; water mass is conserved in both systems. If the water-table levels of the 'drainage' system were subtracted from those of the 'non-drainage' system, the resulting head residuals would represent a pattern of dissipated energy and would show how streams in the 'drainage' system reduce the energy level from the levels shown

in the 'non-drainage' system. The residuals would also show the redirection of outflow and change in flow components relative to the 'non-drainage' system.

Figure 7 shows the residuals of heads resulting from subtracting the heads in the top layer of the 'drainage' system from those of the 'non-drainage' model. The highest residuals and, thus, the highest dissipation of energy occurs in a teardrop-shaped area centered over the streams. This does not mean, however, that the highest discharges occur along these reaches but, rather, that the water table is most significantly lowered in this area of the system (see also figure 4). Moderately high residuals cover a broad area in the upper two-thirds of the aquifer. In general, residuals decrease gradually with proximity to the surface water body; and consistently higher residuals are seen along the lower reaches of the streams.

*Relations between water table and specific discharge*

In this section, the relation between water table and Darcy-velocity profiles are evaluated along each coordinate direction for the 'drainage' and 'non-drainage' systems. (The discharges discussed in this section involve inter-cell volumetric flow rates and not discharges to sinks.) Figures 8 and 9 show corresponding water table, *v*, and head-gradient profiles (node-by-node change in head value along a coordinate direction) for various sections through the modeled system. The *v* profiles for the indicated direction closely match the head gradient profiles that are predicted by Darcy's Law. The figures show water-table profiles in the top panel, and the corresponding head gradients and *v*

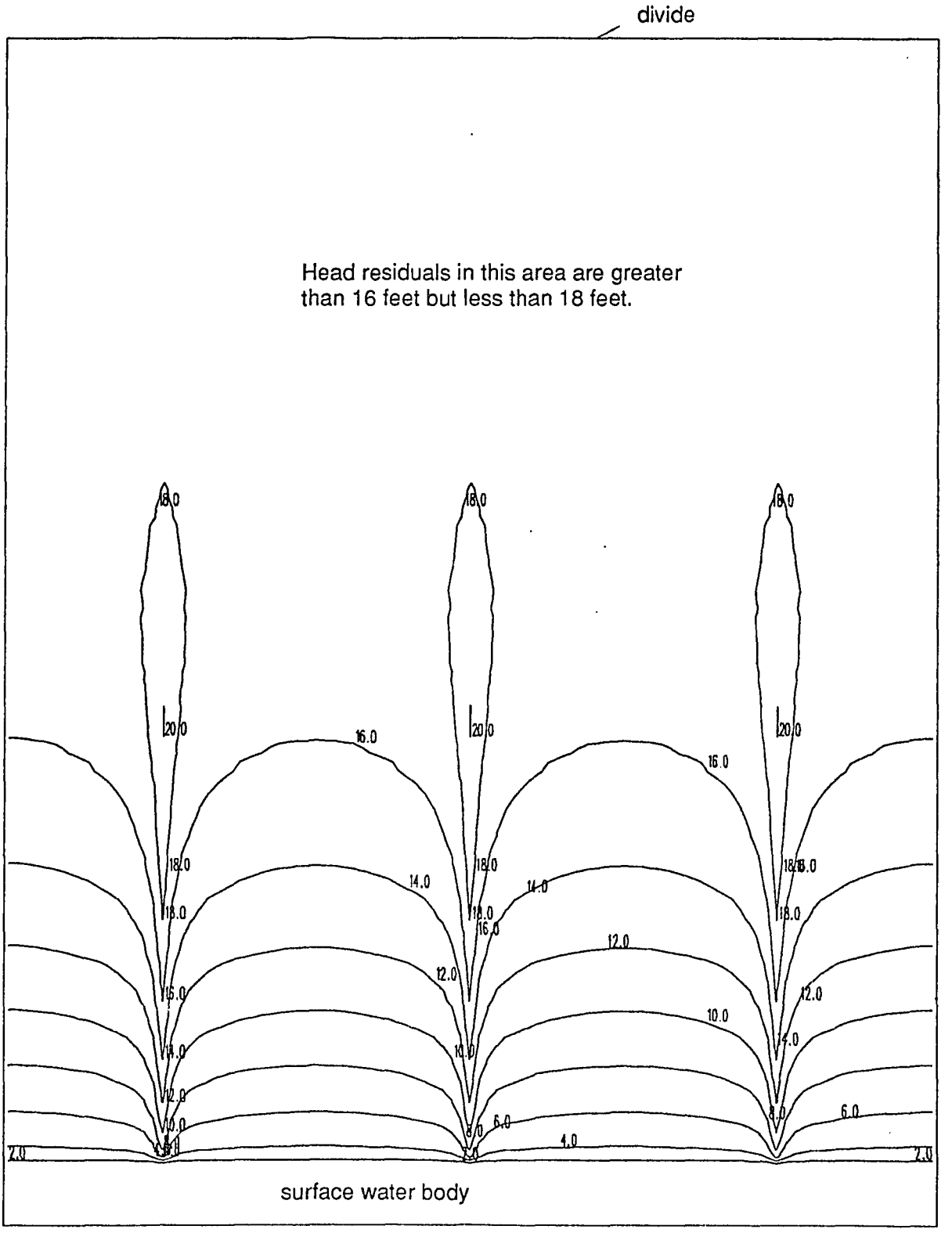


Figure 7--Head residuals resulting from difference in free surfaces between reference and non-drainage simulations. Contour intervals are 2 feet.

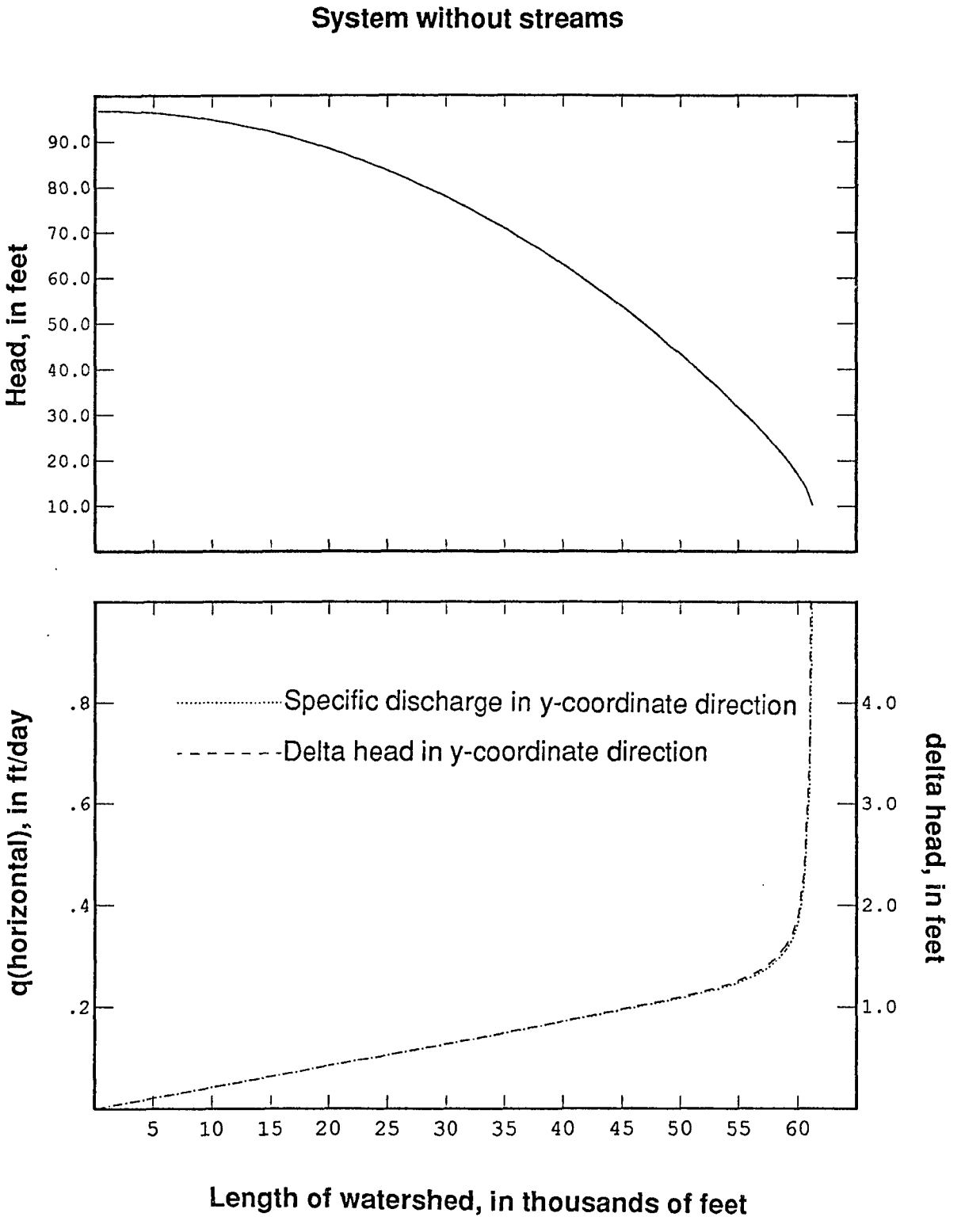


Figure 8--Profiles of water-table head, head gradient, and specific discharge along column of non-drainage simulation.

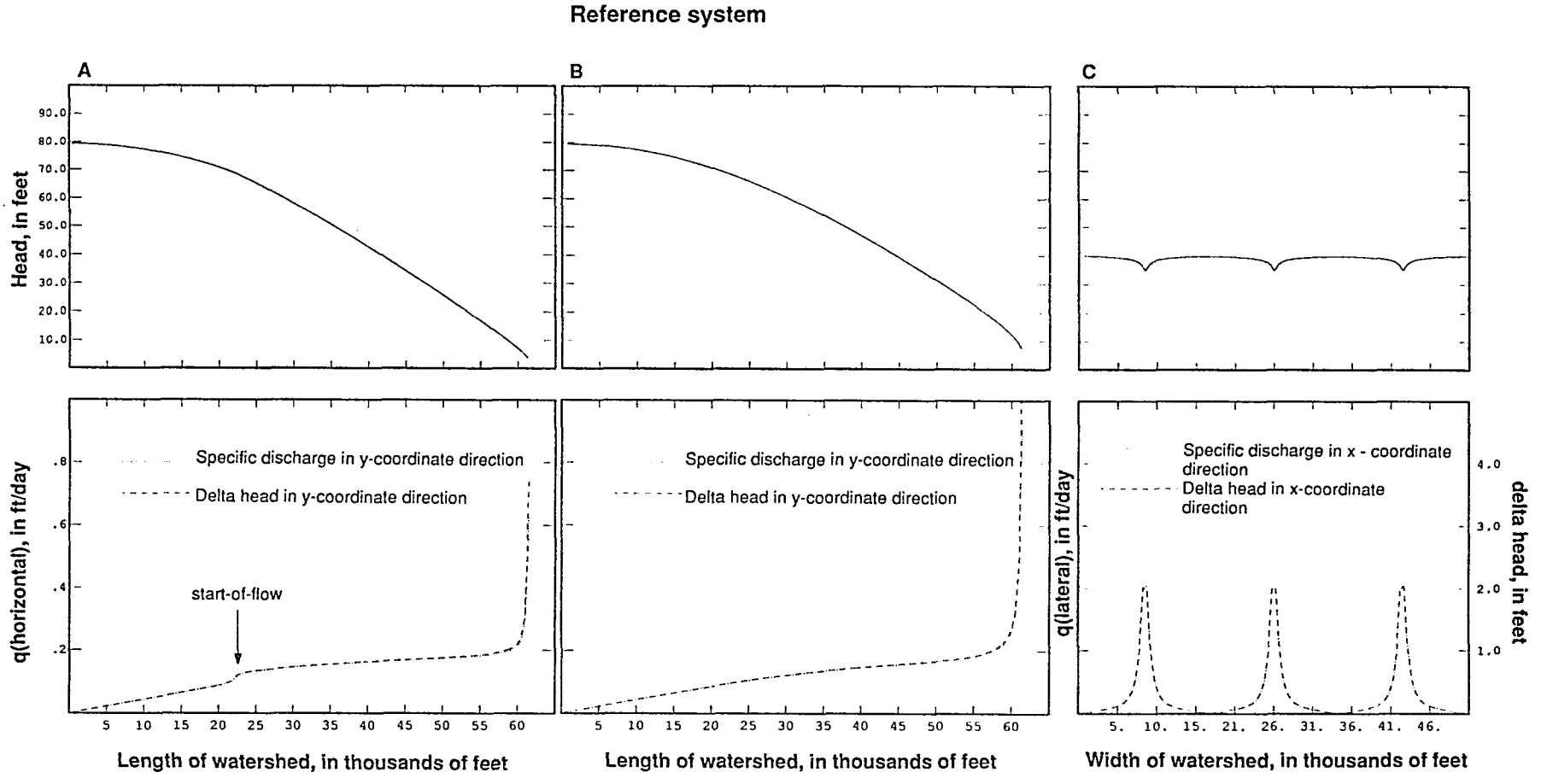


Figure 9--Profiles of water-table head, head gradient, and specific discharge for the reference simulation along A) center stream channel (column 52), B) inter-stream divide (column 35 or 69) and, C) across the system along model row 90.

in the lower panels. The sections illustrated in 8 are sections of the 'non-drainage' system; 9a, a section along the center stream channel; 9b, a section along the inter-stream divide and, 9c, a section of the 'drainage' system perpendicular to the streams along row 90.

The profile of the y-components of *v* shown in figure 8 (from divide to water body) increases at an increasing rate and is characterized by a hyperbolic shape; the profile bears an inverse relation to the parabolic form of the water table which decreases at an increasing rate. The profiles also demonstrate the geometric properties implicit in the mathematical expressions of unconfined flow. A comparison of 8 to 9a and 9b shows that the head gradients in the 'non-drainage' system are steeper and result in higher *v* in the y-direction then for those of the 'drainage' system. (The profiles for left- and right- handed streams, not shown, are slightly but not significantly higher than that of the center stream.)

The profiles of figure 9c follow transects along row 90 and show *v* components in the x-coordinate direction along with the corresponding head and gradient profiles. The *v* in the x direction increases sharply with proximity to the stream channels, the center stream receiving a little less discharge than the other two. The slight depression in the head profile across the watershed can be seen in figure 9c. The highest head value located on either edge of this profile, 40 feet, is significantly less then the head value at the same location in the 'non-drainage' system (which is 60 feet).

Figure 10a compares the *v* profiles in the y direction for both the 'non-drainage' and 'drainage' systems. The 'non-drainage' *v* profile is shown as a solid line and has the higher profile of the two systems; initially it increases at an almost constant rate then increases at an increasing rate as it approaches the stream terminus. The *v* approach high values close to the surface water boundary. This is due, in part, to proximity to the water body that, in this system, functions as a major sink and exerts a strong influence on the flow field along its boundary. In a real-world system head profiles would generally not be nearly as steep here because shore areas would function as a broad, low-angle seepage face and would effectively dissipate the head near the mouth of a stream.

The stream channel and inter-stream *v* profiles for the 'drainage' system shown in figure 10 are shown as solid and dotted lines respectively. The inter-stream profile coincides with that of the 'non-drainage' system near the divide but, farther away, it increases at a decreasing rate. At the zone adjacent to the surface water body discharge increases rapidly. The *v* profile of the stream channel also coincides with that of the 'non-drainage' system near the divide but increases abruptly at the start-of-flow and then increases at a decreasing rate. Finally, the profile crosses below the level of inter-stream profile and quickly rises to a high value at the boundary.

The relatively flatter discharge profiles from the start-of-flow forward indicate that there is lower energy in terms of less specific discharge in the y-direction than there is for the 'non-drainage' system. The sudden profile

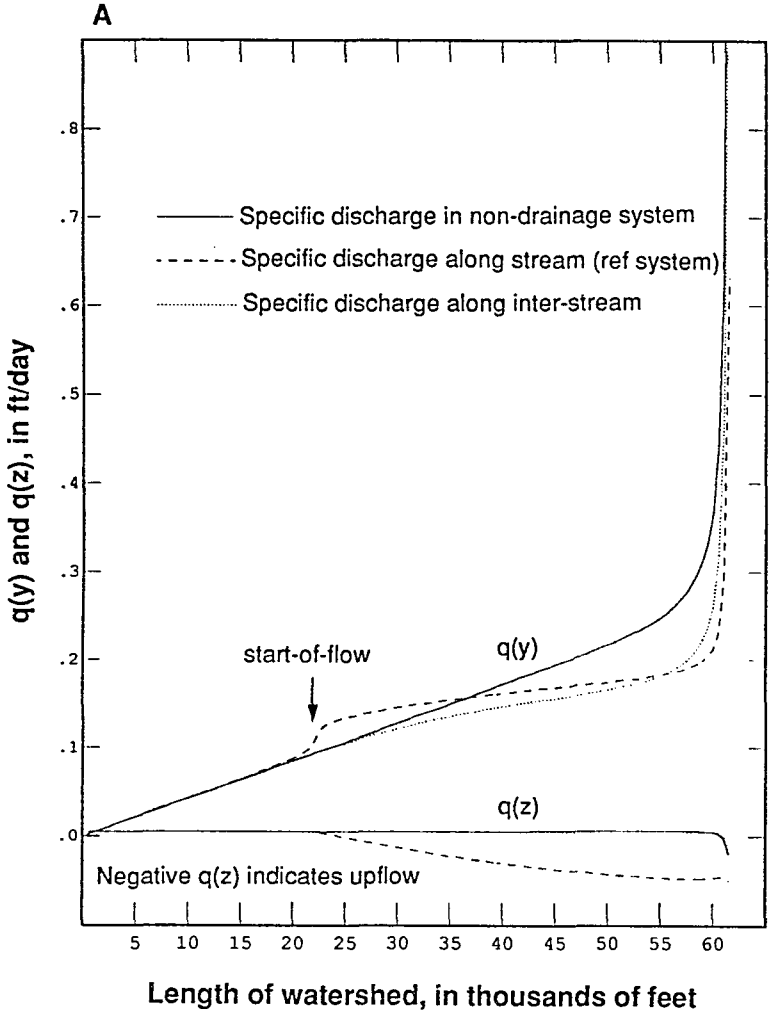


Figure 10a--Profiles of y- and z-coordinate components of specific discharge for non-drainage and reference systems.

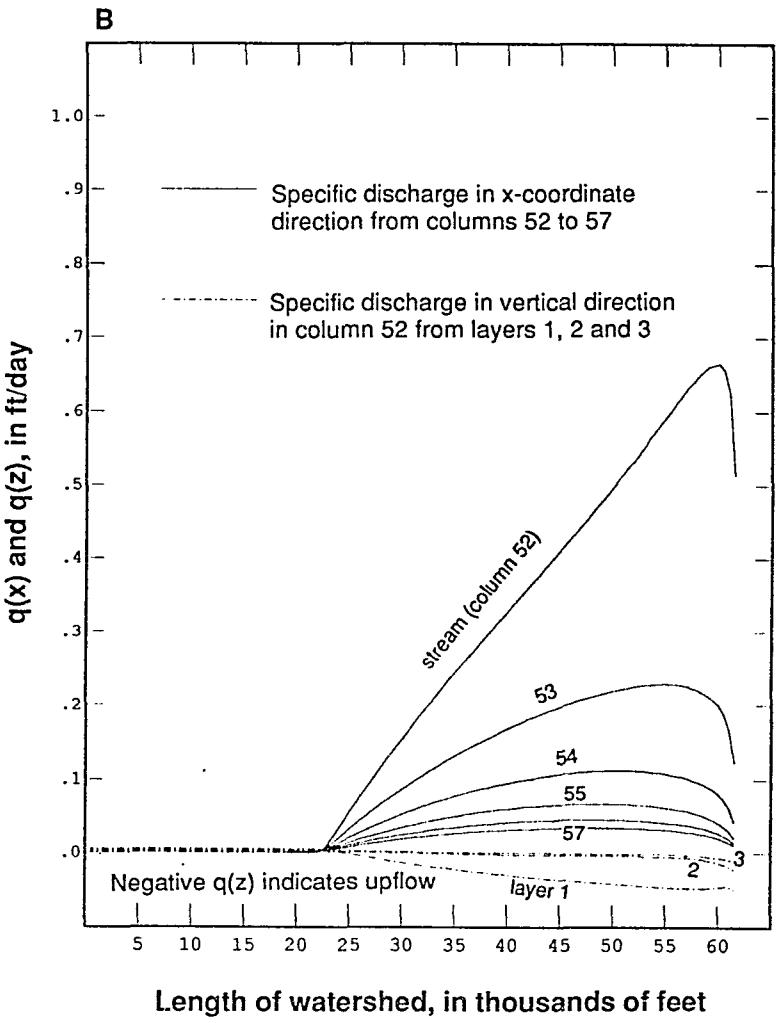


Figure10b--Profiles of x-coordinate component of specific discharge along columns adjacent to the center stream channel at increasing distances away.

increase at the point where start-of-flow occurs on the channel indicates that the flow gradient is locally steepened.

The *v* profiles of vertical-discharge component are negligible compared to profiles of *v* in the y direction. The profile in the 'non-drainage' system is also negligible. In the 'drainage' system the inter-stream specific discharge profile indicates a downward flow direction that is slightly greater than for that of the 'non-drainage' system. Under the stream channel, vertical specific discharge increases abruptly upward at the start-of-flow as would be expected (negative values signify upward flow direction). The marked change in specific discharge occurs only in or very close to the stream channel; however, vertical flow along columns between the inter-stream divide and the stream channel are not significant and decrease rapidly with distance from the channel.

The *v* component in the x-coordinate direction close to the stream is clearly a dominant component of flow in the drainage system. Figure 10b shows the x-direction component of *v* in the top model layer for lateral flow to streambed cells and for five additional profiles for columns of cells adjacent to the stream channel. The profile of lateral *v* into the stream column shows relatively large increases from the start-of-flow almost to the terminus. In contrast, the profile of lateral *v* for the inter-stream is almost negligible. Each of the five profiles adjacent to the stream channel show a substantial decrease of lateral *v* with increased distance from the modeled stream channel. The suite of profiles have the form of parabolic curves that become progressively flatter; each profile is spaced at 500 foot increments from the channel. Figure 10b also shows

a similar pattern of profile flattening with depth. The dotted lines indicate lateral *v* profiles at progressively lower model layers directly underneath the stream channel.

The profiles show that lateral *v* is most significant very close to the stream and in the shallow part of the system. Viewed in terms of energy, most lateral *v* and, hence, the greatest energy dissipation is concentrated adjacent to the stream which, for this system, is only a few hundred feet. This observation is consistent with what is shown by previous vector representations and head residuals.

*Stream sub-system bounding surface*

Because the source area to streams on the water table delimits part of the stream system, its description is included here as part of the characterization of stream sub-system bounding surfaces. The stream sub-system flow creates a broad, V-shaped depression on the overlying water table directly over the channel (see also figure 32). Although streams can depress the position of the water table over large areas of watershed, the depression is most prominent adjacent to the stream. Figure 11 shows a map of the water table and the outline of the contributing area of stream flow. As discussed previously, the unconfined surface perpendicular to the main surface-water body has a parabolic form that is shown by lines of equal head; the decreasing spaces between equipotential lines from the divide to the surface water body represent the increasing slope along the water table's profile. Most equipotential lines form a V-shaped pattern

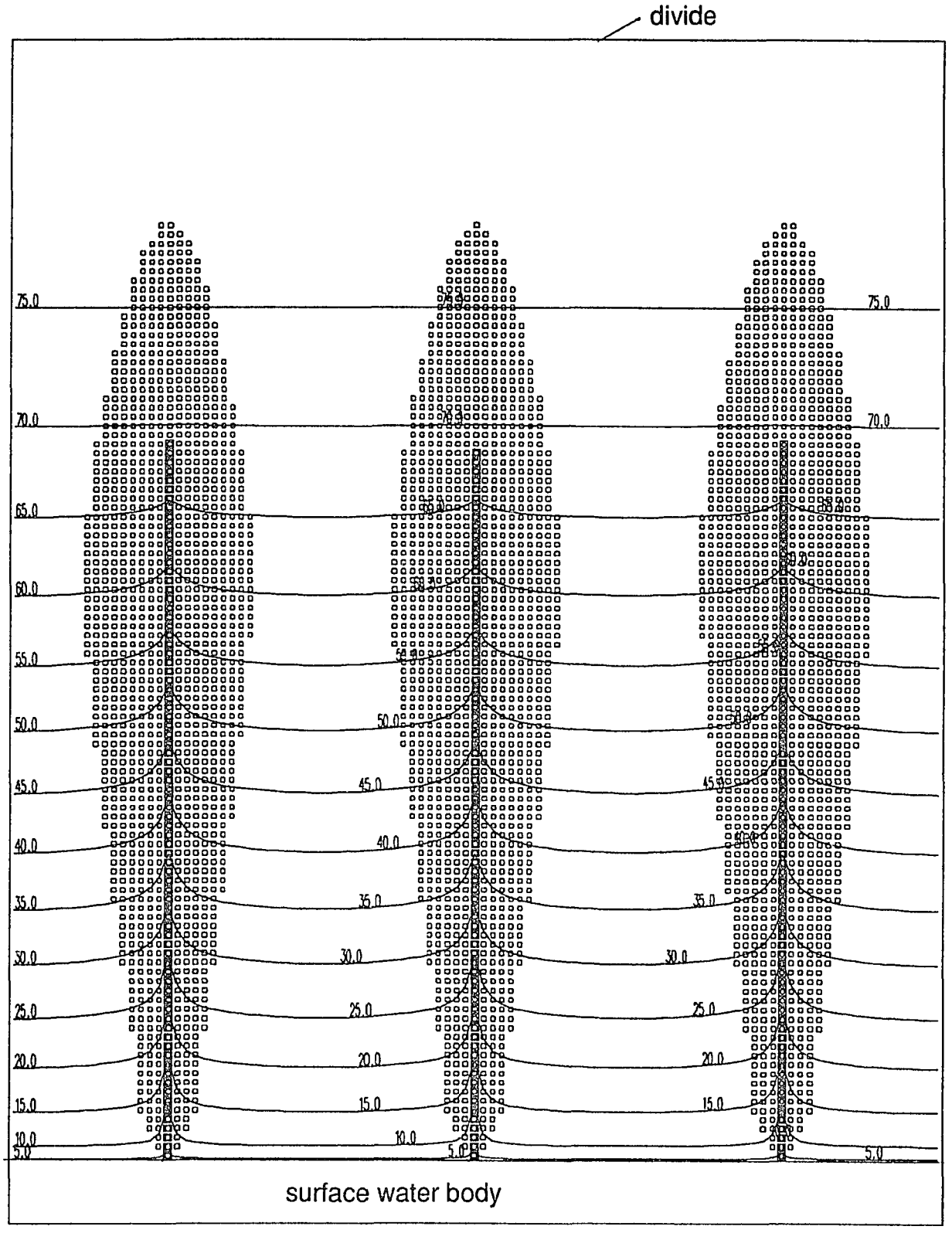


Figure 11-- Map view showing lines of equal elevation head and the source areas of streams on the free surface for the reference simulation. Squares along stream channels indicate where groundwater discharge occurs. Octagons indicate that model cell is at least partially a source for stream discharge.

as they cross the stream channel. In areas near the divide where the elevation of the stream channel is higher than that of the free surface, equipotential lines cross the channel without deflecting. The degree of deflection of an equipotential line at the stream channel is an indication of the depth to which the water table is depressed over the stream, and the stronger the deflection, the stronger the discharge. The depression varies from slight (on the third contour from the top) to relatively deep (fourth up from the terminus), then becomes less pronounced near the end of the stream.

Whereas the top surface of the stream sub-system can be considered a hydraulic surface, the bounding surface of the stream sub-system beneath the water table is a conceptual surface or zone inasmuch as it serves to distinguish flow that discharges to a stream channel from flow that discharges to the surface water body. This surface can also be thought of as an envelope containing all flow that originates within the stream's source area on the water table and that terminates along the stream channels. Generally, this surface is an interface zone between adjacent flow sub-systems that distinguishes flow of one sink's source area from flow that originates in other adjacent source areas. Flow emanating from other source areas discharge to other outlets. These outlets may be any other type of sink including other stream systems. This bounding surface defines a volumetric flow zone within the aquifer. As is discussed further below, this surface does not necessarily correspond to a hydraulic surface such as a stream surface as defined by Bear (1972, p.226) or to an equipotential surface.

The relationship between the position of stream lines that mark the limiting extent of the stream sub-system and this surface are illustrated in figures 11 and 12. The perimeter of the stream system's source area (as shown in figure 11) is represented by the endpoints of flow lines that mark the limiting extent of each stream sub-system on the water table. As these flow lines enter into the system they penetrate the bounding surface, enter the interior of the stream sub-system and terminate at a point on the stream channel. This bounding surface is, therefore, defined only by the initial segments of streamlines because upstream streamlines are progressively overlain by streamlines entering the system further downstream. Figure 12 illustrates how two streamlines originating at the outer edge of the stream system on the water table travel into the interior of the stream flow sub-system. They travel for only a negligibly small distance along the bounding surface.

One noteworthy exception is made by a streamline that originates in the center of the middle stream channel closest to the divide and that terminates closest to the surface water body. This streamline travels along the bottom of the stream sub-system and characterizes the longitudinal profile of the middle-stream system (fig 10b). This is a special case, however, and is due to the bilateral symmetry of flow in the watershed, the axis of which runs along the middle stream. The left- and right-handed streams are asymmetric and do not contain an equivalent streamline of symmetry. Other streamlines close to this streamline of symmetry closely parallel the boundary surface but are not embedded in the surface over their entire path.

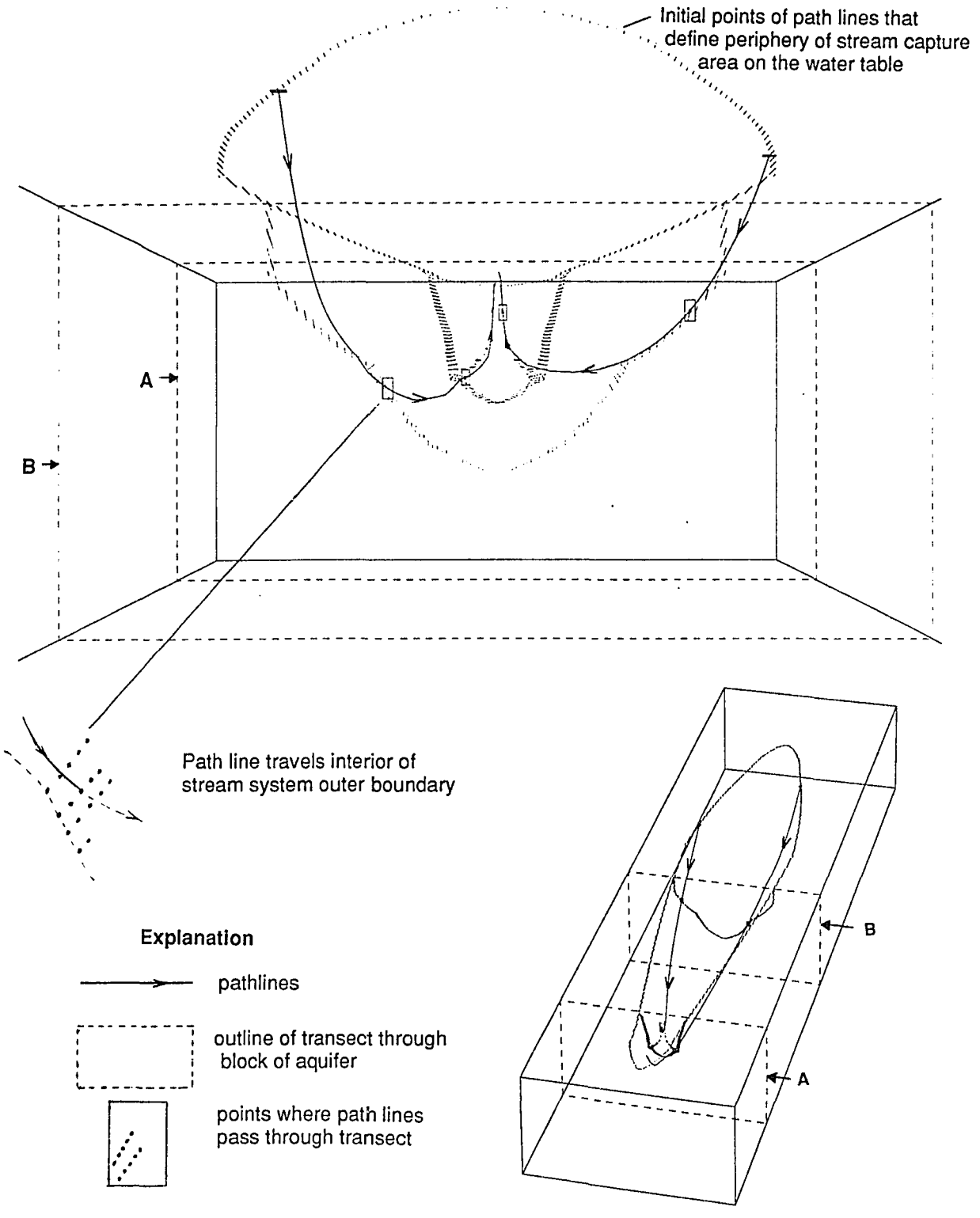


Figure 12--Relation of points of recharge that define the edge of the source area and points of intersection on two transects in the aquifer.

Figure 13 shows three mutually perpendicular views of the center stream system's profile. Although only one stream is shown, the left- and right-handed streams of this simulation are not dissimilar. The map view is similar to the trace of the stream source area in figure 11; it shows the outline of stream systems which begins about 10,000 feet from the divide, centered at the stream channel, extends out from its upper tip to a maximum width of about 9500 feet and converges toward the stream channel. The section along the column is a longitudinal cross-section. The bottom of the profile is defined entirely by one streamline of symmetry which starts at the head of the system, travels down to about 700 feet below datum plane, and terminates at the mouth of the stream. The top of the profile is defined by streamline endpoints along the edge of the source area on the water table; these are the endpoints in the map view projected onto a vertical section. Finally, the section along rows shows three different profiles in vertical sections that are perpendicular to the stream channel. Their locations are indicated in map view. The profiles are formed by tracing the points that mark where the outermost streamlines of the stream sub-system intercept the vertical sections (see also figure 10) but are not necessarily perpendicular to these sections.

The sections along rows of the figure show that the depth, width, and shape of the system's bounding surface vary considerably along the stream channel. The profile farthest upstream has a simple arch shape and is fairly typical of the system's shape near the stream start-of-flow. Profiles further downstream, however, have more complex shapes. In the mid-stream area the

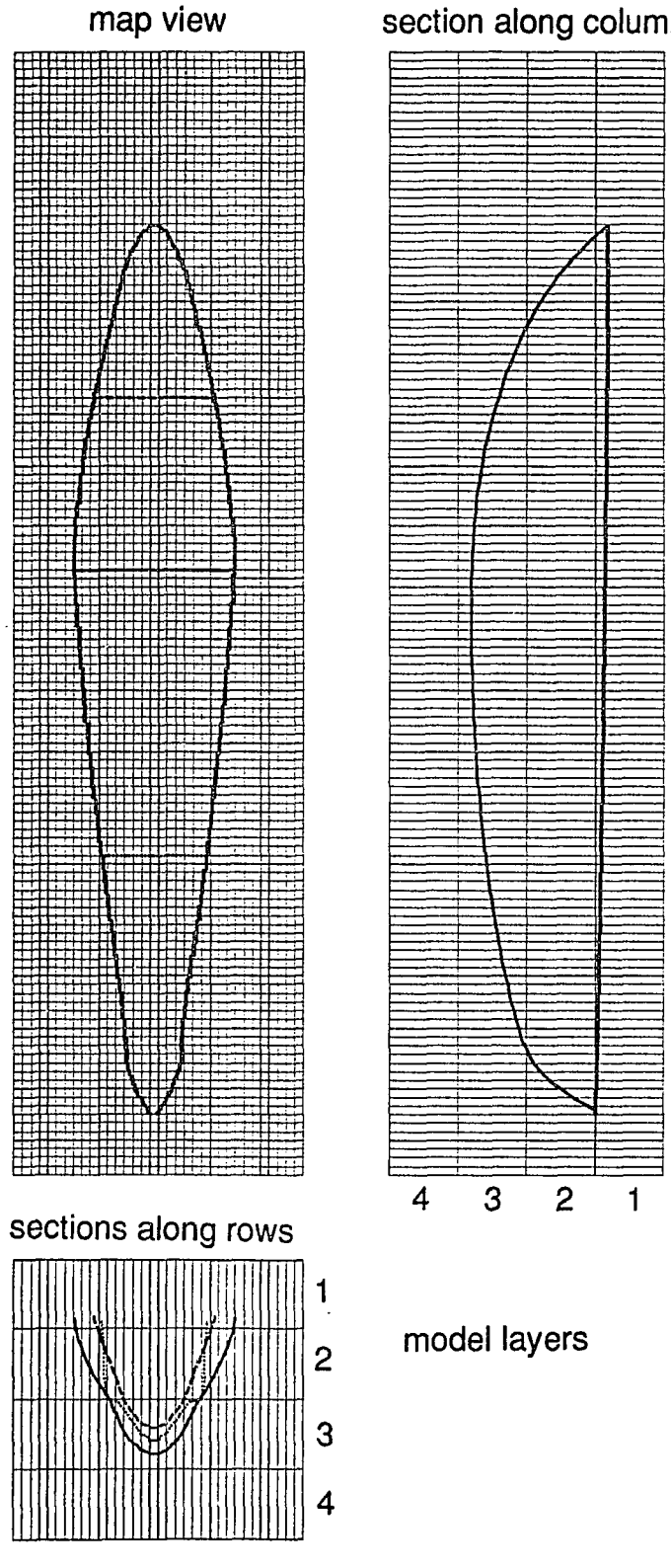


Figure 13--Profiles of bounding surface for the center stream sub-system flow for the reference simulation. Three orthogonal views, map, section parallel to model columns, and section parallel to model rows are shown.

sides are straight and nearly vertical. The section farthest downstream becomes more shallow and narrow. Inflections on the transect profiles are simulation artifacts and reflect some discontinuity in the flow solution at the boundaries of model layers. (see also figure 16b, page 56).

The shape of the stream system's groundwater boundary surface is also shown by a structure-contour representation in figure 14. Contour lines are in 50 foot intervals. A noteworthy feature of this surface is the occurrence of a relatively flat surface that begins along the sides below where the stream system is widest and increases in extent with distance downstream. This flat surface is shown by contour lines that appear to become truncated in the figure but, in actuality, change direction abruptly; the close spacing of these contours indicate a steep edge. This edge and portion of abrupt change that are prominent along the lower stream reach is shown in perspective view in figure 15. All stream system boundary profiles perpendicular to the stream channel that correspond to the model rows are shown. The view is from beneath looking up toward the bottom of the stream flow system, the divide located farthest from the viewer (see section on boundaries for discussion on edge).

Finally, several of the features previously discussed are summarized in two additional three-dimensional perspectives of the single stream system boundary surface shown in figures 16a and 16b. These figures show the structure contours at 50 foot intervals.

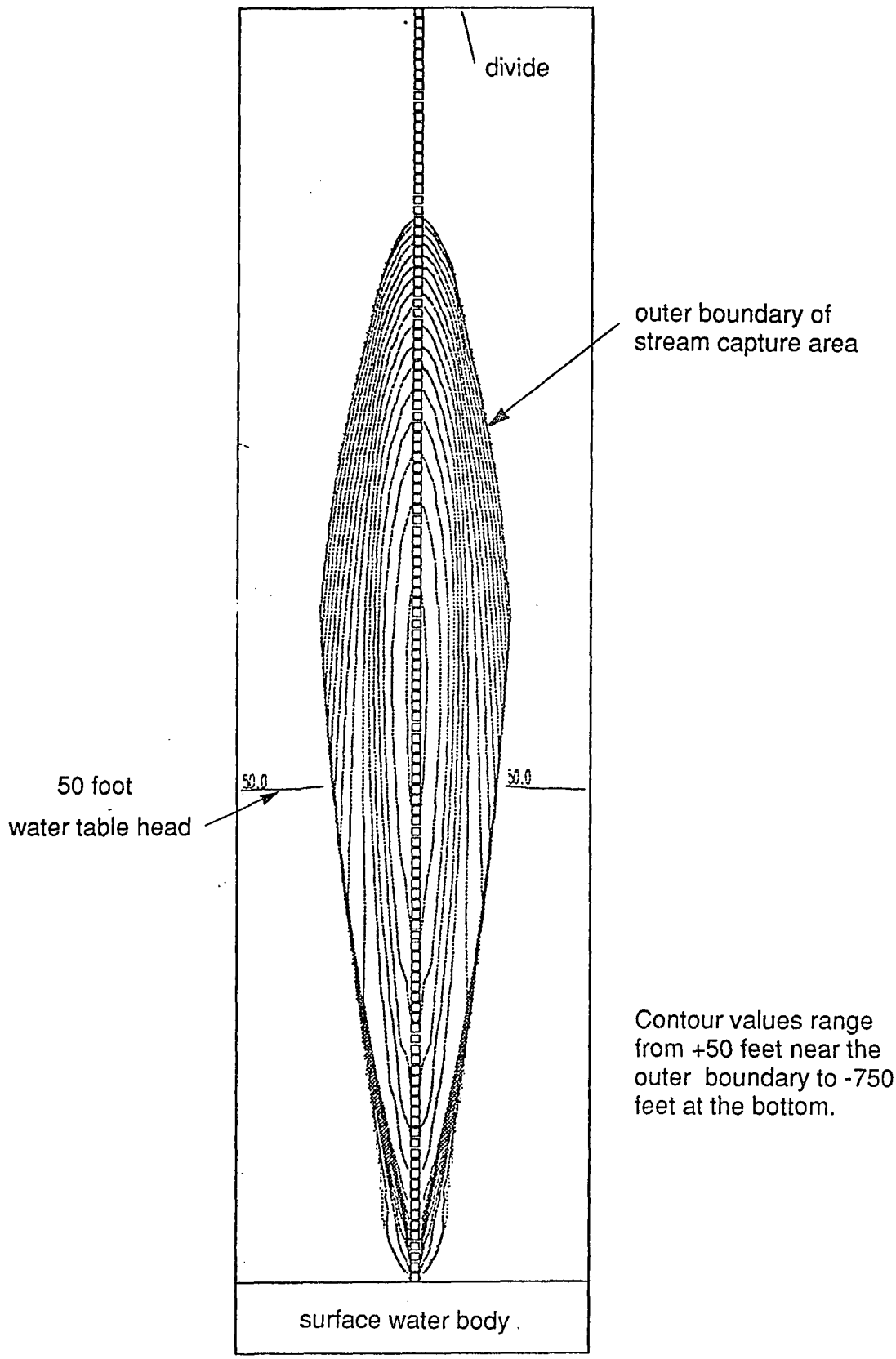


Figure 14--Lines of equal elevation that define the center stream lower boundary surface for the reference system. Contour interval is 50 feet.

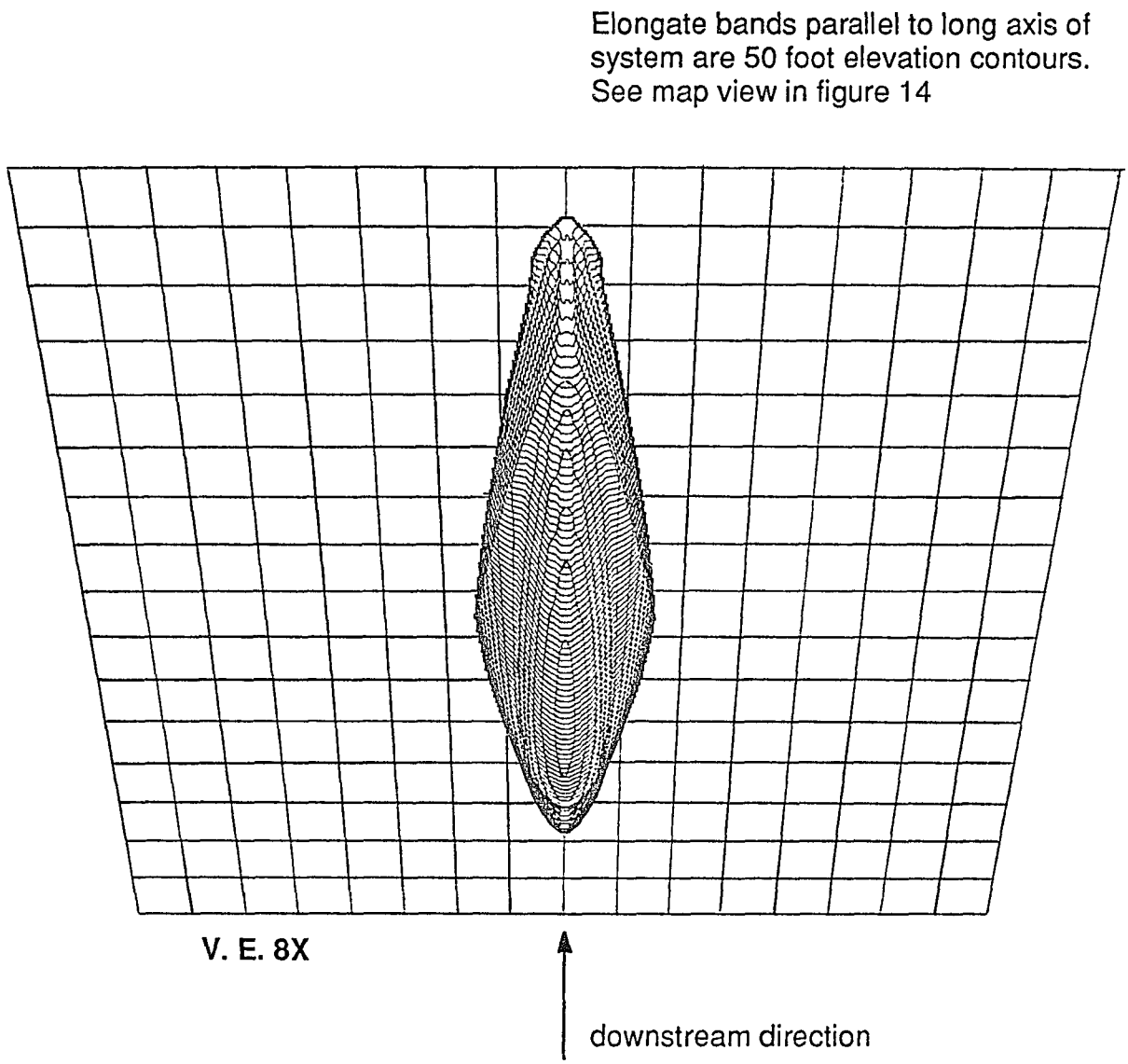


Figure 15--Lower boundary surface of the center stream sub-system flow viewed from downstream and below the system looking upward. An evenly divided grid is positioned near the free surface and is used to show distortion of the perspective. Other views of stream sub-system flow are shown in figure 16.

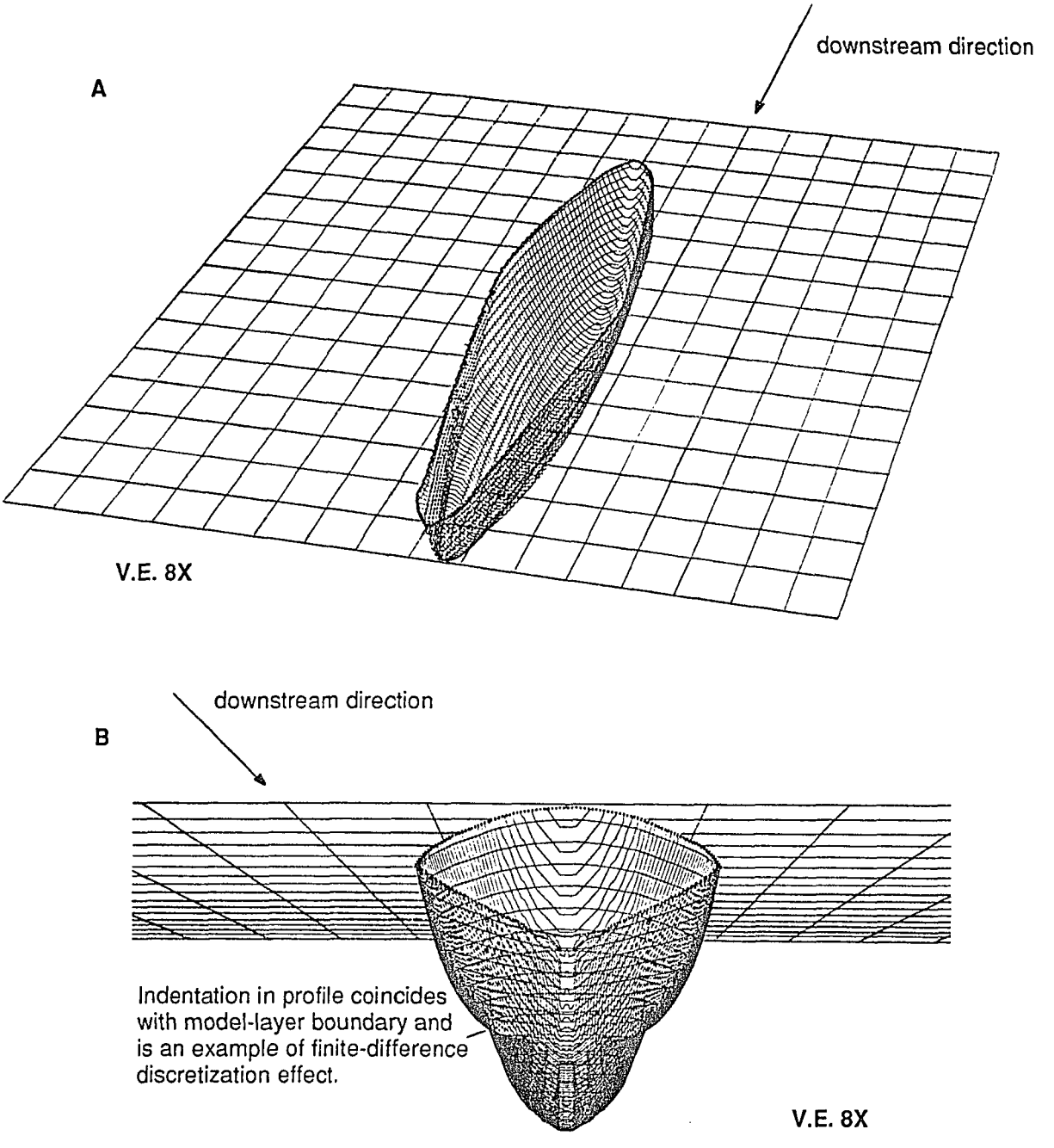


Figure 16a--Lower boundary surface of the center stream sub-system flow looking upstream and downward from front-right view.

Figure 16b--Lower boundary surface of the center stream sub-system flow looking downstream along longitudinal axis of system.

*Hydraulic principles of point-sink galleries and their application to line-sinks*

Although the geometric and hydraulic parameters for the hypothetical system were made simple, the resulting flow patterns are, nevertheless, complex owing to the sub-system flow created by streams in a three-dimensional flow field. In order to understand the complex flow patterns created by the stream system, it is desirable to learn some of the 'line-sink' characteristics of streams and their effects on flow by evaluating the flow processes of similar but much simpler systems.

A line-sink can be thought of as a continuous distribution of wells along a line. Whereas flow to a well converges at a point, flow to a line converges uniformly along its extent (Strack, O. D. L. and Haitjema, H. M., 1981). In a real system a gaining stream functions as a line-sink because groundwater is discharged from the aquifer continuously over much of the stream's reach, albeit at varying rates. In a finite-difference formulation, however, a line-sink is represented by a train of separate nodes. Several wells positioned in tandem would produce hydraulic responses similar to those of a discretely represented line-sink. The streams of the reference system function as a train of closely spaced wells with the distinction that flow to each point is determined by head differences and is not a pre-determined quantity. The finite-difference character of the numerical model can be applied to evaluate aspects of flow to a gallery of wells which are, in turn, similar to flow to a discretized line-sink.

In this section, 5 different simulations involving a well field are discussed. In each simulation individual wells, or several wells in a gallery, are selectively

activated. Each simulation shows an aspect of flow that is applicable to the flow dynamics of a stream system. The wells are positioned along a line bisecting the aquifer on the surface. The aquifer system has geometrical properties and boundary conditions like that of the reference stream system, including constant areal recharge to the water table, except that wells are substituted for streams. A pumping rate of -30000 cfd was used for each active well of each simulation all of which are assumed to run to steady state.

Figure 17a shows how groundwater would discharge to a single well located in the upper half of the system pumping at a constant rate. A map view and two mutually orthogonal cross-sectional views show some of the flow lines that define the well's flow sub-system, from their points of recharge at the water-table to where they discharge at the well. Flow lines above the well travel longer distances down the sloping water table whereas flow lines just below the well travel much shorter distance and against the general direction of flow of the system. Figure 17b represents this same simulation but shows the initial locations of flow lines that enter the well system on the water table. The points collectively define a contributing area of flow for the well. The shape of the contributing area is widest close to the well and tapers in the upgradient direction.

In the second simulation another well (well 3) further from the divide is pumping instead of the first well, otherwise the hydrologic situation is identical to that of the first case. Because the pumping rate is the same the number of flow lines representing the well sub-system is also the same (see discussion on

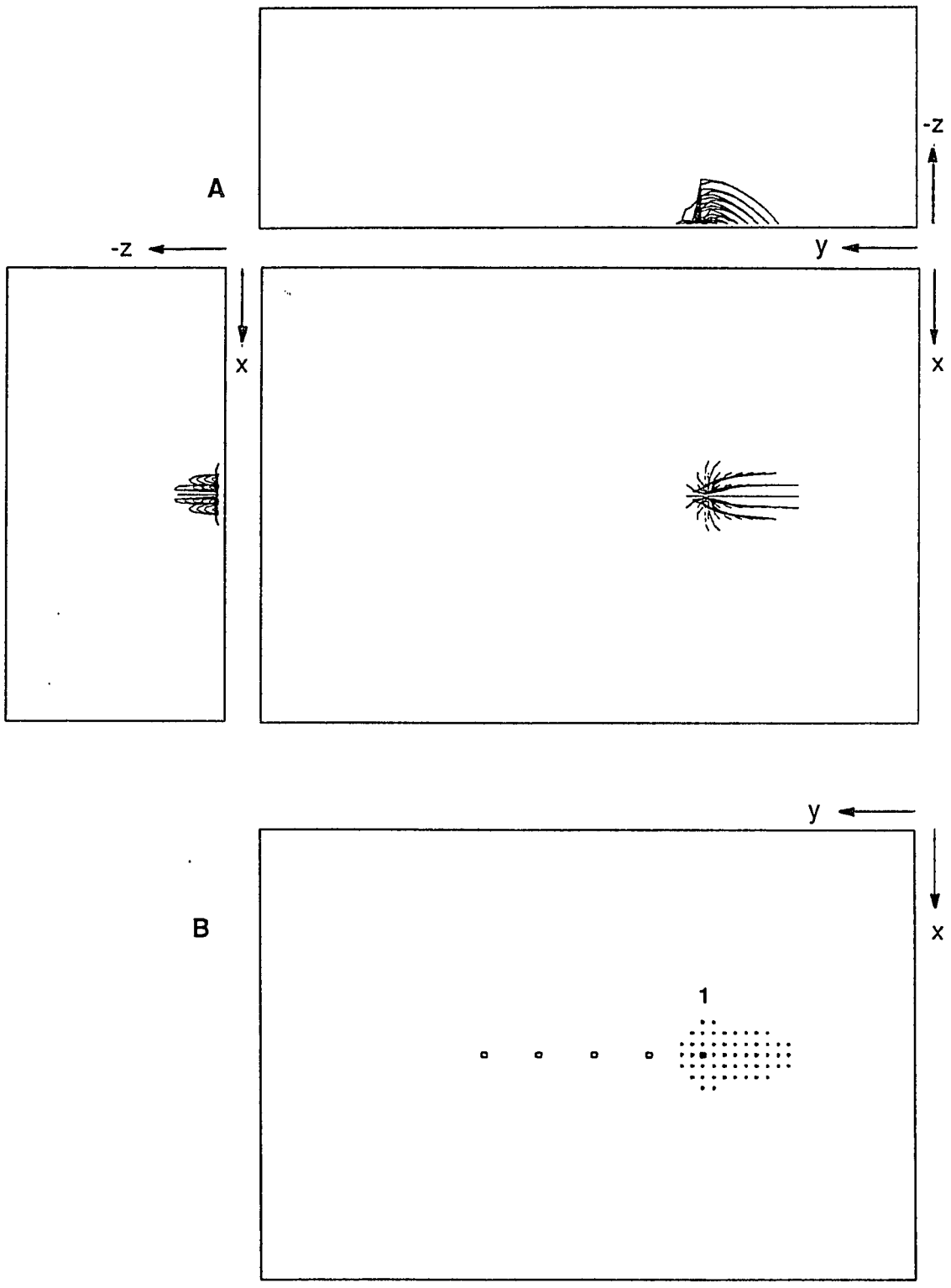


Figure 17a--Flowlines from the water table to a single well (well 1) viewed along each of the three Cartesian coordinate axis.

Figure 17b--Map view of the source area to well 1 as defined by the points of origin of one path line per model cell.

particle tracking algorithm). Figure 18a shows the corresponding flow lines and contributing areas of flow. There are, however, some subtle differences in the shape of the contributing area as well as in the flowline patterns. The flow lines in this case are more elongate than in the previous case as can be seen in map and longitudinal section in figure 18b. The most lateral flow lines are more shallow than that of the previous case. The endpoints also show the longer catchment area in the upgradient direction on the water table.

In the third simulation well 5 is active. Flow lines in the well flow sub-system are longer and occur in a shallower domain of the system than the previous two cases (figure 19a-b). It appears that the shape of the well flow sub-system is related to the well's location along the free surface, specifically, its distance from the divide. Because the water table increases in slope in the y-coordinate direction, the $v$ should also increase. The effect of the increase is seen in the progressive elongation and shallowing of the well flow sub-system geometry.

Figure 20 shows a scenario where three wells in tandem are pumping at the same rate (wells 1, 3 and 5). The resulting contributing area is equivalent in area to the sum of each well's individual contributing area. Yet, its area exceeds the outlines of the superimposed contributing areas for the wells as they pumped individually. This apparent enlargement is explained by the two areas of overlap; note that the 'tail areas' of the contributing area to wells 3 and 5 lie over the 'head areas' of the contributing areas of wells 1 and 3 respectively. Flow lines within these overlapping areas, the longer flow lines that discharge to the well

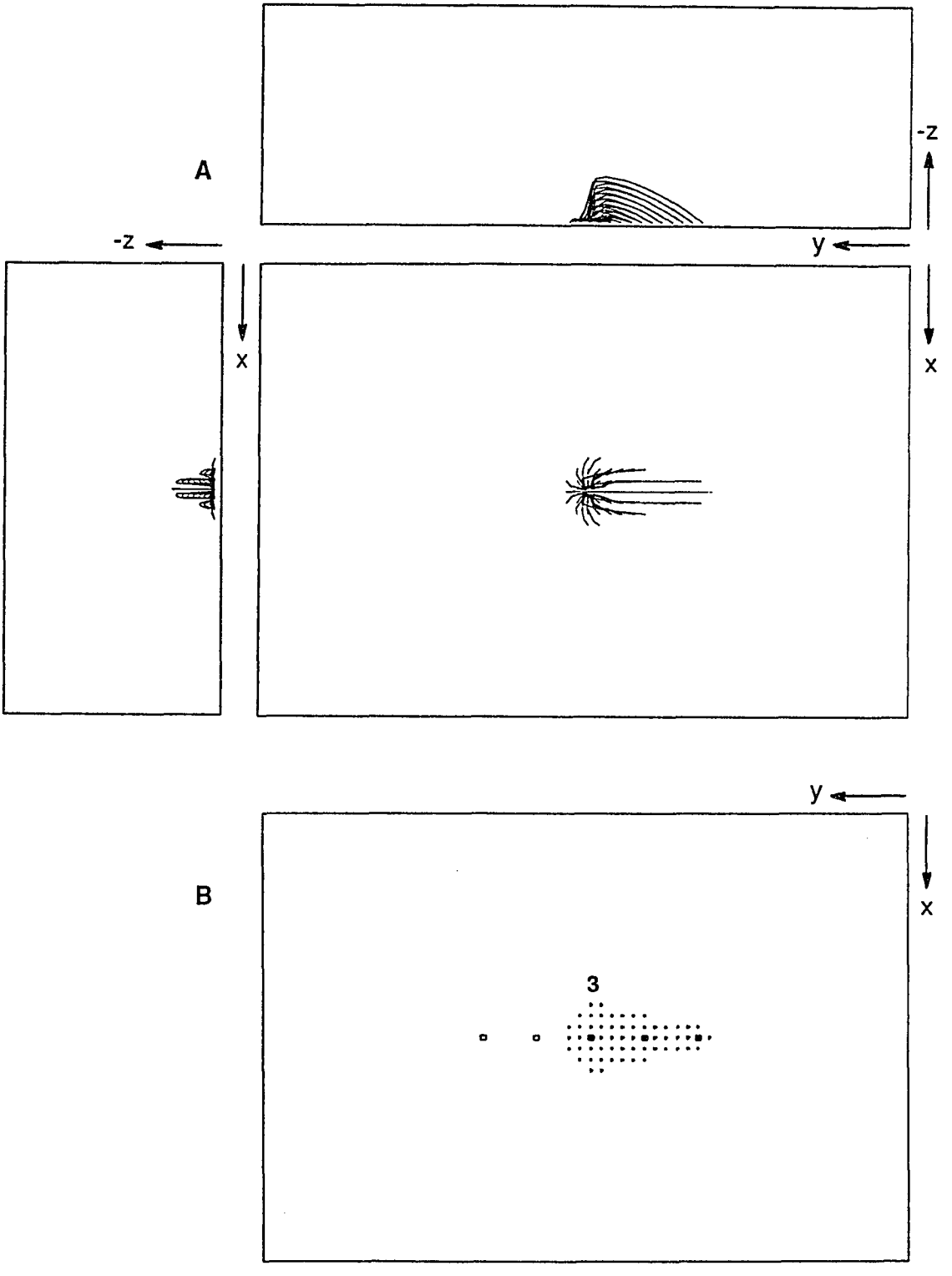


Figure 18a--Flowlines from the water table to a single well (well 3) viewed along each of the three Cartesian coordinate axis.

Figure 18b--Map view of the source area to well 3 as defined by the points of origin of one path line per model cell.

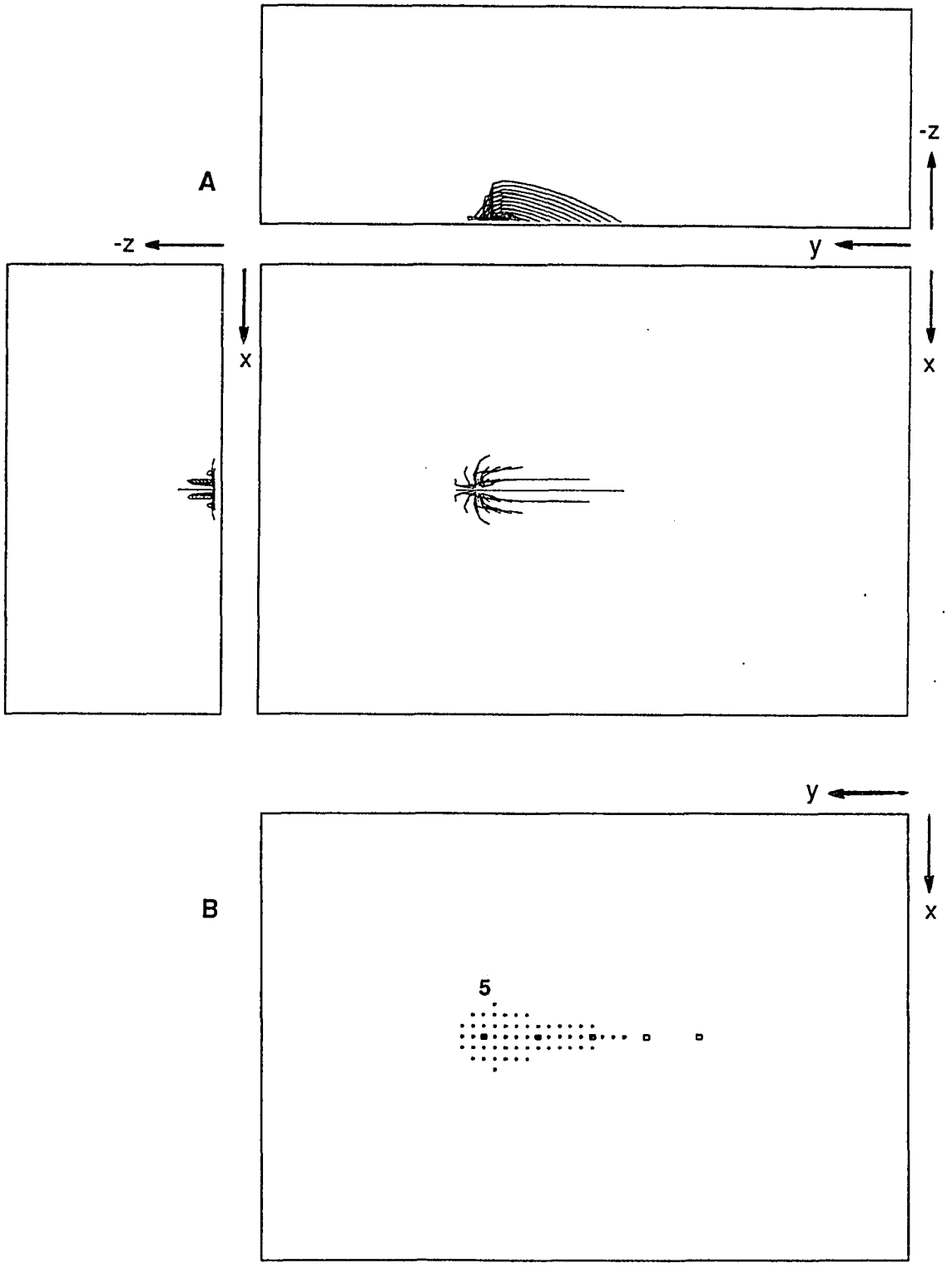


Figure 19a--Flowlines from the water table to a single well (well 5) viewed along each of the three Cartesian coordinate axis.

Figure 19b--Map view of the source area to well 5 as defined by the points of origin of one path line per model cell.

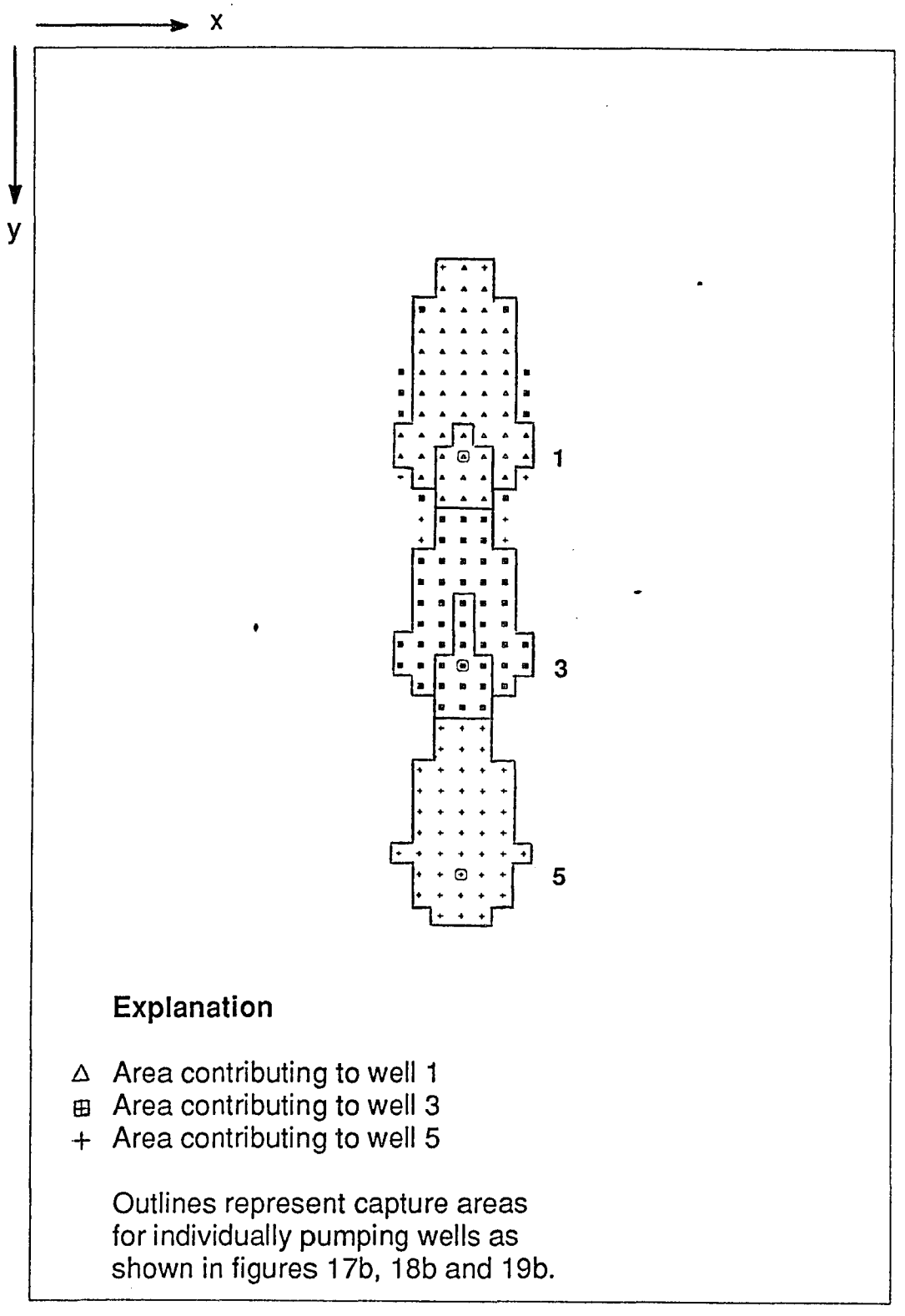


Figure 20--Source area defined by initial points of pathlines to wells 1, 3, and 5 pumping simultaneously.

immediately down-gradient of them in the single-well simulation, are the shorter flow lines that discharge to the up-grade well in the multiple-well simulation. For example, the tail of the contributing area to well 3 is displaced by the part of contributing area created by well 1. However, because water mass balance must be maintained, the displaced portion of the contributing area to well 3 must be compensated for in the system. This compensation is achieved by an enlargement of source areas to all wells.

Thus, figure 20 shows that the contributing area of flow for the triple well gallery has been enlarged in order to compensate for the displaced areas. Well three draws groundwater adjacent to it, upgradient from its discharge point around the upper end of the second well, and above the first well. Much of the accretion of contributing area occurs around the upper portion of the well field.

Recharge near the gallery of wells is more readily captured in the well's sub-system flow as more wells are added to the line. Because the horizontal, rather than vertical, component of flow dominates in the system, recharge that enters the system too far left or right of the line of wells would remain entrained in the regional flow field. In contrast, recharge originating nearer to the divide but close to the alignment of wells is captured in the well flow sub-system; because the horizontal component of flow is weaker in this zone, recharge is more readily captured in the well sub-system. However, recharge in this zone moves deeper into the aquifer and also travels down-gradient near the bottom of the well flow sub-system before it eventually discharges further down-gradient.

Figure 21 shows the pathlines for three closely-spaced points of recharge that are located near well 1 in the triple-well flow simulation. The pathlines indicate that recharge originating at the indicated entry points would discharge to different wells that are widely separated. These flow lines trace paths having sharp directional changes in three-dimensional space from their respective points of origin to their different points of discharge. The particles entering the system within the contributing area of the well flow field travel paths that define a response to the perturbations created by well-water-table interaction. In effect, they define the paths of least resistance for groundwater relative to their entry point that is traced in the well flow field and that must discharge within this system.

The final simulation shows the effect of five wells in tandem that are pumping simultaneously, the two additional wells positioned between, and at equal distances to, the previous three. Figure 22 shows the resulting contributing area of flow for this five-well system. The additional displaced flow from the triple-well system has resulted in a substantial increase in the contributing area especially near the divide. The widest section is adjacent to the first well and the tapering, characteristic of the individual well fields, is evident in this system but is inverted with respect to the y-axis of the model. Another feature apparent in this flow system is that the contributing area of flow to each individual well is an arrangement of discontinuous, concentric, bands around the well field. Flow lines that discharge to the lowest well (well five) are arranged, not only around the

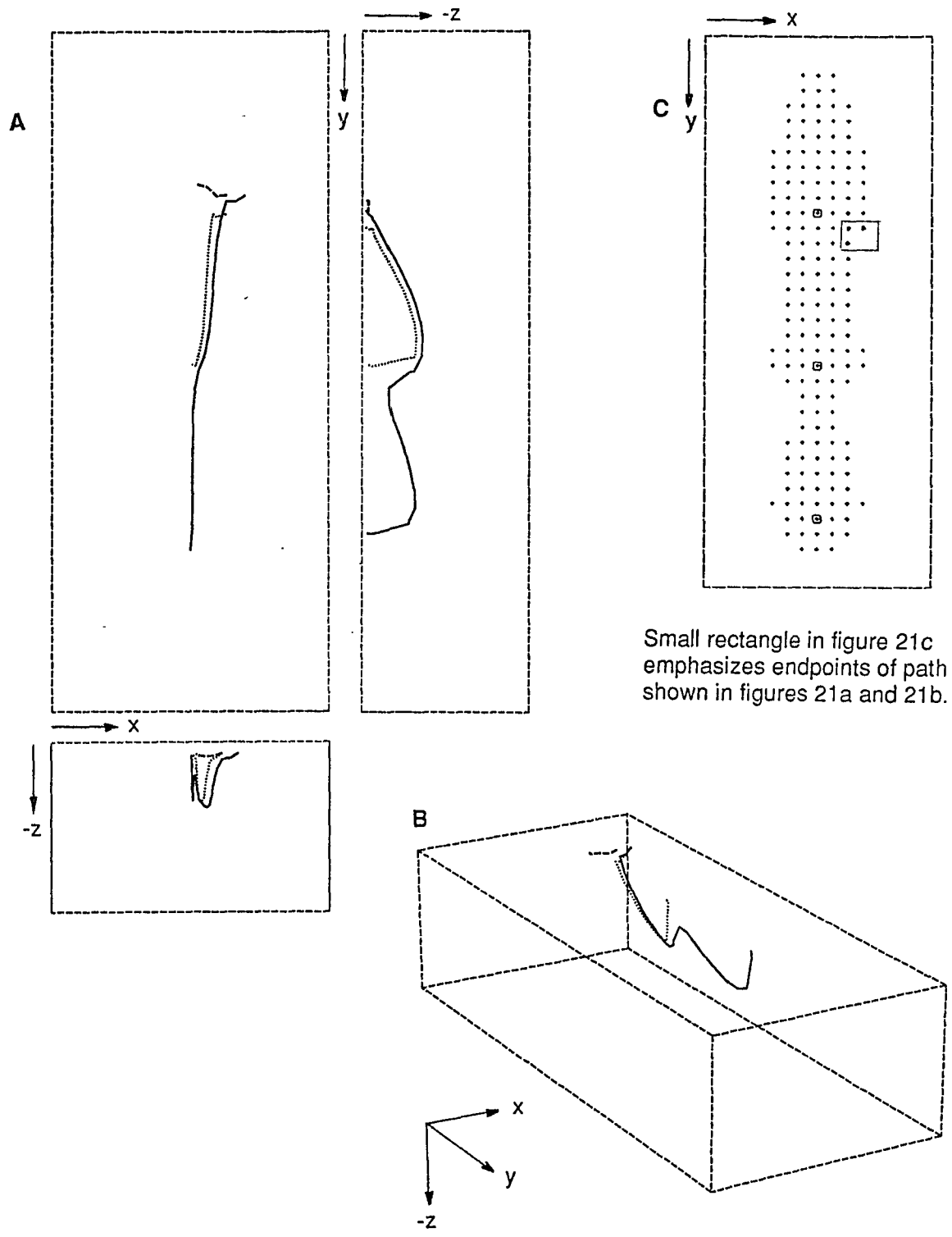


Figure 21-- Pathlines from three closely-spaced points of recharge near well 1.
a) Three orthogonal views along each coordinate. b) 3-D perspective view.
c) Map view of endpoints of pathlines for wells 1, 3, and 5 (see figure 20).

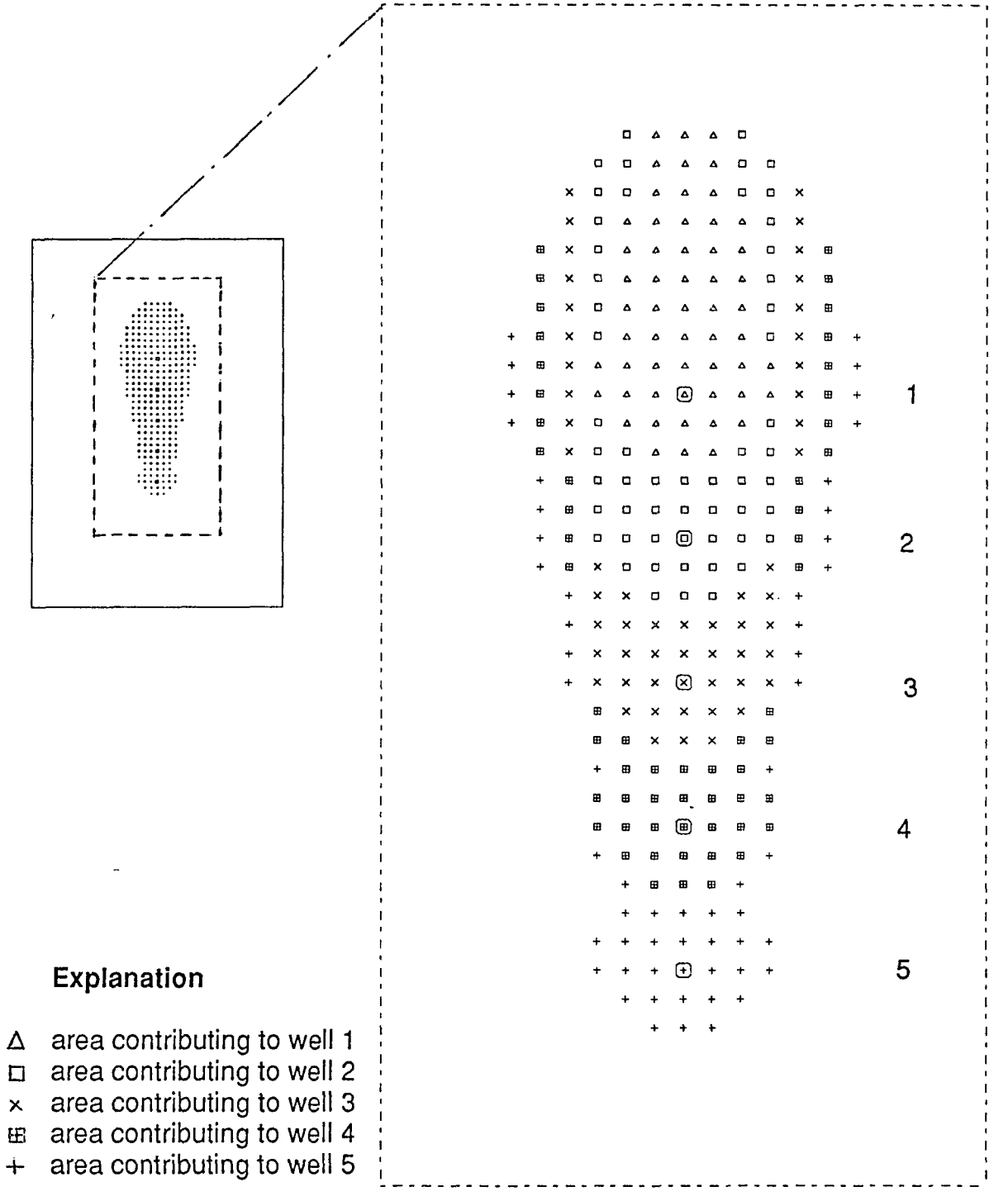


Figure 22--Source area defined by initial points of pathlines to wells 1 through 5 pumping simultaneously.

well, but define parts of the outer edge of the system. Well four displays a similar pattern except that bands of its flowline endpoints lie interior to those of well five.

From the above simulations it is evident that each well generates its own unique flow sub-system. The configuration of its contributing area and subsurface geometry are related to the flow gradients at the location of the well. Secondly, when additional wells are incorporated into the active gallery the well that loses part of its source area to another well will compensate by tapping into new recharge areas. Additional source water is drawn into the well flow sub-system from areas that are in closest proximity to the line of wells and in areas near the divide. As more point-sinks are added to the system its source area must expand; wells farthest down-gradient draw part of their discharge from source areas nearer the divide as well as the area adjacent to the well.

Many point-sinks in a gallery take on the hydraulic characteristics of a line sink. A line-sink generates a complex pattern of flow whereby each discharge point on the line taps into discontinuous patches of source area that are arranged as elongate bands. These bands are arranged in concentric patterns and collectively make up the stream contributing area.

*Flow patterns in hypothetical stream sub-system*

The complex pattern of the contributing area of flow shown in the previous well field simulations are apparent in the stream sub-system flow of the reference system. Figure 23 shows the initial points of flow lines for the center stream of the reference simulation. Only initial points of streamlines that

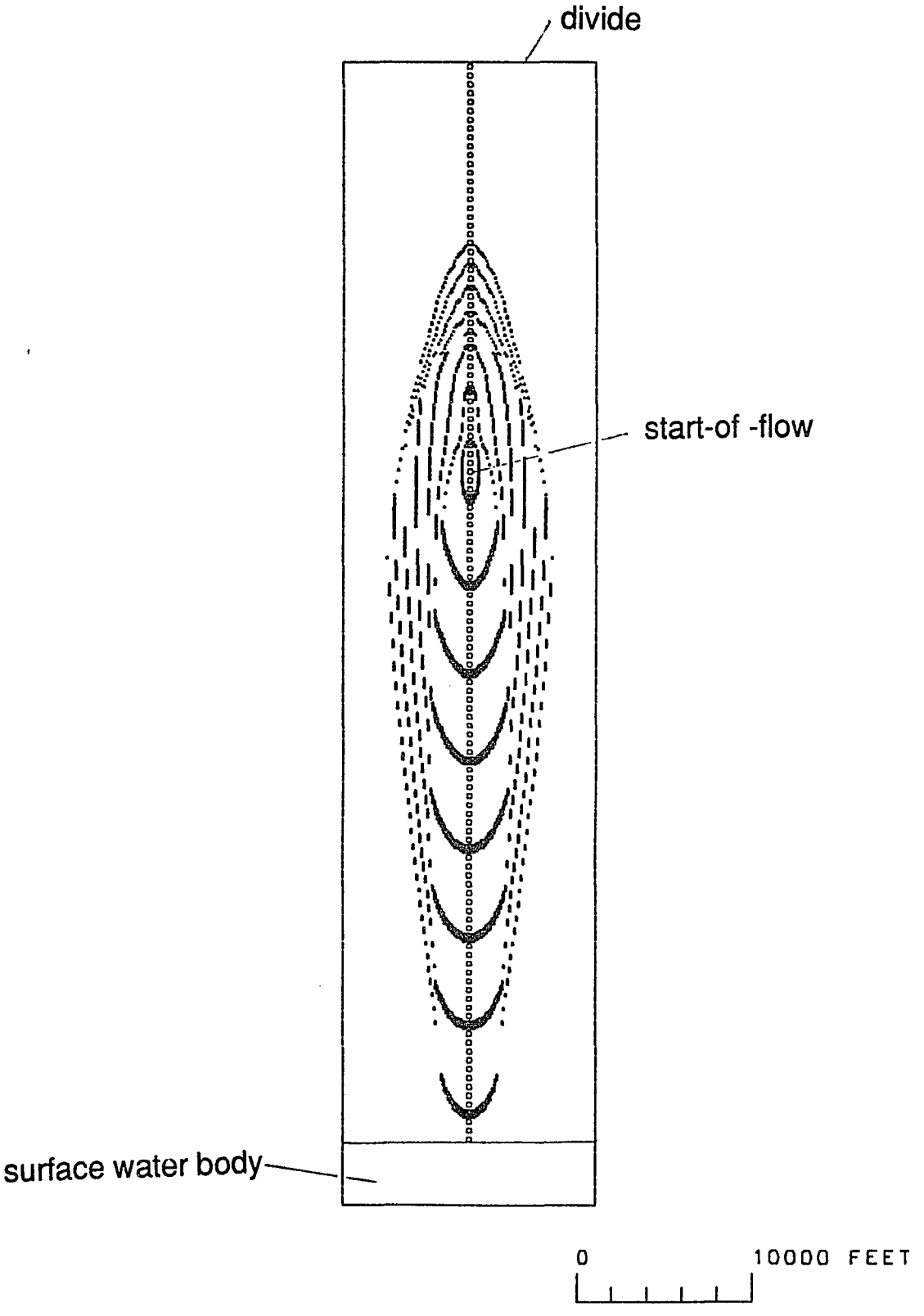


Figure 23--Areal distribution of initial points of pathlines that discharge to every tenth node of the center stream.

terminate at every tenth node are illustrated for clarity of presentation. The initial points of flow lines are arranged as concentric bands or loops. The outermost bands do not completely encircle the system but are truncated near the widest section of the contributing area. The bands for a common discharge point along the stream, consisting of clusters of initial points arranged in loops, are discontinuous. The shape of each cluster varies; for example, crescent-shaped clusters of initial points are centered on their associated discharge points along the stream channel. However, other clusters on the loop form short, linear patterns of various sizes. The start of flow for the stream system occurs within the smallest, innermost loop. The upstream tip of the contributing area, closest to the divide, is characterized by an arch-shaped pattern of initial points. As will be discussed in another section, these initial points represent the flow lines that travel deepest in the stream sub-system before they discharge to points closest to the terminus of the stream channel.

The relation between the pattern of initial points on the free surface and the pattern of sub-surface flow lines is shown as an exploded perspective view in figure 24. Only flow lines that terminate at four points along the stream channel are illustrated. The pattern of concentric loops that would appear on the free surface is shown on the top of the block. The corresponding sets of flow lines for each of the four discharge points make up what appears to be a set of nesting shells. These shell-like features represent the flow fields for the four discharge points on the channel and are approximately defined by the flow lines. The clustering of flow lines into distinct groups indicates that these flow fields are

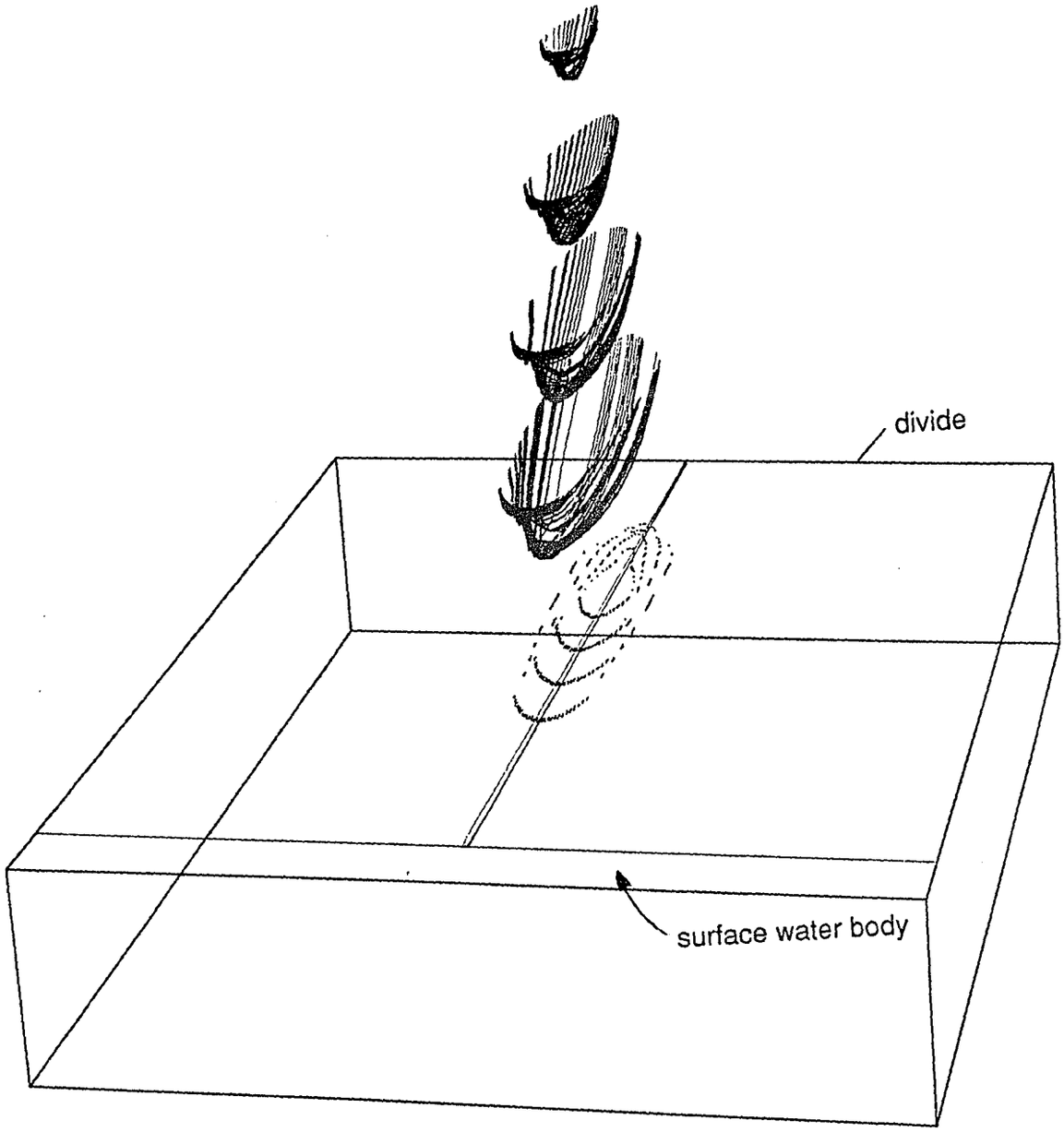


Figure 24--Exploded view of flowlines that terminate at four different points along the center-stream channel. The corresponding recharge patterns on the free surface are also shown.

discontinuous and are made up of distinct plugs of flow within the stream sub-system that start at separate recharge areas on the surface but converge at a common discharge point along the stream. The apparent gaps within each shell-like flow domain are actually occupied by plugs of flow that belong to adjacent flow fields discharging to nearby points along the stream. Collectively, these groups of flow lines inter-finger to form an entire stream flow field.

A hydrologic concept gleaned from the previous well simulations is that the shape of the contributing area and flow field for groundwater discharging to a given point is affected by the gradients and water-table slope near the point of discharge. The horizontal component of specific discharge increases with distance from the divide towards the surface water body. This is true even though the stream system itself depresses the water table position and decreases the gradient. Figures 25 and 26 illustrate the geometric properties of flow lines that originate at two different distances from the divide. Figure 25 shows the flow lines that travel into the system from where they originate along a row 15,000 feet from the divide. The map view and two mutually perpendicular cross-sections show only these lines. The same type of flow patterns are illustrated in figure 26 except that the flow lines originate at 30,000 feet from the divide. A comparison of both figures shows that flow lines that enter the system further downstream travel in the more shallow part of the system. Flow lines originating from rows located at progressively greater distances from the divide would show continued shallowing.

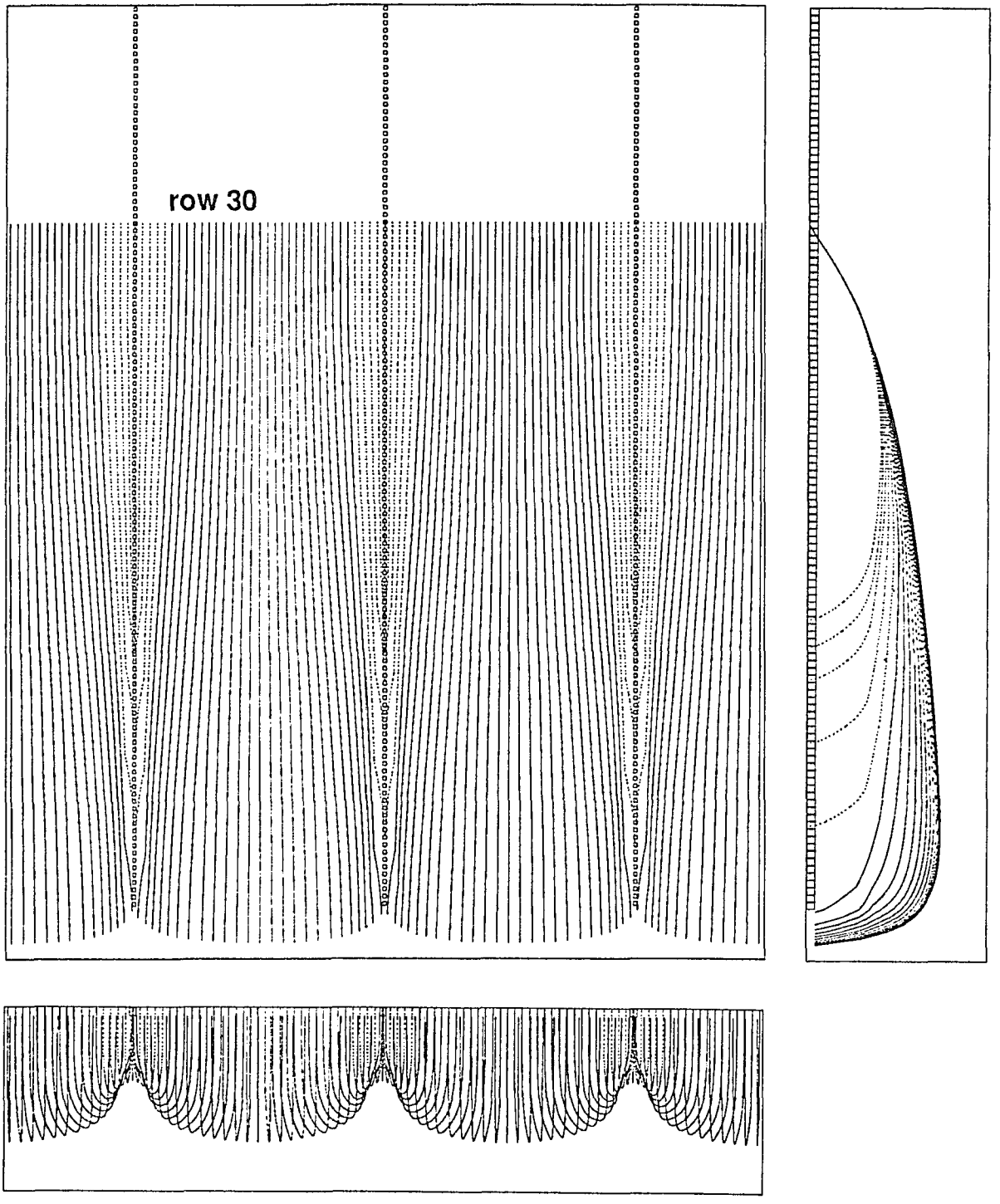


Figure 25--Three mutually perpendicular views of flowlines that enter the system 14750 feet from divide (along model row 30).

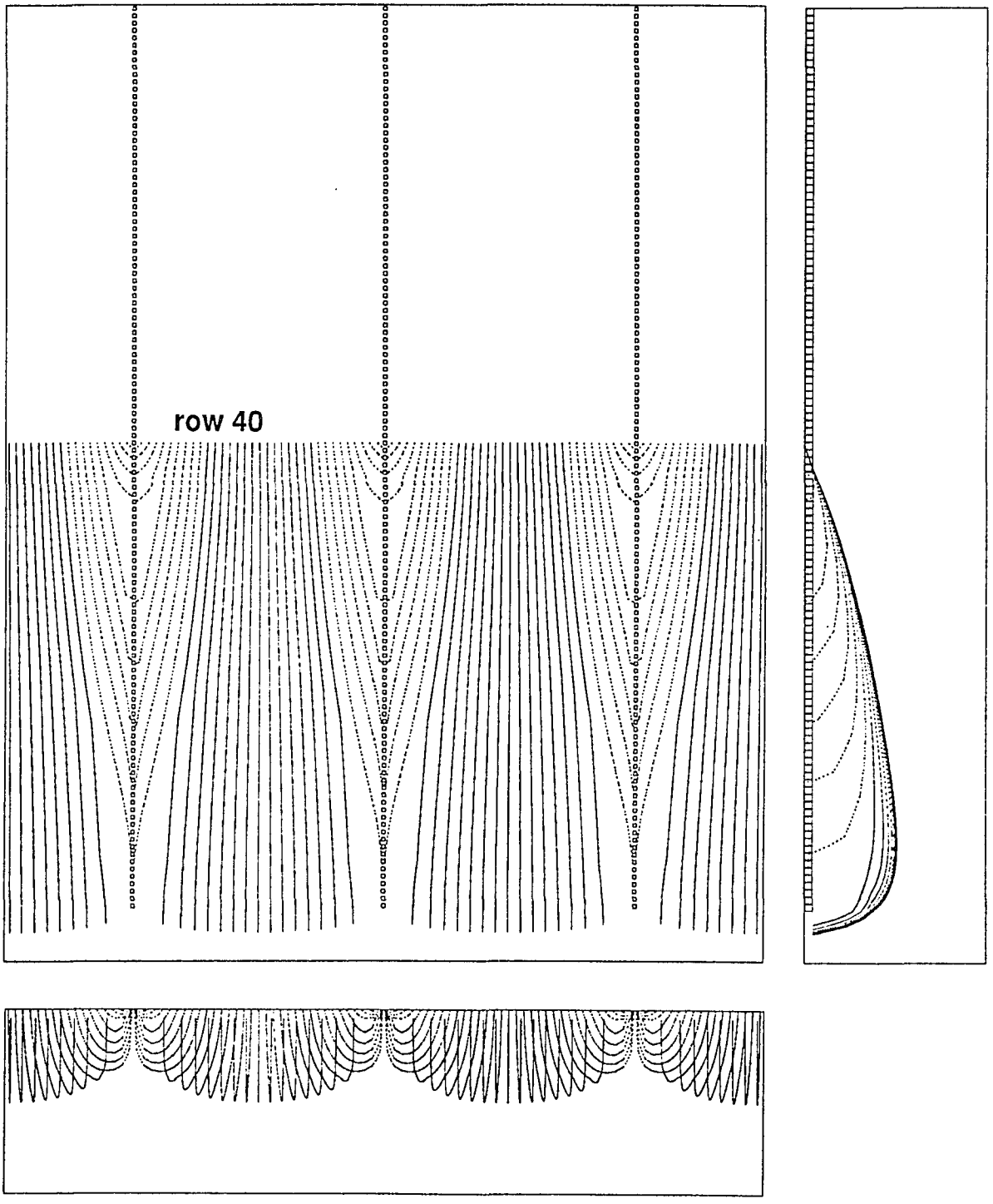


Figure 26--Three mutually perpendicular views of flowlines that enter the system 29750 feet from divide (along model row 60).

Flow lines that originate at the inter-stream divide have a negligible lateral flow component and travel downstream to discharge into the surface water body. Flow lines that enter the system at progressively greater distances (in the x-direction) from the inter-stream divide acquire an increasing lateral flow component. This is shown in the transect views of projected streamlines in figures 25 and 26.

Some of the more complex aspects of flow in the stream sub-system are seen more clearly by studying in isolation the pattern of flow lines that originate along several sections parallel to the system's y axis. Figures 27a-c show the flow pattern made by flow lines that enter the system along a) the center stream channel, b) a column 1500 feet from the channel and, c) a column 2500 feet from the channel. For each case only one flowline per model cell is simulated. Figure 27a shows true cross-sectional flow because pathlines are generated from recharge along the center-line of the stream; flow entering the system along this column discharges only to points within this column. Flow lines that discharge to the channel are shown as solid lines. The point where start-of-flow begins is within the interval defined by the flowline that travels to the shallowest depth and forms the smallest loop along the surface. The flow lines in this section appear to indicate that the stream channel is recharged only between the stream system's limiting flowline (outermost solid line of stream system shown in figure 27A) and the start-of-flow and that discharge occurs only between the start-of-flow and the stream terminus. However, as discussed in a previous section, recharge is distributed over the entire water table including this interval

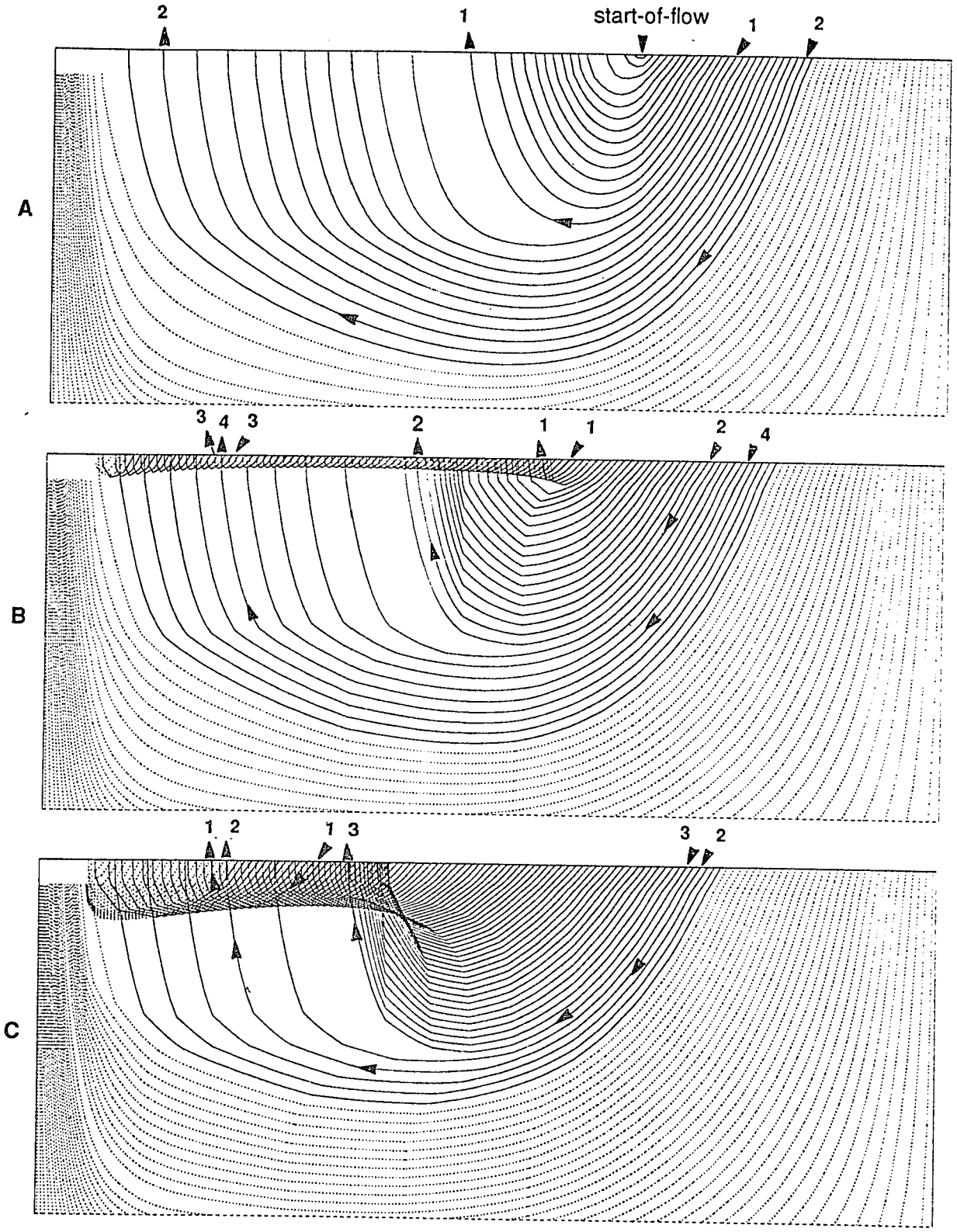


Figure 27--Projection of flowlines to three longitudinal sections. Flow lines originate from (A) the center-stream channel, (B) along a column 1500 feet from the channel and, (C) along a column 2500 feet from the channel.

constituting part of the stream channel. Because blocks in this interval act as a sink, both recharge and discharge occur concurrently; however, the model shows only a net flux exiting the system through the top of this interval. Therefore, the streamlines within this interval represent a net flux that leave the system (see discussion on simulation artifact).

Figure 27b shows a projection of flow lines that enter the system three-column widths away from the stream channel. In map view this is a cut through the flank of the stream contributing area. All flow lines that discharge to the stream channel travel 1500 feet in the x-coordinate direction. The downstream and vertical travel directions are, therefore, the only directional components apparent from this view. Discharge to the channel occurs over a shorter reach, from a point about 6000 feet downstream from the start-of-flow to the end of the channel (interval shown in stippled pattern). The flow that discharges within this interval originates from near and far recharge locations.

The near recharge locations are represented by the shallow, tightly-curled pattern of flow lines. For these flowlines, flow enters the system nearly adjacent to its point of discharge; here, flowlines travel shallow paths that are almost lateral toward the stream. Flowlines 1 and 3 in figure 27B are examples of streamlines that represent shallow groundwater flow originating from near recharge locations.

The discharge that originates from far recharge locations is characterized by deep and relatively long downstream components of flow. Labels 2 and 4 show flow lines that are examples of this group; these originate upstream of the

zone of discharge and travel much longer flow paths than do the flow lines from near recharge locations. Flow lines from near and far recharge areas can also discharge to a common area as shown by labels 3 and 4. The implication is that seepage to stream outlets can represent groundwater with mixed residence times that are significantly different.

Figure 27c shows a projection of flow lines that enter the system five column widths from the stream channel. Flow must travel about 2500 feet in the lateral direction to the stream. In general, the flow characteristics for this projection are similar to those of the previous figure in terms of flow from near and far recharge areas mixing at common areas along the stream. However, flow that originates in near-recharge-areas travels deeper and farther downstream than does flow that enters the system closer to the channel (see stream system flowlines in transect view in figures 25 and 26, and longitudinal view in figure 27B). Also the reach of the zone of discharge is shorter and begins about 17,000 feet down stream from the start-of-flow. Flow lines 1 and 2 are examples of near and far points of recharge that discharge to a common area. The variation of residence times at the discharge location for these two flowlines would be less than for flowlines 3 and 4 in figure 27B where recharge occurs closer to the stream column. However, the actual discharge water would be a combination of waters of many different ages.

The three sections containing projected flow patterns are only three of an unlimited number of sections between the stream channel and inter-stream divide that show differences in flow geometry with distance from the middle

stream system. If all sections of the stream flank could be shown, then each would reveal a progressive but subtle variation in flow pattern from stream to inter-stream in a way suggested by the three figures.

The sense of flow direction in the vertical sections can be related back to the map view of endpoints of figure 23. Each of the eight loops of endpoints illustrated represent a sub-set of flowline endpoints originating on the free surface that discharge to a single node along the streambed. The crescent-shaped pattern of endpoints centered on the stream channel are shallow flow lines that discharge close-by. Other flow lines that discharge to this point are seen as clusters encircling the area of start-of-flow. The flow lines of these initial points must travel progressively longer and deeper paths to their discharge points. The arch-shaped patterns near the upstream tip of the stream contributing area represent the longest paths.

The stream flow system can be thought of as a flow complex consisting of shallow and deep flow sub-systems that are 'intertwined'. The shallow flow is characterized by a strong lateral component of flow, is confined to the very shallow part of the system and, is relatively close to its discharge points. The deeper flow originates farther up the stream system, the farthest recharge originating above the start-of-flow, but within the source area of flow to the stream. This recharge follows deep and long paths in the aquifer but within the bounding surface of the stream system; deep flow rises up and inter-fingers with shallow flow where both discharge to common locations on the channel. This

division is somewhat contrived inasmuch as there is, in actuality, a gradation of flowline lengths and corresponding travel times.

Figure 28a-c shows three vertical sections coinciding with model rows 30, 65, and 100 that are oriented perpendicular to stream channels. The patterns shown on these sections are points where flow lines intersect the vertical plane although not necessarily perpendicular to it. One particle was used for each node on the water table to generate the flow lines. The flow lines that are closest to the bottom of the section can be traced to flow lines that decend deepest in the system and originate at the surface far from the section. Conversely, flow lines appearing near the top of the section can be traced to shallow flow lines that originate on the aquifer surface close to the section.

Figure 28a is an example of a section of the reference system upstream of the start-of-flow where streamlines in section are stacked vertically. Figure 28b and 28c show how stacks of flow lines bend toward the stream channels. Vertical alignment of a section is controlled by proximity to the surface and to the stream channel. As discussed previously, the stream system induces a lateral flow in the system which increases in strength downstream until the flow gradients induced by the surface water body begin to dominate. The degree of offset from vertical shows in a qualitative way the relative strength of the lateral component of flow.

Figure 29 illustrates the three sections as they would appear in a three-dimensional perspective of the system; there are also two groups of pathlines that are included to show the relation between their orientation in the

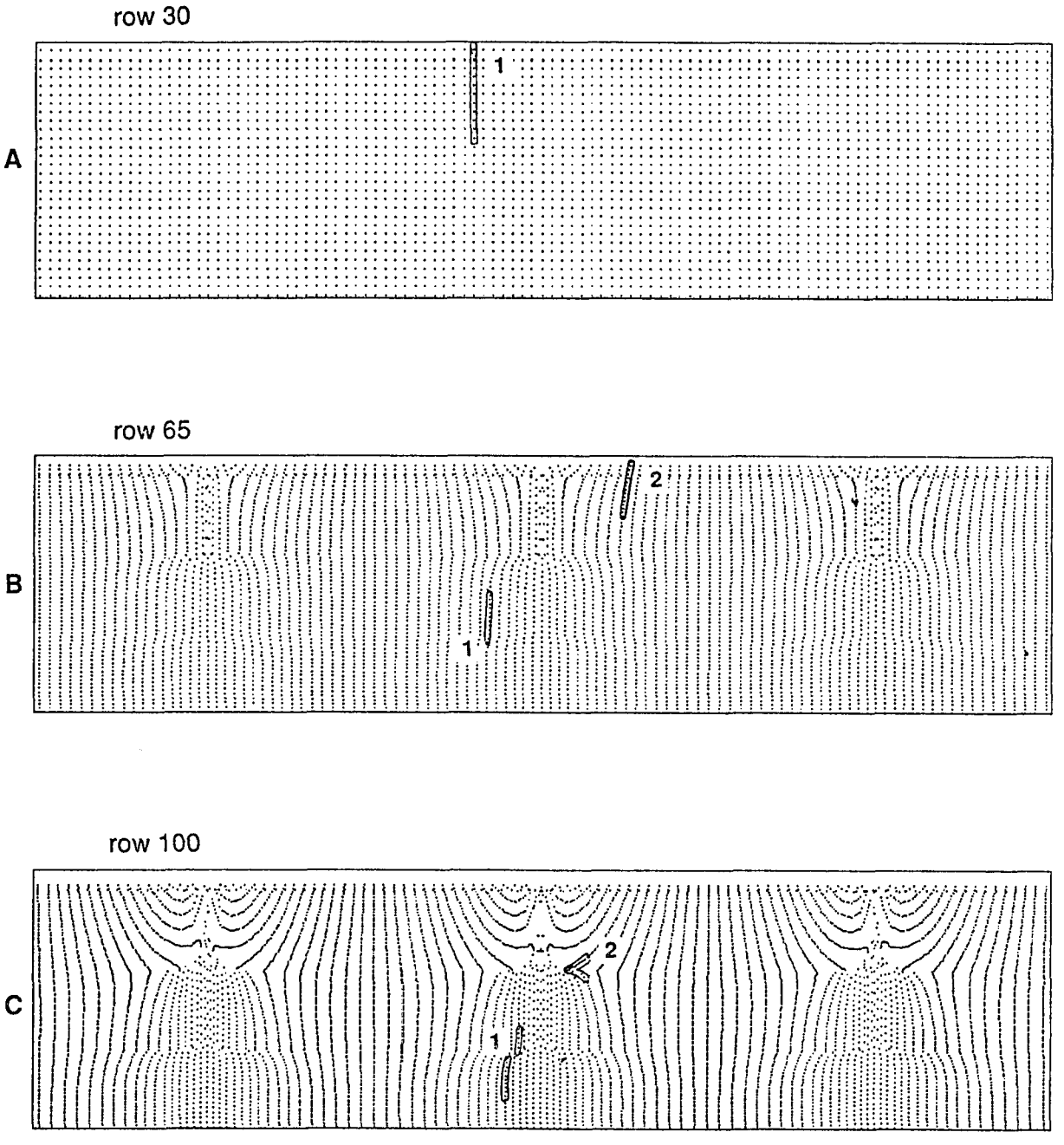


Figure 28--Three transverse sections through the modeled aquifer showing points where flowlines intersect the sections. (sections shown in 3-D perspective in figure 29.)

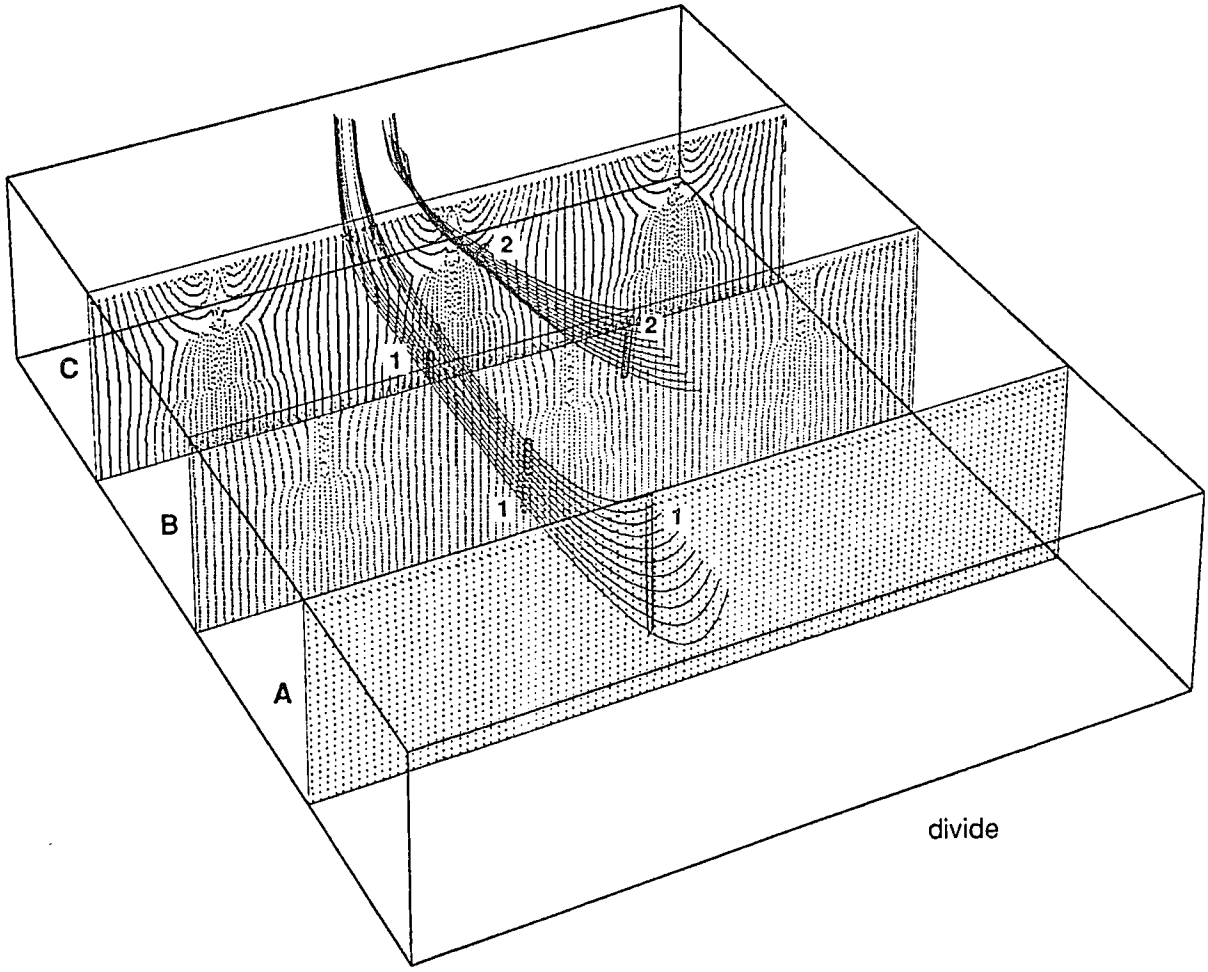


Figure 29--View of aquifer system from rear-upper-right showing the three transverse sections containing flowline intersection and orientation of two groups of flowlines.

aquifer and those of the previously described sections. The pathlines in group 1 (see figure 29), originating from an evenly spaced array of recharge points on the surface, appear in section A as a stack of points in a perfectly vertical column. Because this section is above the start-of-flow, the flow lines are not affected by stream sub-system flow and enter the aquifer following their linear recharge alignment.

In zones of the system where the effects of the stream on the adjacent flow field become more prominent, streamlines appear in a section as a string of points that bulge toward the stream channel. Note that where flow lines in group 1 intersect sections B and C their alignment patterns are affected by the stream sub-system flow. Flow lines of group 2, which originate in the system in an area close to the influence of stream flow, show a pattern that is tilted toward the stream in section B and a pattern that is acutely flexed toward the stream in section C.

*Residence times*

Residence time refers to the period during which groundwater remains in the aquifer between the moment it enters the system as recharge and the moment when it leaves as discharge. The concept of residence time has important applications with respect to the length of time that a contaminant plume migrates through the aquifer. It is also critical to understanding the chemical evolution of groundwater.

The previous discussions on flow patterns within the stream flow sub-system have indicated that discharge to streams can be composed of a mixture of groundwater that originates from very widely separated recharge areas and, hence, represents waters with a wide range of residence times.

The time for a particle to move through the system is easily calculated by the particle tracking algorithm from inter-cell specific discharge data that is used to calculate flow paths. Figure 30 shows contour lines of equal residence times for the reference simulation. The figure indicates how long it would take for recharge entering the system at a given point on the water table to move completely through the aquifer system. It is evident that residence times of water recharging the contributing area (shown as stippled) of the stream sub-system are strongly affected by the stream sub-system flow. The lines of equal residence time are markedly refracted where they cross the boundaries of the stream system.

The ages that are indicated by the lines within the stream contributing areas are consistent with the flow patterns previously discussed. Lines that virtually parallel the stream channel indicate relatively short residence times. The flow lines originating here would remain shallow and travel short lateral distances. With increased lateral distance away from the channel, the flow lines would travel deeper and farther down stream. This observation suggests also that residence time should increase outwardly away from the stream channel. Flow lines originating in the upper part of the stream contributing areas indicate much longer residence times. This is also consistent with the observation that

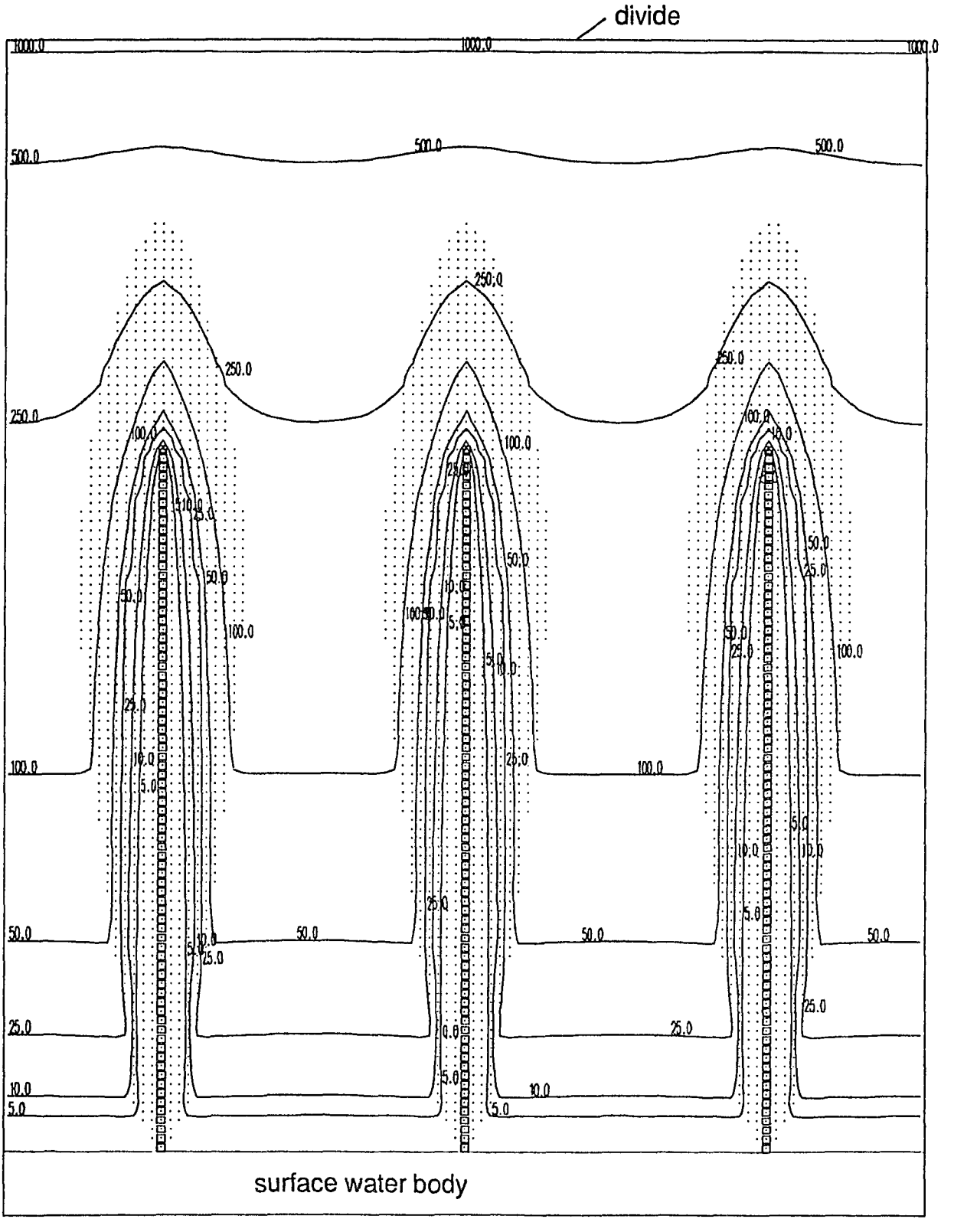


Figure 30--Map view of lines of equal residence time for recharge locations on the free surface. Stippling indicates stream source areas.

flow lines originating in this area travel deep into the system before discharging. Also the lines of equal residence time originating in this area have a similar pattern to the looping initial points in figure 23.

## SIMULATIONS OF OTHER HYPOTHETICAL SYSTEMS

The next aspect of the analysis involves studying the effects of selected parameter changes on the flow patterns and hydraulic characteristics of the stream sub-system. The hydraulic parameters and aquifer geometry of what has been called the "reference simulation" were selected because of their similarity to those of Coastal Plain systems. A reference system also serves as an index for comparing the series of simulations that are shown in this section which involves changes in parameters relative to those used in the reference simulation.

Table 1 lists these additional simulations along with the specific parameter changes. In general, a lower and higher value for each parameter relative to the value used in the reference case was used. The choice of values was, to some degree, arbitrary although generally the range of values falls within the realm of values found in the real world. However, several of the parameter values have no real-world analogues. For example, a purely isotropic system would be difficult to find as would streambeds with constant slopes. Clearly, the latter would not persist as an equilibrium configuration unless there were some structural control.

The values chosen do not necessarily represent extreme or limiting parameter values nor is there necessarily a linear progression of hydrologic and geometric characteristics between the simulated systems that assume these values and those of the reference system. The range over which a parameter

## LIST OF SIMULATIONS AND MODEL-IMPUT MODIFICATIONS

| Simulation | Recharge | Depth | Anisotropy | Stream Conductanc | Stream Density | Stream Slope |
|---|---|---|---|---|---|---|
| Reference | .0054 ft/day | 1200 feet | 1 :33 | 5000 $ft^2$/day | 3 | 0.1° constant |
| One stream | | | | | 1 | |
| Five stream | | | | | 5 | |
| Seven stream | | | | | 7 | |
| Thin | | 900 feet | | | | |
| Thick | | 1800 feet | | | | |
| Anisotropic | | | 1:100 | | | |
| Isotropic | | | 1:1 | | | |
| High recharge | .0066 ft/day | | | | | |
| Low recharge | .0044 ft/day | | | | | |
| High conductance | | | | 50,000 $ft^2$/day | | |
| Low conductance | | | | 500 $ft^2$/day | | |
| Low slope | | | | | | 0.05° constant |
| High slope | | | | | | 0.15° constant |
| Concave slope | | | | | | $z = (.0058)(e^{0.098x} - 1)$ |

table 1

can affect the flow system and the nature of that effect is determined by parameter sensitivity analysis, that is, the changing of a parameter value by increments and determining the corresponding response in the hydraulic heads of the aquifer (Gillham and Farvolden, 1974). Such an analysis is not within the scope of this study. However, an impression regarding how responsive the stream sub-system's hydraulic and geometric properties are to each of the listed parameters can, nevertheless, be gained.

Figure 31 shows the groundwater budget for each of the simulations including that of the reference case. Because of the imposed boundary conditions for these systems, discharge can only occur either to the simulated surface water body (flow to constant head) or to the stream system. As discussed earlier, slightly higher values of stream discharge occur for the left- and right- handed streams wheres the lowest stream discharge is observed for the central stream.

The basic geometric stream-basin relations are listed in table 2. In the following analysis the various distances are normalized to the respective watershed dimensions for easy comparison. The length of the watershed is taken to be the distance between the divide and boundary of surface water (123 500-foot row widths = 61500 feet) whereas its width is the full modeled width (103 500-foot column widths = 51500 feet). Aquifer depth is normalized to 1200 feet except for the shallow- and deep-system simulations. The stream contributing area is listed as a percentage of the total watershed area in table 2

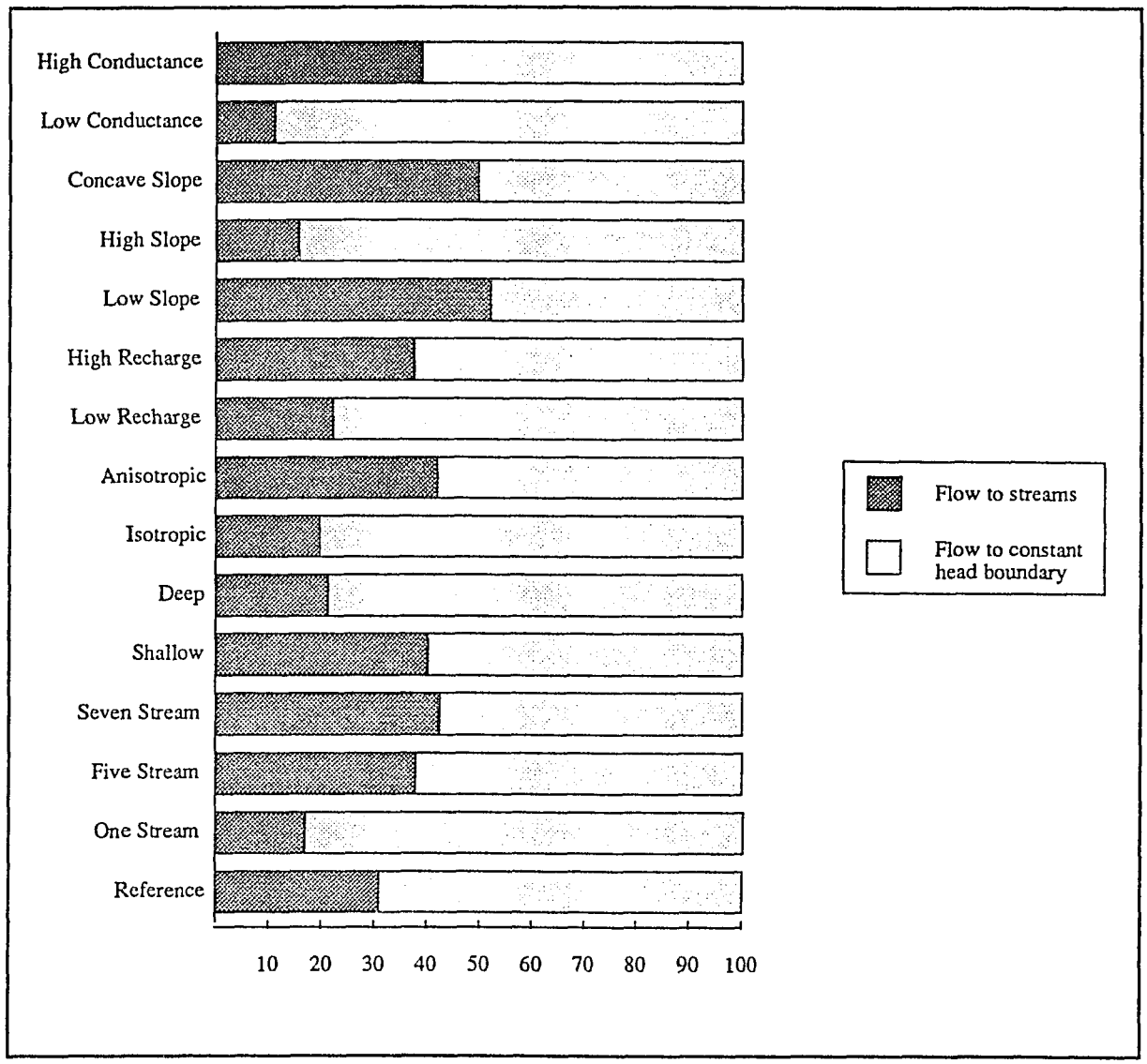


Figure 31--Comparision of proportion of simulated discharge to streams (head-dependent flux) and to the surface water body (constant heads) for hypothetical systems used in study.

# GEOMETRIC CHARACTERISTICS OF STREAM SYSTEMS IN DIFFERENT FLOW SIMULATIONS

| Simu-lation | Stream Length / Basin Length | Distan-ce from Divide | Strm Width / Basin Width | Source Area / Basin Area | Max Depth | Position of Max Depth | Pos of Start of Flow | Pos of Max Base flow |
|---|---|---|---|---|---|---|---|---|
| Reference | 0.84 | 0.16 | 0.17 | 30.9% | 0.59 | 0.56 | 0.37 | 0.82 |
| One stream | 0.93 | 0.07 | 0.28 | 16.8% | 0.73 | 0.46 | 0.27 | 0.74 |
| Five stream | 0.78 | 0.22 | 0.15 | 37.9% | 0.52 | 0.63 | 0.42 | 0.89 |
| Seven stream | 0.74 | 0.26 | 0.11 | 42.5% | 0.48 | 0.68 | 0.46 | 0.93 |
| Thin | 0.94 | 0.06 | 0.19 | 40.3% | 0.79 | 0.61 | 0.26 | 0.70 |
| Thick | 0.67 | 0.33 | 0.15 | 21.3% | 0.45 | 0.95 | 0.54 | 0.92 |
| An-isotropic | 0.83 | 0.17 | 0.24 | 42.0% | 0.54 | 0.73 | 0.3 | 0.85 |
| Isotropic | 0.99 | 0.01 | 0.09 | 19.8% | 0.98 | 0.93 | 0.45 | 0.76 |
| High recharge | 0.89 | 0.11 | 0.17 | 37.6% | 0.65 | 0.64 | 0.27 | 0.75 |
| Low recharge | 0.75 | 0.25 | 0.12 | 22.2% | 0.53 | 0.93 | 0.52 | 0.9 |
| High conduct | 0.88 | 0.12 | 0.22 | 39.1% | 0.72 | 0.89 | 0.44 | 0.85 |
| Low conduct | 0.79 | 0.21 | 0.07 | 11.3% | 0.24 | 0.57 | 0.22 | 0.8 |
| Low slope | 0.75 | 0.25 | 0.12 | 52.0% | 0.53 | 0.93 | 0.52 | 0.9 |
| High slope | 0.59 | 0.41 | 0.09 | 15.7% | 0.45 | 0.79 | 0.65 | 0.94 |
| Concave slope | 0.95 | 0.05 | 0.2 | 49.7% | 0.82 | 0.63 | 0.2 | 0.63 |

table 2

and is identical to the percent of volumetric flow leaving through the stream system.

Finally, some comments are needed regarding the figures that depict three mutually perpendicular views (figure 13, page 52) for each simulation: These figures include one lengthwise section, three transects of the stream system, and the outline of the source area for each simulation. The lengthwise profile is defined by one path line herein referred to as the streamline of symmetry. With respect to the sections that are perpendicular to the stream channel, the middle section is located across the stream's widest contributing area; and the other two transects are placed midway between the widest contributing area section and the extremes of the system. As the lengths vary considerably for each simulation, so do the positions of the transects.

**Effect of surface water body on stream system configuration**

The incorporation of a large water body into the hypothetical reference system was necessary in order to induce a general, regional gradient in the systems flow field. The effect of the water body on the system is simulated by simply setting the nodes at the lower end of the model to a low constant-head value. Under these conditions recharge that is continuously applied over the aquifer would cause the free surface to mound, the heads of which would be everywhere higher than heads of the surface water body (assuming sufficient recharge). When a stream system is included in the simulation, groundwater is diverted to the streams. Although streams lower the gradients of the water table,

a flow field is, nevertheless, created whereby groundwater is drawn to both the water body and the streams. The combined effect of the two sinks work together to create a boundary surface around stream sub-system flow that is unique to this system. The stream sub-system configuration is a signature that is, in part, a hydraulic response to the specific boundary conditions of this system. It will be shown how the alteration of different aspects of these boundaries (as well as some aquifer properties) will translate into a different stream system configuration.

Because the surface-water body exerts significant control over the flow in the system, its effect on the stream system needs to be evaluated. In order to evaluate the nature of this effect a simulation was made of a drainage system without the water body. Figures 32 through 35 show hydrologic and geometric features of such a hypothetical system, herein referred to as the 'no-flow' system. This system is identical to that of the reference system in all other respects. Although this system is rather contrived, inasmuch as there are no regional discharge outlets, it demonstrates pertinent hydrologic concepts for systems of this study. For this 'no-flow' system the stream configuration is constrained by five sides of a rectangle, each side representing a no-flow boundary.

Intuitively, it would appear that each stream sub-system flow domain should occupy about one third the volume of the aquifer system (the middle stream system actually occupies a smaller volume due to discretization effects). The lateral and bottom boundaries of each stream system should be flat as they

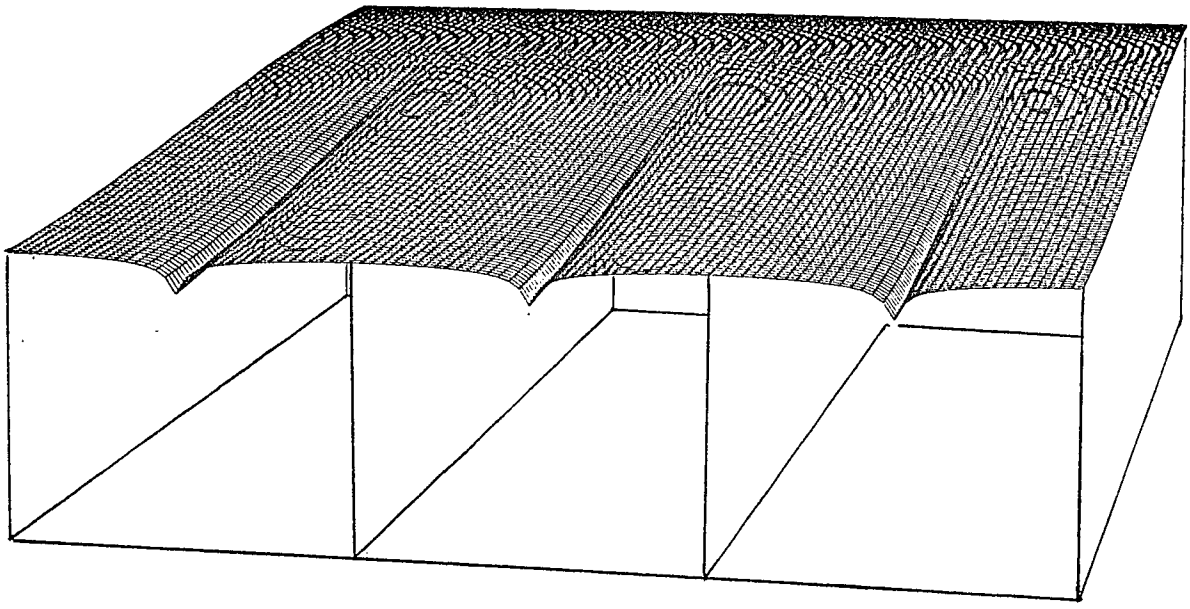

Figure 32--Bounding surfaces containing three stream sub-system flow domains in a rectangular aquifer in which surface-water body (constant-head sink) is not simulated.

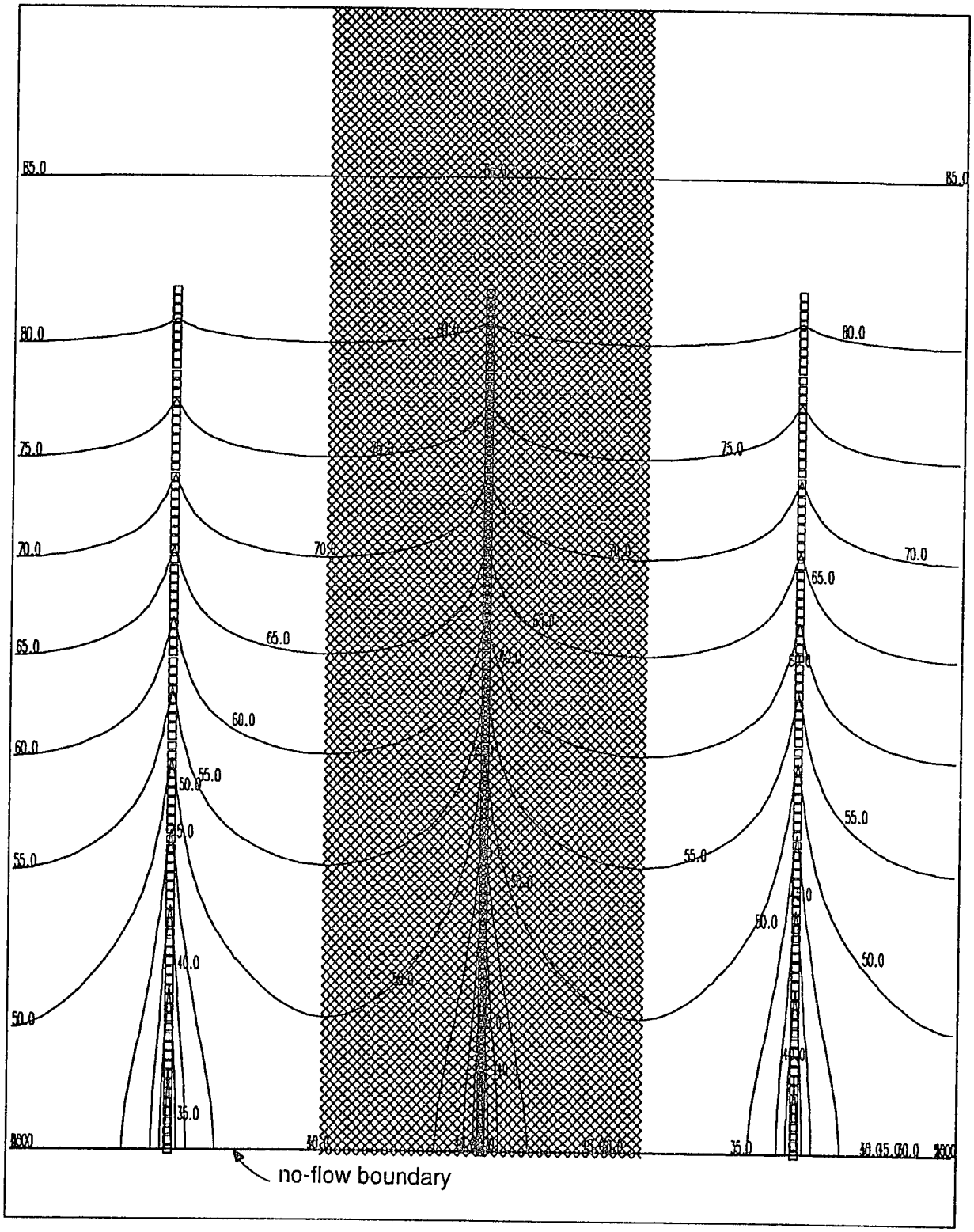


Figure 33--Map view showing lines of equal elevation head for a three stream system without a constant-head sink. Hatched pattern indicates source area of center stream; blank areas are sources of flow to respective lateral streams.

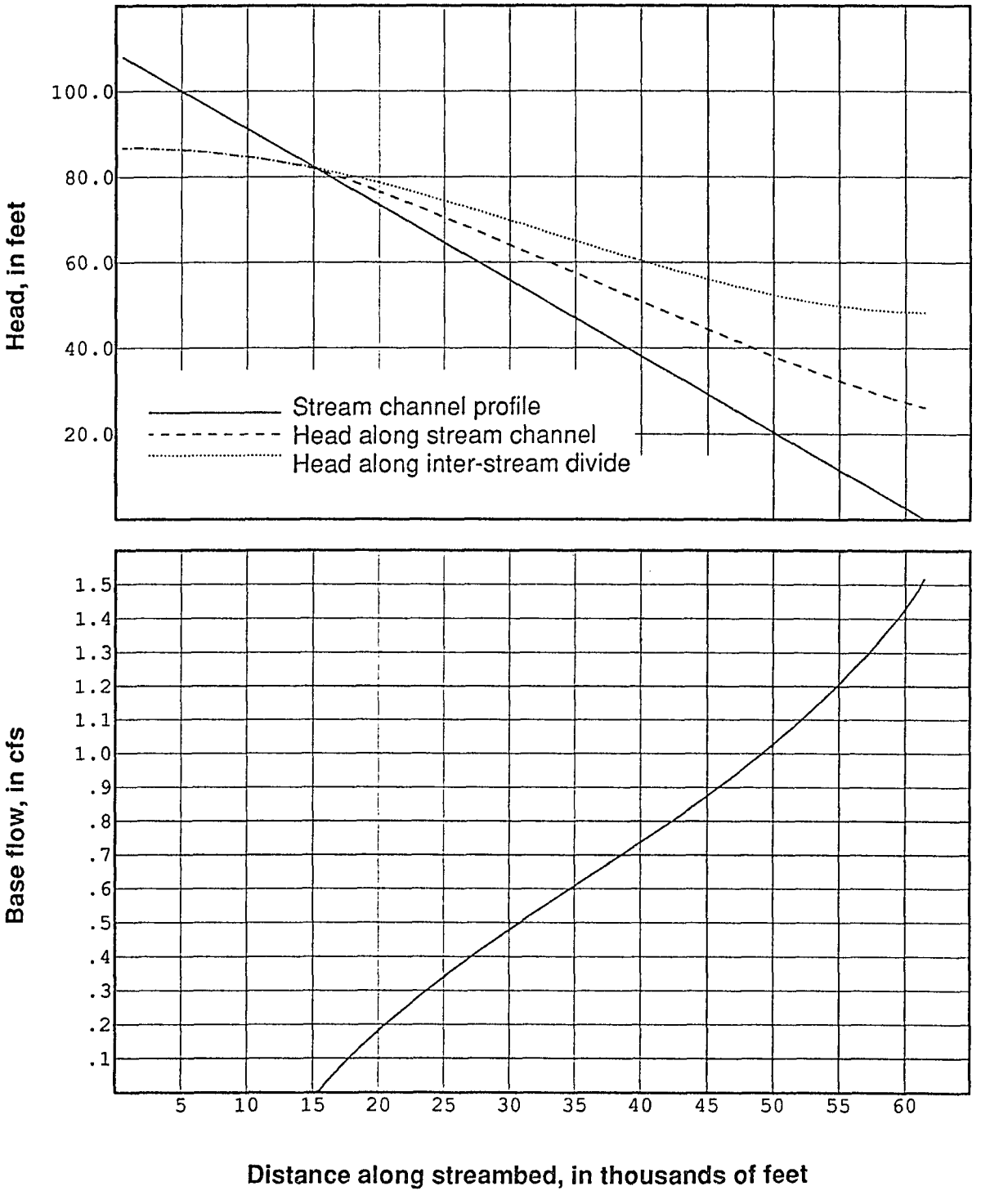


Figure 34a--Profiles of water table along stream channel and inter-stream divide for three-stream system without surface-water body.

Figure 34b--Profile of groundwater discharge to center-stream channel (along model column 52) for three-stream system without surface-water body.

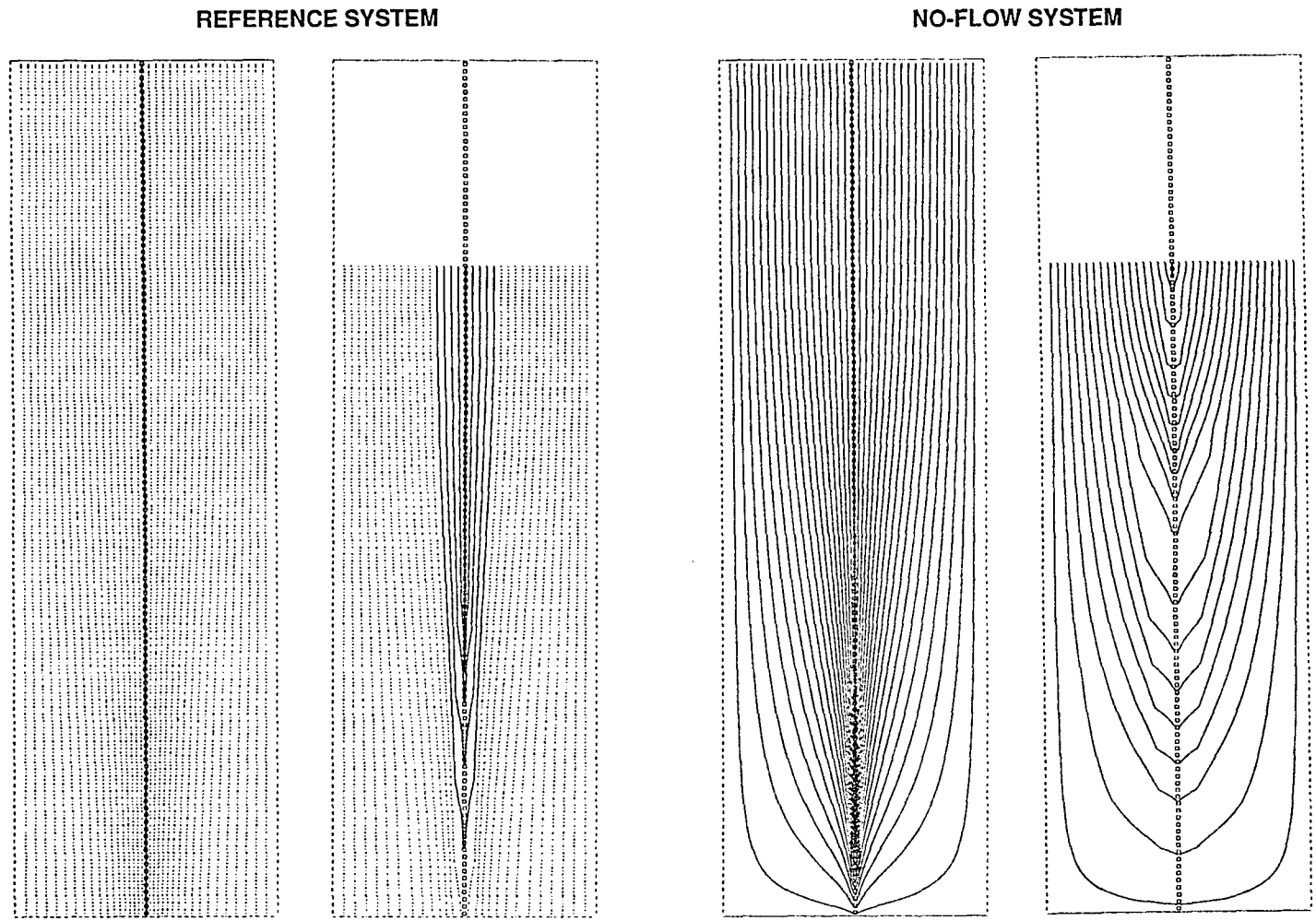


Figure 35--Map view of pathlines that enter the reference and no-flow systems along column one and column thirty. View is between the inter-stream divides for the center stream. Solid lines show flow discharging to stream; dotted lines indicate pathlines that discharge to the water body.

are constrained by the planar, no-flow hydraulic surfaces. Figure 32 shows this simple stream sub-system geometry. As in the reference simulation the free surface of this system reflects the discharge along the stream channel except that the contributing area would have a rectangular shape.

The head distribution of this simulation is shown in figures 33 and 34a. In the area from the divide to the middle of the system the water table assumes the characteristic shape of unconfined flow but, because there is no sink across the lower end of the model, the head profiles (parallel to the y-axis) do not fall off at the increasing rates that are typical of the reference system but, instead, fall off at decreasing rates. The base flow, which begins at about 0.23 from the divide, increases at a decreasing rate but then increases up to the terminus (figure 34b). Head profiles along the y-axis of the system are relatively flatter than for those of the reference simulation. The difference in head between the divide and stream terminus is 60 feet in the channel and 38 feet along the inter-stream divide in this system; for the reference system they are 76 and 72 respectively. However, near the mouth of the streams in the direction of the no-flow boundary, there is a head difference of 21 feet between inter-stream divide and channel compared to a 3.6 feet difference for that of the reference system. The 21 foot difference in heads between channel and inter-stream accounts for high discharge along the lower reach of the streams. Clearly, the high heads in the lower end of this system could not develop adjacent to the water body.

Another effect that the no-flow boundary imparts on the flow patterns of the system is shown in figure 35. The figures compare a line of path lines

originating along columns 1 and 30 of both the reference and no-flow systems. Path lines terminating in the water body (reference system only) are shown as dotted lines. Path lines in the reference system tend to be relatively straight and closely spaced irrespective of their destination. The lines will converge more strongly as they approach the discharge zone. Path lines of the no-flow system, however, tend to make strong directional changes as they approach the discharge zone. This is especially true of path lines originating closest to the inter-stream divide. The spacing of path lines is greatest closest to the no-flow boundary and suggest that groundwater velocities near the no-flow and inter-stream boundaries are extremely slow or virtually stagnant.

Another effect of the no-flow boundary is that flow is forced to discharge further upstream than is the case for the reference system. A comparison of path lines on column 30 of both systems will show that equivalent path lines that discharge to the stream system terminate at nodes higher on the stream channel in the no-flow system.

Other aspects of flow line geometry, such as the confluence of shallow and deep path lines at common points in the discharge zone, the concentric banding and nesting of inner stream lines discussed for the reference system, hold true for this system as well. Flow lines that originate near the divide wrap around the system and discharge near the terminus.

In contrast, the bounding surface of the reference system is quite different. The upstream end of the reference stream sub-system is shaped like the tip of a spoon. The path lines that originate in the divide and corner portions

along the inter-stream divide become entrained in the flow field that discharges to the water body. In the no-flow system this same recharge would discharge to the streams. The outline of the stream contributing area and the stream system boundary comprise, in effect, an interface formed by flow fields discharging to different sinks. The streams' flow system is constrained by the boundary of flow that is part of another sub-system.

The outline of the reference system along transects to the stream (figure 13) show that the edge is rounded along the bottom; this shape is, to some degree, a mirror of the outline of the upstream catchment area of the stream system. Corresponding irregularities along the section perimeter can be traced back to the edge of the catchment area via connecting path lines. Therefore, the shape of the bottom of the stream sub-system represents a zone of interaction between two sinks.

Sections and perspective views of the reference system show a relatively flat side starting at about 0.51 from the divide that becomes progressively wider with distance downstream (figure 15). The width of the stream section also becomes more narrow with distance toward the mouth. The relative flatness of the bounding surface in this zone suggest that influence from the hydraulic surfaces on the stream system's flow configuration becomes more dominant in the lower part of this aquifer system. Thus, the stream sub-system flow boundary appears to be an interface between two flow sub-systems in the upper end of the aquifer and influenced more by hydraulic surfaces toward the lower end of system.

**Anisotropy**

The anisotropy of porous material refers to the difference in water transmitting properties between the vertical and horizontal directions of flow. Aquifer conductivity in the vertical direction of flow reflects, in part, layered deposition and subsequent compaction of the sediments that comprise the aquifer. While aquifer conductivity can vary with azimuthal direction due to preferential fracturing or solution of aquifer material, variation between horizontal and vertical directions is regionally more prevalent.

Layered aquifer systems can show appreciable vertical to horizontal anisotropy when there are large conductivity contrasts between layers. The effect of composite vertical conductivity is typically represented as 'layers in series', that is, the sequential alignment of two or more prisms of material in the direction of flow. Layers in series are described by equivalent conductance or the harmonic mean. On the other hand, composite horizontal conductivity is represented as 'layers in parallel' that is described by an arithmetic mean. Because layered aquifer systems typically have large contrasting conductivities, their arithmetic mean is generally larger than their harmonic mean and, therefore, their vertical to horizontal anisotropy is large.

The ratio of horizontal to vertical conductivities can vary widely. The reference system assumes a 33:1 anisotropy and falls within the range of typical values for sand-silt material. The two simulations discussed in this section were modified by setting horizontal to vertical conductivities to 1:1 (isotropic) and 100:1 respectively. Real isotropic systems are rare because all sediments

compact in time. Nevertheless, a purely isotropic system was used in order to demonstrate the degree to which the anisotropic ratio can control stream sub-system geometry.

A comparison of the contributing areas of flow for both systems shows strongly contrasting geometries. Figure 36 shows the contributing area for streams of the anisotropic system; stream contributing areas are wider and have less inter-stream distance at their widest section then for those of the reference. The maximum width of each area in the anisotropic system is 0.24 with an inter-stream distance of 0.09 (compared to 0.18 width and 0.15 inter-stream distance for the reference system). The percentage of watershed area that forms the contributing area to stream is 42%, which is 10% greater than that of the reference system. Figure 37 shows the isotropic system's long and narrow stream source areas as having considerably more distance between them. The length virtually spans the length of the watershed (0.99). Its maximum width is 0.09 and inter-stream width is 0.24, just the reverse of the widths found in the anisotropic system.

Figure 38 shows the three mutually perpendicular views of the center stream for the anisotropic system. The cross-sectional views indicate that the stream sub-system flow does not penetrate the groundwater zone as deeply as does that of the reference system. In contrast, the cross-sectional views of the isotropic system shown in figure 39 show that its stream system penetrates deep into the aquifer, almost to the full depth. The path lines that travel deepest are constrained by the aquifer thickness and by the position of the divide. The

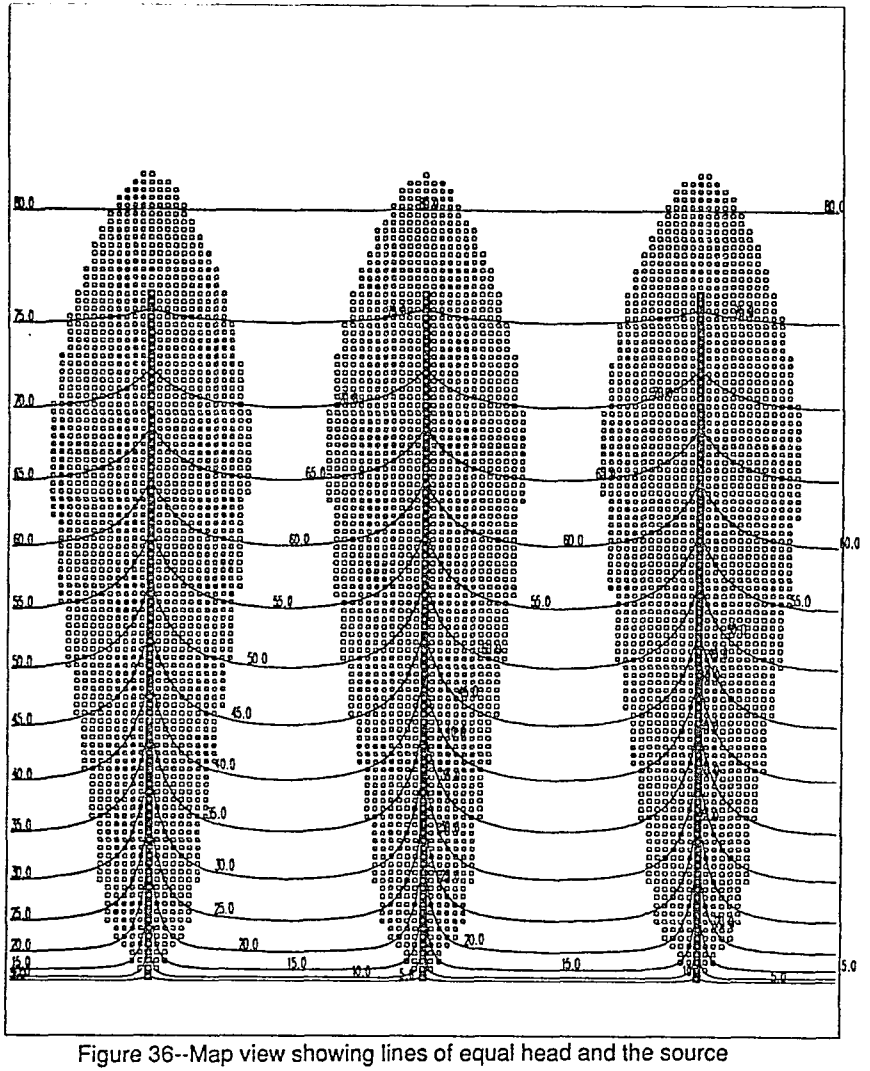


Figure 36--Map view showing lines of equal head and the source areas of streams on the free surface for the **'anisotropic'** simulation. Squares along stream channels indicate where groundwater discharge occurs. Octagons indicate that model cell is at least partially a source for stream discharge.

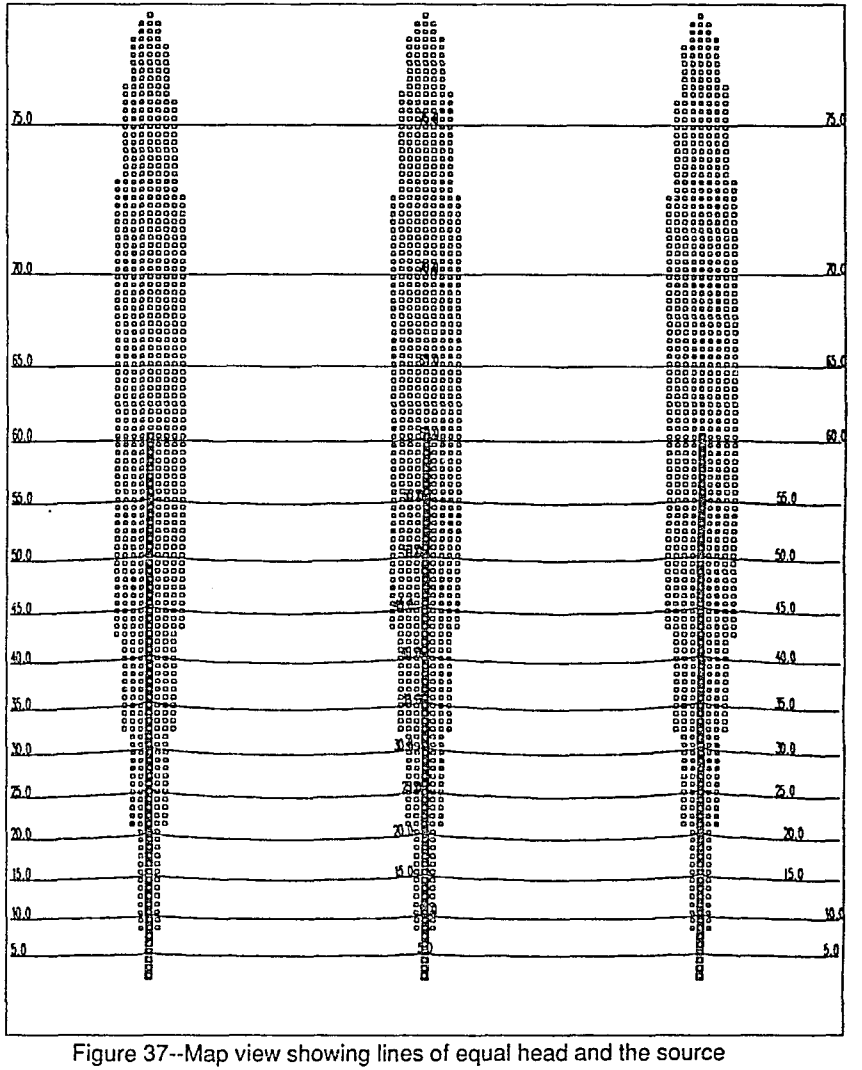


Figure 37--Map view showing lines of equal head and the source areas of streams on the free surface for the **'isotropic'** simulation. Squares along stream channels indicate where groundwater discharge occurs. Octagons indicate that model cell is at least partially a source for stream discharge.

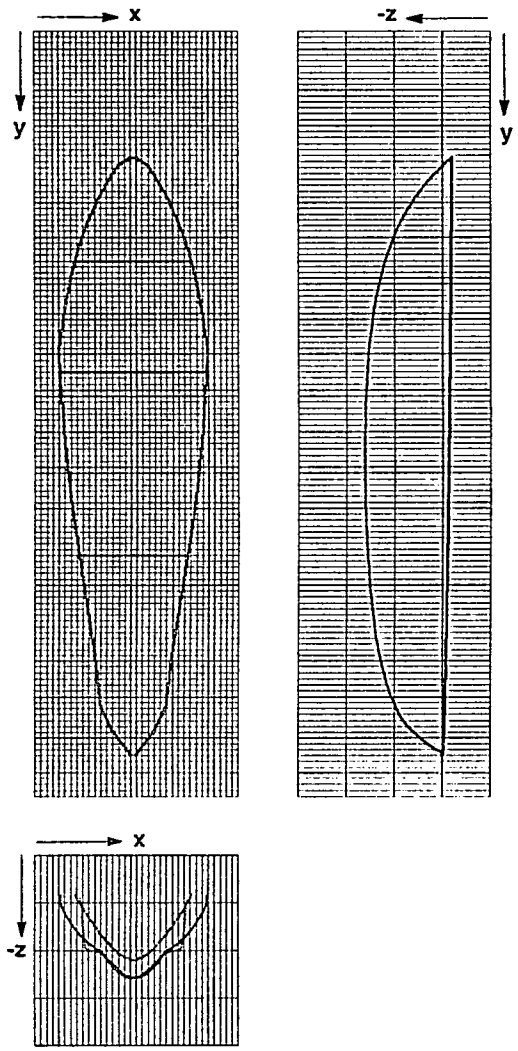


Figure 38--Profiles of bounding surface for the center stream sub-system flow for the '**anisotropic**' simulation viewed along each of the three Cartesian coordinate axis.

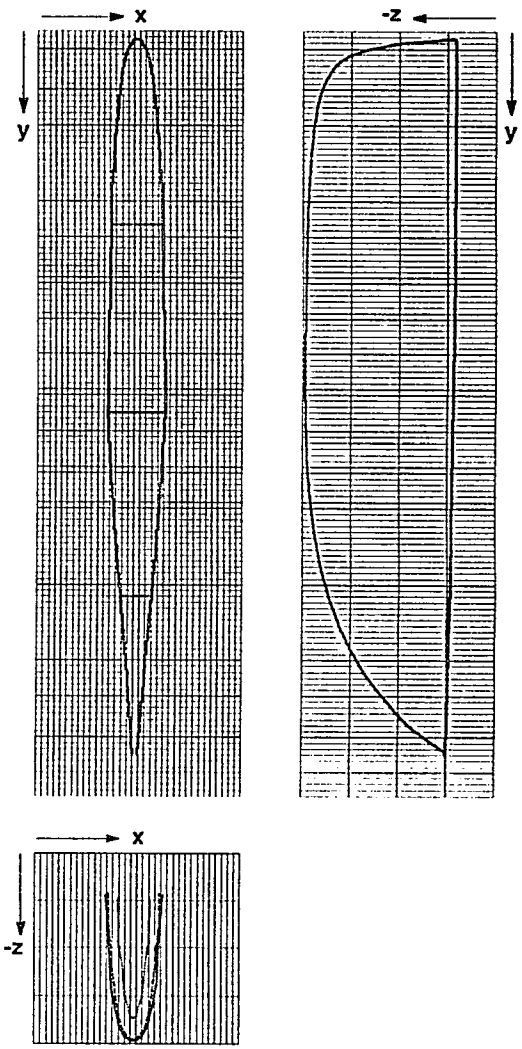


Figure 39--Profiles of bounding surface for the center stream sub-system flow for the '**isotropic**' simulation viewed along each of the three Cartesian coordinate axis.

relatively high vertical conductivity of the isotropic aquifer causes the stream sub-system to propagate downward at the expense of the contributing area. In contrast, the low vertical conductivity of the anisotropic systems inhibits vertical propagation of the stream system but causes areal expansion near the free surface. From these simulations it appears that high anisotropic values may contribute to coalescence of stream catchment areas in multiple stream systems.

A sense of the hydraulic behavior of each system can be gained by looking at the water-table contours. Figure 36 shows a pattern similar to the reference but with contour lines bending more steeply as they cross the stream channels. Following the discussions for the reference system, this observation suggests that the lateral component of flow (in the x-direction) adjacent to the stream is strong. By comparison, the contour lines of the isotropic system (figure 37) are only slightly deflected at the intersection of the channel indicating a much weaker lateral flow component. The base flow and head profiles of the stream system are consistent with this (figures 40 and 41). The base flow curve for the anisotropic system shows higher discharge over a longer reach of stream than for the isotropic system; the start-of-flow begins at about a third the way from the divide (0.3) compared to almost halfway down (0.45) for the isotropic system. The maximum base flow for the anisotropic simulation is 0.44 cfs and occurs about 0.85 from divide whereas maximum base flow for the isotropic system is only about 0.27 cfs at 0.76 from the divide.

Figures 40a and 41a show the head profiles based on simulation of the 'non-drainage' system for the corresponding anisotropy values. Following the

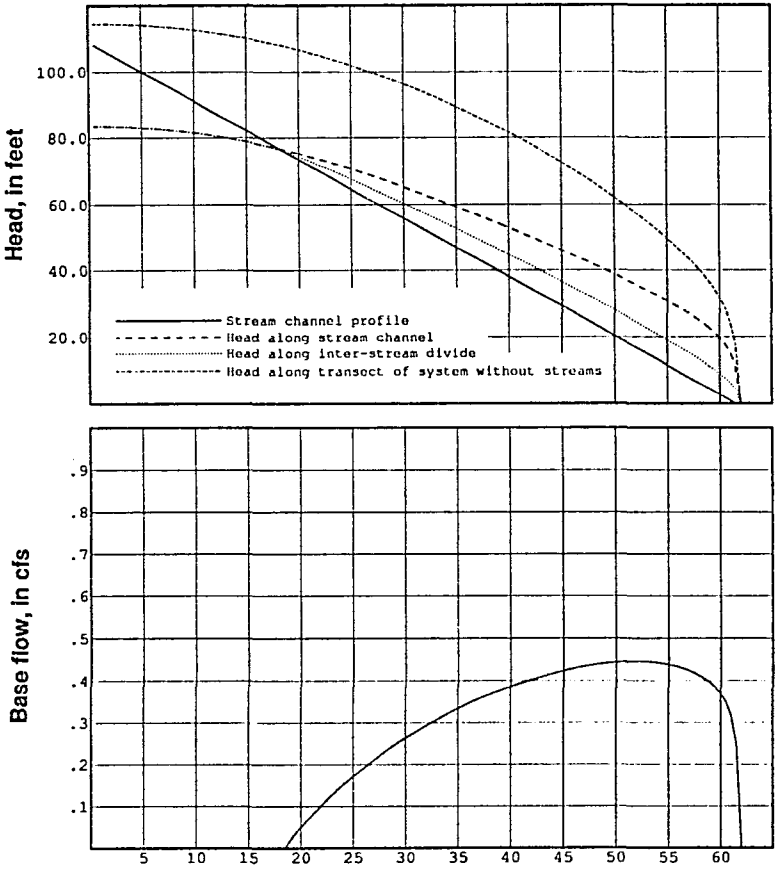


Figure 40a--Profiles of water table along stream channel and inter-stream divide for the '**anisotropic**' simulation and typical profile for corresponding non-drainage simulation.

*Figure 40b--Profile of groundwater discharge to center-stream channel* (along model column 52) for '**anisotropic**' simulation.

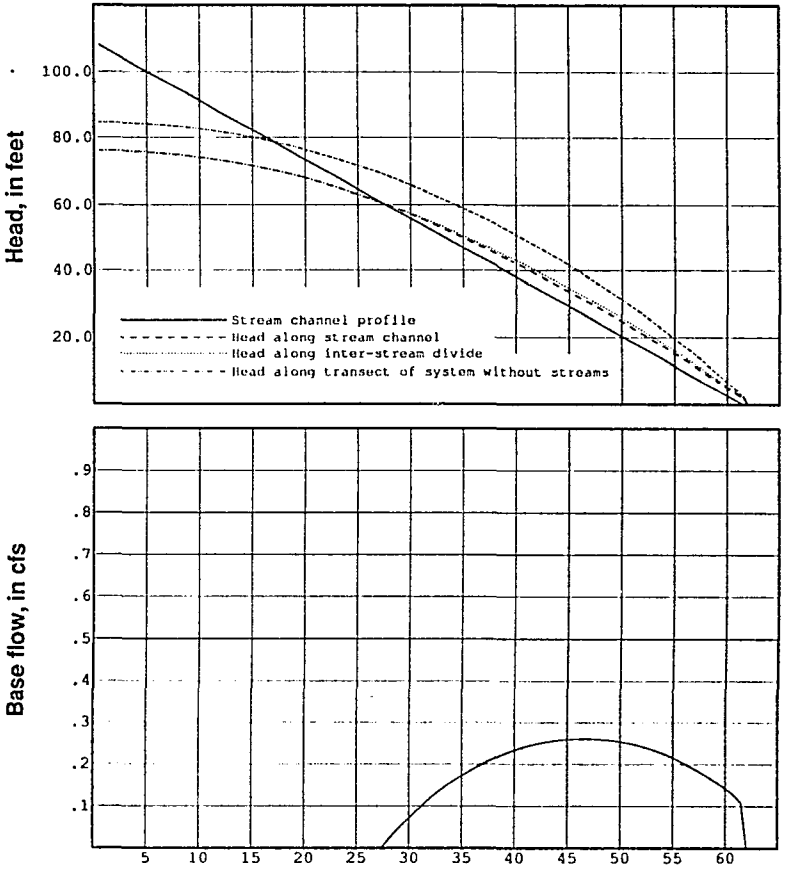


Figure 41a--Profiles of water table along stream channel and inter-stream divide for the '**isotropic**' simulation and typical profile for corresponding non-drainage simulation.

Figure 41b--Profile of groundwater discharge to center-stream channel (along model column 52) for '**isotropic**' simulation.

earlier discussion that head profiles represent the potential energy in the system, the anisotropic system has a higher energy then the corresponding system that is isotropic. Consequently, the dissipated energy is greater in the anisotropic system as is seen by greater differences between drainage system heads and 'non-drainage' heads. This energy release is shown in the model budget which indicates that total flow to the stream system accounts for 40% of recharge in the anisotropic system but only 20% in the isotropic.

**Recharge**

The recharge rate of 0.0054 feet/day used for the reference simulation represents an average recharge in Atlantic Coastal Plain areas. The next two simulations involve increasing and reducing this rate by 20%. A steady-state simulation made with either a 20% recharge reduction or increase would represent the equilibrium flow configuration resulting from the continuous, steady-state application of these lower or higher recharge rates.

The interruptions of average recharge periods by unusually wet years or periods of drought are not shown by these simulations. Wet and dry spells are climatic conditions that represent temporary departures from more average, persistent conditions. In reality, if a system experiences a departure from the average recharge, such as would occur during several years of drought, the aquifer would respond continuously by adjusting its flow; the system would tend toward, and eventually attain, a new equilibrium state as long as the abnormal recharge rate persists.

Different recharge rates affect the size and shape of the catchment area of flow to streams as figures 42 and 43 illustrate. Higher recharge rates generate a longer and wider stream source area, that is, a larger area of the watershed contributes to stream flow when compared to streams of lower recharge rates (see table 2). The shapes of the upstream ends of each system are also quite different. The most upstream stream recharge area of the high-recharge system is rounded and arch-shaped compared to the pointed, V-shape of the low recharge system.

In figures 44 and 45 the cross-sectional views show that the high-recharge system reaches a maximum depth at almost 800 feet below datum (and constitutes 0.65 of aquifer thickness) whereas the low-recharge system is more shallow going to slightly more than 700 feet (0.53 of aquifer thickness). The longitudinal streamline of symmetry of each system also delineates a distinctive profile at the upstream end; the low-recharge profile forms a narrow, tapered wedge at the upstream end whereas the high-recharge profile is wider and fuller (figure 45).

The larger contributing areas and their rounder, fuller configurations in the high-recharge stream system is indicative of stronger discharge. Inspection of head contours, head profiles, and base flows show this to be the case (figures 46 and 47). Table 2 shows that recharge to streams is 37% for high recharge compared to 22% for the low-recharge system. The position of the start-of-flow for the high-recharge system is closer to the divide than for the lower-recharge system.

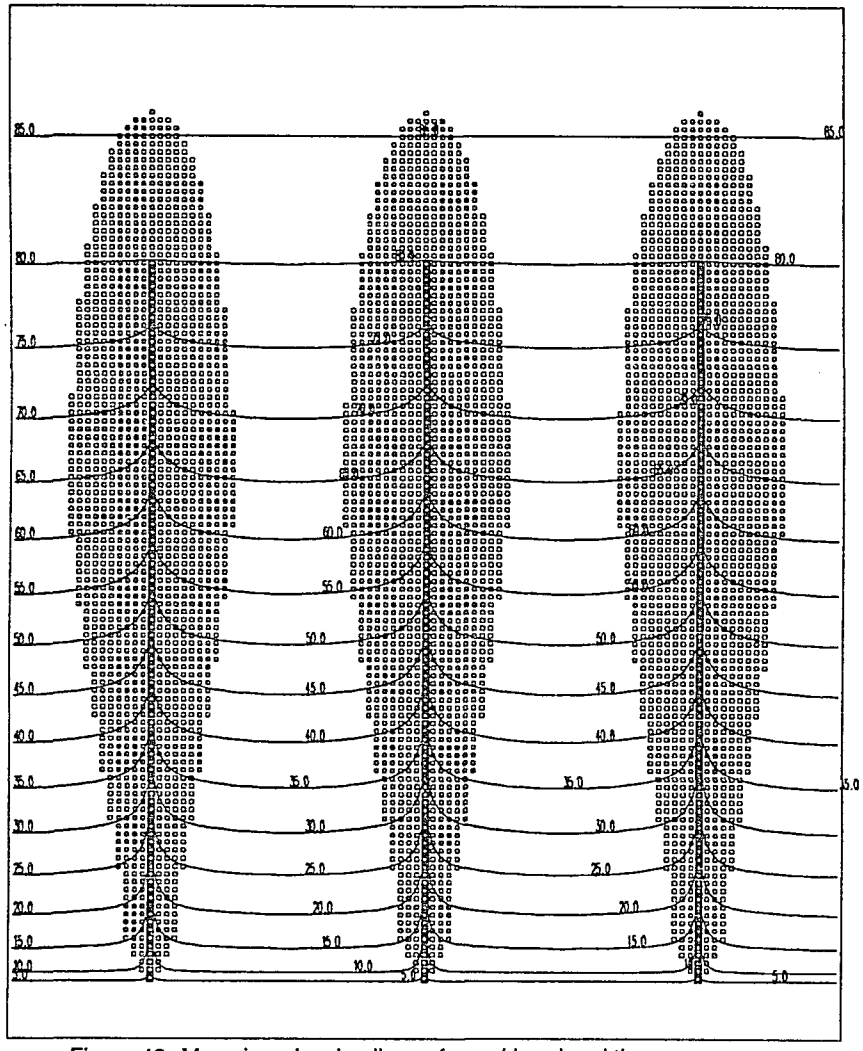

Figure 42--Map view showing lines of equal head and the source areas of streams on the free surface for the '**high recharge**' simulation. Squares along stream channels indicate where groundwater discharge occurs. Octagons indicate that model cell is at least partially a source for stream discharge.

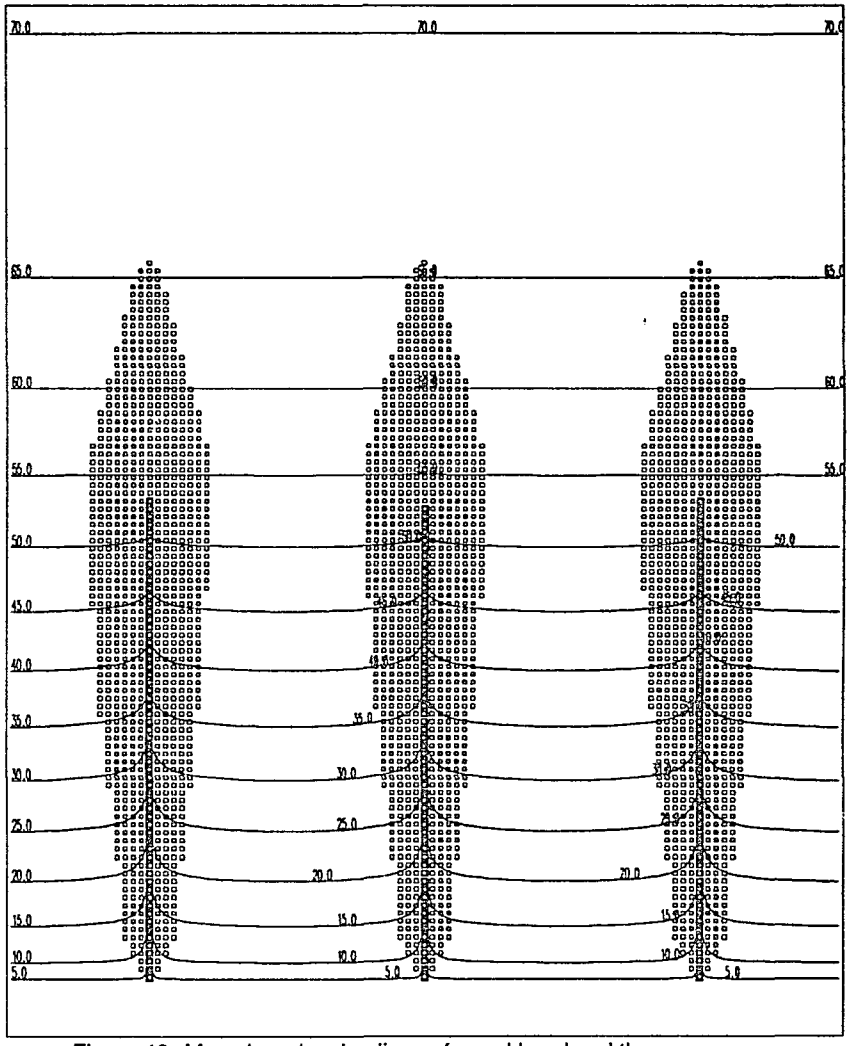

Figure 43--Map view showing lines of equal head and the source areas of streams on the free surface for the '**low recharge**' simulation. Squares along stream channels indicate where groundwater discharge occurs. Octagons indicate that model cell is at least partially a source for stream discharge.

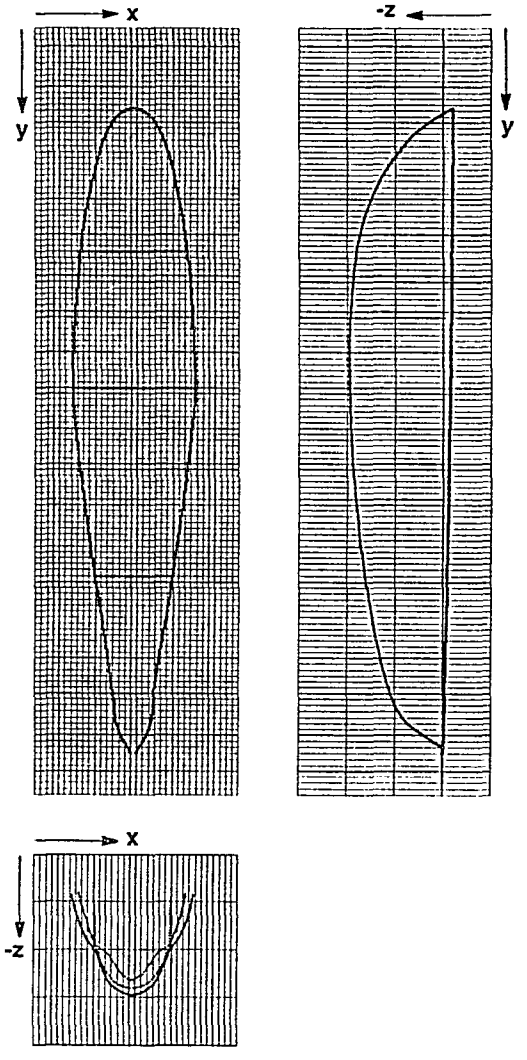


Figure 44--Profiles of bounding surface for the center stream sub-system flow for the '**high recharge**' simulation viewed along each of the three Cartesian coordinate axis.

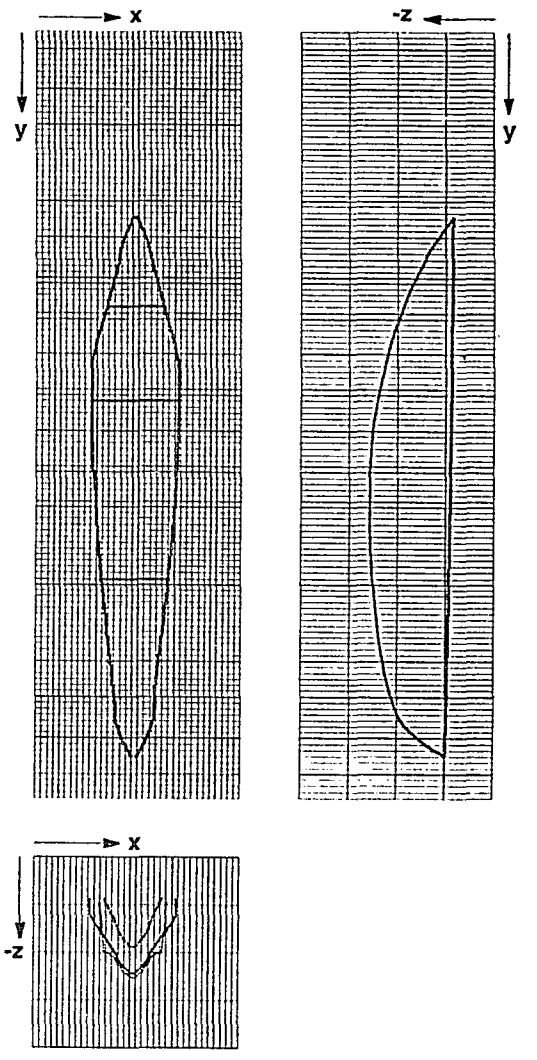


Figure 45--Profiles of bounding surface for the center stream sub-system flow for the '**low recharge**' simulation viewed along each of the three Cartesian coordinate axis.

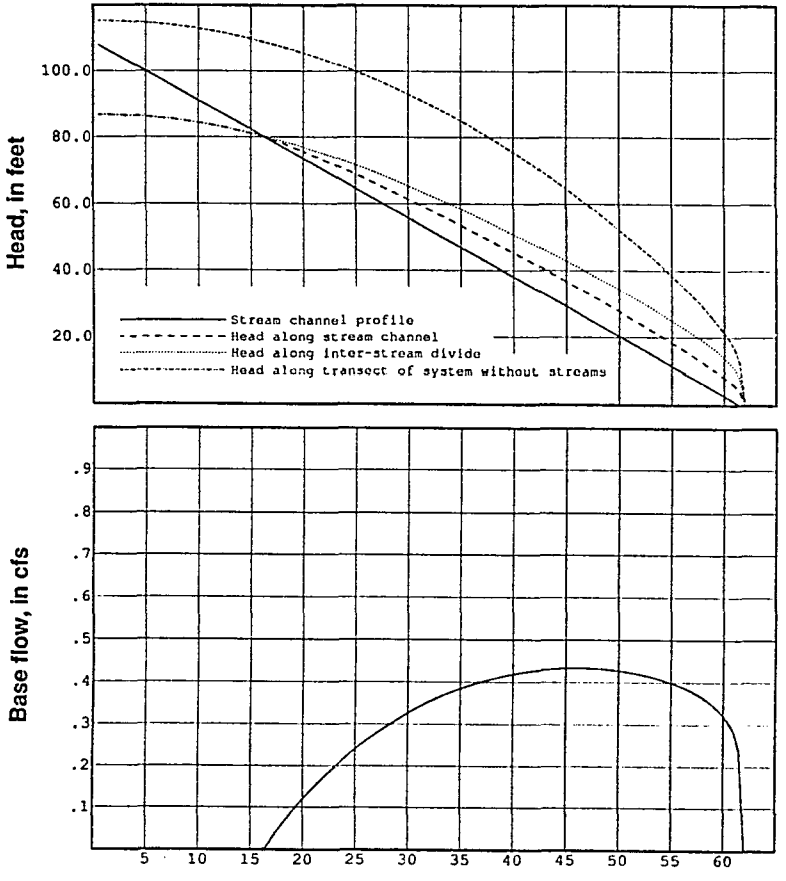


Figure 46a--Profiles of water table along stream channel and inter-stream divide for the '**high recharge**' simulation and typical profile for corresponding non-drainage simulation.

Figure 46b--Profile of groundwater discharge to center-stream channel (along model column 52) for '**high recharge**' simulation.

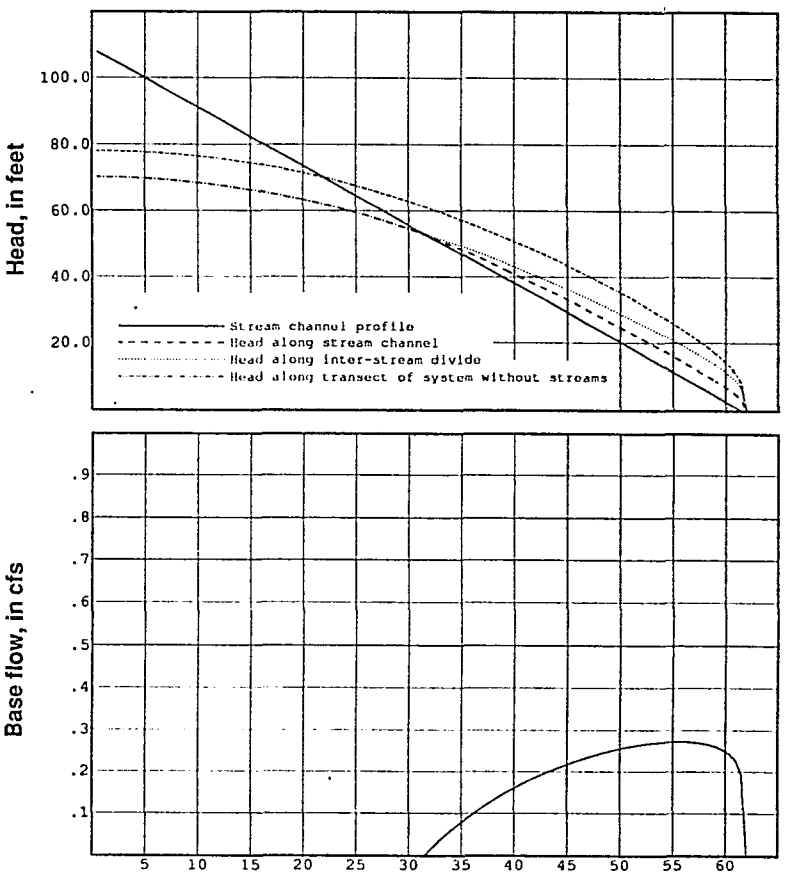


Figure 47a--Profiles of water table along stream channel and inter-stream divide for the '**low recharge**' simulation and typical profile for corresponding non-drainage simulation.

Figure 47b--Profile of groundwater discharge to center-stream channel (along model column 52) for '**low recharge**' simulation.

The 'non-drainage' profiles for each of these systems show how the energy level is raised or lowered in each system similar to those of the anisotropic systems. There is greater dissipation of energy in the high-recharge system than for the low-recharge system. This is not surprising inasmuch as equation (3) shows that aquifer conductivity and recharge are inversely related.

Whereas capture areas for streams contract at lower recharge rates, capture areas for 'fixed' discharge entities, such as wells, expand at lower recharge rates. This seemingly paradoxical behavior of the capture areas is explained by the nature of the sinks involved. In the case of the stream, discharge depends on head differences between the free surface and the streambed elevation (in a water-table aquifer). Because lower recharge rates result in lower heads, discharge to the stream is also correspondingly lower. The lower discharge requires less of a capture area as is demonstrated by the above simulations. Wells, in contrast, have a fixed discharge rate. As recharge rates are lowered, wells must tap larger source areas to compensate for the diminished recharge rate per unit area of free surface in order to insure mass balance in the system.

**Aquifer Thickness**

The thickness of an aquifer plays an important part in constraining flow in a system. The analytical solutions of Toth discussed earlier show how the flow of thin systems propagated deeper into the aquifer as thickness is increased (Toth, 1963). Conversely, thin aquifers constrain the depth to which regional flow can

descend and cause thin flow sub-systems to 'tap' into a larger catchment area on the free surface. Examples of thick and thin aquifer systems found in the Atlantic Coastal Plain is Long Island's groundwater system and Upper Rancocas Drainage Basin in Central New Jersey, respectively. These systems will be discussed in a later section.

Figures 48 and 49 show the contributing areas of flow and water table position for a simulated thin and thick system. The thin system was set at half the thickness of the thick system. The former represents a 25% reduction over the thickness of the reference simulation whereas the latter is 50% deeper.

The basic differences in size and shape of the contributing areas found in low- and high-recharge systems and between isotropic and anisotropic systems are also evident for the thin and thick systems. The contributing areas for the thin system are longer (0.94 of watershed length) and wider (0.19) than for those of the thick system, extending up to within 0.06 feet of the divide. By contrast the thick system is over 0.33 from the divide. Also, the shape of the upstream tip of the thin system is round and dome-like compared to the wedge-like shape in the thick system. A comparison of percentage of water table area that forms the contributing area for each of these simulations shows that the thin system is virtually double that of the thick system (see table 2).

Figures 50 and 51 show the three sectional views. The sections have been adjusted to show the aquifer thickness used for these simulations. The view of the thin system's lengthwise section indicates that the stream line of symmetry is close to -700 feet (0.79 of a 900 foot thick aquifer) in the aquifer and

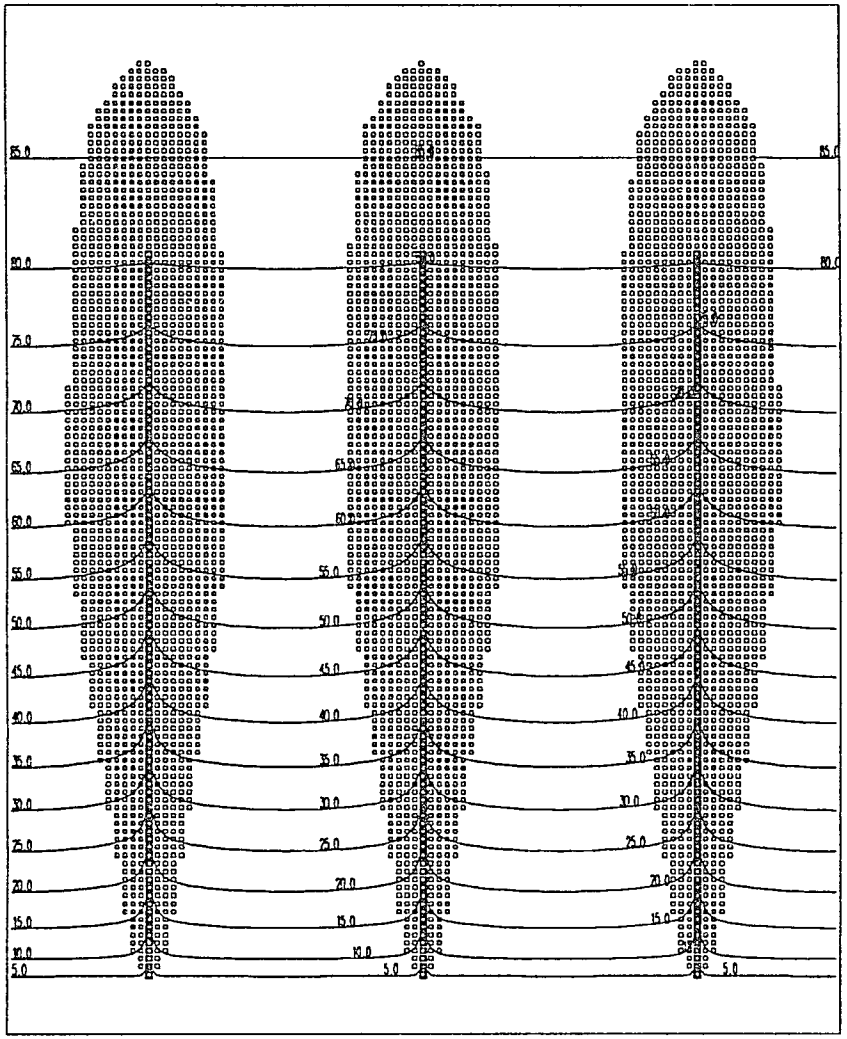

Figure 48--Map view showing lines of equal head and the source areas of streams on the free surface for the **'thin aquifer'** simulation. Squares along stream channels indicate where groundwater discharge occurs. Octagons indicate that model cell is at least partially a source for stream discharge.

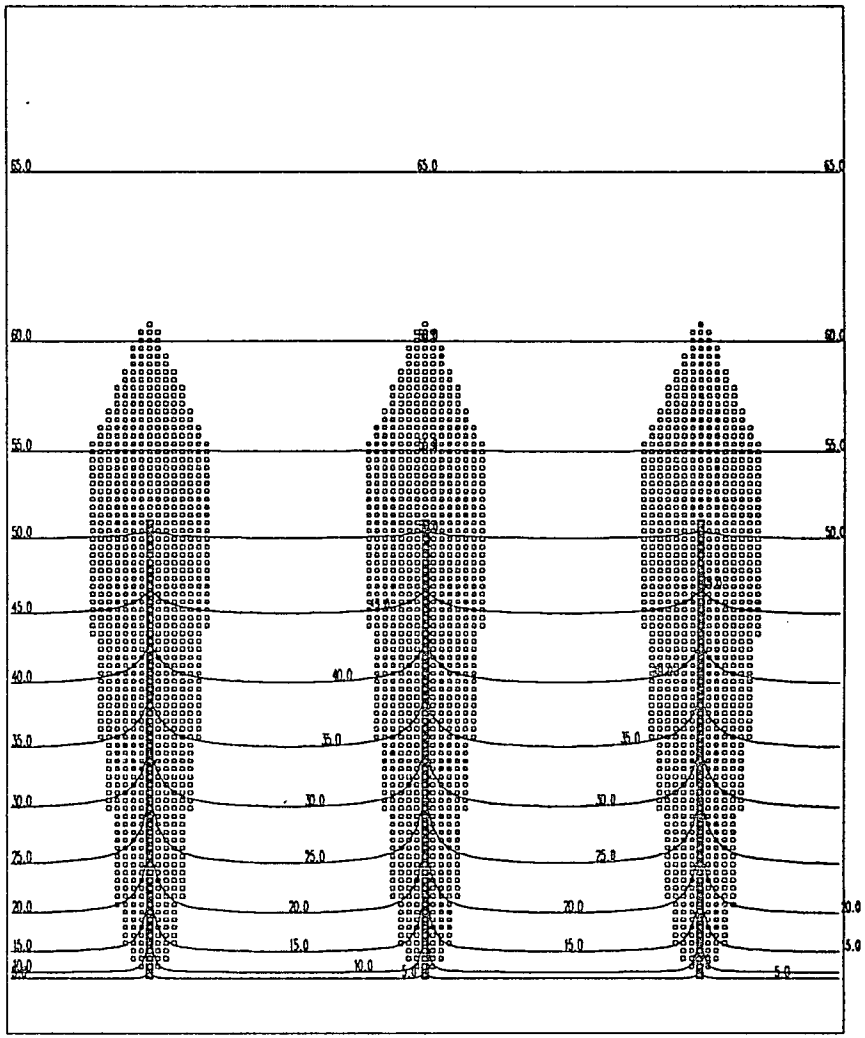

Figure 49--Map view showing lines of equal head and the source areas of streams on the free surface for the **'thick aquifer'** simulation. Squares along stream channels indicate where groundwater discharge occurs. Octagons indicate that model cell is at least partially a source for stream discharge.

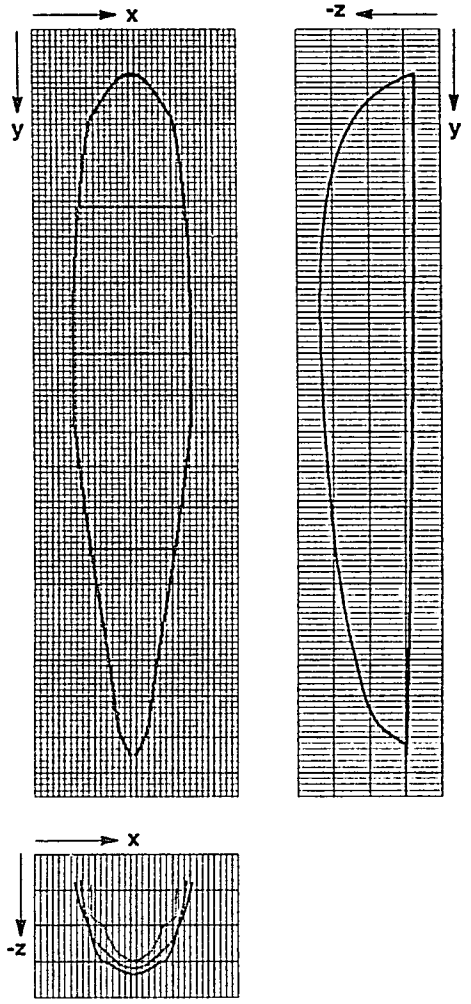


Figure 50--Profiles of bounding surface for thecenter stream sub-system flow for the '**thin aquifer**' simulation viewed along each of the three Cartesian coordinate axis.

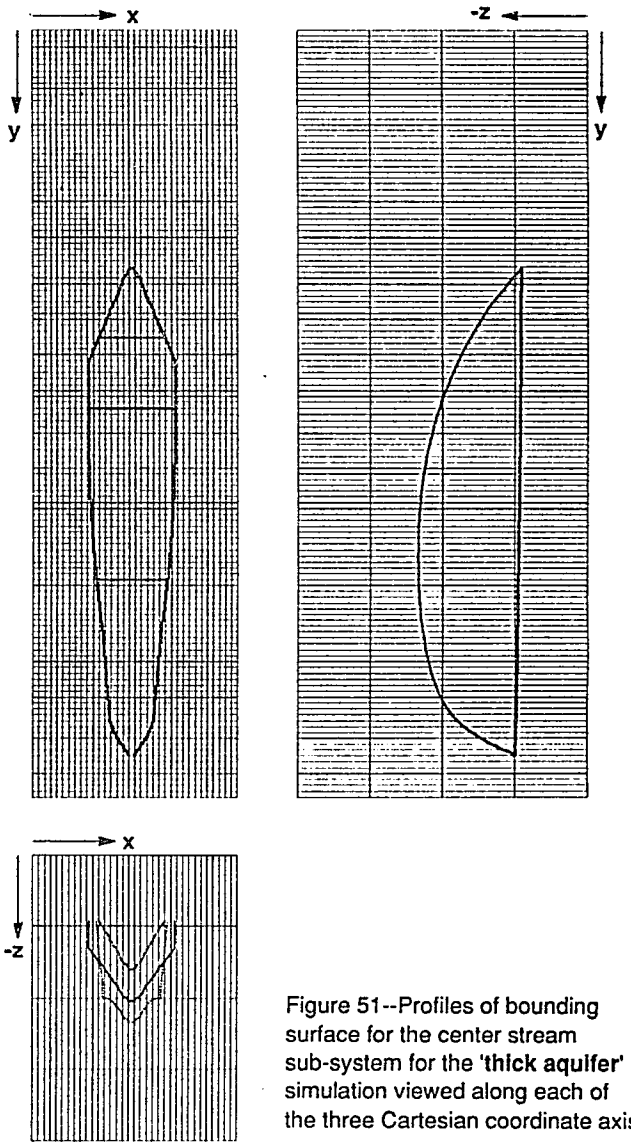


Figure 51--Profiles of bounding surface for the center stream sub-system for the '**thick aquifer**' simulation viewed along each of the three Cartesian coordinate axis.

enters the system at a steeper angle compared to that of the thick system. The stream line of symmetry for the thick system descends to about -800 feet (0.45 of an 1800 foot thick aquifer) and enters the system at a shallower angle; its maximum depth is found closer to the front of the system whereas the maximum depth of the thin system is found closer to the divide. The transverse profiles of the thin system show a relatively wide and fuller shape whereas those of the thick system show narrow, wedge-shape profiles. The outlines of the upstream ends of these catchment areas are similar in form to the profiles of the cross-sections.

Although the heads in the thick system are lower than those of the thin system, the lines of equal head on the water table indicate that there is appreciable lateral flow near the downstream end of the system. This is also indicated by the base-flow profile that reaches a maximum near the terminus of stream. The start-of-flow for the thin system is about 0.26 of the basin length from the divide whereas that of the thick system is at 0.54. The thin system base flow and head profiles are broader and uniformly distributed whereas the thick system profiles are strongly peaked near the stream terminus. The stream discharge of each system is reflected in the differences in the contributing flow areas; the proportion of stream catchment area to basin is 0.4 for the thin system and 0.21 for the thick system.

Simulations for 'non-drainage' system was made using the aquifer-thickness changes in this section. The water-table profiles are shown in figures 52 and 53. The difference in head profile between 'non-drainage' type thin and

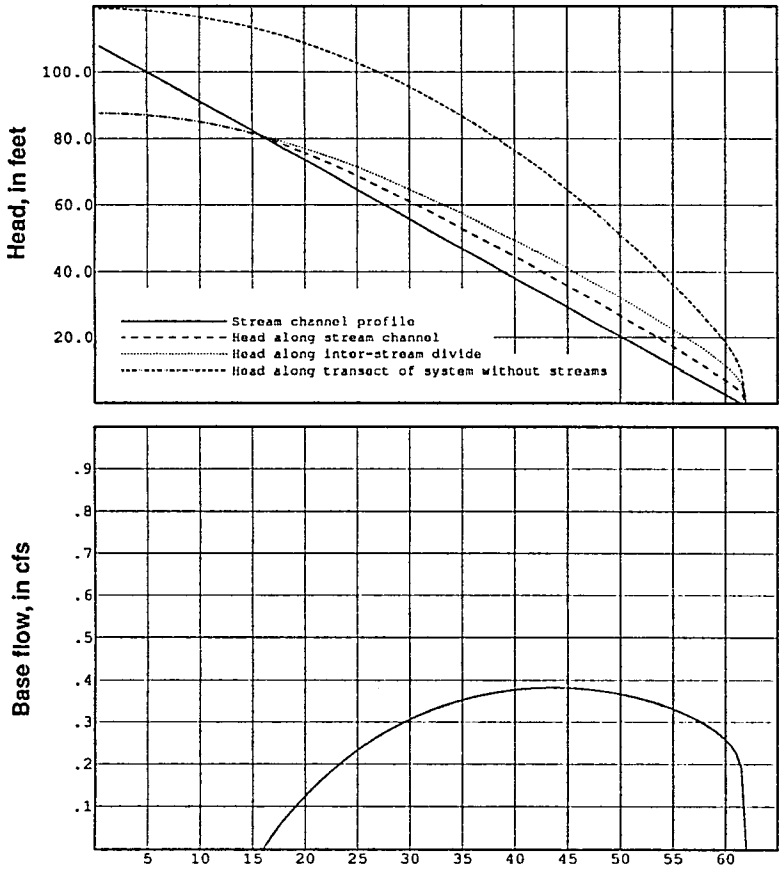


Figure 52a--Profiles of water table along stream channel and inter-stream divide for the **'thin aquifer'** simulation and typical profile for corresponding non-drainage simulation.

Figure 52b--Profile of groundwater discharge to center-stream channel (along model column 52) for **'thin aquifer'** simulation.

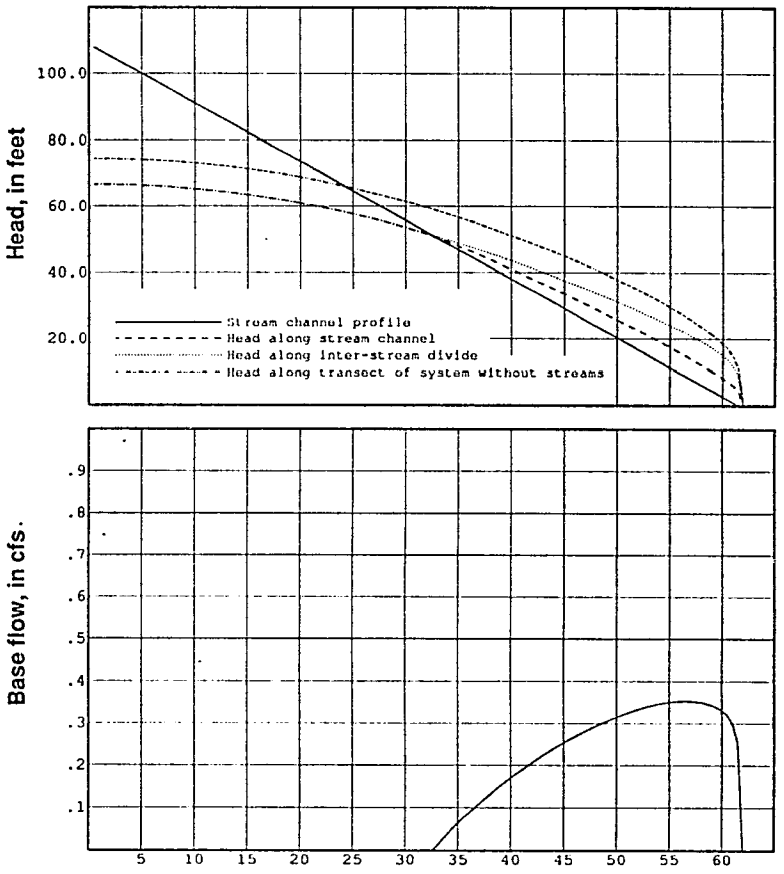


Figure 53a--Profiles of water table along stream channel and inter-stream divide for the **'thick aquifer'** simulation and typical profile for corresponding non-drainage simulation.

Figure 53b--Profile of groundwater discharge to center-stream channel (along model column 52) for **'thick aquifer'** simulation.

thick systems is large; heads are 120 feet at the divide of the thin system compared to 75 feet at the divide for the thick system. When viewed in terms of energy levels, the thin system has a markedly higher level of potential energy. When these profiles are compared to the corresponding 'drainage' systems, the head differences are larger in the thin system than in the thick system. These head differences suggest that stream systems dissipate more energy in a thin aquifer than in a thick aquifer.

**Streambed Conductance**

As discussed on page 19, the streambed conductance parameter is a simulation term that combines several factors affecting resistance to groundwater discharge along streams. Resistance to discharge along a reach of stream can be controlled by such factors as streambed-deposit thickness, clay content of deposits, narrowness of channels, or even clay lenses in the aquifer itself which are close to the stream but that retard discharge to streams. For all of these cases the resistive effects are simulated by simply reducing the conductance term. Although combinations of some or all of the above factors are also simulated by changes in conductance, the effects attributed to individual factors cannot be differentiated at the scale of discretization used for these simulations.

As table 1 shows, the conductance terms used for the high streambed conductance simulation was 50,000 feet$^2$/day; the low conductance simulation

used a value of 500 feet$^2$/day. Each value represents a change from the reference by an order of magnitude.

Figures 54 and 55 show the extent to which the catchment areas are affected by the change in conductance values. This parameter change has a prominent effect on the widths of the contributing areas. The high-conductance system is generally much wider, reaching a maximum width of 0.22. The low-conductance system is uniformly narrow and reaches a maximum width of only 0.07. The high-conductance system is closer to the reference simulation in terms of its general shape and hydraulic behavior than is the low-conductance system.

Figures 56 and 57 show the three mutually perpendicular views of each system. The lengthwise profile of the low-conductance system remains shallow, reaching a maximum depth of -287 feet which is 0.24 of aquifer thickness, compared to -862 (0.72 of thickness) for the high- conductance and -720 (.60 of thickness) for the reference simulations.

The base flow of each simulation shows a distinct distribution pattern (figures 58 and 59). The start-of-flow for the high-conductance system is at 0.44 from the divide, nearly halfway downstream, with a maximum flow of almost 0.6 cfs at 0.8 the way downstream. In this system the inter-stream head is similar to that of the reference configuration. The stream heads, however, are lower and more base flow occurs as there is a 10% increase in flow to streams compared to the reference simulation. In contrast, the low-conductance system shows a much lower but more uniformly distributed base flow, starting at 0.22 from the

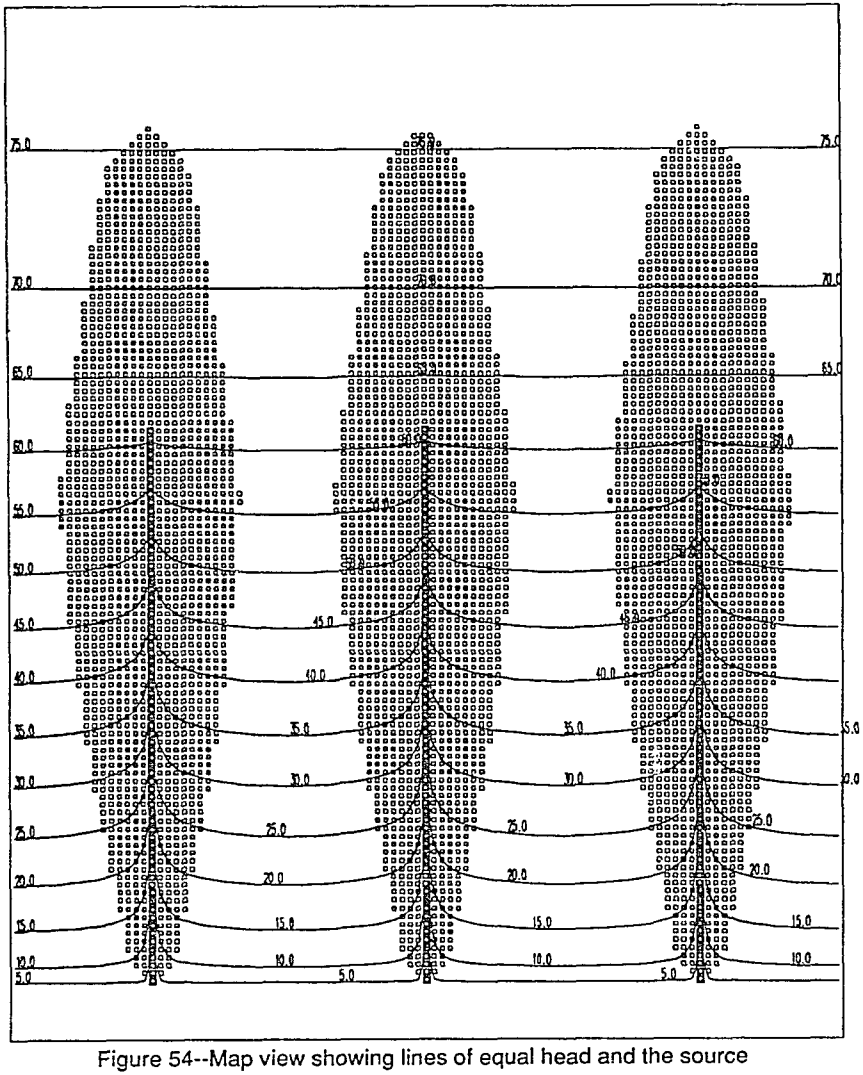

Figure 54--Map view showing lines of equal head and the source areas of streams on the free surface for the **'high stream conductance'** simulation. Squares along stream channels indicate where groundwater discharge occurs. Octagons indicate that model cell is at least partially a source for stream discharge.

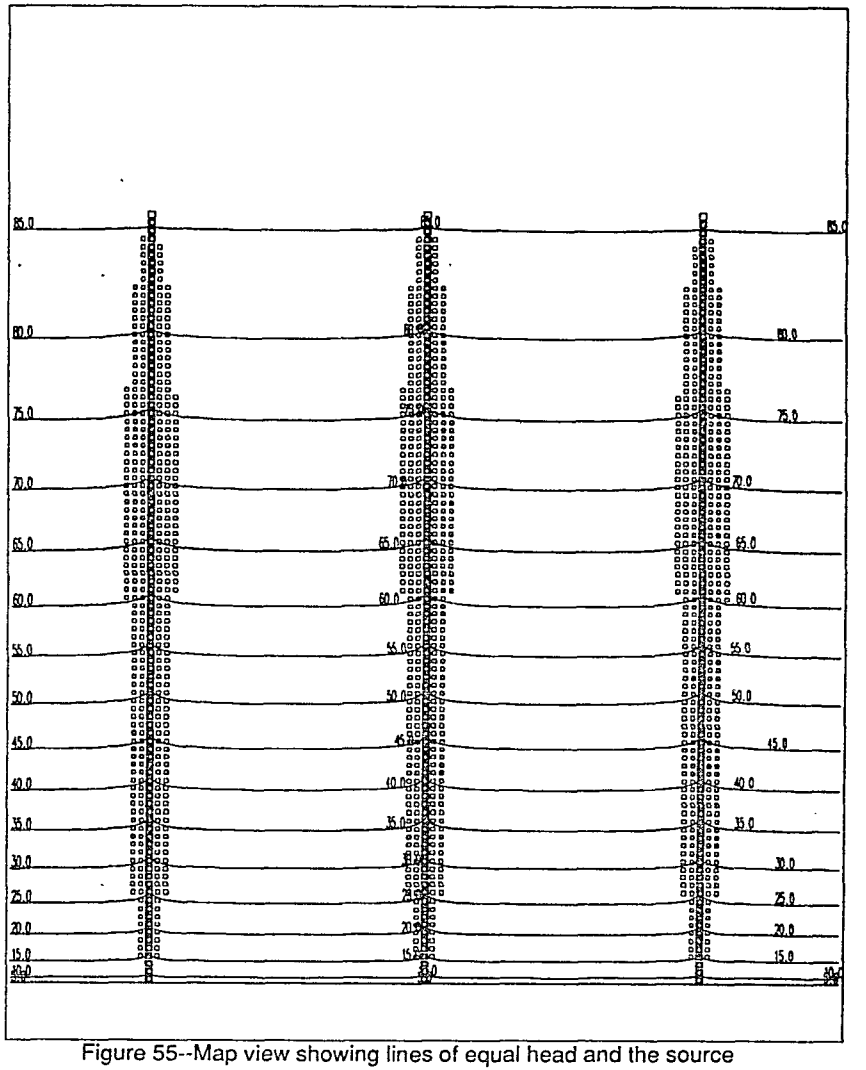

Figure 55--Map view showing lines of equal head and the source areas of streams on the free surface for the **'low-stream conductance'** simulation. Squares along stream channels indicate where groundwater discharge occurs. Octagons indicate that model cell is at least partially a source for stream discharge.

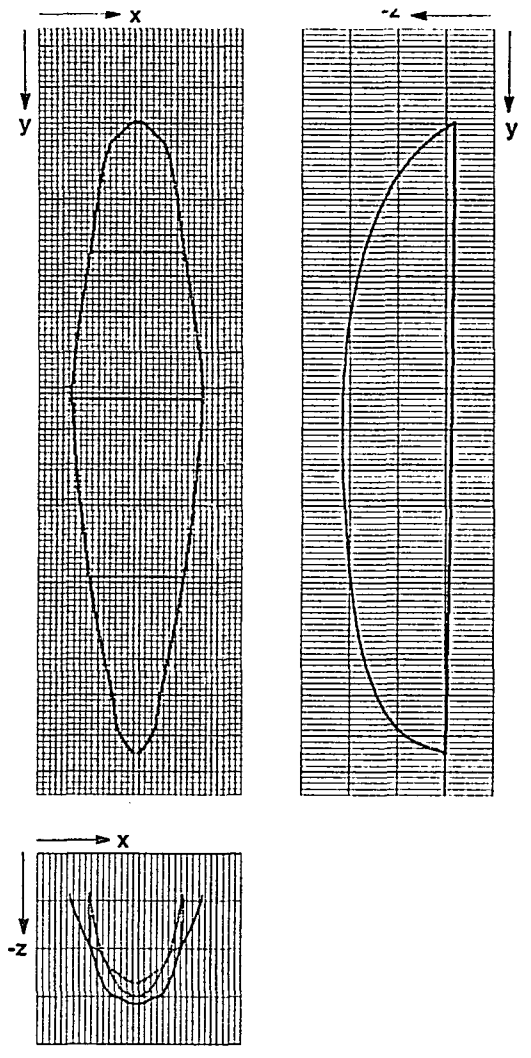


Figure 56--Profiles of bounding surface for the center stream sub-system flow for the '**high-stream conductance**' simulation viewed along each of the three Cartesian coordinate axis.

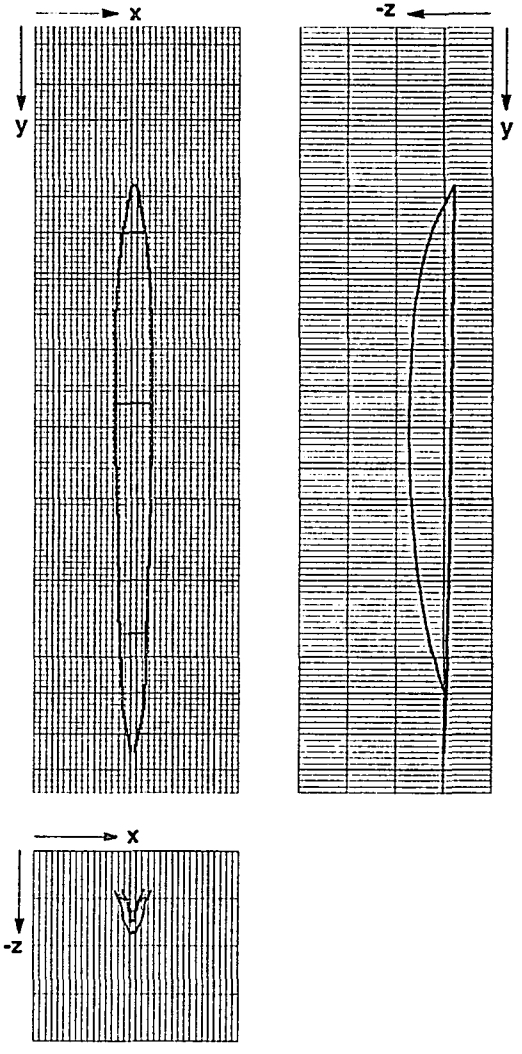


Figure 57--Profiles of bounding surface for the center stream sub-system flow for the '**low-stream conductance**' simulation viewed along each of the three Cartesian coordinate axis.

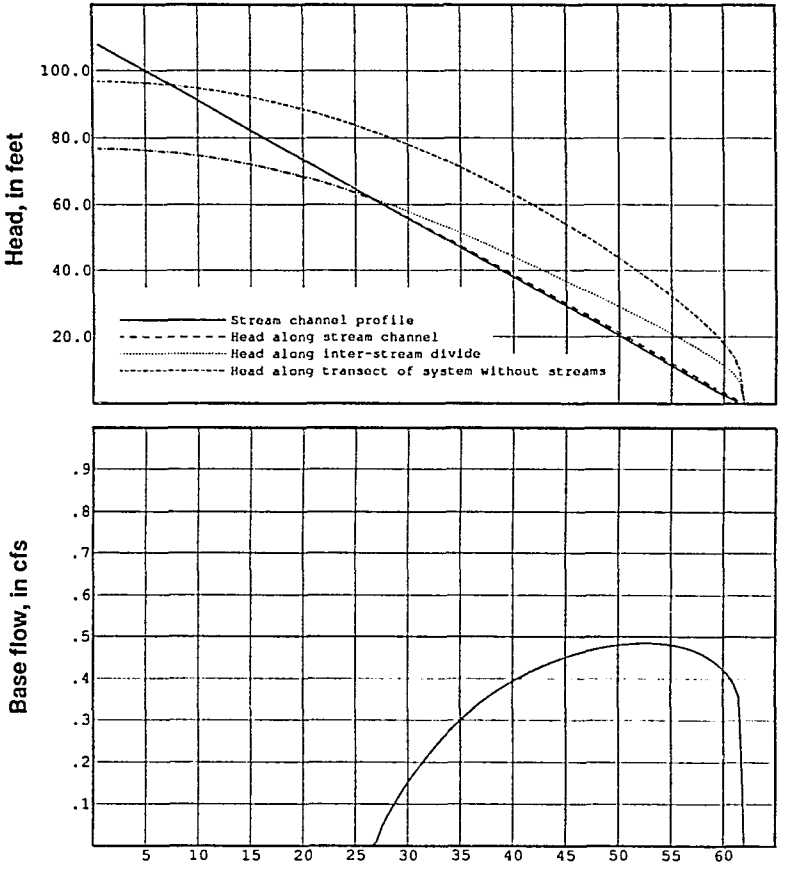


Figure 58a--Profiles of water table along stream channel and inter-stream divide for the '**high-stream conductance**' simulation and typical profile for corresponding non-drainage simulation.

Figure 58b--Profile of groundwater discharge to center-stream channel (along model column 52) for '**high-stream conductance**' simulation.

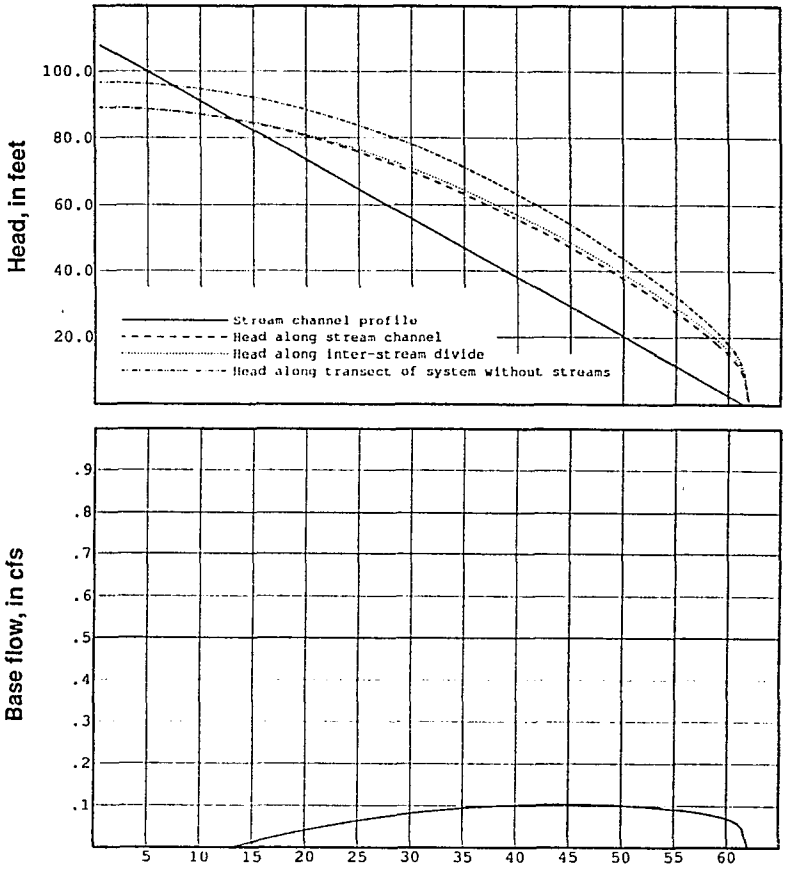


Figure 59a--Profiles of water table along stream channel and inter-stream divide for the '**low-stream conductance**' simulation and typical profile for corresponding non-drainage simulation.

Figure 59b--Profile of groundwater discharge to center-stream channel (along model column 52) for '**low-stream conductance**' simulation.

divide but reaching a maximum flow of 0.1 cfs at a position 0.6 downstream from the divide.

A comparison shows that the geometric and hydraulic character of the high-conductance system are closer to those of the reference system than are those of the low-conductance system. Because conductance values in each simulation were set an order of magnitude apart it appears that the sensitivity of conductance values relative to that used in the reference simulation increases in the direction of the lower values. In contrast, increasing conductance has a progressively minimal effect. Figure 60 shows a range of head and base flow profiles along the middle stream channel for simulations in which the conductance values were increased by an order of magnitude in the range of 0 to 500,000 feet$^2$/day. The greatest sensitivity in this part of the system appears to be in the range of 500 and 5000 feet$^2$/day. Figure 60 also compares the base flow over this same range. When stream conductance is small, base flow is distributed in smaller quantity but over a long reach of stream. When stream conductance is large, base flow is distributed over a shorter stream reach but at higher discharge rates.

**Stream-Channel Slope**

Discharge along stream channels is, to a large degree, sensitive to the channel's elevation. The streambed profile relative to the hydraulic head in the aquifer determines the distribution of groundwater discharge. In the reference system a constant slope was used. For regional scale coastal plain models this

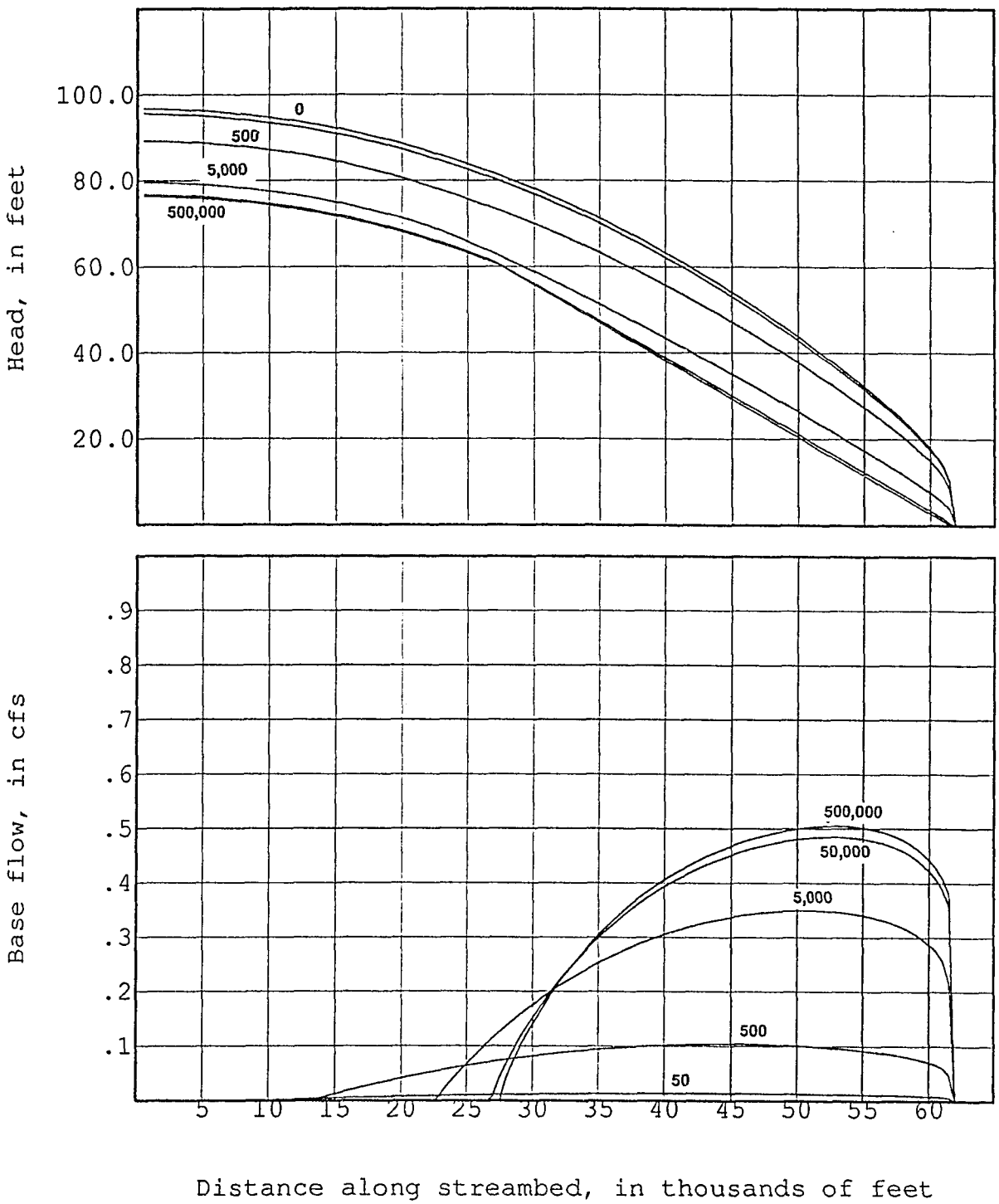


Figure 60--Profiles of water table and corresponding base flow along center stream channel for simulations of systems with stream conductance values ranging from 0 to 500,000 feet$^2$/day.

slope represents an average land surface gradient from a typical divide to a baseline at the shore. However, stream channels are more realistically expressed as an exponential function of distance from their terminus (Shulits, 1941; Hack, 1958; Yatsu, 1955). Furthermore, at local scales the departures from a general expression of slope become more common and the base flow or stream 'pickup' also departs from those of the predicted expression and vary with local perturbations in the channel slope.

In order to understand some aspects of the effect that variation in stream channel position has on base flow and, consequently, on the streams' character, three simulations were made: two involved changing the channel angle by 0.05 degrees less and greater than slopes used in the reference simulation. In each case the channel gradient remained constant. In a third simulation the channel profile was generated according to the exponential relation (from Shulits, 1941):

(7) $z = (.0058) \times (e^{0.098x} - 1)$ where,

z is elevation

x is the horizontal distance from the starting point of the stream channel

e is the exponential

Equation (7) is one of several forms of the stream profile equation.

Although the change in angle for the constant slope simulations were quite small, the effects that these slope-changes had on flow were large. The 0.05 degree change results in a 50 foot increase or decrease in height at the divide and thus helps to explain how subtle changes in slope have large effects

on stream pickup. In actuality, constant slopes would not persist as equilibrium stream-profile configurations but rather the exponential form represents a more typical equilibrium profile that would reflect a landform response to climatic and geologic factors over time.

The contributing areas to flow for each of the systems are shown in figures 61 through 63. The lower-slope stream system is longer (0.94 of watershed length) and wider (0.20) then for the high-slope system, the length and width of which are 0.59 and 0.09 respectively. The total catchment area of the low-slope system is over three times that of the high-slope system (0.52 compared to 0.16). In general, the exponential-slope system shows similar dimensions to that of the lower-slope system although there are differences in its shape and position of the start-of-flow.

The configurations of the contributing areas for the low- and high-slope systems are generally similar to those of the previous simulation pairs with some differences. The upstream end of the low-slope system has a broad dome shape and begins within 0.02 from the divide. Its maximum width is located about 0.23 from the divide; this is unusual compared to other simulations of this study as the average position of maximum-width is located about 0.50 from the divide. In contrast, the high-slope contributing area begins at 0.38 from the divide, the farthest downstream of all simulations; the short length over which stream discharge occurs is explained by the fact that a large upstream reach of channel remains above the free surface due to the higher channel slope. The position of

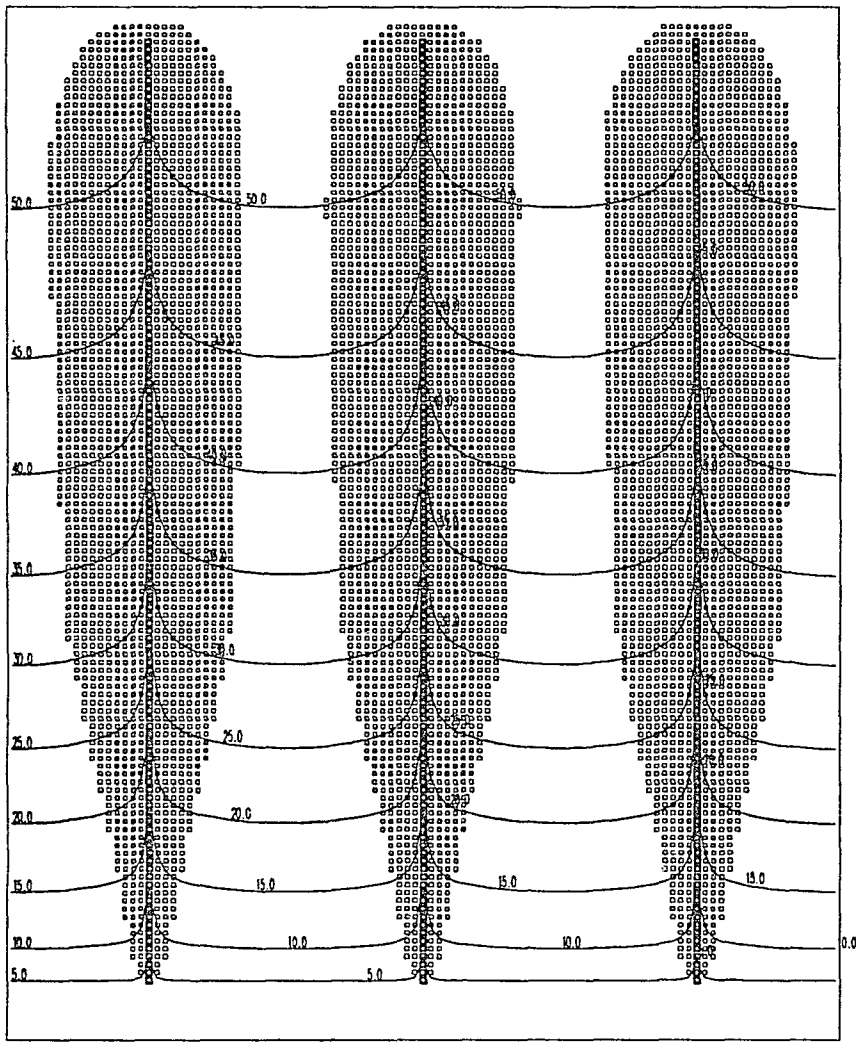


Figure 61--Map view showing lines of equal head and the source areas of streams on the free surface for the '**low stream-channel slope**' simulation. Squares along stream channels indicate where groundwater discharge occurs. Octagons indicate that model cell is at least partially a source for stream discharge.

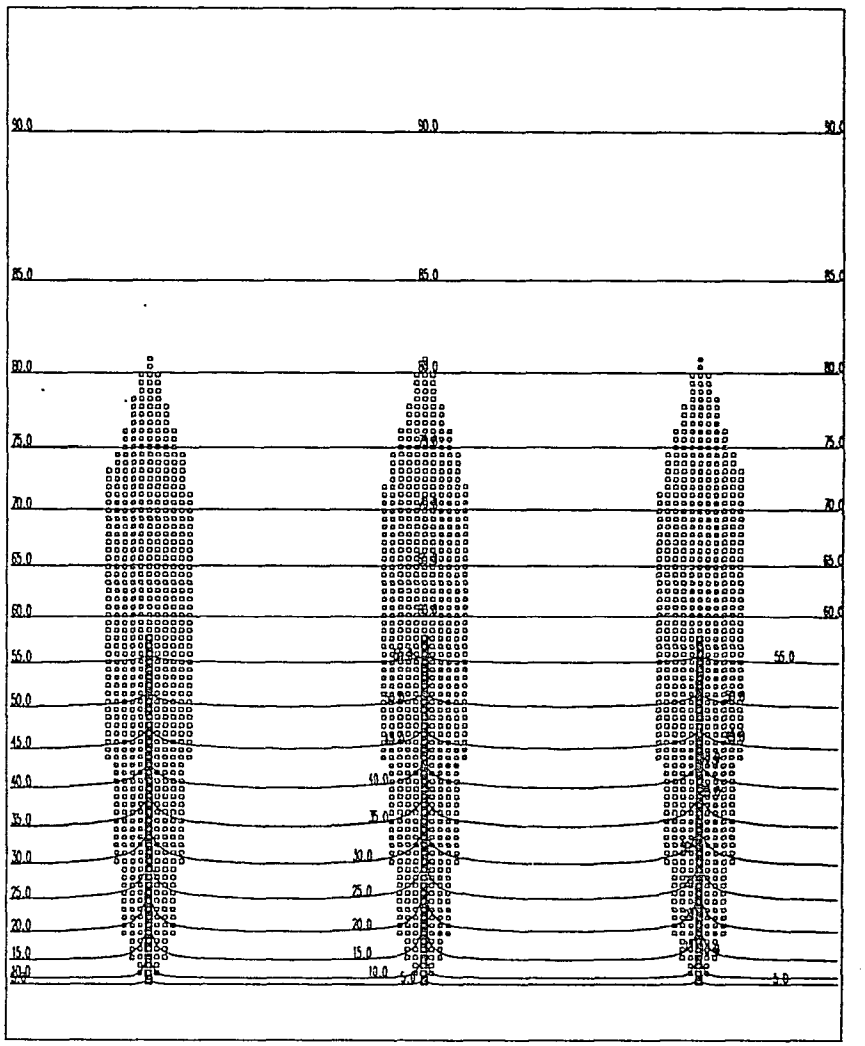


Figure 62--Map view showing lines of equal head and the source areas of streams on the free surface for the '**high stream-channel slope**' simulation. Squares along stream channels indicate where groundwater discharge occurs. Octagons indicate that model cell is at least partially a source for stream discharge.

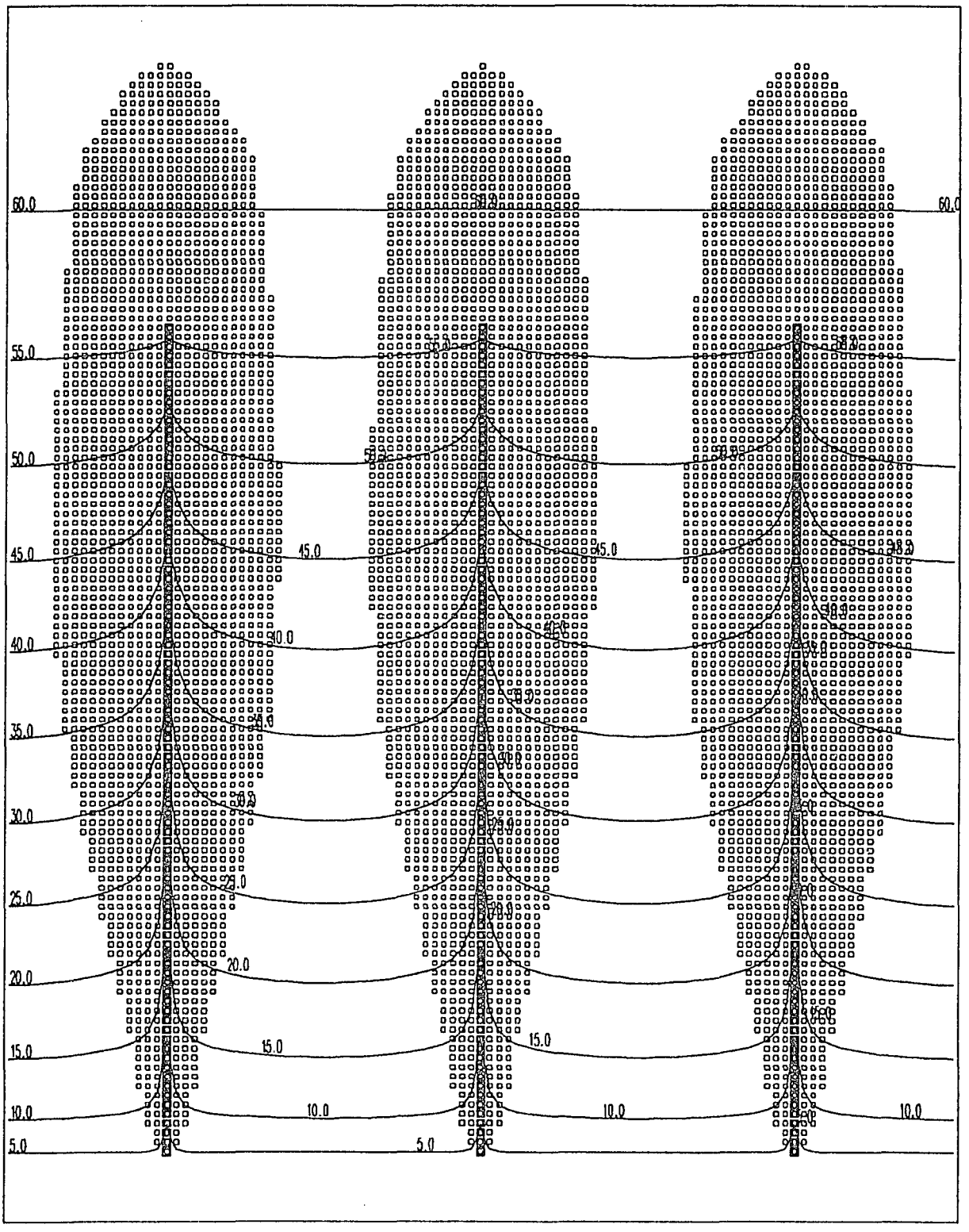


Figure 63--Map view showing lines of equal elevation head and the source areas of streams on the free surface for the **'concave stream-channel slope'** simulation. Squares along stream channels indicate where groundwater discharge occurs. Octagons indicate that model cell is at least partially a source for stream discharge.

the start-of-flow is thus shifted far downstream. The upstream end of this system is wedge-shaped with concave limbs.

The longitudinal sections in figure 64 show that the maximum depth of the low-slope system is -957 feet which is 0.80 of the aquifer thickness and a distance of 0.27 from the divide. The maximum depth to which the high-slope system penetrates the groundwater zone is -546 feet, which is 0.45 of thickness at a distance of 0.79 from divide (figure 65). The shapes of each system's lengthwise profile are also quite different; the upstream end of the profile for the low-slope system makes a steep angle with the horizontal lines compared to the relatively shallow angle of entry seen for the high-slope profile. The transects of each reflect the shape of the upstream end of their respective catchment areas.

Figure 66 shows the three mutually perpendicular views for the exponential-slope system. The outline of the upstream end of the catchment area is broad and dome-shaped. The discontinuities on either side are related to irregularities found on the transect profiles that coincide with the model layer boundary. They are artifacts of a finite-difference solution. The widest section of the stream system is about 0.41 from the divide. The maximum depth shown in longitudinal profile is -988 feet and is located at 0.67 from divide. The longitudinal profile makes a steep angle with the horizontal lines although it does not follow the divide as closely as does the streamline of symmetry in the low-slope system.

The head distribution for each of the three simulations is distinctive and is a distinguishing characteristic of the low-slope and exponential-slope systems

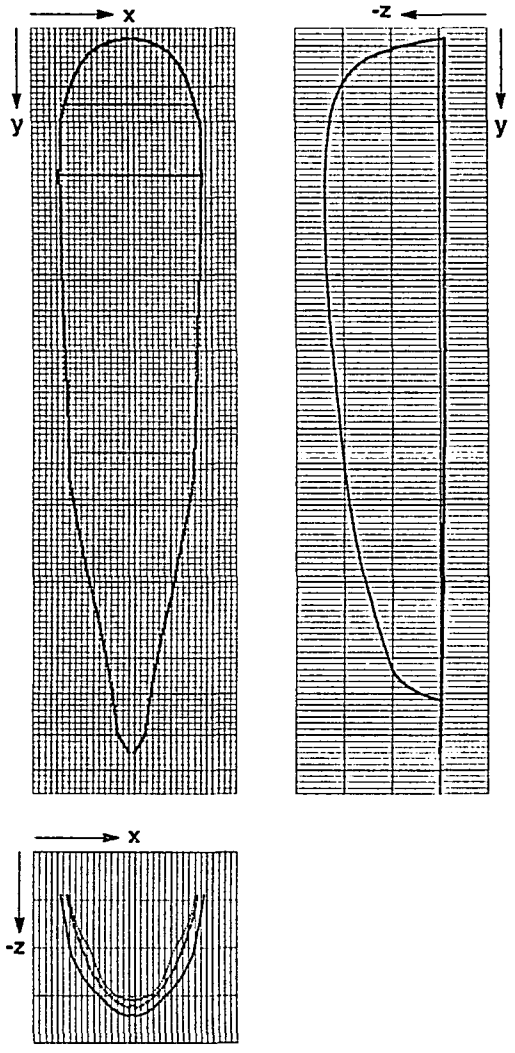


Figure 64--Profiles of bounding surface for the center stream sub-system flow for the '**low stream-channel slope**' simulation viewed along each of the three Cartesian coordinate axis.

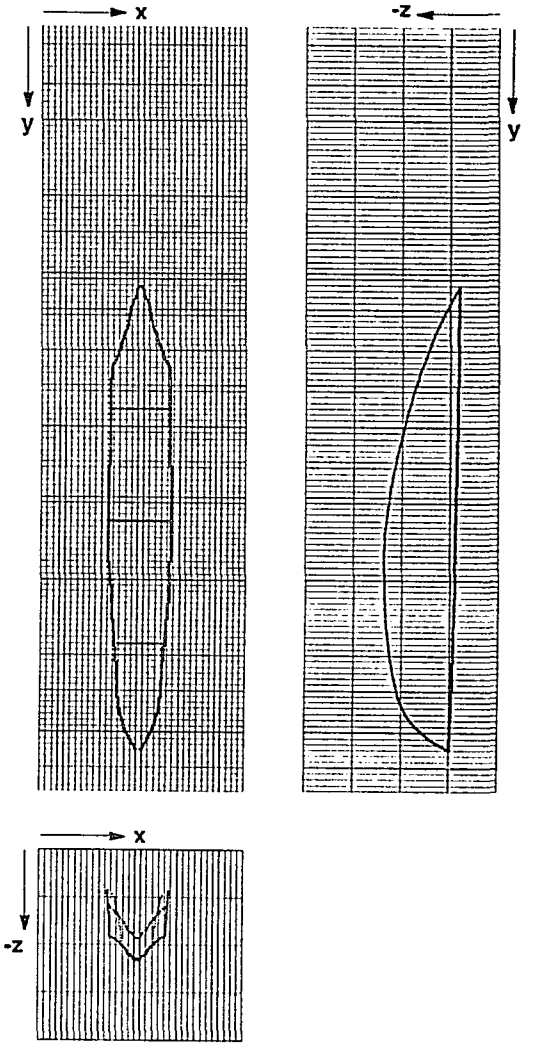


Figure 65--Profiles of bounding surface for the center stream sub-system flow for the '**high stream-channel slope**' simulation viewed along each of the three Cartesian coordinate axis.

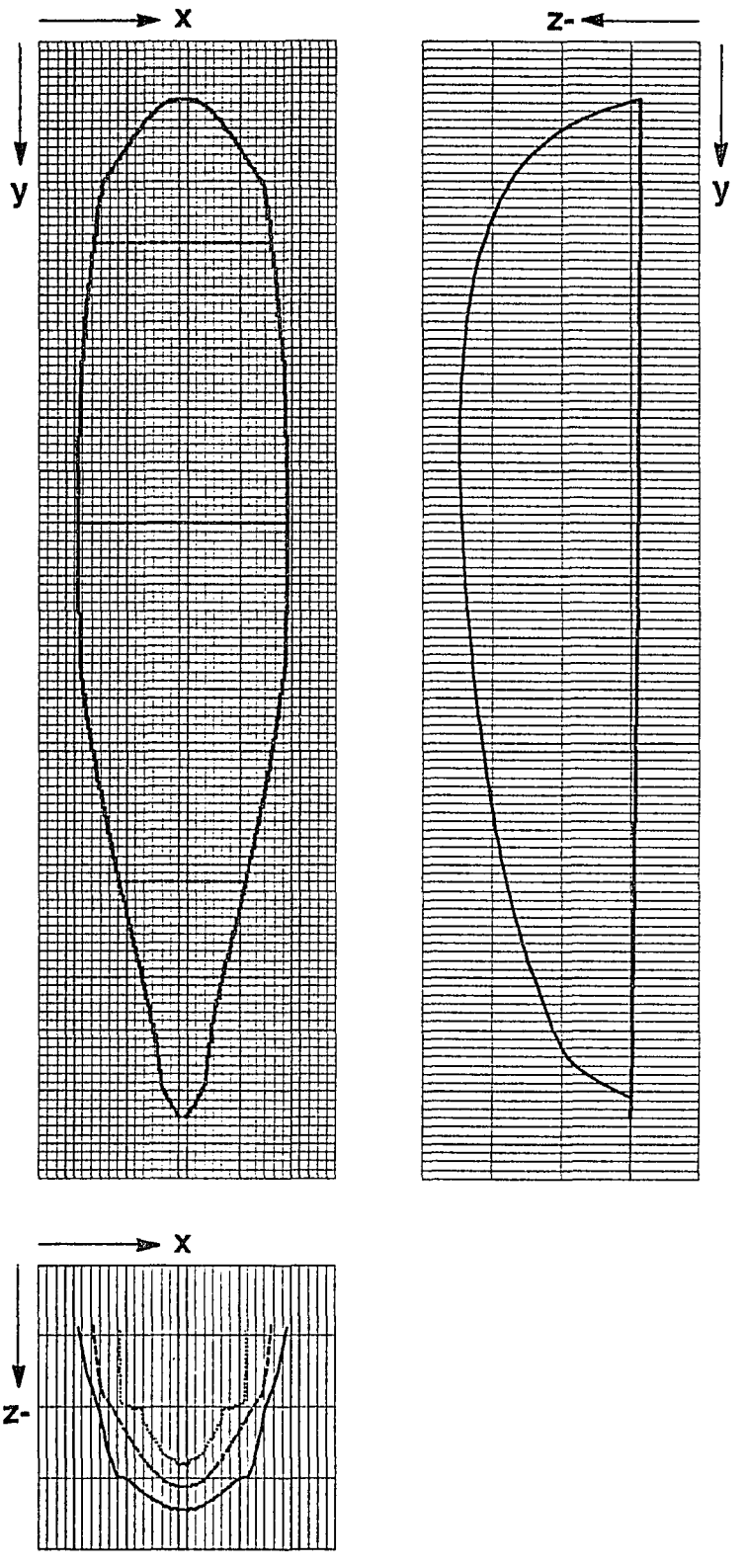


Figure 66--Profiles of bounding surface for the center stream sub-system flow for the **'concave stream-channel slope'** simulation viewed along each of the three Cartesian coordinate axis.

which otherwise have similar lengths, maximum widths, and areal extent. The contours of the low-slope system shown in figure 61 indicate that an unusually strong component of lateral flow occurs in the upstream reach. In contrast, the exponential-slope system of figure 63 indicates negligible lateral flow in the upper stream reaches which is consistent with other simulations.

Figures 67 through 69 show base flow and corresponding head profiles. A look at the base flow and head relations in figure 67a and 67b show that base flow for the low-slope system occurs over virtually the entire stream length (start-of-flow begins at 0.04 from divide). A maximum discharge of less than 0.4 cfs occurs at 0.59 from divide. The exponential-slope system, however, starts flowing at 0.20 from the divide and attains a maximum discharge of 0.5 cfs at 0.63 downstream. Discharge rises sharply and attains a maximum rate much closer to the start-of-flow because of the exponential drop in channel elevation that develops higher head differences within a shorter distance than for a linear slope.

The head contour map of the high-slope system (figure 62) shows that lateral flow is restricted to the lower reach of the stream and that heads remain high near the divide. This is explained by flow starting at 0.65 from the divide with peak flow of 0.34 cfs occurring at 0.94 from the divide near the stream terminus. As mentioned previously, the small increase in channel angle causes it to intersect the free surface at a position far from the divide and, therefore, precludes flow to much of the channel.

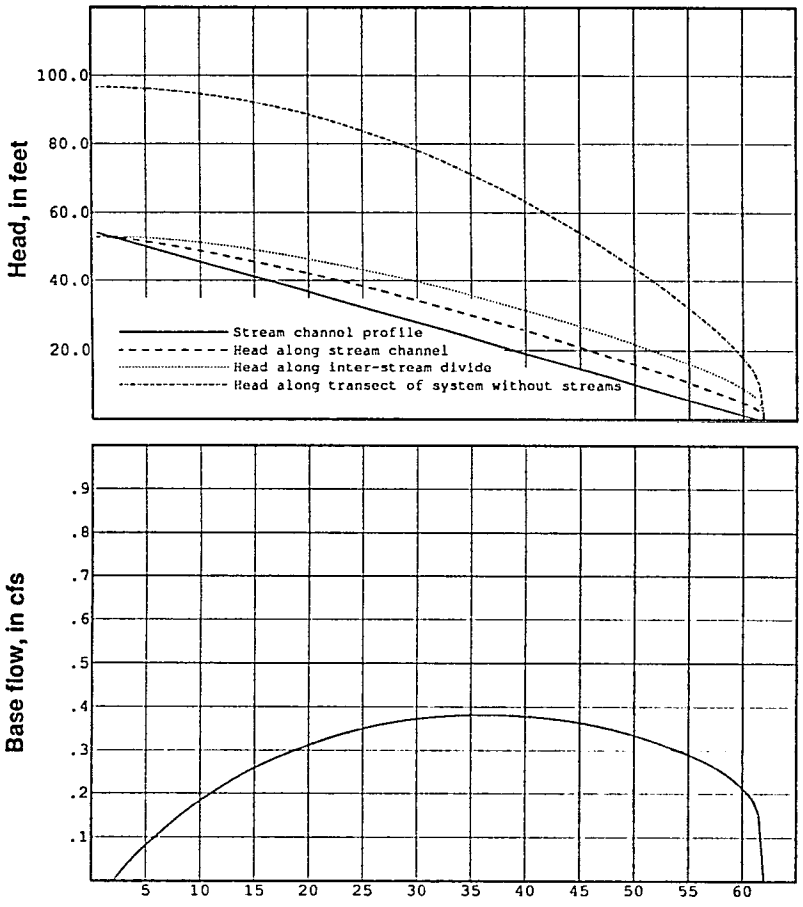


Figure 67a--Profiles of water table along stream channel and inter-stream divide for the '**low stream-channel slope**' simulation and typical profile for corresponding non-drainage simulation.

Figure 67b--Profile of groundwater discharge to center-stream channel (along model column 52) for '**low stream-channel conductance**' simulation.

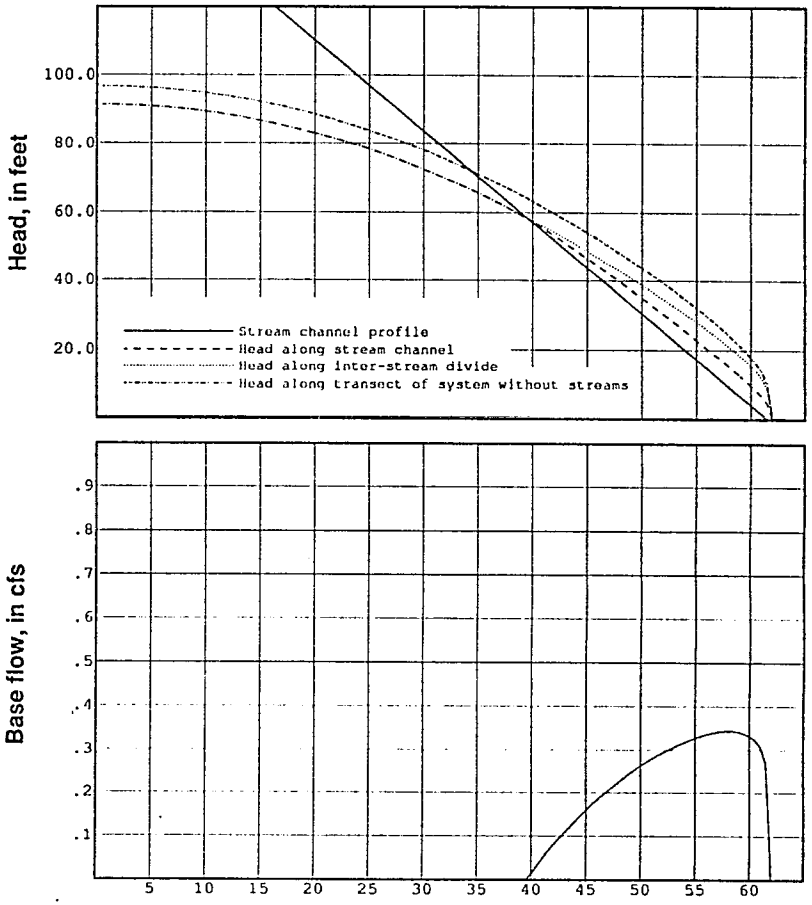


Figure 68a--Profiles of water table along stream channel and inter-stream divide for the '**high stream-channel slope**' simulation and typical profile for corresponding non-drainage simulation.

Figure 68b--Profile of groundwater discharge to center-stream channel (along model column 52) for '**high stream-channel slope**' simulation.

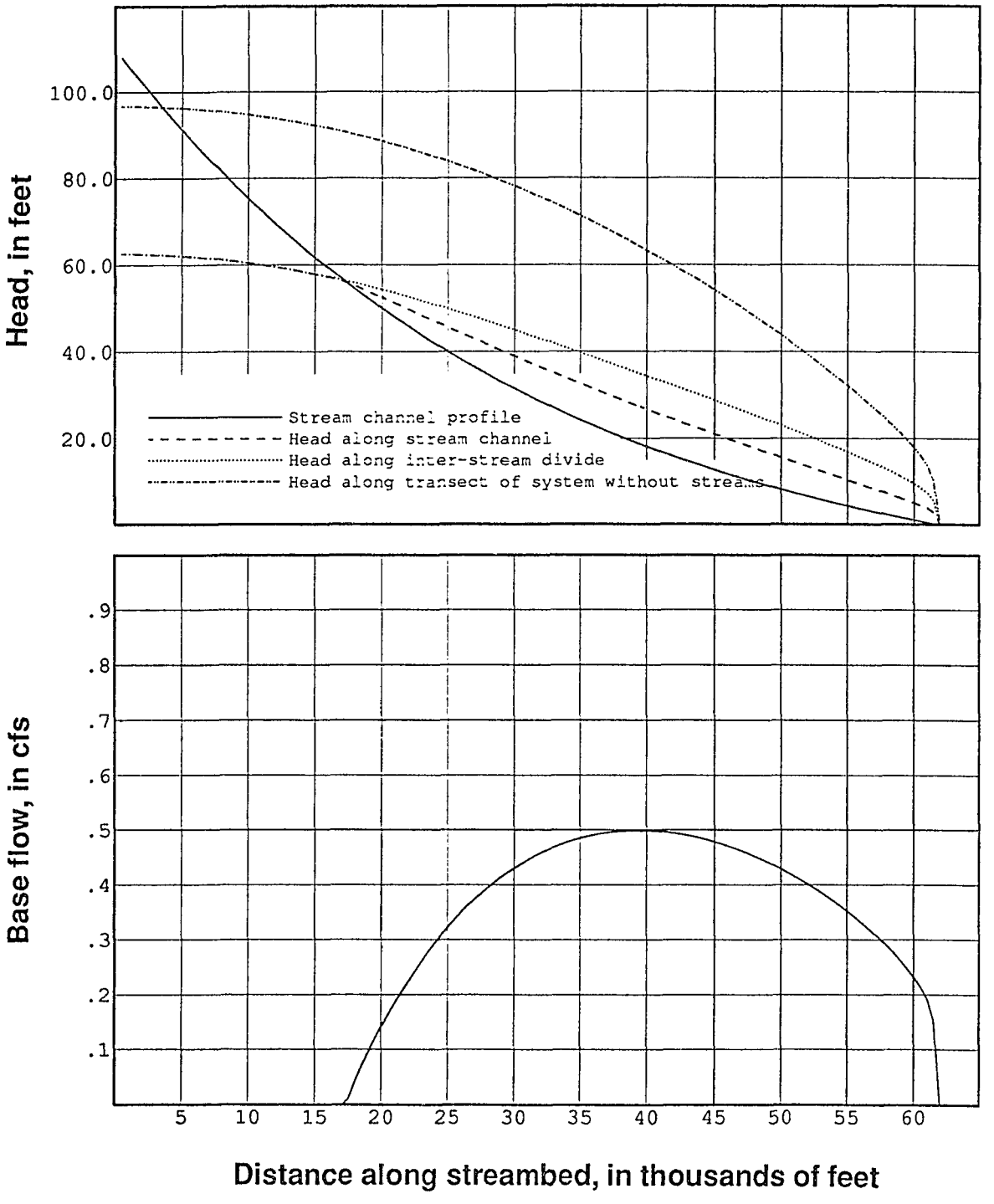


Figure 69a--Profiles of water table along stream channel and inter-stream divide for the **'concave stream-channel slope'** simulation and typical profile for corresponding non-drainage simulation.

Figure 69b--Profile of groundwater discharge to center-stream channel (along model column 52) for **'concave stream-channel slope'** simulation.

## Stream Density

Stream density, or total stream length per given area of watershed, is one of several linear measures used in quantitative basin analysis to characterize the closeness of spacing of channels and for comparing topographic features (Strahler, 1956). Drainage density is controlled by interaction between climate and geology and, therefore, varies widely from region to region. In general, resistant surface materials or those with high infiltration capacities have widely spaced streams or low drainage density. As resistance or surface permeability decrease, runoff is removed in a greater number of closely spaced channels. Stream density raises questions as to what degree streams will mutually interfere or modify each others flow patterns and whether contributing areas of adjacent streams meet or coalesce in high stream density basins. Another related question is what effects do boundary conditions have on stream systems.

### *Single stream systems and boundary effects*

In this section four simulations with different stream density configurations are considered. Figure 70 shows the contributing area for a single stream positioned along the center of the system, otherwise all other parameters are kept identical to those of the reference system. An interesting feature is the increased size of the contributing area when compared to the reference stream system. The length, width and area for the one-stream system is 0.93, 0.28, and 16.8% compared with 0.84, 0.16, and 10.3% of the reference system respectively.

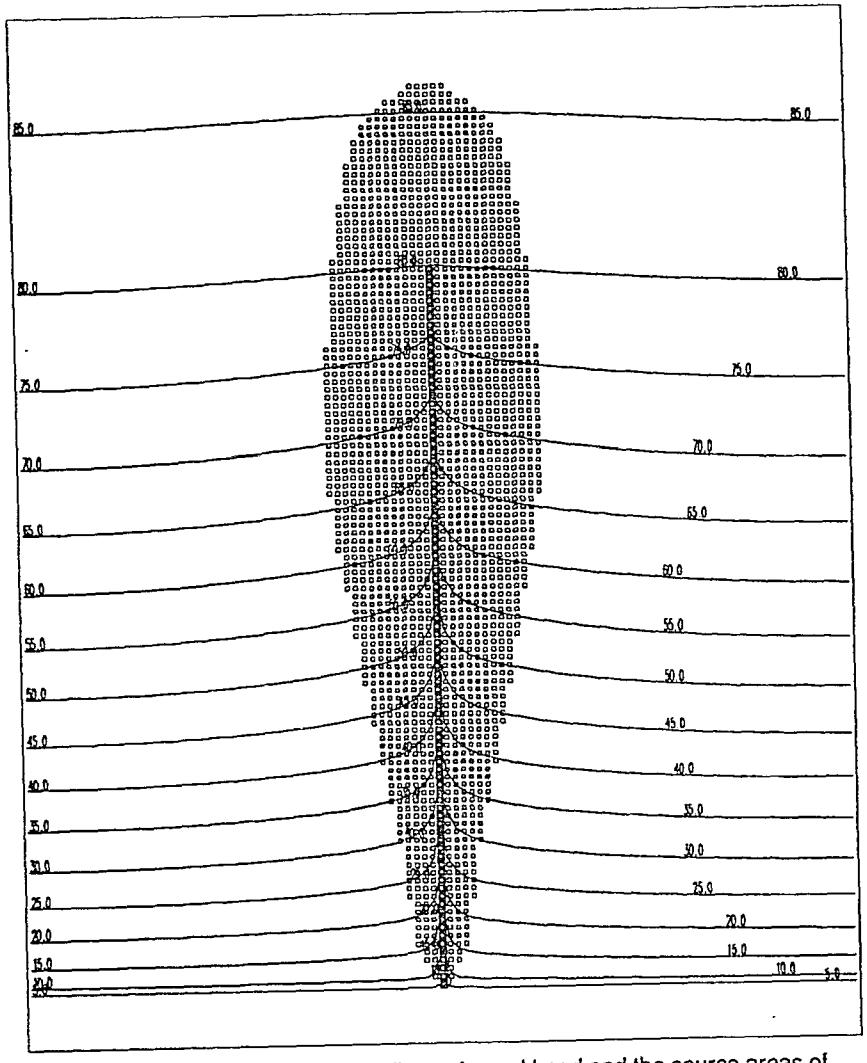


Figure 70--Map view showing lines of equal head and the source areas of streams on the free surface for the '**single stream**' simulation. Squares along stream channels indicate where groundwater discharge occurs. Octagons indicate that model cell is at least partially a source for stream discharge.

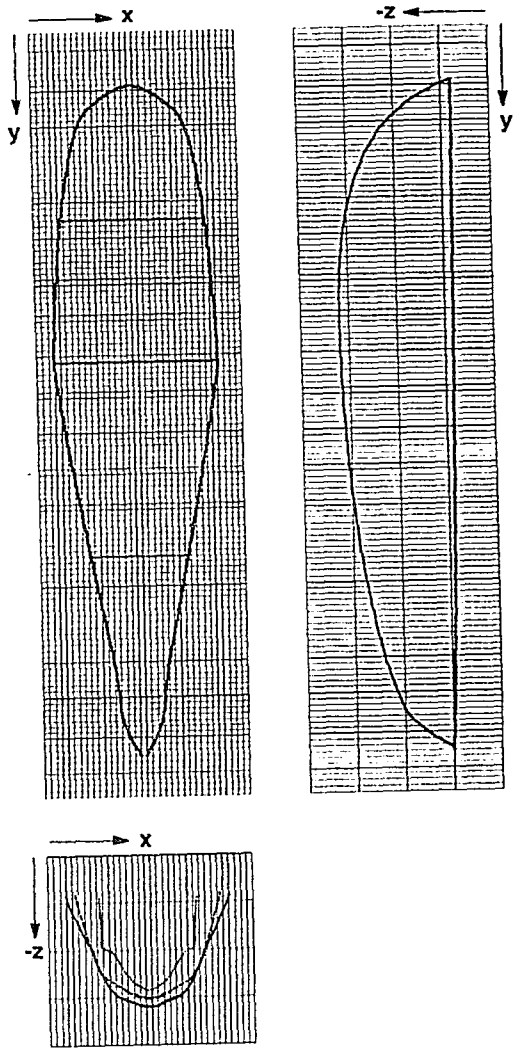


Figure 71--Profiles of bounding surface for the center stream sub-system flow for the '**single stream**' simulation viewed along each of the three Cartesian coordinate axis.

The difference in the shapes from each of the three mutually perpendicular views is also evident when comparing figure 71 to figure 13. The upstream end of the single-stream system has a broader, rounder shape compared to the longer tapered arch-shape of the reference system. Also the maximum depth of the single-stream system is 0.73 of total depth (0.60 for the reference). There is also a difference in head contours and base flow. The contours for the single-stream system indicate that a stronger lateral flow occurs in the upstream reaches; the start-of-flow is only 0.27 from the divide for this system compared to 0.37 in the reference case.

The comparison of a single-stream system to the three-stream reference case shows how several streams in a common flow field will affect each others configuration and flow. Thus, the central stream of the reference would increase in size and in quantity of discharge if the two lateral streams were eliminated or moved further away. The flow and geometry of the single-stream system is itself constrained by the lateral no-flow boundaries imposed on the system. Implicit with the use of the two lateral no-flow boundaries is that the watershed is situated adjacent to similar watershed systems and, thus, the no-flow boundary is a stream surface common to two adjacent watersheds.

If the single-stream system is not restricted by lateral hydraulic surfaces, then its stream system should increase its size and discharge to an even greater degree. Figure 72 shows the center section of the simulated flow system that contains a single stream. The lateral boundaries of this system extend nearly five-hundred columns in the x-coordinate direction. The aquifer is ten times the

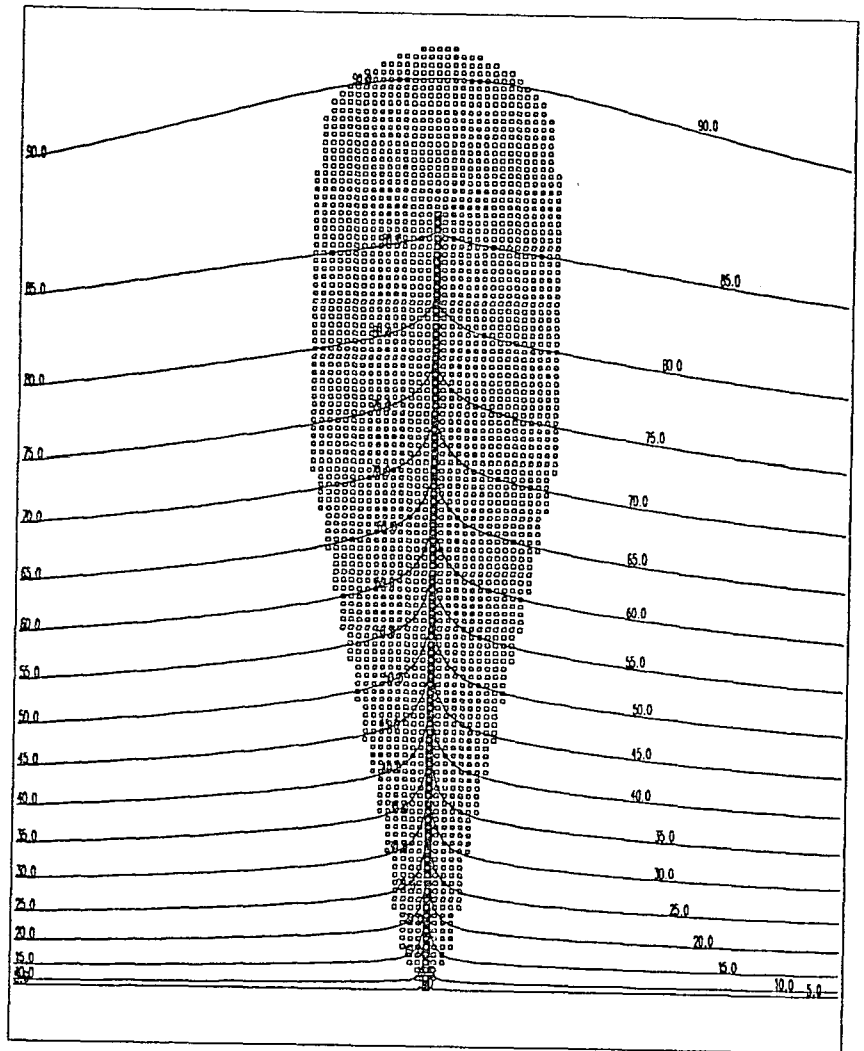


Figure 72--Map view showing lines of equal head and the source areas of streams on the free surface for the **'single stream in wide watershed'** simulation. Squares along stream channels indicate where groundwater discharge occurs. Octagons indicate that model cell is at least partially a source for stream discharge.

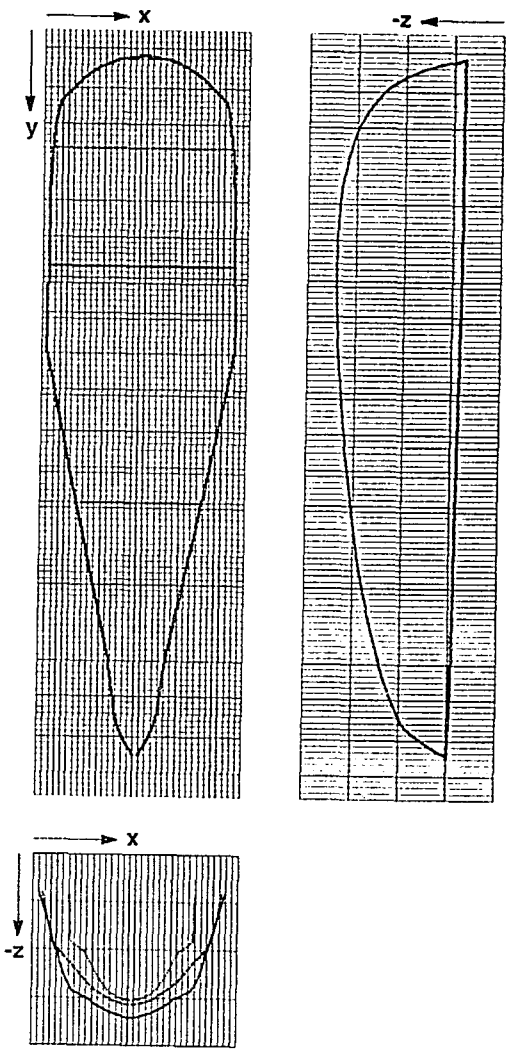


Figure 73--Profiles of bounding surface for the center stream sub-system flow for the **'single stream in wide watershed'** simulation viewed along each of the three Cartesian coordinate axis.

width of the reference system and is equivalent to a ninety-five-mile wide watershed with a single stream in the center. It was necessary to extend the aquifer this far in order to reduce the x-component of flow from the extreme columns to negligible amounts. This was done in order to insure that potential lateral flow to the stream was not restricted by placing no-flow boundaries too close to the stream. The head profiles of these end columns approach the configuration of the 'non-drainage' profile (note inter-stream head and 'non-drainage' head profiles in figure 79a).

Figure 73 shows the contributing area to the stream for this system. It is evident that size and shape have adjusted to the additional lateral flow into the stream system. The outline of the lower section of the contributing area is similar to shapes in previous simulations as this region is strongly controlled by the constant head boundary. However, the edges of the upstream section of the stream catchment area parallel the straight lateral boundaries. The upper tip is also straight and parallel to the divide. These linear features suggest that the bounding surface of the stream sub-system is controlled, in part, by the geometry of the aquifer boundaries when no other interference is present. For this system the rectilinear outline of the aquifer boundaries is reflected in the contributing-area outline.

*Multiple stream systems*

It is evident that multiple streams in a watershed system must generate flow geometries that vary depending on the number of streams present in a

system. This is demonstrated by the five-stream and seven-stream systems shown in figures 74 through 76. In the five-stream system although the total contributing area of flow increases to 37.9%, the average area is only 7.6% for each stream. The area for one stream is less than half the area of the one-stream system (16.8%) and 3% smaller than for the average stream in the reference simulation (10.3%). All of these streams in the five-stream system have correspondingly smaller lengths and widths, they are more shallow and show the characteristic wedge-shape of the upstream end that has become associated with relatively weaker-discharge systems (see figure 75).

The total contributing area for the seven-stream system increases to 42.5%, but each stream covers an area slightly more than 6%. All other stream measurements also decrease. An examination of all the geometrical and hydraulic features of the simulations involving the one, three, five and seven stream systems show that non-linear decreases of lengths, widths and areas result with additional streams added to the system (figures 76a and 76b). For the three- five- and seven- stream systems the inter-stream distance is 0.15, 0.08, and 0.03 respectively. In a nine-stream system the stream catchment areas would still not coalesce, although the inter-stream distance would be between 0.01 and 0.015.

In figure 77 the variations of several stream flow system topology measurements are shown as a function of drainage density. The plots are based on the topologies of 7 different stream systems, 4 odd-numbered stream systems previously discussed, and 3 even-numbered stream-system simulations

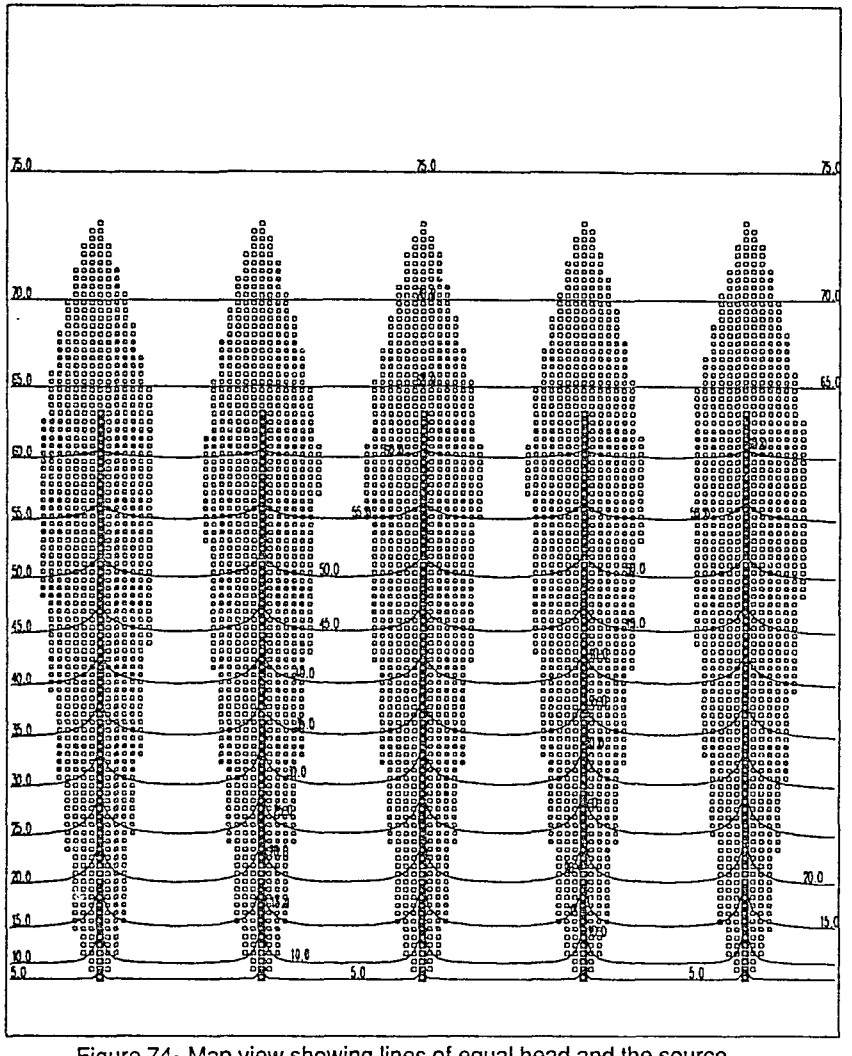

Figure 74--Map view showing lines of equal head and the source areas of streams on the free surface for the **'five stream'** simulation. Squares along stream channels indicate where groundwater discharge occurs. Octagons indicate that model cell is at least partially a source for stream discharge.

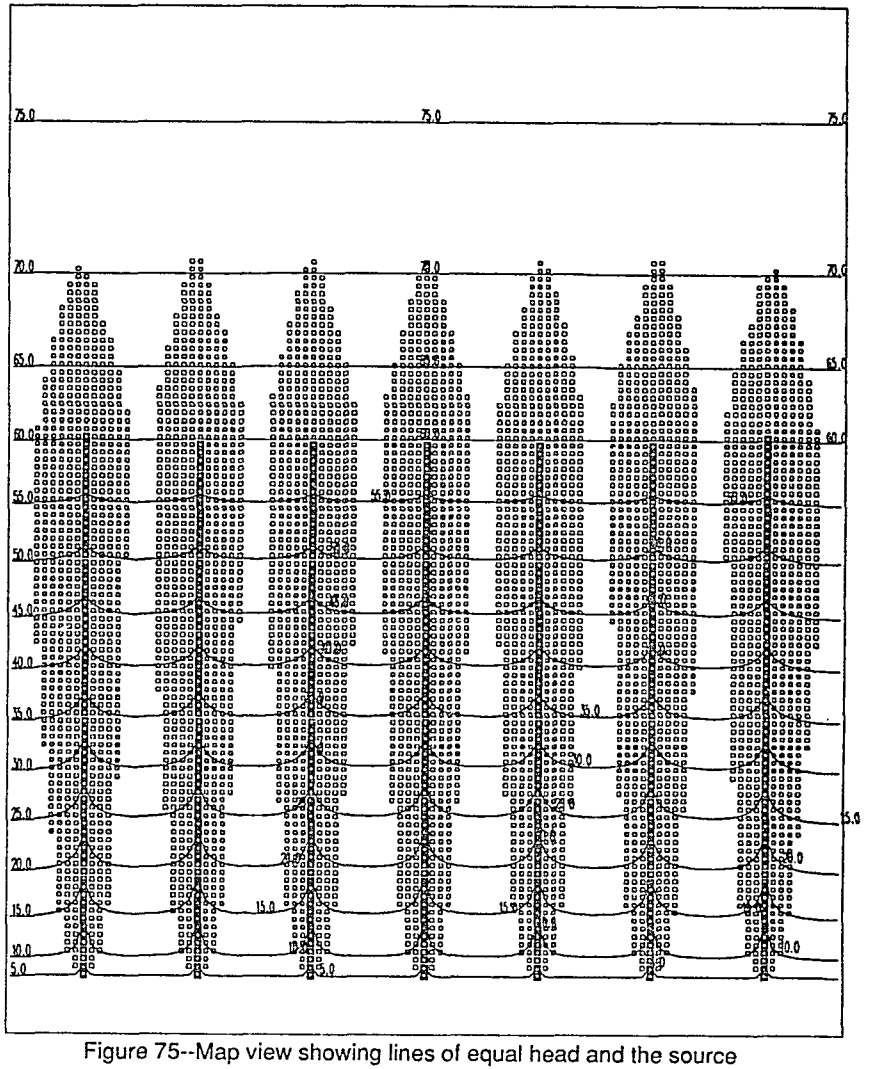

Figure 75--Map view showing lines of equal head and the source areas of streams on the free surface for the **'seven stream'** simulation. Squares along stream channels indicate where groundwater discharge occurs. Octagons indicate that model cell is at least partially a source for stream discharge.

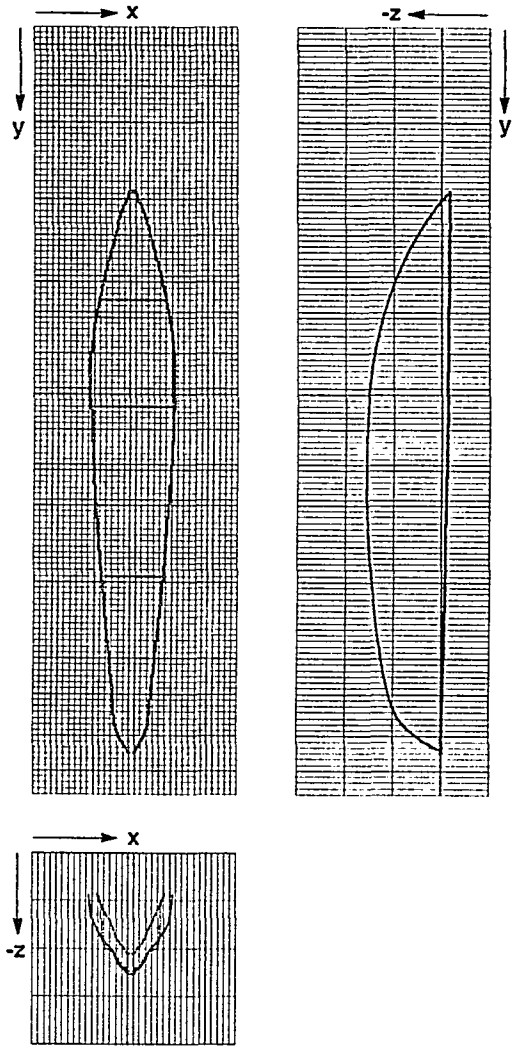


Figure 76a--Profiles of bounding surface for the center stream sub-system flow for the '**five stream**' simulation viewed along each of the three Cartesian coordinate axis.

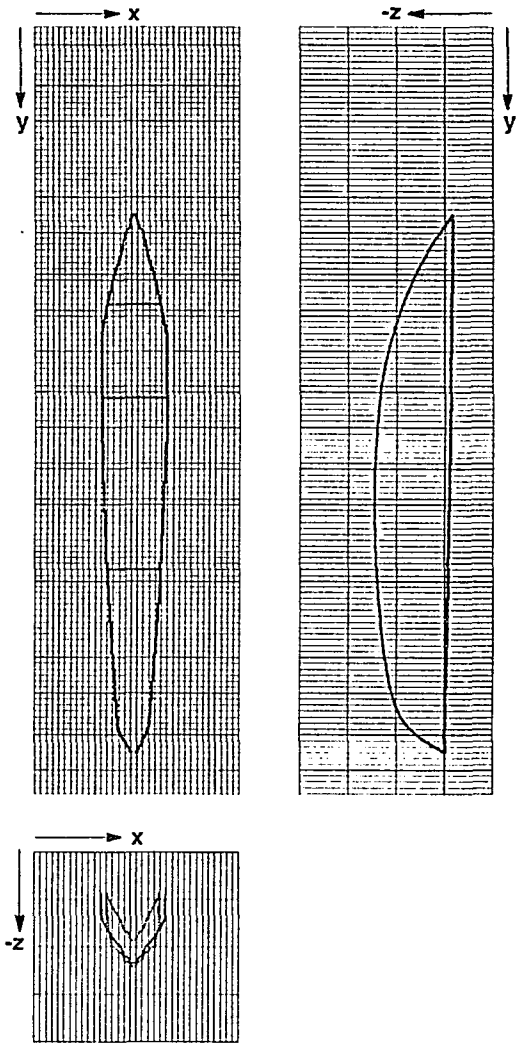


Figure 76b--Profiles of bounding surface for the center stream sub-system flow for the '**seven stream**' simulation viewed along each of the three Cartesian coordinate axis.

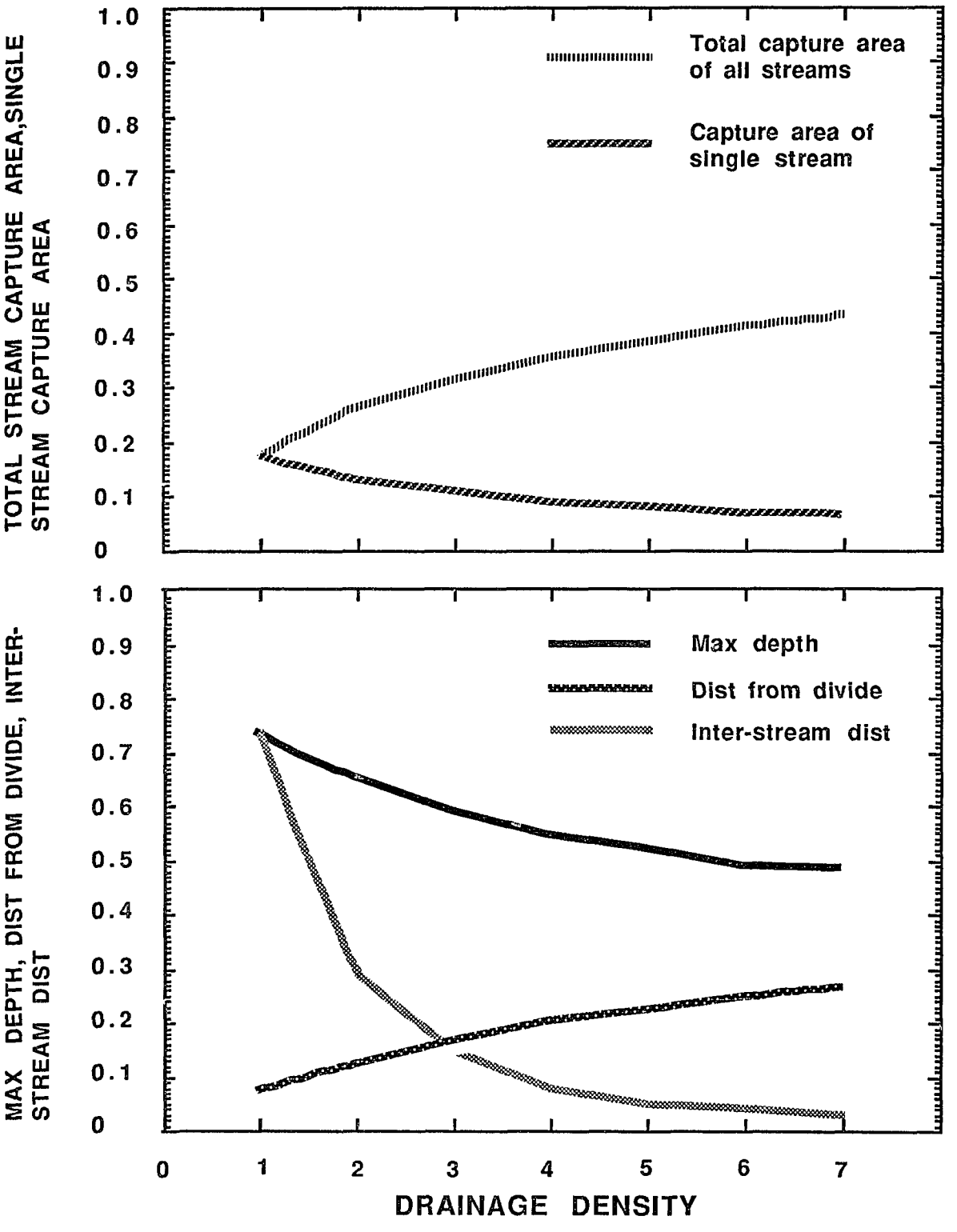


Figure 77--Line-graphs showing non-linear relations between drainage density and geometric characteristics of the system.

not discussed in this study. The upper plot of figure 77 shows the capture area of all streams and of a single stream in each system as a decimal fraction of watershed area. The capture areas vary asymptotically with increasing drainage density. There is a nearly-inverse relation between total stream and individual stream capture areas. The lower plot of figure 77 shows the relation between drainage density and maximum depths, the inter-stream widths, and the distances between divide and upstream ends of stream capture areas. These distances also vary asymptotically with increasing drainage density.

It appears that the magnitude of change in topological measures of the stream systems diminishes with increased drainage density. Size and shape changes are greatest between systems of low drainage density but become negligible between systems of high drainage density. This may relate to previously discussed concepts of energy levels in the aquifer system: increasing the number of discharge outlets in a system that has few outlets causes larger drops in the potential energy of the system whereas increasing the number of discharge outlets in a system where many outlets already exist has negligible effects on the potential energy. The energy drops are seen here as magnitudes of change in the size and shape of the stream sub-sytem flow.

Figures 78 through 81 show the base flows and head profiles for the entire suite of simulations from the extended-boundary to the seven-stream system. Each shows a progressive decrease in maximum base flow and increase in distance of start of flow from the divide.

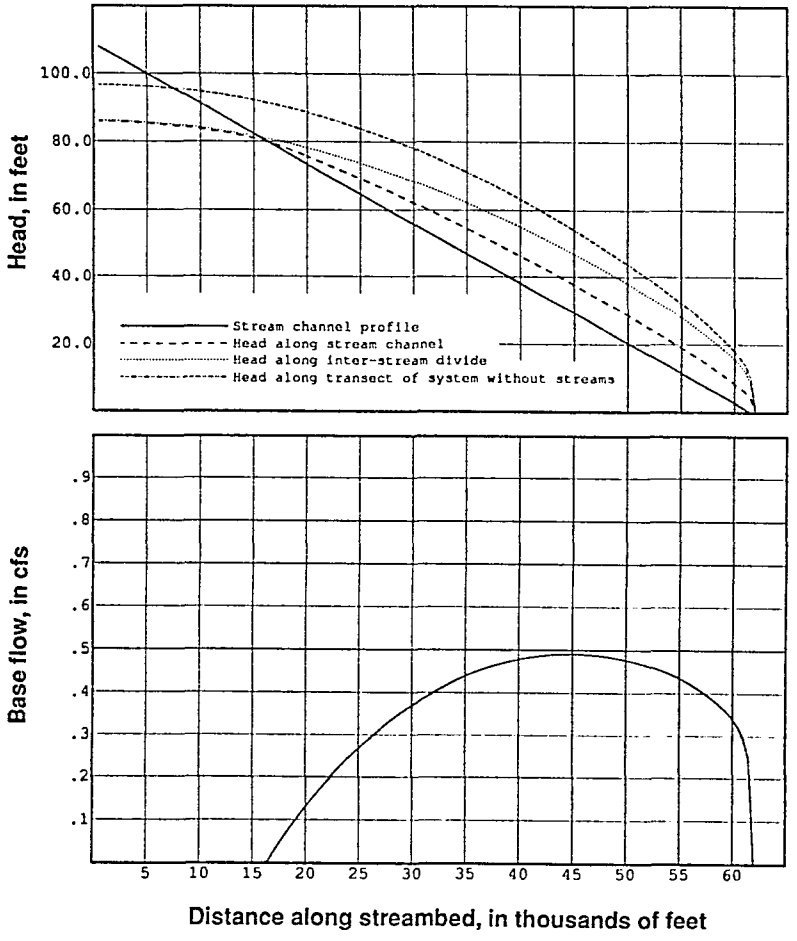


Figure 78a--Profiles of water table along stream channel and inter-stream divide for the **'single stream'** simulation and typical profile for corresponding non-drainage simulation.

Figure 78b--Profile of groundwater discharge to center-stream channel (along model column 52) for **'single stream'** simulation.

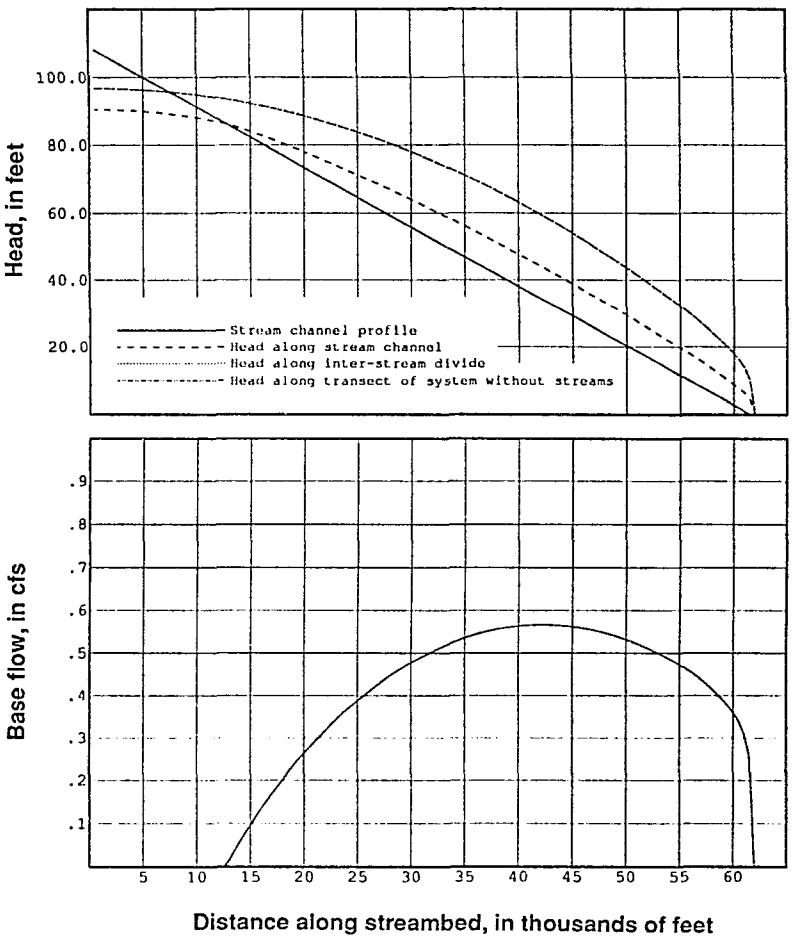


Figure 79a--Profiles of water table along stream channel and inter-stream divide for the **'single stream in wide watershed'** simulation and typical profile for corresponding non-drainage simulation.

Figure 79b--Profile of groundwater discharge to center-stream channel (along model column 52) for **'single stream in wide watershed'** simulation.

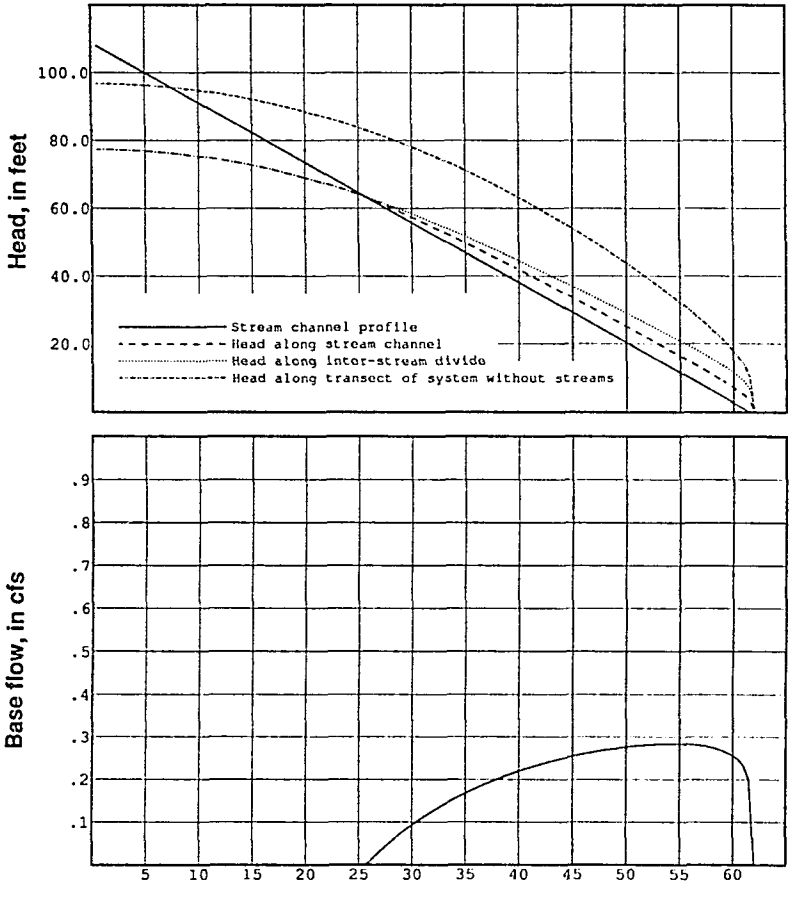


Figure 80a--Profiles of water table along stream channel and inter-stream divide for the '**five stream**' simulation and typical profile for corresponding non-drainage simulation.

Figure 80b--Profile of groundwater discharge to center-stream channel (along model column 52) for '**five stream**' simulation.

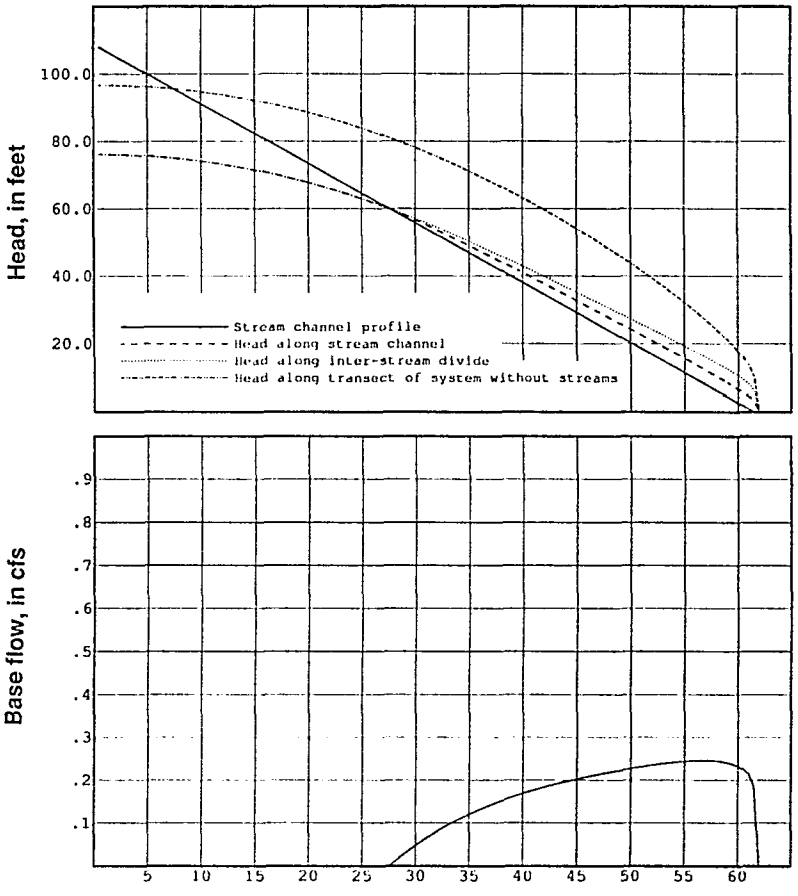


Figure 81a--Profiles of water table along stream channel and inter-stream divide for the '**seven stream**' simulation and typical profile for corresponding non-drainage simulation.

Figure 81b--Profile of groundwater discharge to center-stream channel (along model column 52) for '**seven stream**' simulation.

**Weak- and strong-discharge type systems**

There are several generalizations that can be made from all the previous simulations; the flow characteristics are controlled not only by the nature of the line-sink boundary but, to a large extent, by the boundaries of the aquifer system itself. The surface water body plays a role in shaping the nature of the interface between the deeper, regional flow and stream sub-system flow particularly in the upstream domain. The shape of the 'hull' of the system is affected by depth of aquifer and proximity of stream sub-system to it. This shape is reflected in the shape of the catchment area. Also, the proximity and shape of stream surfaces that border the system will control some stream properties.

Because all of these hypothetical systems involve symmetrical, rectilinear geometry, the stream sub-system flow has a high degree of symmetry and its boundaries are smooth and regular. In real systems where all of these boundaries are quite irregular, the stream system configuration must, necessarily, reflect irregularities of aquifer boundaries (see simulation of real-world aquifer systems).

There are generally two types of systems in which these simulations can be grouped, those with strong discharge and those with relatively weak discharge characteristics. Strong discharge systems have fuller catchment areas, that is, they are long and wide and occupy larger percentages of watershed area. They also are deeper with rounder shapes at the upstream end. In these systems the start-of-flow and point of maximum base flow occur closer to the divide.

The weak discharge systems are shorter, their start-of-flow occurs farther from the divide, they are narrower, and have wider inter-stream distances; also their contributing areas tap into less of the water table. Their upstream ends are V-shaped which reflects their cross-sectional profiles.

Changes in recharge rates, anisotropy, streambed conductance or profile, drainage density, and aquifer thickness can all potentially restrict or increase the head difference between the aquifer and the stream channel. These factors will, in turn, directly affect the quantity of base flow. Greater discharge to streams implies that more of the free surface must provide a source area of stream flow whereas less stream discharge means less area. Consequently, there is no unique parameter that will increase or decrease catchment area. All of the parameters used previously can be adjusted to simulate large or small catchment-area systems, although not in an identical way.

**Coalescence of Catchment Areas**

The coalescence of catchment areas is herein defined as the partial or complete merging of catchment areas of adjacent streams. In effect, parts of the perimeter of two adjacent stream source areas act as a common divide to both systems. Thus far, for all simulations, catchment areas coalesced only in the system without the surface-water body. All other systems show areas of varying sizes between adjacent streams that are source areas to flow for the surface water body. It may appear that the parameter changes of previous simulations were not of sufficient magnitude to induce coalescence. However, for the

hypothetical systems of this study, coalescence actually relates to the degree of control that the surface-water body has on stream sub-system flow.

Two additional flow models were developed in which parameters were purposely manipulated to induce coalescence of stream-source area. Of the parameters that were used in previous simulations to examine cause-and-effect relations, only anisotropy and aquifer thickness were found to affect source-area configuration to a significant degree. Both of these parameters constrain the depth to which the stream system will descend. Increased anisotropy limits the vertical direction of stream system propagation because it imposes increased preferential resistance to recharge. A thin aquifer system limits the space of propagation. The responses of the contributing areas to shallowing and increase of anisotropy are similar although not identical.

For both of the additional simulations the rate of recharge, horizontal aquifer conductivity, and position of the three streams were the same as those used in the reference simulation. Also, the boundary conditions and area were the same. However, an exponential- instead of constant-angle profile was used, the highest elevation of which was adjusted to 95 feet above sea level near the divide. In addition, stream conductance values were set to 10,000 feet$^2$/day. These modifications were made to the streams in order to increase stream discharge and catchment width near upper reaches. The anisotropy ratio was set to 1:1000 for the first simulation. For the second simulation the anisotropy ratio was restored to 1:33, but the aquifer thickness was decreased to 300 feet.

An inspection of the catchment areas of the two simulations (figures 82 and 83) show that, although both parameter adjustments succeeded in significantly increasing stream-catchment areas, true coalescence actually occurs only in the thin system simulation.

The first highly anisotropic system shows that stream source areas in the zone next to the divide are nearly coalescent but are separated by a narrow line of flow lines that form part of the source of flow to the surface-water body. Furthermore, the upstream end forms a broadly rounded border with a contributing area of flow to the water body. Increases in the anisotropy ratio cause further increase in contributing area but do not induce true coalescence.

In the anisotropic system the stream sub-system flow has been restricted to the shallow domain of the aquifer; flow to the surface water body has ample space in which to interact with flow to the stream sub-system and, thus, influence its boundary configuration. The thickness of this system is 1200 feet and allows for development of a source area of flow in remote parts of the watershed system that ultimately discharge to the water body.

In the thin aquifer system the three streams coalesce in their uppermost reaches without the source area of flow to the regional sink separating them. Coalescence is discontinued after a short distance from the divide. The thinness of the aquifer limits the influence that the 'regional' sink has on the most distant part of the stream system. In this simulation the shape of the stream catchment area in the divide zone is rectangular and takes on the shape of the constraining aquifer boundaries as there is no regional sink to affect the flow field and

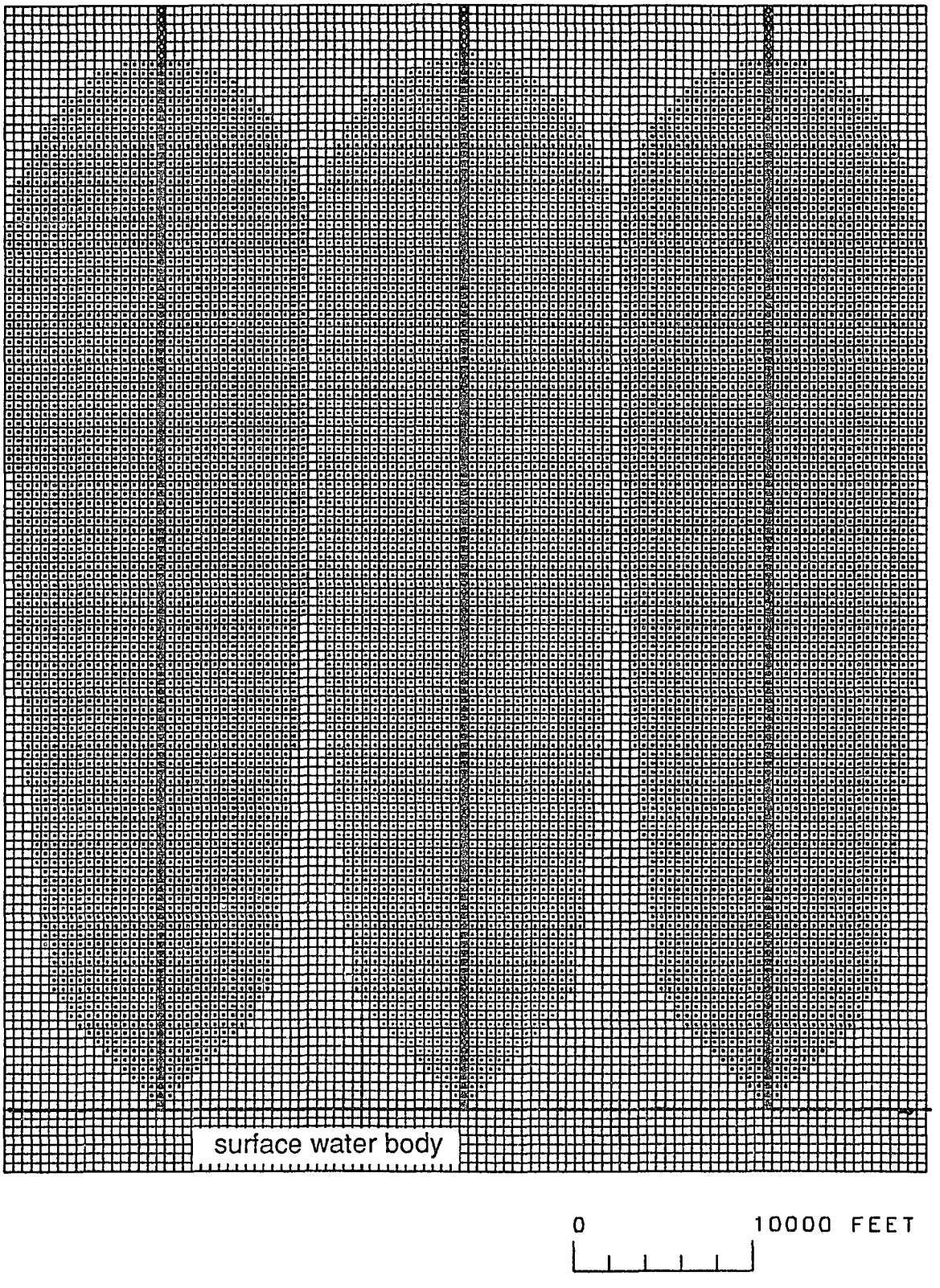


Figure 82--Near-coalesce of stream source areas. Anisotropy is 1000:1

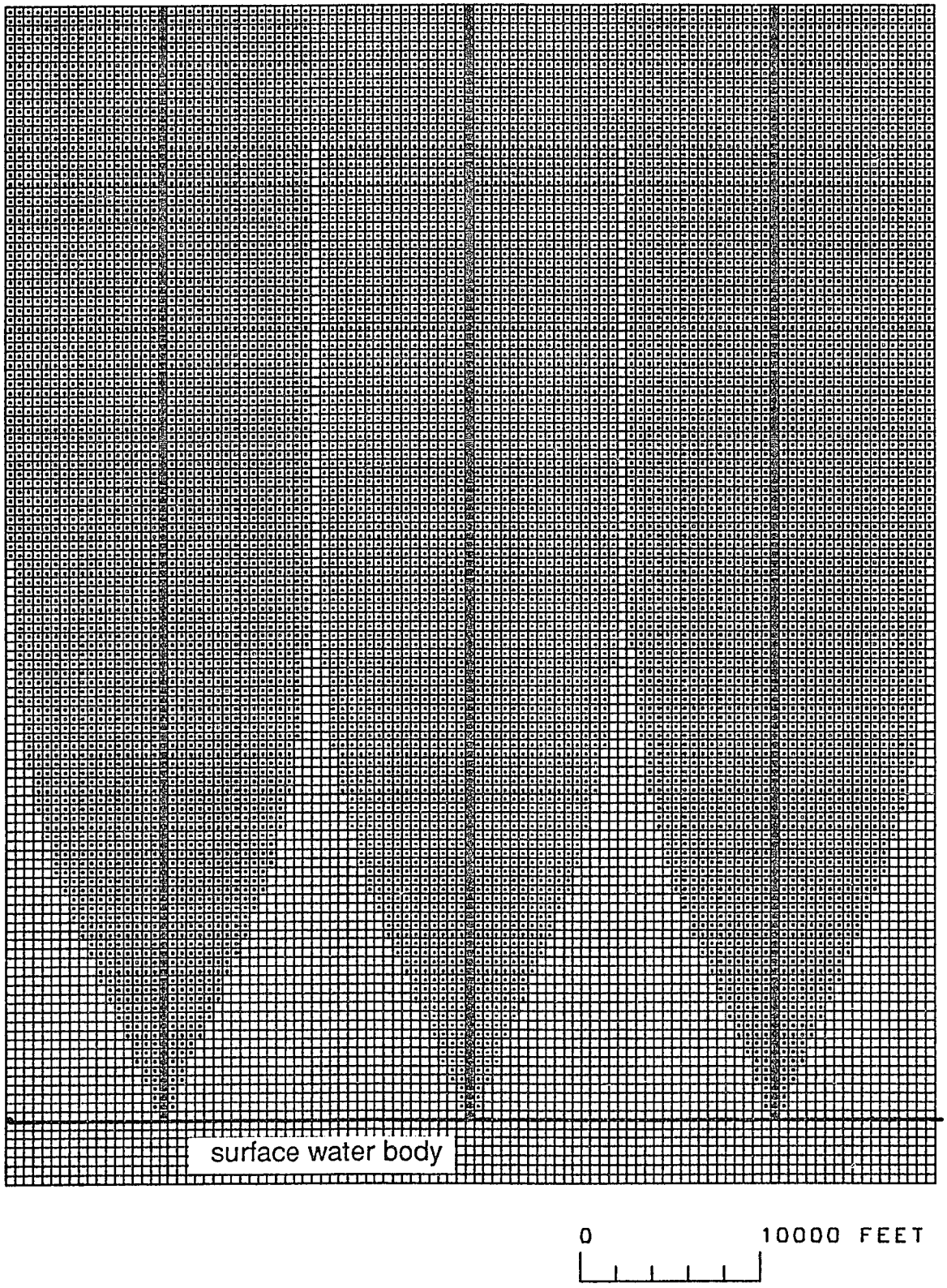


Figure 83--Coalesce of stream source areas. Aquifer thickness is 300 feet.

interaction with the stream sub-system flow. Simulations of progressive decreases in aquifer thickness would show progressive increase of source-area coalescence propagating downstream, while the influence of the water body is progressively restricted to the downstream end of the system.

Clearly, the thickness of the aquifer has greater control than anisotropy ratio over limiting the influence of the regional sink on stream sub-system flow for these simulations. Although the parameters listed in table 1 affect stream catchment size to varying degrees, they will not dampen the effect of the regional sink as well as the aquifer-thickness parameter for this system. This observation suggests that only factors that affect the relative strength of outflow induced by a regional sink will significantly affect the stream system configuration.

## SIMULATION OF A REAL-WORLD AQUIFER SYSTEM

Many simplifications were built into the generic models with respect to aquifer homogeneity and geometry in order to make clear the cause-and-effect relations between hydraulic phenomena simulated in the stream system and the factors that contribute to their occurrence. Yet the analysis would be of little value unless it could be demonstrated that the flow patterns and hydraulics produced in simple, hypothetical systems are, to some degree, valid for real systems.

In this section a finite-difference flow model of an actual system is described and compared to the hypothetical reference model in order to

determine the similarities and differences of each. The differences are an important aspect of evaluation inasmuch as they show how boundary irregularities and variations in water transmitting properties of real-world systems can alter the cause-and-effect relations observed in simulations of highly simplified hypothetical systems.

It is worth noting that even though the finite-difference formulation of flow is patterned after the more complicated geometric and hydraulic properties of an actual system, the flow model of a real system is, nevertheless, still a simplification. For example, the Upper Rancocas system, described in detail in this section, is calibrated to heads in observation wells and stream-gage data at several benchmark stations. On a watershed-scale these data provide a way to determine how closely water mass is estimated by the model. However, it is not practical to determine the discharge along each individual tributary of the drainage system as a prohibitively extensive stream-gaging network would be needed for this purpose. Therefore, simulated discharge tends to be hypothetical on a more local scale. In fact, it is generally impossible to adequately represent all spatial variations in a real system.

## Upper Rancocas flow system

### *Physiography of the Upper Rancocas drainage system*

A three-dimensional, steady-state flow model of Upper Rancocas drainage system of Central New Jersey was developed. The modeled area encompasses a part of the Pine Barrens and is within the Atlantic Coastal Plain

physiographic province. The landform is characterized by low relief; the highest elevations are about 235 feet and are located along the topographic divide which meanders in the north-south direction (see figure 84). Drainage within the upper Rancocas system is to the west of the divide toward the Delaware River. Surface slopes typically vary between 2 to 10 feet/mile. Because of the low relief, swamps, impoundments, and wetlands are widespread features of the landscape.

*Hydrogeology*

The Upper Rancocas watershed drains a portion of the Kirkwood-Cohansey aquifer system; the units comprising the system are part of a layered sequence of unconsolidated marine deposits of Tertiary age that dip to the east-southeast. Figure 85 shows a generalized section of the hydrogeologic units that immediately underlie the watershed. The Cohansey Sand, the upper portion of the aquifer system, is predominantly a quartz sand that contains minor amounts of pebbly sand, silty and clayey sand, and inter-bedded clay. The Kirkwood Formation forms the lower part of the aquifer system and consists of fine to medium sand and silty sand. The Kirkwood grades down to a massive clay at the base of the system and functions as an aquiclude below the aquifer. The Piney Point Aquifer underlies part of the Kirkwood and is separated from the overlying aquifer by 50 to 100 feet of basal Kirkwood clay. It underlies the eastern boundary of the modeled area under the divide. In contrast, the western boundary of the modeled area is underlain by the eastern margin of the

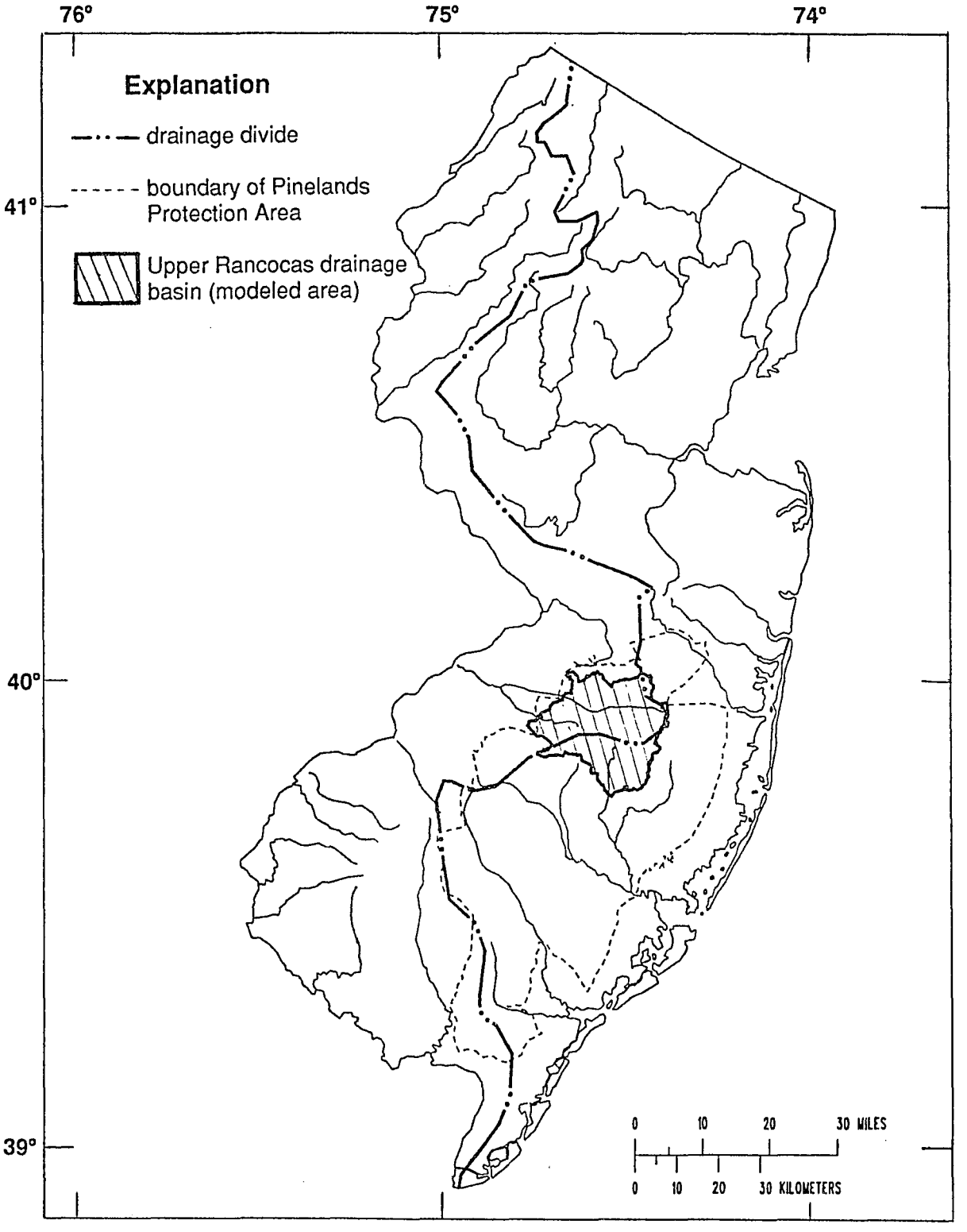


Figure 84--Map of New Jersey showing primary drainage network, drainage divide and outline of the Upper Rancocas drainage basin.

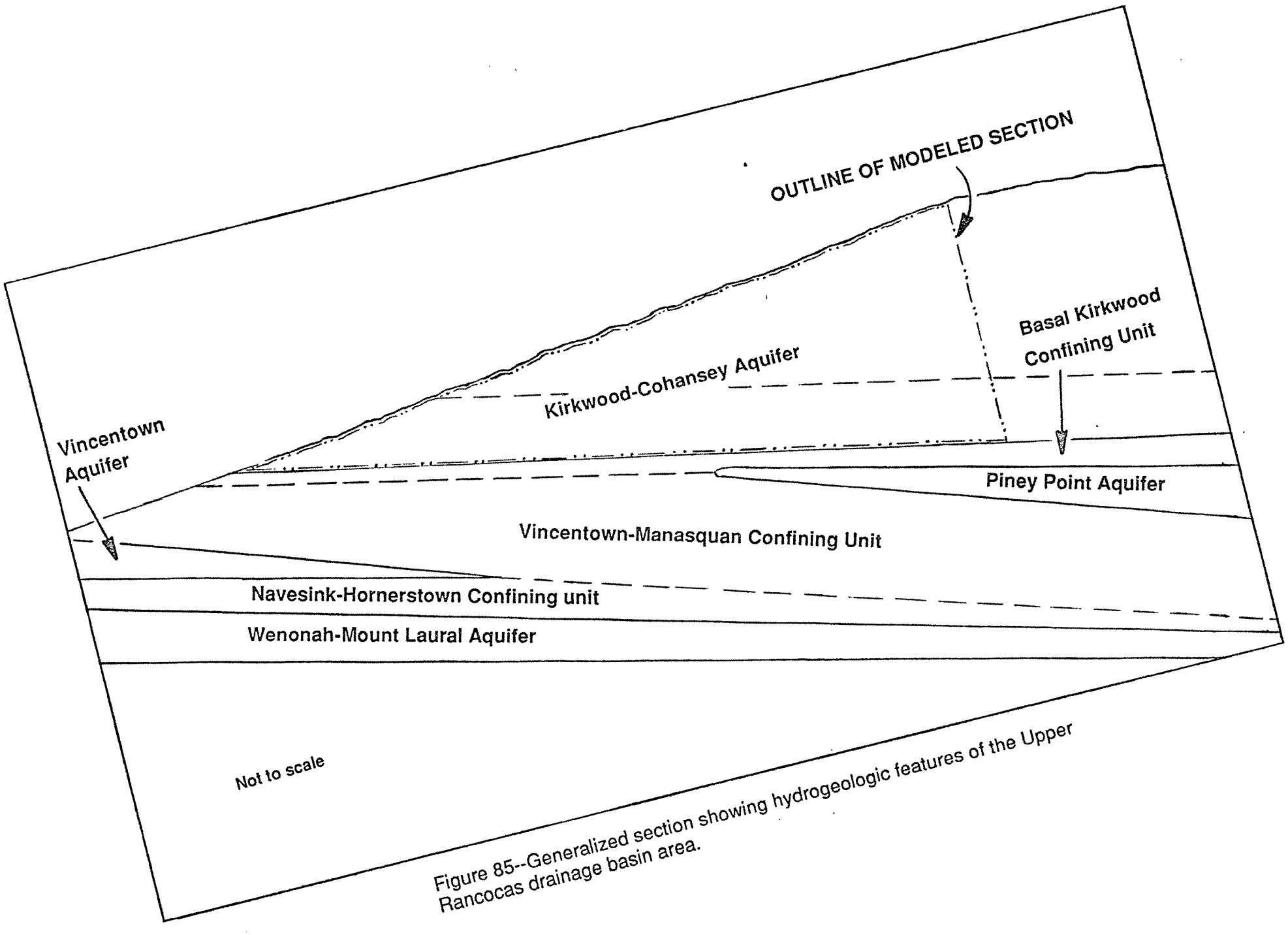


Figure 85--Generalized section showing hydrogeologic features of the Upper Rancocas drainage basin area.

Vincentown aquifer; it is separated from the overlying Kirkwood-Cohansey aquifer by about 200 feet of the Vincentown-Manasquan Confining unit (Rhodehamel, 1973, Zapecza, 1989).

The top layers of the Kirkwood Formation are hydraulically connected to the overlying Cohansey sands. The thickness of the modeled system varies from about 360 feet, under the divide, to 0 at the updip limit to the west where the basal layers of the Kirkwood crop out. Flow in the aquifer is unconfined, although inter-bedded clays create locally confined flow conditions.

*Finite-difference Formulation*

Figure 86 shows the horizontal division of the aquifer and simulated drainage network of the system. The modeled aquifer is divided into two layers of evenly-spaced blocks 1500 x 1500 feet. The perimeter of the model represents the trace of hydraulic surfaces; the dash-double-dotted lines are watershed boundaries and include a segment of the regional drainage divide. The solid line along the top represents the updip extent of the outcrop of the Kirkwood Formation. The drainage network is simulated at cells shown with octagons within the blocks; these cells function as head-dependent seepage boundaries. The streams in the system are effluent, and the stream network serves as the system's major sink. The bottom of the system is modeled as a head-dependent seepage boundary in order to simulate seepage to the Piney Point aquifer and seepage from the Vincentown Aquifer to the north. These aquifers were not explicitly represented in the model.

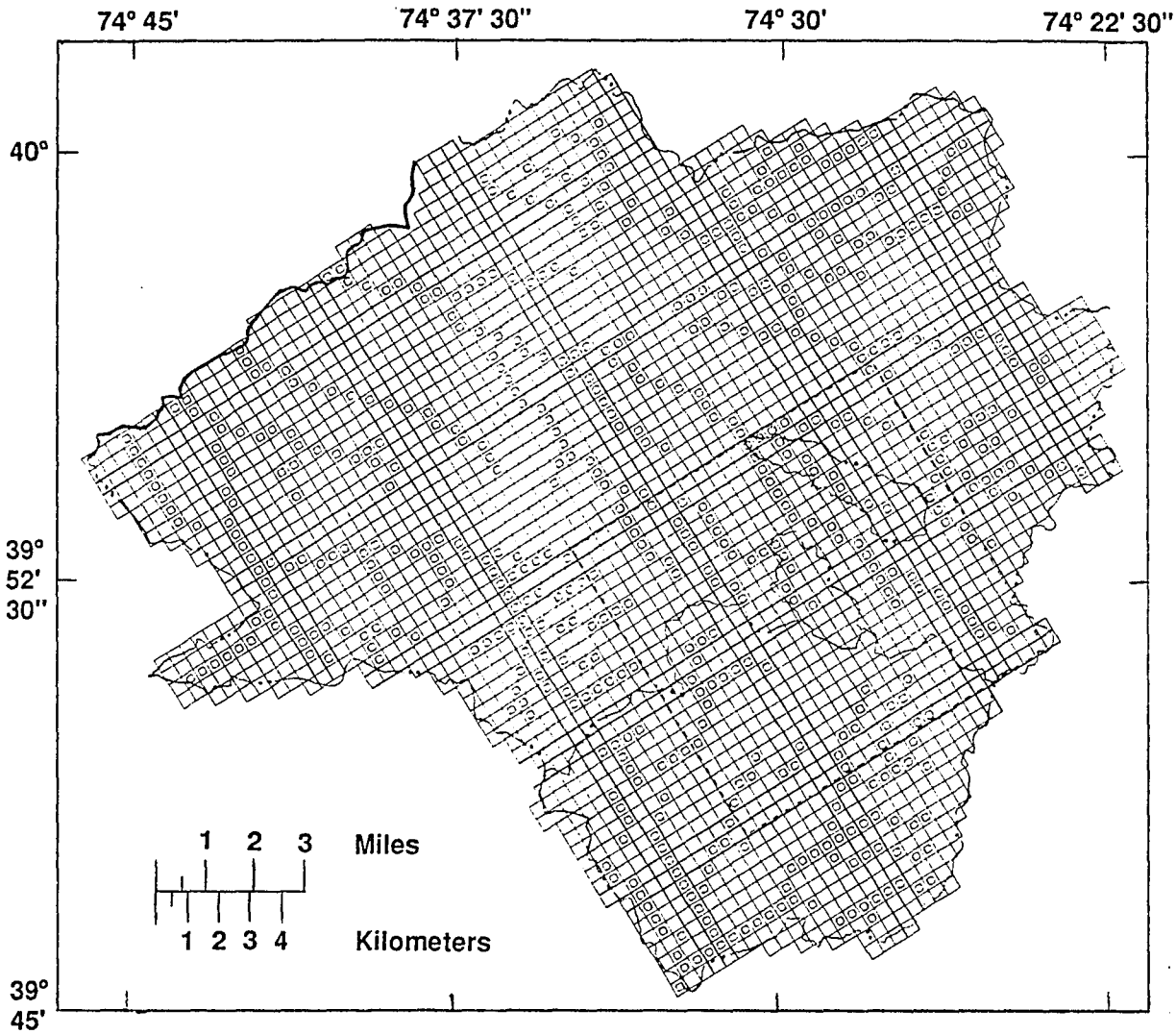


Figure 86--Horizontal discretization of aquifer and drainage network. Grid spacing is 1500 X 1500 feet. Octagons represent cells that function as drains. Dash double-dot lines indicate watershed boundaries. Thick solid line shows updip extent of Kirkwood Formation in modeled area. Dashed rectangle is sub-area of model analysed in detail (see figures 92a and 92b); area includes McDonalds and Middle Branch basins and part of the regional drainage divide.

Figure 87 shows the vertical division in a generalized section of the system from the divide to outcrop of the Kirkwood. The two lithologic components of the Kirkwood-Cohansey hydrologic unit are represented by separate model layers except along the zone where the Kirkwood crops out. The thickness of the Cohansey Sand is assumed to be two-thirds of the total aquifer thickness. Data from geophysical logs on the altitude of the base of the Kirkwood formation was used to determine total aquifer thickness (Zapecza, 1989). In actuality, there is no distinct contact nor marker-bed that separates the lithologic units. However, the water transmitting properties of the Cohansey Sand are considered to be greater then those of the Kirkwood Formation and are, therefore, represented by different layers in order to assign distinct conductivity values to each unit.

An aquifer test was performed in the Wharton Tract area in 1960, about 2.5 miles south of Batsto, for the purpose of determining the effects of induced infiltration from the Mullica River on the adjacent aquifer (Lang and Rhodelhamel, 1963). The test indicated a transmissivity of about 20,000 $ft^2$/day and was thought to represent values for the entire Kirkwood-Cohansey aquifer. However, well logs from the study and adjacent areas indicate that Cohansey sands have higher conductivities than the Kirkwood Formation. Consequently, a conductivity value of 120 $ft^2$/day was used for the Cohansey Sand and a value of 60 $ft^2$/day was used for the Kirkwood Formation. A horizontal to vertical anisotropy ratio of 10 to 1 was assumed for each unit. The conductivity and recharge values were adjusted by trial and error until head values and base

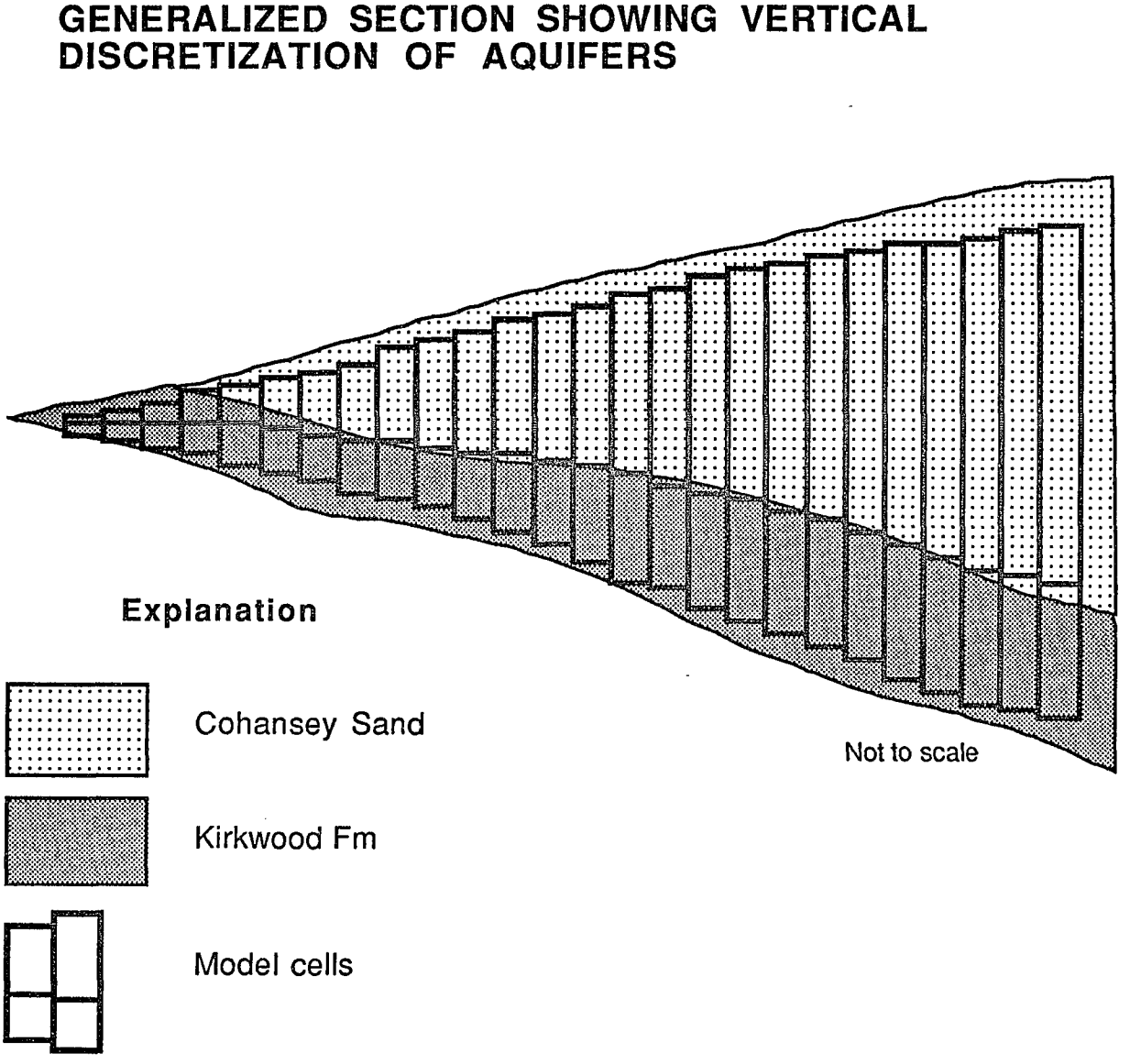


Figure 87--Generalized section showing relation of aquifer units and model layering in Upper Rancocas flow model.

flows matched values recorded in wells and gaging stations within the area. Table 3 shows hydraulic parameters used in the calibrated simulation:

*Flow Operations of the System*

Figure 88 illustrates the general flow patterns in a representative cross section of the system. About 50% of the average precipitation in the area (45 inches per year) recharges the system. Recharge that enters the system at the divide moves vertically downward toward the base; some groundwater seeps through the basal clays and into the Piney Point aquifer. Most groundwater travels horizontally away from the divide to the west and east; for the modeled area flow moves to the west in the updip direction. Deeper groundwater rises and mixes with shallow groundwater, and finally seeps to local surface depressions or discharges into streams. A small quantity of groundwater seeps upwards from the Vincentown Aquifer near the western border of the system.

## Comparison of Rancocas and hypothetical systems

*Major Dissimilarities*

It is clear that the irregularity of boundaries, variations in aquifer thickness, and drainage characteristics in the Rancocas system induce a different flow situation than for that of the hypothetical model. For this system asymmetrical flow is the norm; the nearly perfect bilateral symmetry that facilitated the evaluation of cause-and-effect relationships of the generic system

## HYDRAULIC PARAMETERS USED IN UPPER RANCOCAS FLOW SIMULATION

HYDRAULIC CONDUCTIVITY (IN FEET/DAY):

| Unit | Horizontal | Vertical |
|---|---|---|
| *Aquifers* | | |
| Kirkwood-Cohancey | | |
| upper | 80 - 120 | 8 - 12 |
| lower | 60 | 6 |
| *Confining Units* | | |
| Basal Kirkwood | - | $2x10^{-4}$ - $5x10^{-3}$ |
| Vincentown-Manasquan | - | $5x10^{-4}$ - $2.5x10^{-3}$ |
| Navesink-Hornerstown | - | $3x10^{-6}$ - $3x10^{-5}$ |

RECHARGE (IN INCHES/YEAR):

15.0 - 20.0

Table 3

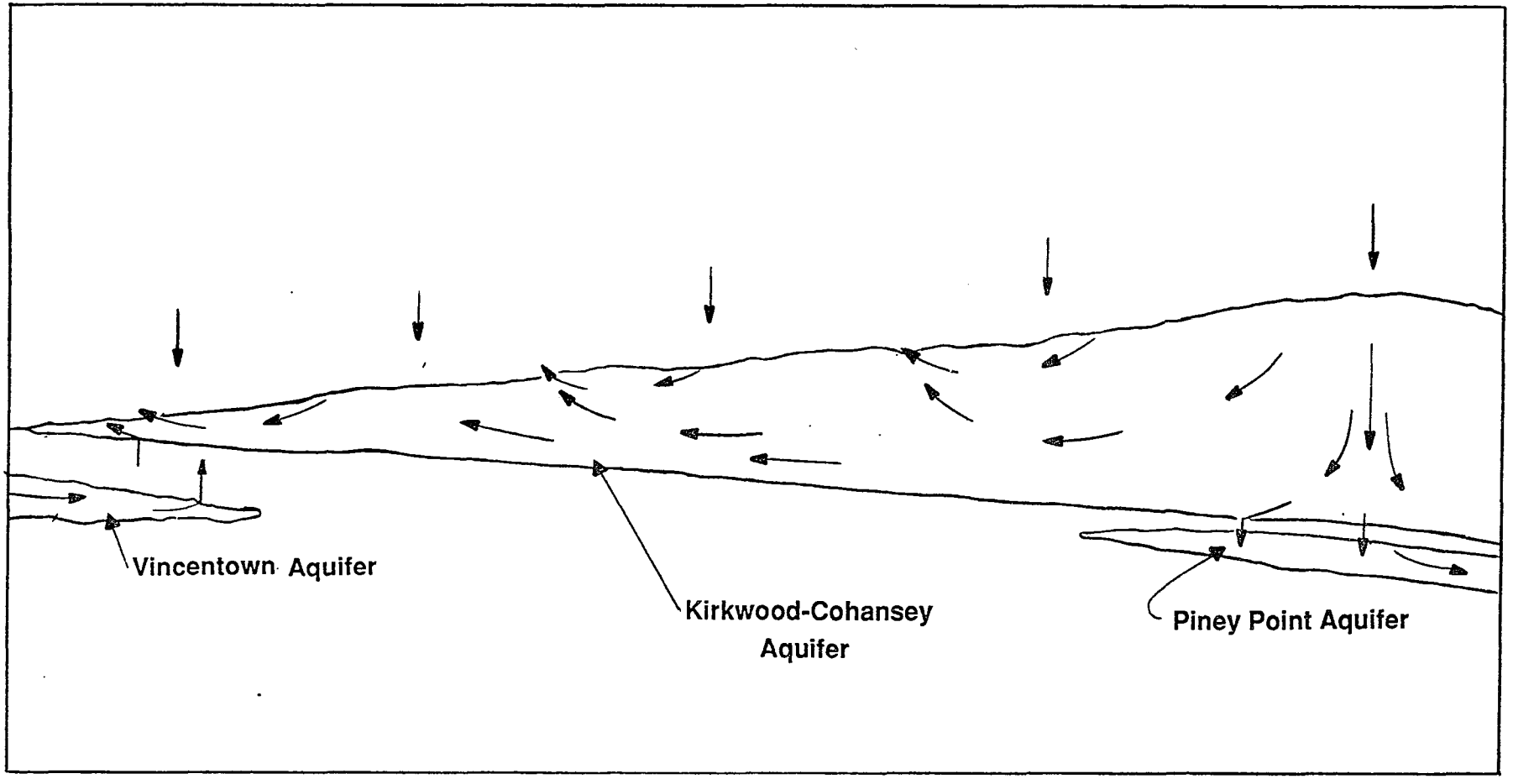


Figure 88--Generalized section of Upper Rancocas hydrologic system and flow operations in aquifer.

is practically non-existent in the real-system simulation. The hydrologic divide has an irregular and meandering trend that follows the topographic highs. Flow adjacent to the divide area moves in divergent paths away from the divide; the horizontal components of velocity, represented as vectors in figure 89, show that flow directions vary considerably within the modeled section. Flow directions range from west to southwest over a relatively short distance near the divide area.

The wedge-shaped thickness of the Rancocas system is unlike the uniform thickness of the hypothetical system; the tapering thickness of aquifer affects the paths and mixing of deeper flow and of shallow flow at discharge areas.

Another major distinction between the two systems is found in the drainage pattern. In the reference system the drainage 'network' is represented as single-stream systems with perfectly straight channels. Clearly, these are over-simplifications of real drainage systems but were used to establish cause-and-effect relations that would otherwise not be apparent in models based on actual systems. Flow in each stream sub-system of the hypothetical simulation is constrained by the deeper flow to the surface body. In contrast, the drainage pattern of the Rancocas system is a bifurcating stream network. In areas where smaller order streams join larger members, the stream boundaries mutually interfere and affect the shape of their flow sub-systems. The convergence of vectors and their increase in magnitude near the drainage network is also evident in figure 89.

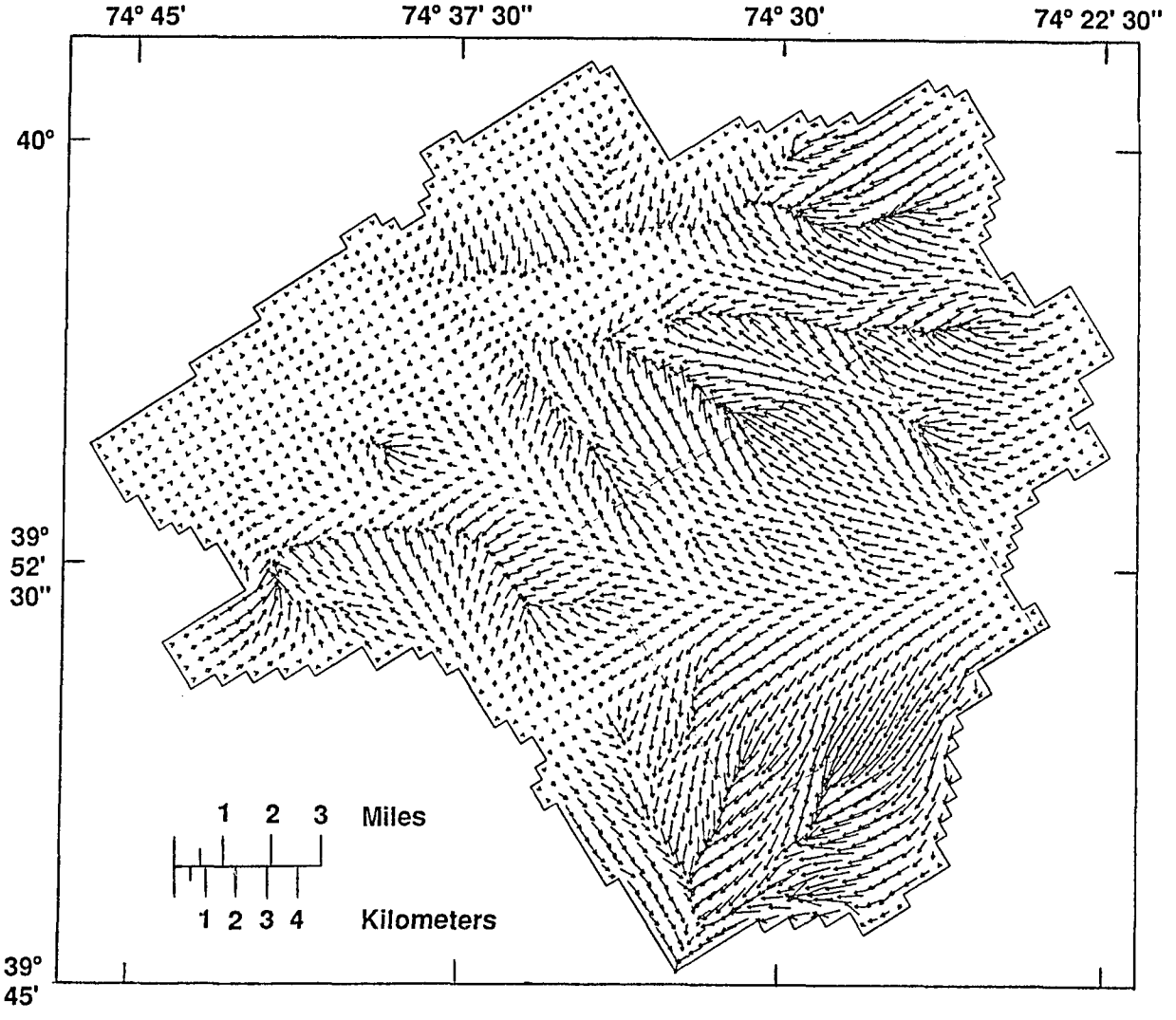


Figure 89--Map view of horizontal velocity components represented as vectors in upper layer of modeled watershed area.

*Base flow and water-table profiles*

The simulated base flow along streams in the Rancocas system can change abruptly from point to point and is unlike the smooth parabolic pattern of the hypothetical simulations. The saw-tooth pattern shown in figure 90 for South Branch shows a typical base-flow profile of the system (map view shown in figure 92b). The pattern is partly attributed to the inability of the finite-difference model to represent the continuous variation of stream channel slopes at larger scales. Nodes that comprise the drainage network are set to a stream-channel elevation. Only an average value of elevation can be specified for the stream reach represented by the length of the block. Steep gradients along the stream are approximated in steps; stream gradients over short reaches cannot be represented when they are smaller than the size of blocks. Hence, the more subtle and continuous variations in base flow elude the finite-difference formulation at a coarse scale. Because changes in stream channel profiles in the hypothetical system were simple and more finely discretized than those of the Rancocas system, a better approximation of the continuous variation of base flow was achieved.

Figure 90 also shows oscillations of base flow and corresponding head profiles along the stream channel. Base flow of streams can decrease locally due to natural diversion of groundwater caused by competing stream systems or other sinks in the aquifer or even because of local increases in aquifer conductivity. Streams may also experience surges due to local constriction in the aquifer. In all cases, however, the base flow is still proportional to the difference

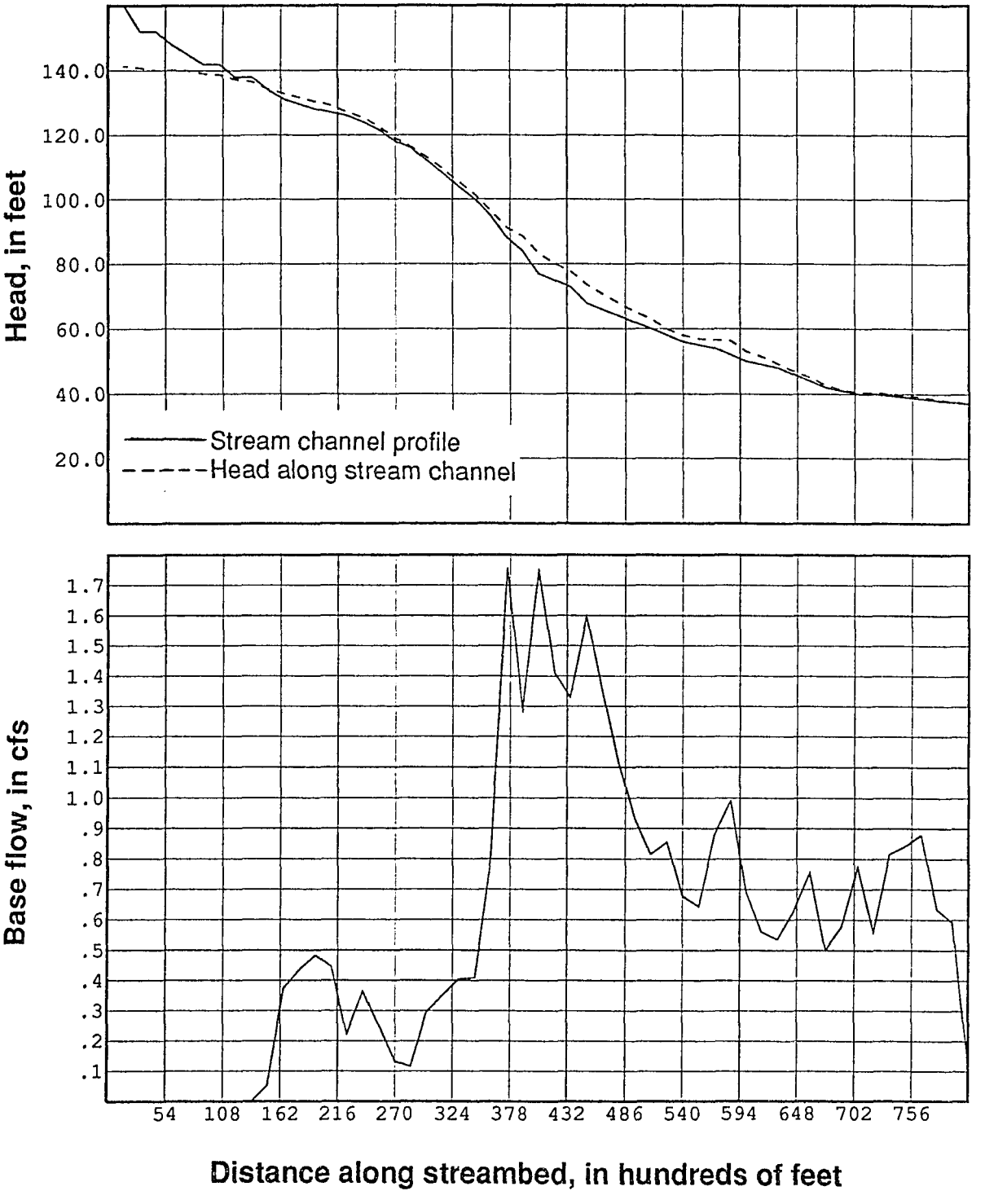


Figure 90--Simulated groundwater discharge along reach of South Branch.

in head between aquifer and streambed. In the hypothetical systems stream conductance values for all nodes were uniform. In the Rancocas system the conductance values are generally quite variable as a result of the model calibration. The discharge irregularities are effected by these conductance variations.

The shape of the water table for the Rancocas system is similar to that of the reference system in spite of the drainage and aquifer heterogeneities. Head values traced along inter-stream positions are higher than for stream channels. Figure 91 show the profile and location of section AA'; the familiar parabolic shape along the water table is evident.

*Source Areas of Flow to Streams*

The drainage system of the Upper Rancocas comprises the predominant system sink for the surficial aquifer (92%); the rest of the groundwater seeps into the Piney Point aquifer (see table 4). In most areas of the basin the recharge area consists of a mosaic of source areas of flow that discharge to different parts of the stream network. Because the modeled system is deepest near the divide, there is opportunity for deeper flow to develop there. Some of this groundwater seeps into the underlying aquifer. However, most groundwater traveling deeper into the system flows under the local shallow flow systems above and moves toward the surface to a more distant part of the surficial aquifer. Consequently, the recharge zone near the divide consists of a mosaic of source areas of flow that discharge to the Piney Point, to local streams, or to higher order streams

## GROUND-WATER BUDGET FOR UPPER RANCOCAS FLOW MODEL

| | Percent | MGD[1] |
|---|---|---|
| **In:** | | |
| Surface water bodies | 0.5 | 1.1 |
| Recharge | 98.3 | 195.3 |
| Bottom leakage | 1.2 | 2.4 |
| **Out:** | | |
| Surface water bodies | 4.6 | 9.2 |
| Streams | 87.3 | 173.5 |
| Bottom leakage | 8.1 | 16.1 |

[1] Millions of Gallons per Day

Table 4

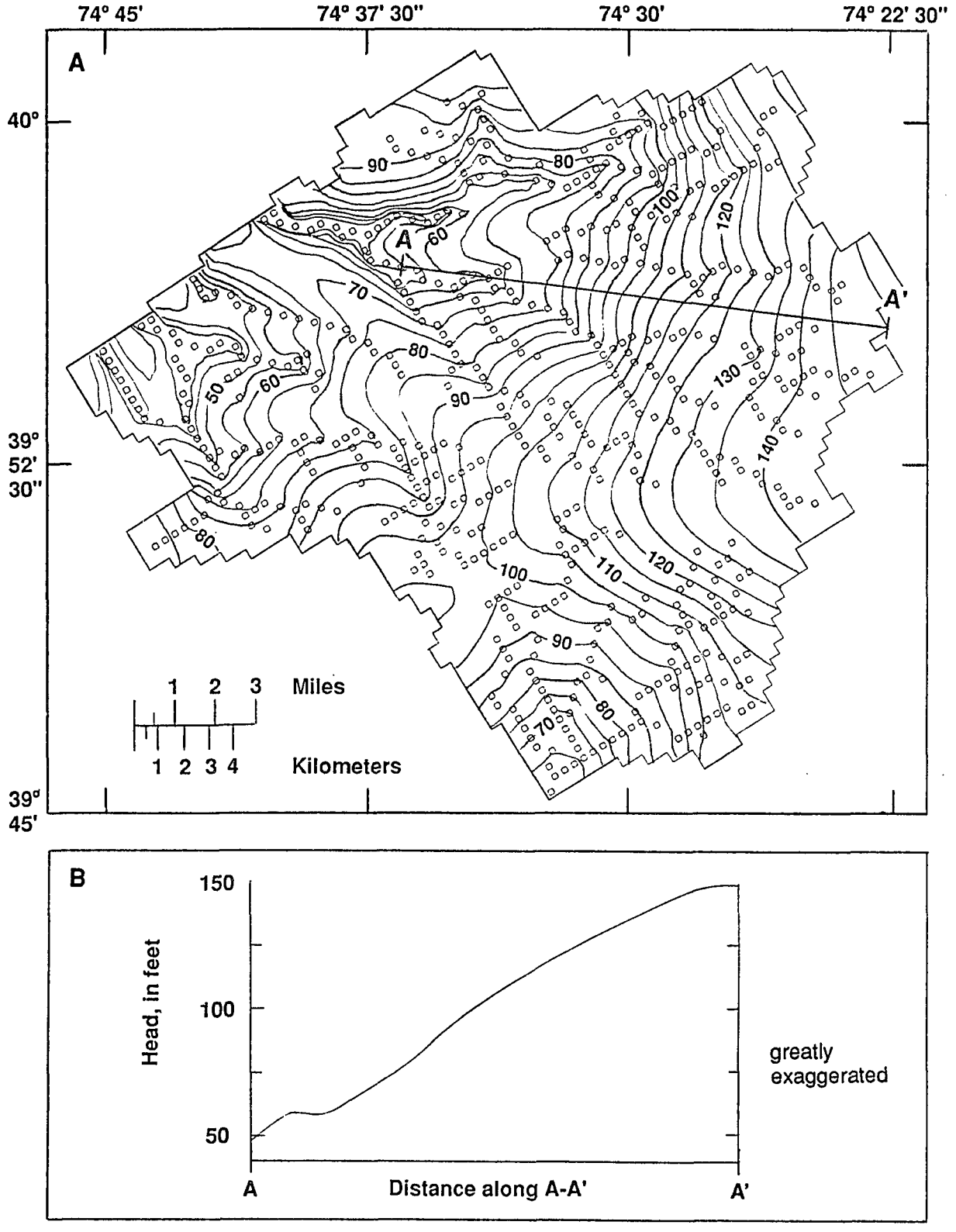


Figure 91a--Lines of equal head in upper layer of modeled watershed area. Contour interval is 5 feet.

Figure 91b--Water-table profile from divide to confluence at Rancocas Creek along A-A'.

in a more remote part of the stream network. In contrast, recharge areas near the divide of the reference simulation are sources of flow for the surface water at the far end of the system and to the remote part of the stream channel .

Figure 92a is a particle tracking simulation that shows the points of origin of flowlines that constitute the contributing areas of flow to stream nodes located within a sub-area of the model (sub-area is shown as grey rectangle in figure 86). The contributing area of flow that seeps to the Piney Point is also shown. Areas that are blank are the source areas to flow to streams out of the sub-area in the system. Flow to streams of different orders and to the Piney Point are differentiated by different symbols. There are some similarities between the shapes of the source areas to streams in this simulation and the reference simulations. The trailing-off upstream ends of the streams are evident in both systems. The second order streams engulf the first order streams. In general, the catchment areas for higher order streams are further downstream and will envelop lower order streams to the degree that the aquifer thickness will permit. The stream system Tibbs Branch on the left side of figure 92a is an example. Also note the separate components of the source areas for South Branch.

Because of the changing course of the groundwater divide, flow diverges away from the divide in a range of directions from due west to due south. This is evident in the varying orientations and bending of the catchment areas. Also, the areas are not evenly apportioned around the stream channels as is the case for the highly symmetric reference model. Note the skewed apportionment of source areas along South and Middle Branch channels (see figure 92b).

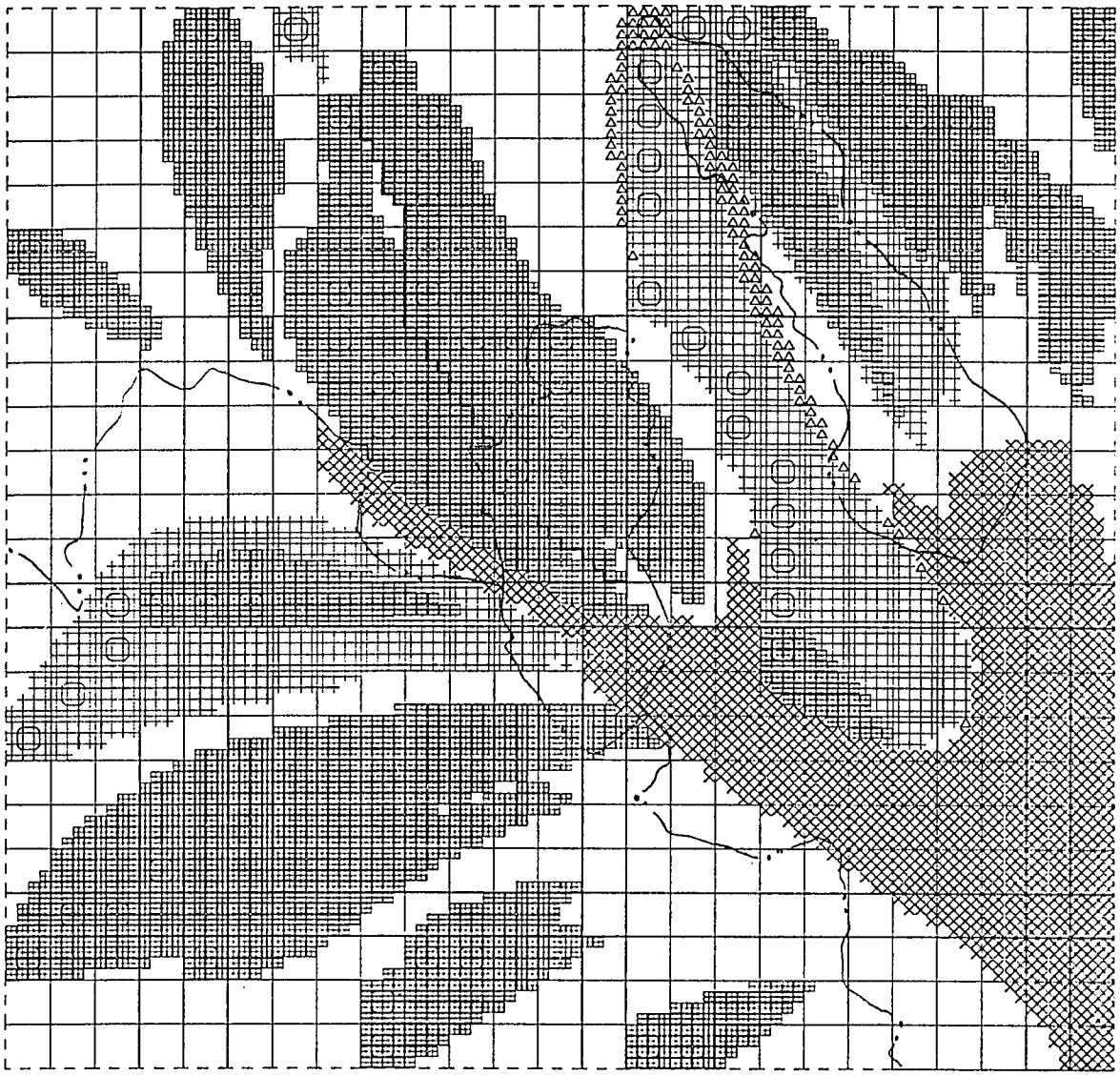

**Explanation**

⊞ capture area of first order streams
\+ capture area of second order streams
Δ capture area of third order streams
X capture area of seepage to the Piney Point Aquifer
▢ node that behaves as sink in simulation

Figure 92a--Source areas of flow to first three orders of streams and to Piney Point Aquifer within sub-area of modeled system. (Location of sub-area is shown in figure 86. Names of streams is shown in figure 92b.)

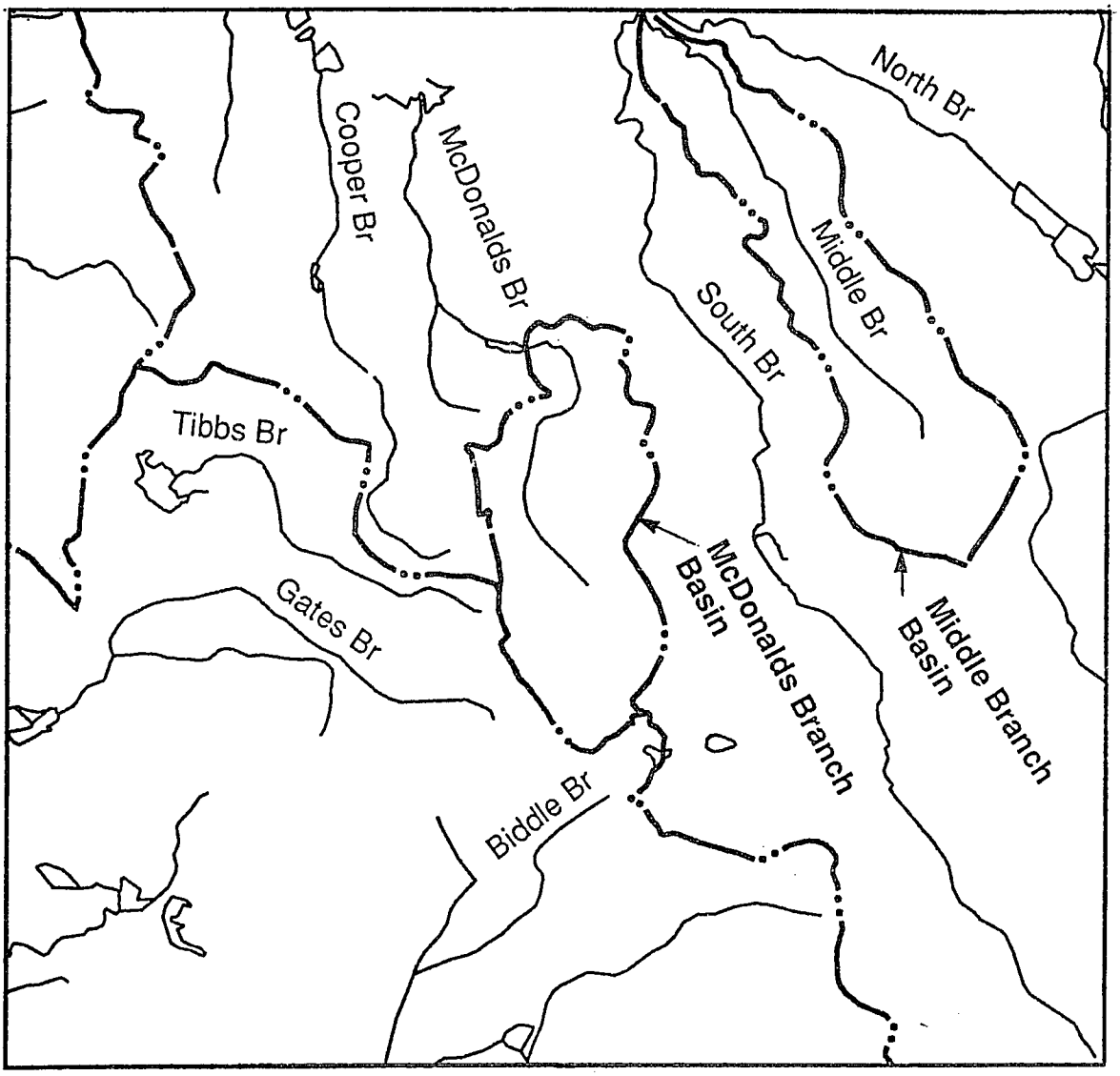


Figure 92b--Map of stream system within a forty-eight square mile area of the Upper Rancocas drainage system near the regional divide. (Location shown in figure 86.)

These departures from symmetry can be attributed to the varying proximity of a stream to neighboring streams and to varying degrees of channel sinuosity. In reality these variations in stream channel distribution develop in response to heterogeneities in aquifer media and landform. However, the model shows only the effect of stream channel distribution on the watershed. The local variations in aquifer material are not modeled at the regional scale.

The Rancocas flow model also demonstrates relations between contributing areas of small-order streams and basins in which they occur. A basin's physiographic borders do not necessarily coincide with the borders of source areas of flow to its streams. An example is the McDonald's Branch basin. Here the stream source area extends over its northern basin boundary. In fact, flow to other first-order streams can be traced to recharge areas within the confines of McDonald's branch basin. (see Coopers and the left-bottom). This is true in sensitive parts of the watershed where flow directions change over relatively short distances.

The source area of flow to the Piney Point is adjacent to source areas of first and second order streams; the presence of this flow sub-system affects the shape of flow in the adjacent stream systems. An indication of this observation can be seen at the upstream end of South Branch's catchment area. The source area to the Piney Point embays part of the source area of the nearby stream systems.

Figure 93 shows an exploded view of the limiting pathlines that define the catchment areas of flow to the Piney Point, McDonald's Branch and South

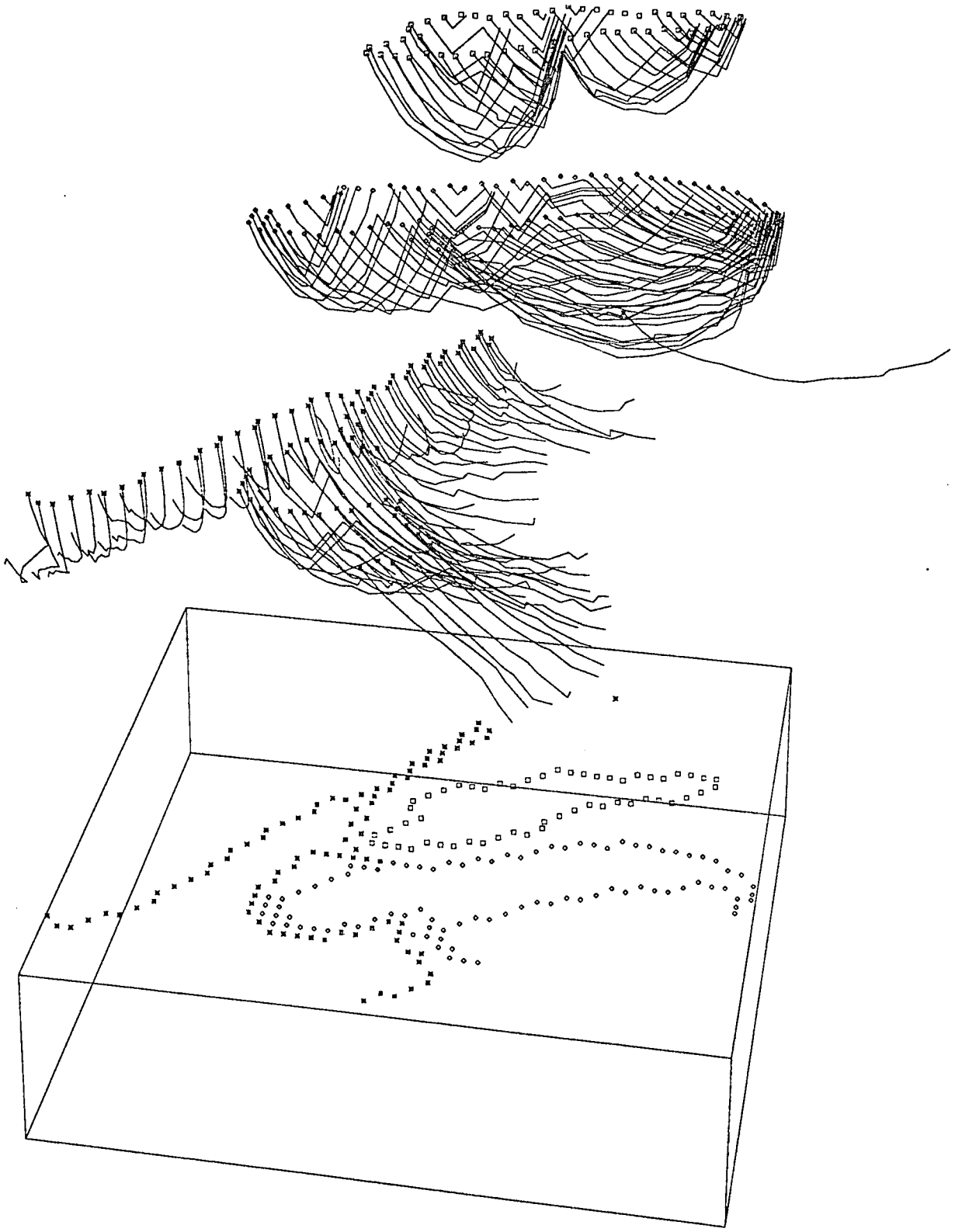

Figure 93--Exploded view of flowlines from source areas to Piney Point Aquifer, McDonald's Branch, and South Branch streams.

Branch. In each flow sub-system the shapes are controlled both by the flow dynamics within the sub-system and mutual effects of these and other systems not shown.

## RESIDENCE TIMES AND GROUNDWATER MIXING

The capability of determining residence time of groundwater is important to applied hydrology, especially with respect to determining how long it takes a constituent that is introduced into an aquifer system to reach a discharge boundary. Because streams function as natural sink networks for portions of the aquifer system (and in some systems for significantly large portions), the issue of groundwater residence times in stream systems is of interest to studies involving solute transport.

Figures 23 and 27 demonstrated how discharge to a point on the stream channel could originate from widely different source localities within the stream's catchment area. The flow paths that converged at a point on the channel originated from both shallow and deep parts of the stream system. In general the travel times of groundwater are related to the length of flow paths as was shown in figure 27. Short flow paths typical of shallow flow usually mean short residence times whereas long flow paths of the deeper system are equated to longer residence times. This observation is, to some degree, an oversimplification because short flow paths in or near stagnation zones can travel at exceedingly slow rates due to low gradients.

**Relation between residence time and stream-source area**

Discharges to a point on the stream channel will have a range of residence times. Figure 94a illustrates the configuration of contributing areas associated with two points of discharge on the channel. The first discharge point is located about 1.3 miles downstream from the start-of-flow. The source area for this point is the smaller, innermost, concentric band. Its range of residence times varies from greater than zero to about 89 years. In this upstream section of the stream channel the residence-time range is not extreme because most flowlines are relatively short and restricted to the shallow system. In figure 22 they are represented by the smallest 'nested shell' of flow lines.

The second discharge point is located at 5.1 miles downstream from the start-of-flow. Its contributing area is the outer, larger band. The range of residence times at this point varies from greater than 0 to about 272 years. Flow that originates from remote localities within the stream's catchment area travel longer and deeper paths in the system; when some of these eventually discharge at point two, they mix with shallow flow that also discharges to this point. In figure 24 these flow lines would be embedded in the relatively larger 'nested shells'. The range of residence times for point two is wider than that of point one.

Points of discharge located near the stream's terminus would show the widest range of residence times because the limiting flow lines originating closest to the divide discharge to this point along with the adjacent shallow flow. It is apparent that the range of residence times for any point along the stream

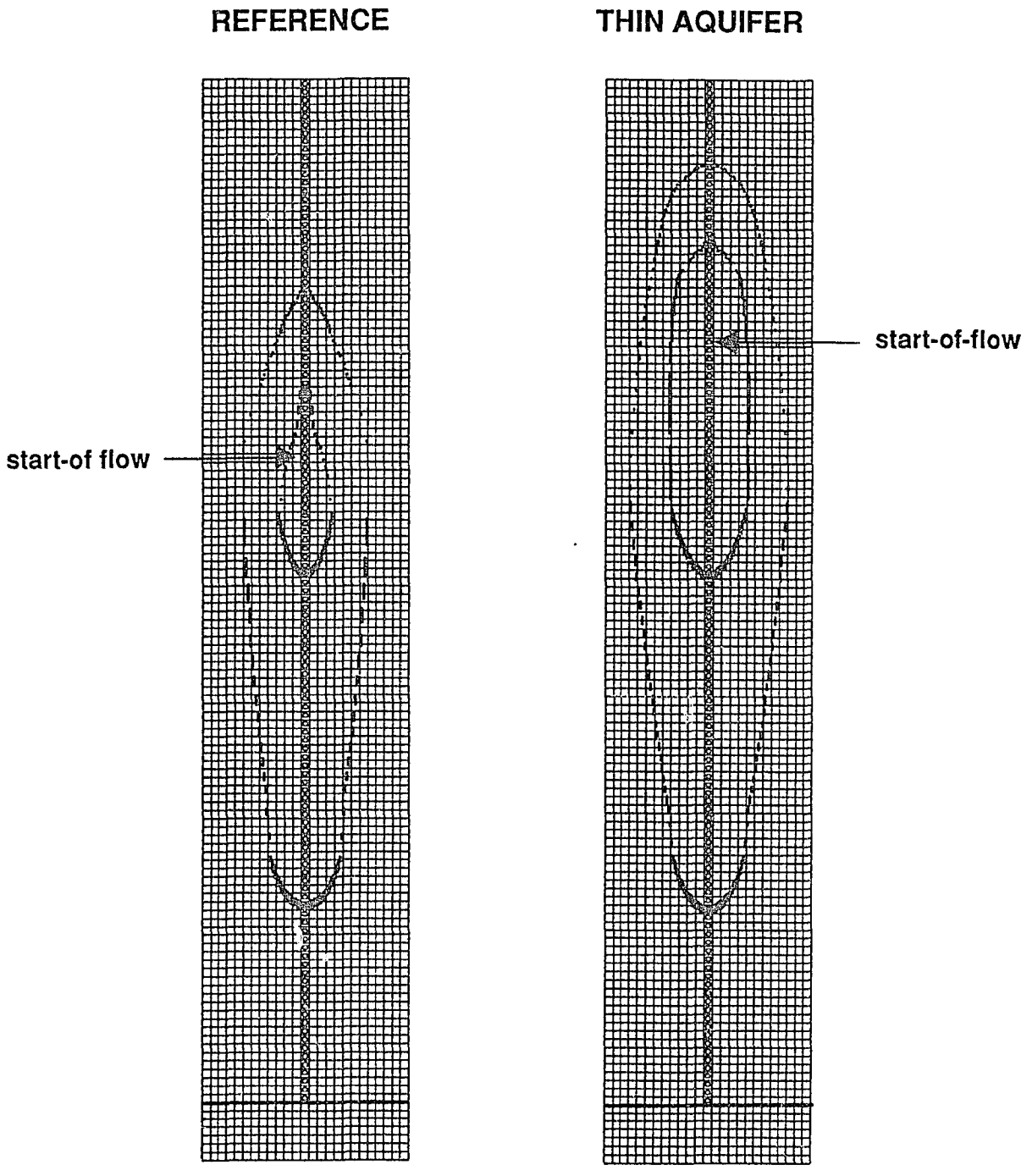


Figure 94a--Contributing areas of flow to nodes 60 and 100 of the center stream in the 'Reference' system. Residence times of flow that discharges to node 60 range up to 89 years whereas those of node 100 range up to 272 years.

Figure 94b--Contributing areas of flow to nodes 60 and 100 of the center stream in the 'Thin Aquifer' system. Residence times of flow that discharges to node 60 range up to 164 years whereas those of node 100 range up to 357 years.

channel is a function of position between the start-of-flow and the stream terminus, with higher ranges associated with increasing distances from start-of-flow.

It should be emphasized that, in practice, it is difficult to define or quantify what constitutes shallow and deep flow. In fact, residence times are sensitive to system parameters and boundaries. In figure 94b an identical residence time determination was made for the shallow-system simulation. A comparison of the residence times of catchment areas for the same two discharge points show how a shallow system affects their distribution. Although the system has a relatively shallow aquifer, the flow lines are made to travel longer distances and hence groundwater residence times for discharge to the same points have a higher range that for the reference system. The range of time is from greater than zero to 164 years for the discharge point closest to the start-of-flow, and from greater than zero to 357 years for the point further downstream.

**Temporal relations in sections of stream sub-system**

The previous discussion focused on areal relations with respect to groundwater recharge-discharge locations and the associated residence times. Cross-sections also reveal information regarding the distribution of travel times in different parts of the stream sub-system. The change in distribution of travel times with distance along the stream is clearly demonstrated by transects showing lines of equal age across the stream channel (figure 95).

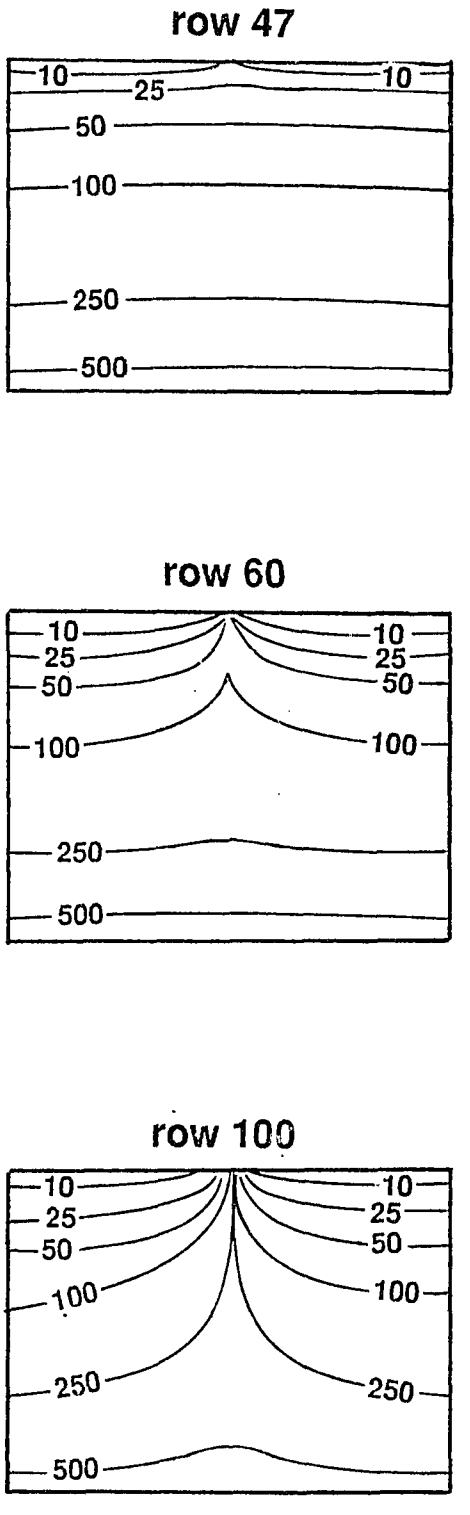


Figure 95--Lines of equal age along three transects between inter-stream divides of the center stream for the reference system.

The transect from row 47 is located 500 feet downstream from the start-of-flow. Lines of equal age of up to 500 years are shown. The age contours are generally parallel to the surface but bulge slightly upward under the stream. The line of equal age closest to the free surface is ten years. The age of groundwater discharging to the channel is relatively young, about ten years or less, with no mixing of older waters.

The section along row 60, located 1.3 miles from the start-of-flow, is similar to that of the previous section except that lines of equal age from 100 years and less are deflected upward directly under the channel. Also, all age lines are slightly closer to the surface. The section indicates that small quantities of older water in the range of 10 to 25 years old discharge with the younger water. The ten-year line of equal age is breached at the stream channel.

The section along row 100 is located about 5.1 miles further downstream from the start-of-flow. Along the sides of the section there is a decreasing age gradient from the bottom upward; here ages increase more rapidly with depth. Directly under the stream, however, the lines of equal age are deflected upward in a spike-like manner. This indicates that 'older' groundwater rises upward at the center of the stream. 'Younger' water discharges adjacent to the older water. The age gradient within the narrow width of the stream bottom is extremely steep and, at the terminus, ranges from greater than zero to about 360 years old. The spike of older water creates a discontinuity in section across the stream. Therefore, discharge along this reach would consist of a range of ages from about 250 years at the center to less then 10 years near the edges.

This age discontinuity is also apparent in the map view of a surface of equal age shown in figure 96. The surface is approximated by points on pathlines that indicate 20 years of travel within the surficial aquifer for particles originating on the water table. The pathlines were generated from four evenly spaced particles for each cell on the water table within the center stream area. These points are shown as a projection to the top of the model. From the figure it is evident that a breach begins 25,000 feet from the divide and continues to widen with distance downstream. Within this breached area 'older' groundwater seeps upward and discharges to the stream channel as shown in the transects.

If a line of wells were screened at regular horizontal and vertical positions along a transect to a stream at some distance from the start-of-flow, it should be possible to map groundwater ages in a manner similar to figure 95 if groundwater samples from each well could be dated. Such an analysis would indicate possible ranges of ages for groundwater discharging to a limited area and a sense of mixing would, thus, be gained. In practice, however, there are some limitations. Various dating techniques rely on different chemical principles for their effective application; a given aquifer system may not have the prerequisite chemical environment. Also, dating strategies have various temporal scales of application which may not be suitable in a particular section.

(One example of a potentially useful technique is dating isotopes that naturally occur in groundwater such as $^{14}C$. Because the half-life of the isotope is 5730 years $^{14}C$ is suitable for dating relatively old water. Groundwater age is correlated to the rate at which the activity of $^{14}C$ decrease with time. The age

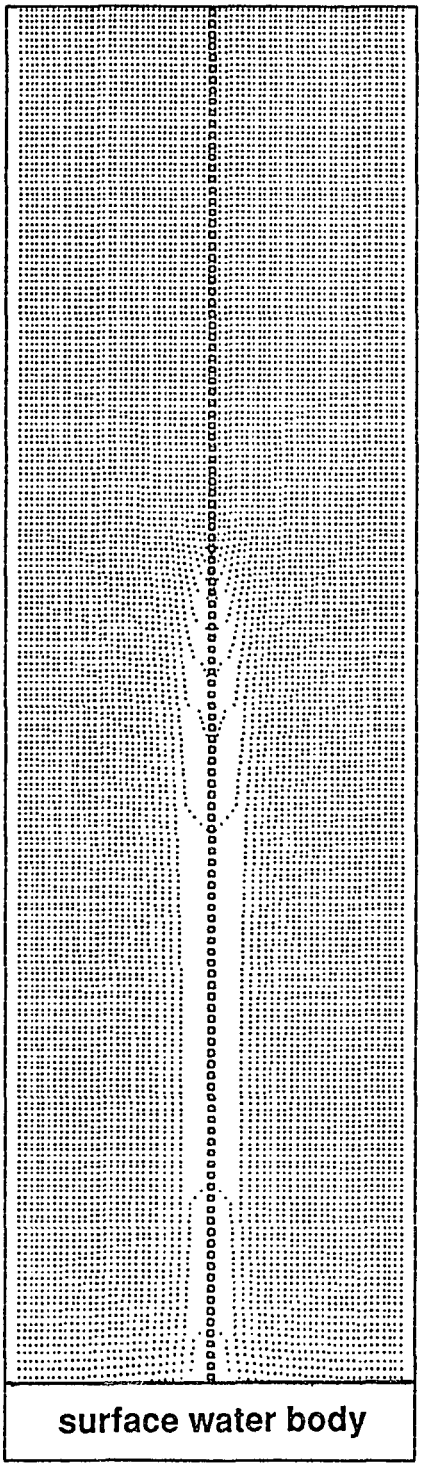


Dots represent points along pathlines that mark 20 years of travel in the aquifer system. Blank area next to stream represents gap in the '20-year equal age surface'.

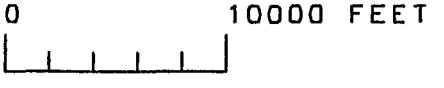


Figure 96--Map view showing 20-year 'surface' of equal age for center-stream area.

refers to the period of time that has elapsed since water has traveled into the aquifer system so as to be isolated from the atmosphere, the presumed source of the $^{14}C$. The technique assumes that the groundwater system is closed relative to other source of Carbon. This approach, of course, becomes problematic when another source of Carbon mixes with atmospheric Carbon, such as the dissolution of limestone or from oxidation of organic material. In such cases, an adjustment factor must be used if the source of the additional Carbon can be determined. The residence time-source area relations that were heretofore discussed would be useful for determining other Carbon sources.)

Another perspective on age relations in stream sub-systems can be seen by determining the relative proportions of 'younger' and 'older' water that discharge along the stream channel. Assuming, for the moment, that in this system residence times of 20 years or less are young and residence times greater then 200 years are old, then it can be seen that older groundwater becomes a progressively larger component of discharge with distance downstream.

The variation in the proportion of young water to older water is shown in a plot (figure 97a) of base-flow distribution along the stream channel. The divisions in this plot assume that young water is less than 20 years of age and very old water is greater than 200 years of age. Thus, there are three age groups for water. The plots are actually a tally of the maximum travel times of path lines, used in the simulation, that terminate along the stream channel. Their distribution reflects the parabolic variation of discharge from start-of-flow to

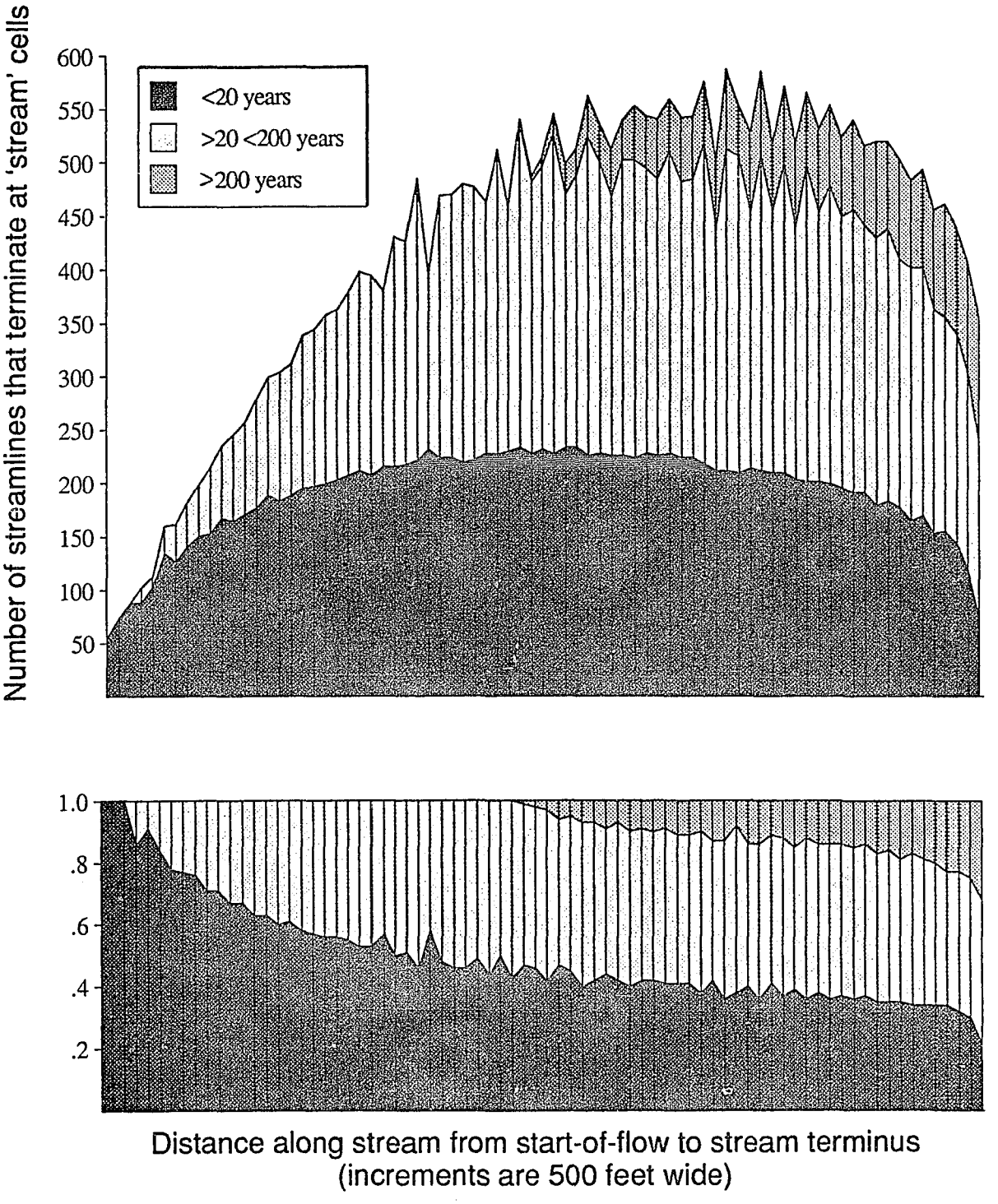


Figure 97a--Distribution of base flow in terms of number of pathlines that discharge along stream channel shown as proportions of 'young', 'middle-aged', and 'old' water.

Figure 97b--Distribution of base flow in terms of normalized number of pathlines that discharge along stream channel shown as normalized proportions of 'young', 'middle-aged', and 'old' water.

stream terminus simulated by the flow model. The proportion of young water along the stream's length follows the parabolic shape of total base flow along the same length. However, compared to the older water, young water makes up a progressively decreasing fraction of stream discharge with distance downstream. Very old water does not begin to discharge until about 3.4 miles from the start-of-flow. Figure 97b shows a normalized version of the same age distribution.

**Fate and residence times of contaminants**

The above models of catchment area and residence time for stream systems can be used for water quality management purposes to demonstrate different scenarios for the fate and natural flushing times of contaminated sources in which constituents behave as conservative tracers. The following demonstration is predicated on the concept of plug flow where constituents introduced into the groundwater system are transported advectively:

Consider the two hypothetical contaminated areas labeled A and B in figure 98. It is assumed that these contaminants are conservative, and are introduced into the system at some point in time within the areas shown and are continuously released thereafter. Because contaminated area A is straddled over the edge of the stream catchment area, part of the contaminated groundwater will discharge to the water body. The area that lies within the stream catchment area will discharge along about 7.2 miles of stream channel beginning about

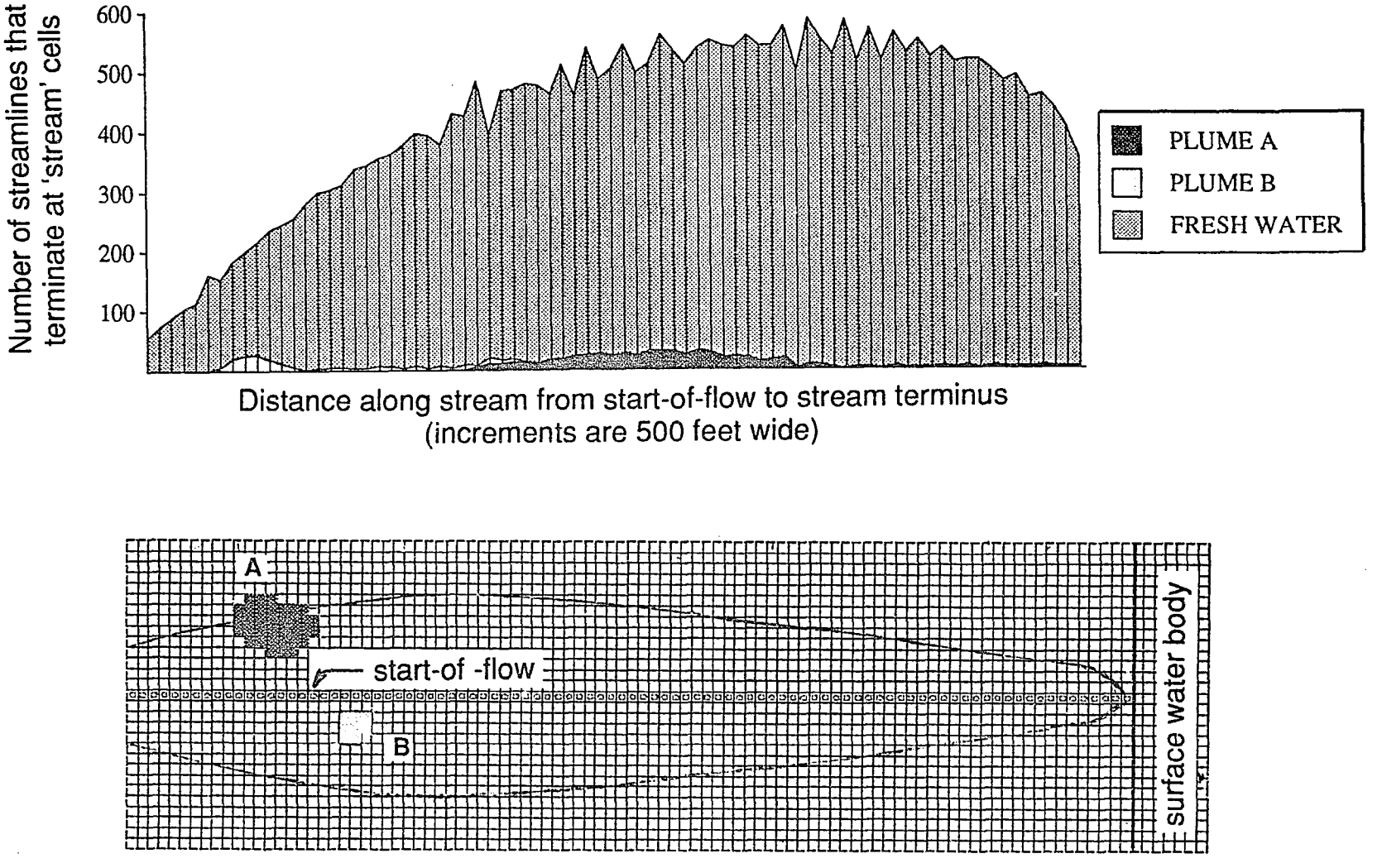


Figure 98--Relative proportions of contaminant A and B mixing with fresh groundwater along center stream channel if source areas A and B are continuous.

3500 feet from the start-of-flow (node 46) to the terminus. However, the highest proportions will discharge within a 1.6 mile reach (between nodes 82 and 99).

In contaminated area B, because it lies entirely within the stream catchment area, it will eventually discharge to the stream along the reach between 3500 feet from the start-of-flow to node 72, about 2.4 miles. The highest concentrations will occur within a 1500 foot reach (between nodes 54 and 57). Contaminant source B is closer to the stream than is contaminant source A; its pathlines are shorter and less dispersed than those from source area A.

Figure 98 shows the relative proportions of contaminants and fresh groundwater that will discharge to each node along the stream assuming continuous seepage. Clearly, the contaminants make up relatively small proportions of discharge even at their peak quantities.

Maintaining the assumption that contaminants A and B are continuously released into the groundwater system after their initial introduction at sites A and B, it would take about 92 years for contaminant A to first appear in the stream system and about 245 years for a steady state solute transport condition to develop with respect to the stream. It would take over 252 years for all flowlines originating at the A-site to completely sweep through the system and discharge to both the stream and surface water body. It would take about 7 years for contaminant B to first appear in the stream system but about 84 years for a steady state condition to develop.

If the contaminants are introduced into the system and then discontinued after a short interval of time, the contaminants would move through the system as a plug that would flush out of the system at different times and to different reaches along the stream. The contaminants would reside longer in the aquifer if they followed pathlines discharging farther downstream. Also the fresh groundwater that mixes in would have a wider range of residence times.

For example, an analysis of the path lines discharging to node 89, as illustrated in figure 98, would show that about 5% of flow would originate from source A. However, because their residence times range from 150 to 200 years the percentage of contaminated flow would be lower than that at any instant in time. The fresh water that discharges with the contaminant would range in age from a little greater than 0 to well over 200 years.

Mixing of groundwater from different source areas is important for determining the fate of solutes that are transported in the system. The stream sub-system functions as an effective mixing mechanism especially in the lower reaches. Concentrations of a constituent introduced in the system may be attenuated because of mixing with fresh water.

**Some controlling factors on groundwater residence times**

Age patterns in aquifer systems are greatly affected by aquifer thickness, the presence of confining units, and other factors. An example of how residence times of groundwater are controlled by geometric properties of aquifers is seen

from evaluation of models of two different systems, Long Island's aquifer system and the Upper Rancocas system.

*Long Island aquifer system*

Figure 99 shows the lines of equal age for a representative section of Long Island's aquifer system (Buxton and Modica, 1992). The system consists of three aquifers and two confining units. The total thickness varies from about 400 feet at the North Shore to well over 2000 feet near and beneath the Atlantic Ocean. Because of the great thickness and the retarding effect that clay deposits have on groundwater movement, groundwater ages on the order of thousands of years are found in the system. Groundwater that moves through the Raritan Confining Unit and into the southern portion of the Lloyd Aquifer travels for extreme durations of greater than 8000 years. However, ages of ground water in the Magothy exceed 2000 years in the off-shore area, even though ground water doesn't pass through the Raritan Clay. An interesting phenomena is that the Raritan Confining Unit generates an age discontinuity in the Magothy Aquifer along the limiting streamline of flow near the southern shoreline; this streamline is a hydraulic boundary that separates flow that stays in the Magothy from flow that moves through the confining unit.

*Upper Rancocas aquifer system*

The deposits in the Atlantic Coastal Plain of New Jersey are more extensive, having more sequences of aquifers and inter-layered confining units,

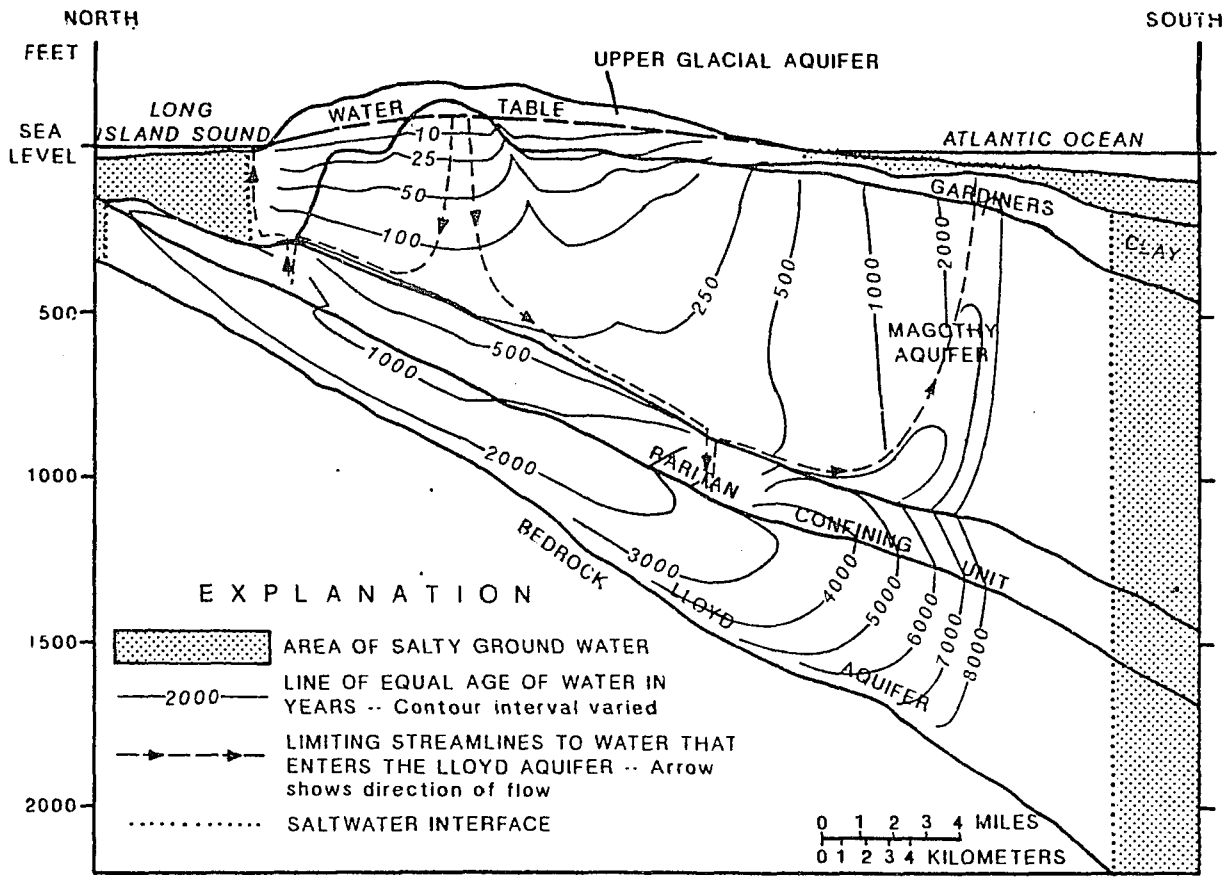


Figure 99--Lines of equal age for representative cross-section of Long Island's aquifer system (after Buxton and Modica, 1992).

than the deposits beneath Long Island. At the regional scale groundwater could attain great ages, perhaps exceeding those of Long Island's system, due to the presence and great thickness of confining units. The Upper Rancocas System constitutes a relatively small sub-system of this larger complex. Therefore, the scale and extent of the Rancocas model are not strictly comparable to Long Island's model.

The modeled portion of the Rancocas system does not contain extensive confining units except at its base. The modeled aquifer has a maximum depth of about 360 feet. Clearly, the shallowness of the system and lack of confining units preclude the propagation of very deep pathlines and, consequently, long travel times. Figure 100 shows lines of equal residence times. Recharge originating along the respective time lines would take the length of time indicated to travel through the system. The maximum time is about 200 years (excluding ground water traveling through stagnation zones such as might occur near hydraulic surfaces).

Figure 101 shows the locations along pathlines to where particles would take 20 and 80 years to travel through the groundwater zone when they originate from a line of particles on column 42. Because the Rancocas model is three-dimensional, the ages can only be shown as projections. The time symbols tend to demarcate lines of equal age. However, the time lines shown are discontinuous. The discontinuities represent an absence of ranges of residence times in different locations and would appear as holes in a time surface similar to that illustrated in figure 96.

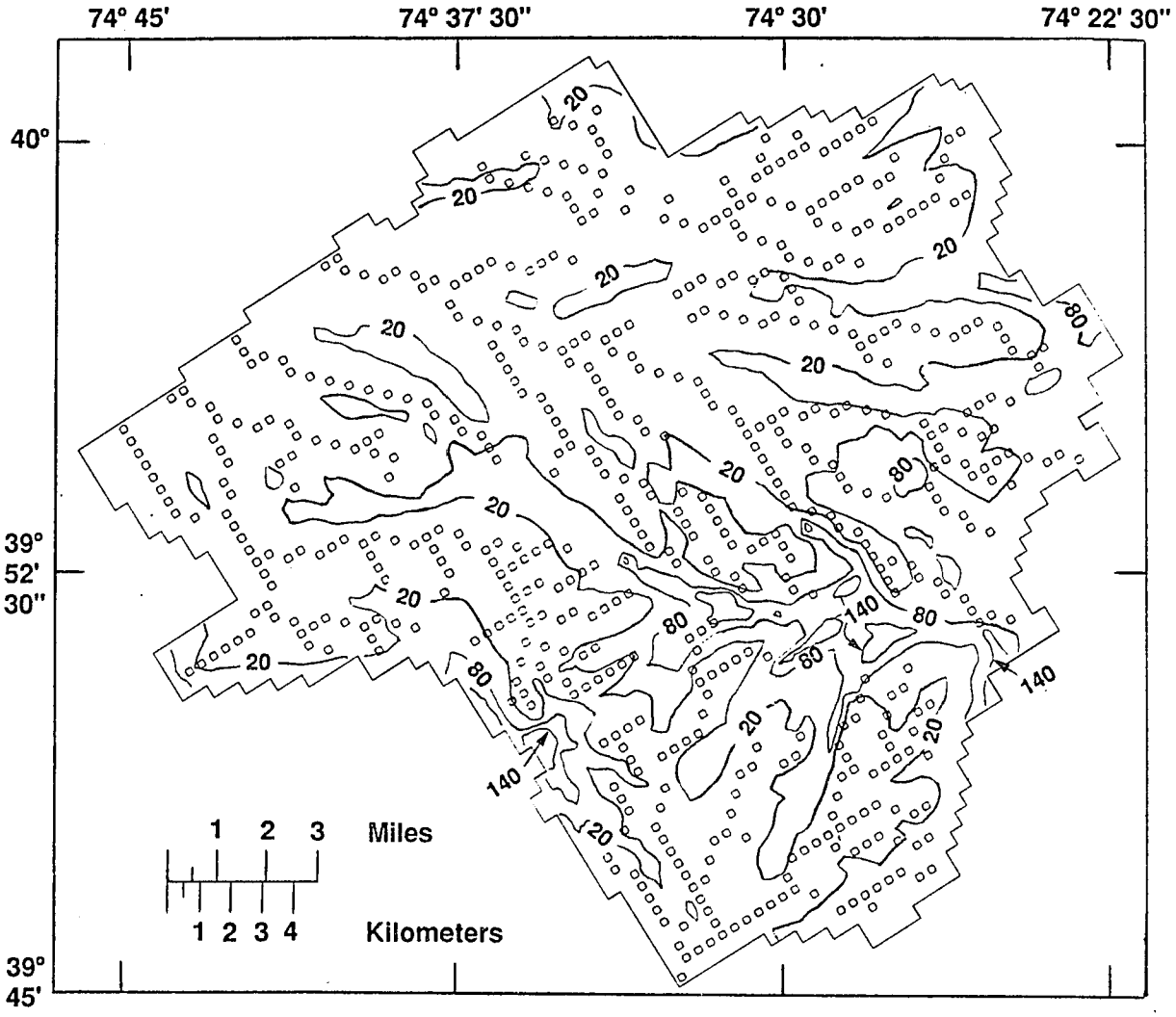


Figure 100--Map view of lines of equal residence time for recharge locations on the free surface in the Upper Rancocas system. Lines shown represent 20, 80 and 140 year residence-time intervals.

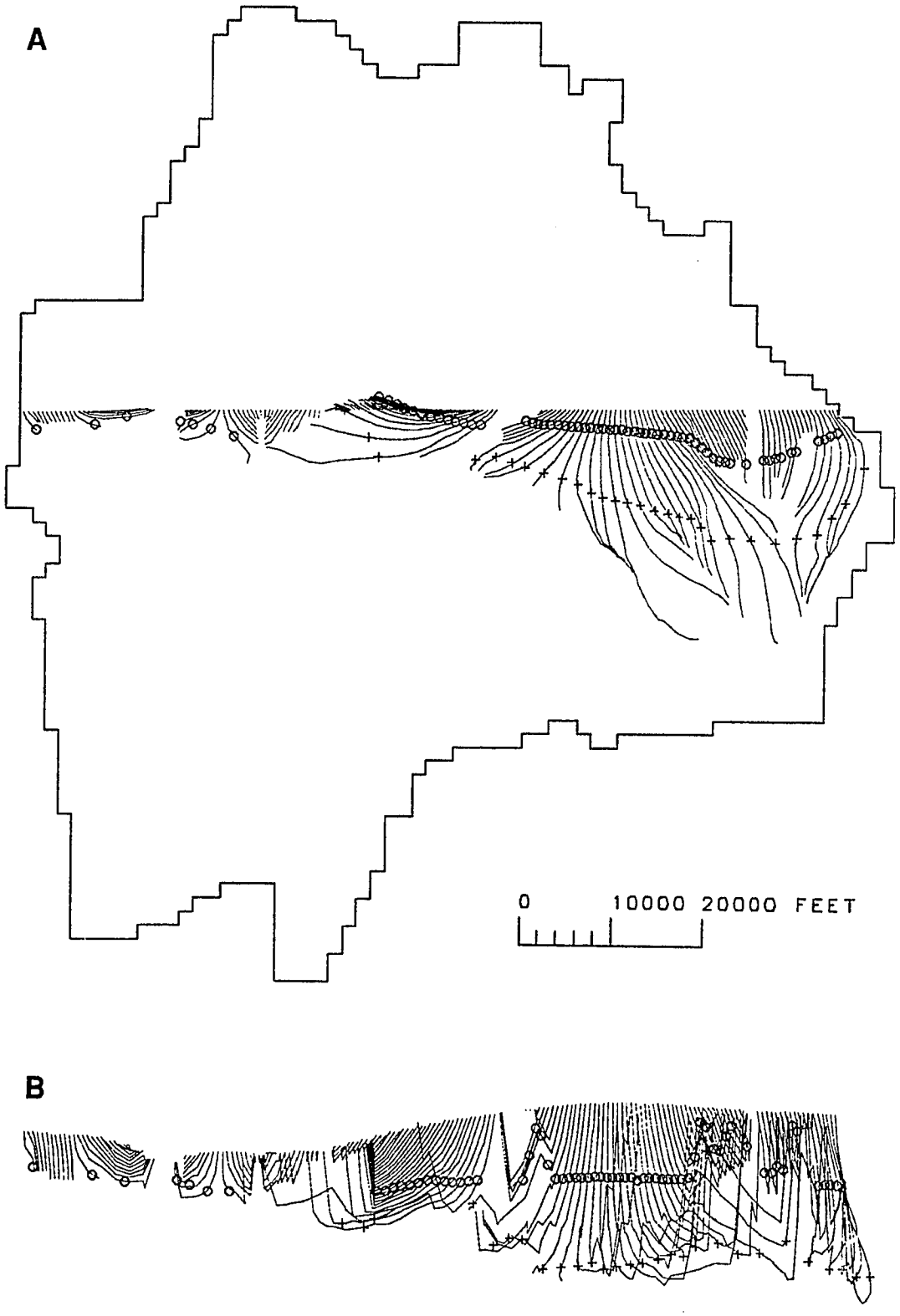


Figure101--Path lines from column 42 of Upper Rancocas model projected to (A) map and, (B) cross-sectional views. Circles indicate 20 years of travel along path lines. Crosses indicate 80 years of travel.

## SUMMARY AND CONCLUSIONS

Several hydrologic concepts that are specific to stream sub-system flow and its interaction with the deeper groundwater zone have emerged from an analysis of the hypothetical and real-world flow models. The models used in this study involved numerical solutions to three-dimensional, steady-state, unconfined flow systems. Numerical solutions provide a convenient and effective vehicle with which to analyze complex flow problems that would not be possible with analytical approaches.

The concepts of stream sub-system flow and interaction with the regional flow can be applied to problems involving the fate and advective transport of contaminants and the confluence of groundwater of different source areas along streams. Groundwater residence times and age distributions in aquifer systems that have major drainage networks are also understood through an analysis of flow patterns in the system. The basic hydrologic concepts derived from this study can be summarized as follows:

Bounding surfaces of stream sub-systems demarcate zones of interaction between adjacent sub-system flow regimes. The surfaces are generally not hydraulic surfaces except along the water table. In cases of flow symmetry, stream lines can coincide with bounding surfaces deeper in the groundwater zone. Bounding surfaces cannot be uniquely defined inasmuch as their position is sensitive to the shape and position of the flow-system boundaries, water transmitting properties of the aquifer and stream, recharge, stream channel geometry, and the disposition of other hydraulic sinks in the system.

Although hydraulic parameters affect stream sub-system flow in different ways, the following generalities can be stated regarding stream sub-system geometry: stream source areas will tend to be shorter and narrower in systems where hydraulic parameters restrict discharge, and flow lines will not propagate as deeply into the groundwater zone. Conversely, source areas will be longer, wider with rounder shapes, and associated streamlines will propagate deeper into the aquifer in systems where hydraulic parameters cause higher rates of stream discharge. Factors that tend to control stream discharge are recharge, stream slopes and profiles, channel geometry and streambed deposits, and number of streams in a given watershed area. Increased anisotropy in a system will cause source areas to expand over larger areas of the free surface while limiting the depth of flow.

Thin aquifers constrain vertical propagation of stream sub-system flow and cause their source areas to tap into larger areas of the free surface. Thin aquifer systems limit the development of flow to more remote sinks or sinks that serve as common discharge outlets for much of the watershed system. Regional divide areas that are underlain by such aquifers tend to have limited deeper, 'regional' flow. Thick aquifers allow for development of deeper flow systems under local stream sub-systems. Divide areas in thick aquifer systems generally contain source areas to remote discharge outlets juxtaposed with local source areas of flow.

Base flow along a gaining stream is related to the difference in head in the aquifer and the elevation of the stream channel. In an unconfined system a

base-flow profile assumes the parabolic form of the water table for constant or concave channel slopes. The water table is a reflection of the system's potential energy. Streams lower the water-table position and reflect the degree to which they dissipate energy from the system.

The lateral component of flow becomes increasingly significant in zones adjacent to the stream and with distance downstream from the start-of-flow. The horizontal component of flow, in the direction away from the major hydrologic divide, increases in magnitude with distance down gradient especially if there is a major regional sink. Horizontal flow tends to be weaker near the divide. Downward flow components are more significant near the divide area in that horizontal flow is less dominant.

Streams behave as line-sinks; they induce complex flow patterns in a flow field whereby flow from near and far source areas are drawn into common discharge locations. Any point along the stream that is downstream from the start-of-flow receives flow from a recharge area shaped like an elongated loop. The recharge areas to points further downstream are larger and encompass upstream loops. The flow field to each successive reach along a stream appears as nested, shell-like zones of flow that are intermingled. Flow traveling from the perimeter of the source area nearest to the divide travels the longest, deepest path in the stream sub-system and discharges at the stream terminus.

The age range of groundwater that discharges along the stream varies as a function of distance downstream from the start-of-flow. The age of groundwater discharging just below the start-of-flow is relatively young and

homogeneous in age but shows increasing range in age downstream. Discharge with the oldest residence times in the stream sub-system are found at the stream terminus. Recharge that enters the stream system close to the channel has short residence times but mixes with much older groundwater along the stream.

## REFERENCES

Barnes, B. S., 1939, The structure of discharge-recession curves, Trans. Amer. Geophys. Union: Reports and Papers, Hydrology, p. 721-725

Bear, J., 1972, *Dynamics of Fluids in Porous Media*, American Elsevier Pub. Co., New York, 764 p.

Bear, J., 1979, *Hydraulics of Groundwater*, McGraw Hill, New York, 569 p.

Buxton, H. T., et al., 1991, Particle tracking analysis of recharge areas on Long Island, New York, Groundwater, vol. 29, no. 1, p. 63-71

Buxton, H. T. and Modica, E., 1992, Ground-water flow patterns in Long Island's aquifer system, Groundwater, vol. 30, no. 6, p.857-866

Cooper, H. H., and Rorabaugh, M. I., 1963, Ground-water movements and bank storage due to flood stages in surface streams, U. S. Geol. Survey Water-Supply Paper 1536-J, p. 343-366

Dunne, T., and Black, R. D., 1970, An experimental investigation of runoff production in permeable soils, Water Resources Research, vol. 6, no. 2, p. 478-490

Dunne, T., and Black, R. D., 1970, Partial area contributions to storm runoff in a small New England watershed, Water Resources Research, vol. 6, no. 5, p. 1296-1311

Eshett, A. and Bittinger, M. W., 1965, Stream-aquifer system analysis, Journal of the Hydraulics Division: Proceedings of the Amer. Soc. of Civil Engineers, vol. 91, no. HY6, p. 153-164

Franke, O. L. and Cohen, P., 1972, Regional rates of ground-water movement on Long Island, New York, in Geological Survey Research 1972: U. S. Geol. Survey Prof. Paper 800-C, p. C271-C277

Franke, O. L. and Reilly, T. E., 1987, The effects of boundary conditions on the steady-state response of three hypothetical ground-water systems - results and implications of numerical experiments, U. S. Geol. Survey Water-Supply Paper 2315, 19 p.

Freeze, R. A., 1972, Role of subsurface flow in generating surface runoff 1. base flow contributions to channel flow, Water Resources Research, vol. 8, no. 3, p. 609-623

Freeze, R. A.,1972, Role of subsurface flow in generating surface runoff 2. upstream source areas, Water Resources Research, vol. 8, no. 5, p. 1272-1283

Freeze, R. A., 1974, Streamflow generation, Reviews of Geophysics and Space Physics, vol. 12, no. 4, p. 627-647

Freeze, R. A., 1971 Three-dimensional, transient, saturated-unsaturated flow in a groundwater basin, Water Resources Research, vol. 7, no. 2, p. 347-366

Gillham, R. W., and Farvolden, 1974, Sensitivity analysis of input parameters in numerical modeling of steady state regional groundwater flow, Water Resources Research, vol. 10, no. 3, p. 529-538

Hack, J. T., 1958, Studies of longitudinal stream profiles in Virginia and Maryland, U. S. Geol. Survey Prof. Paper 294-B, p. 53-63

Hall, F. R., 1968, Base-flow recessions-a review, Water Resources Research, vol. 4, no. 5, p. 973-983

Hall, F. R., and Moench, A. F., 1972, Application of the convolution equation to stream-aquifer relationships, Water Resources Research, vol. 8, no. 2, p. 487-493

Harbaugh, A. W., and Getzen, R. T., 1977, Stream simulation in an analog model of the ground-water system on Long Island, New York, U. S. Geol. Survey Water Resources Investigation 77-58, 15 p.

Hewlett,J. D., and Nutter, W. L.,1970, The varying source area of streamflow from upland basins, Sumposium on Interdisciplinary Aspects of Watershed Management, Mont. State Univ., Bozeman

Hornberger, G. M., et al, 1970, Numerical solution of the Boussinesq equation for aquifer-stream interaction, Water Resources Research, vol. 6, no. 2, p. 601-608

Horton, R. E., 1945, Erosional development of streams and their drainage basins: hydrophysical approach to quantitative morphology, Bull. Geol. Soc. Am., vol. 56, p. 275-370

Illangasekare, T., and Morel-Seytoux, H. J., 1982, Stream-aquifer influence coefficients as tools for simulation and management, Water Resources Research, vol. 18, no. 1, p. 168-176

Jacob, C. E.,1943, Correlation of ground-water levels and precipitation on Long Island, New York, Trans. Amer. Geophysical Union, p. 564-573

Kirkby, M. J., and Chorley, R. J., 1967, Throughflow, overland flow and erosion, Int. Assoc. Sci. Hydrol. Bull., no. 12, p. 5-21

Lang, S. M., and Rhodehamel, E. C., 1963, Aquifer test at a site on the Mullica River in the Wharton Tract, southern New Jersey, International Association Scientific Hydrology Bulletin, vol. 8, no. 2, p. 31-38

McDonald, M. G., and Harbaugh, A. W., 1988, A modular three-dimensional finite-difference ground-water flow model, U. S. Geol. Survey Techniques of Water Resources Investigations, Book 6, Chapter A1

Modica, E., in press, Simulated effects of development on ground-water flow patterns in the Upper Rancocas Basin, New Jersey Pinelands, U. S. Geol. Survey Water Resources Investigation Report 93-xxxx, p.xx

Morel-Seytoux, H. J., 1975, A combined model of water table and river stage evolution, Water Resources Research, vol. 11, no. 6, p. 968-972

Morel-Seytoux, H. J., and Daly, C. J., 1975, A discrete kernel generator for stream-aquifer studies, Water Resources Research, vol. 11, no. 2, p. 253-260

Pinder, G. F., and Sauer, S. P., 1971, Numerical simulation of flood wave modification due to bank storage effects, Water Resources Research, vol. 7, no. 1, p. 63-70

Pollock, D. W.,1988, Semianalytical computation of path lines for finite-difference models, Groundwater, vol. 26, no.6, p.743-750

Pollock, D. W., 1989, Documentation of computer programs to compute and display pathlines using results from the U. S. Geological Survey modular three-dimensional finite-difference ground-water flow model, U. S. Geol. Survey Open File Report 89-381, 188 p.

Prince, K. R., 1988, Quantitative assessment of the shallow ground-water flow system associated with Connetquot Brook, Long Island, New York, U. S. Geol. Survey Water-Supply Paper 2309, 28 p.

Rhodehamel, E. C., 1973, Geology and water resources of the Wharton Tract and Mullica River Basin in Southern New Jersey, New Jersey Dept. of Environmental Protection, Div. of Water Resources Special Report 36, 58p.

Ritter, D. F., 1982, *Process Geomorphology*, Dubuque Iowa, WM. C. Brown Co. Publishers, 603 p.

Shulits, S., 1941, Rational equation of river-bed profile, Trans. Amer. Geophy. Union, vol. x, p. 622-630

Singh, K. P., 1968, Some factors affecting baseflow, Water Resources Research, vol. 4, no. 5, p. 985-999

Strack, O. D. L., and Haitjema, H. M., 1981, Modeling double aquifer flow using a comprehensive potential and distributed singularities 1. Solution for homogenous permeability, Water Resources Research, vol. 17, no. 5, p. 1535-1549

Strahler, A. N., 1964, Quantitative geomorphology of drainage basins and channel networks, p. 4-39-4-76, in Ven Te Chow, Ed, *Handbook of Applied Hydrology*, McGraw-Hill, New York

Toth, J., 1963, A Theoretical analysis of groundwater flow in small drainage basins, Journal of Geophysical Research, vol. 68, no. 16, p. 4795-4812

Toth, J., 1962, A Theory of groundwater motion in small drainage basins in Central Alberta, Canada, Journal of Geophysical Research, vol. 67, no. 11, p. 4375-4387

Venetis, C., 1970, Finite aquifers: characteristics responses and applications, Journal of Hydrology, 12, p. 53-62

Winter, T. C., 1976, Numerical simulation analysis of the interaction of lakes and ground water, Geol. Survey Prof. Paper 1001, 45 p.

Yatsu, E., 1955, On the longitudinal profile of the graded river, Trans. Amer. Geophys. Union, vol. 36, no. 4, p. 211-219

Zapecza, O. S., 1989, Hydrogeologic framework of the New Jersey Coastal Plain, U. S. Geol. Survey Prof. Paper 1404-B, 49 p.